

DESIGNING THERMALLY STABLE IONIC LIQUID STATIONARY PHASES FOR GAS
CHROMATOGRAPHY AND EXAMINING THEIR STRUCTURE-PROPERTY
RELATIONSHIPS

by

RAHUL AVINASH PATIL

Presented to the Faculty of the Graduate School of
The University of Texas at Arlington in Partial Fulfillment
of the Requirements
for the Degree of

DOCTOR OF PHILOSOPHY

THE UNIVERSITY OF TEXAS AT ARLINGTON

December 2018

Copyright © by Rahul A. Patil 2018

All Rights Reserved



I dedicate this dissertation to my parents, Kiran Patil, Avinash Patil and my brother

Sandip Patil

Acknowledgments

I would like to thank my advisor Prof. Daniel Armstrong for believing in me and providing an opportunity for Ph.D. in his group. I am grateful to him for his mentorship, guidance, and motivation throughout my Ph.D. research. I must say that I feel fortunate to receive a Ph.D. under his supervision. I am grateful to my committee members Dr. Purnendu Dasgupta, Dr. Frank Foss and Dr. Kevin Schug for their valuable support.

I thank Dr. Alain Berthod, Dr. M. Farooq Wahab, Dr. Chandan Barhate, Dr. Sumit Bhawal, Dr. Lillian Frink and Dr. John Lang for their valuable guidance throughout my Ph.D. I greatly value the support of my colleague and friend Mohsen Talebi. I thank Len Sidisky (MilliporeSigma) and Ryo Takechi (Shimadzu) for their help during research. I appreciate my friend Ravi Singh for all his help in synthesis projects. I would like to thank Ms. Barbara Smith and Ms. Angel Escalante for their precious administrative support in my research. I am grateful to my mentors Mr. Raymond Zielinski and Dr. Kelly Camozzi for their support during my internship at Zoetis. I am honored to receive the research poster award from Dr. Jim Luong at ISCC 2017 conference and I would like to thank him for his guidance during my Ph.D. I would like to acknowledge Dr. Roy McDougald and Dr. Brian Edwards for training on different instruments and helping me fix them.

I would like to thank my parents for believing in me and giving me everything I needed to become the man I am today. My brother owes a special thank you for motivating me, inspiring me, supporting me and teaching me the value of hard work. I appreciate my cousin Dr. Swapnil Sonawane for mentoring throughout my career. I want to thank my friends Deepanshu, Avin, Rahul, Maria and Apoorva for always keeping me motivated and helping me through the tough times. Finally, I thank Nimisha for her love and support which made this journey easier.

October 25, 2018

Abstract

DESIGNING THERMALLY STABLE IONIC LIQUID STATIONARY PHASES FOR GAS CHROMATOGRAPHY AND EXAMINING THEIR STRUCTURE-PROPERTY RELATIONSHIPS

Rahul A. Patil, PhD

The University of Texas at Arlington, 2018

Supervising Professor: Daniel W. Armstrong

Ionic liquids are popular in diverse scientific applications because of their unique physicochemical properties. The physicochemical properties of ionic liquids can be “tuned” by the modification of their structural moieties. Understanding of structure-property relationship is important if one wants to introduce a desired property in ionic liquid for a specific application. The initial part of this thesis will discuss the understanding of structure-property relationship of dicationic ionic liquids.

Ionic liquids with high thermal stability are useful in many applications from simple solvents for high temperature reactions to high vacuum lubricants for space applications. This thesis presents the design, synthesis, and characterization of different thermally stable dicationic ionic liquids. ILs with TGA thermal stabilities in the range of 330 to 467 °C and inverse gas chromatography stabilities up to 400 °C are reported. The thesis also provides an understanding of the thermal behavior of ionic liquids at higher temperatures. The first, in depth thermal decomposition study of dicationic ionic liquids by using electrospray ionization mass spectrometer is presented, and it discusses the mechanism of thermal degradation of ionic liquids and their degradation products at high temperatures.

Two important applications of thermally stable ionic liquids, stationary phases for gas chromatography and solvents for high temperature reactions are discussed in this thesis. Applications of thermally stable dicationic ionic liquid gas chromatography stationary phases for the high temperature separation of high molecular weight compounds is presented. Applications of ionic liquid stationary phases in the separation of structural isomers of toxic environmental pollutants, compounds with different functional groups and polarities are reported. A fundamental investigation of the effect of structural modifications such as cations, linkage chains, and anions on the selectivities of ionic liquids is discussed.

The last chapter of the thesis presents the application of thermally stable monocationic phosphonium ionic liquid as a solvent in a high temperature synthesis. The advantages of higher thermal stability and the catalytic properties of ionic liquid were utilized for the “rapid” deprotection of *tert*-butoxy amino acids and peptides at higher temperatures.

Table of Contents

Acknowledgments	iv
Abstract	v
List of Illustrations	xiii
List of Tables	xvii
List of Schemes.....	xviii
Chapter 1 INTRODUCTION.....	1
1.1 Introduction to Ionic Liquids.....	1
1.2 Structure-Property Relationship of Ionic Liquids	1
1.3 Thermal Stability of Ionic Liquids.....	3
1.3.1 Short term thermal stability.....	4
1.3.2 Long-term thermal stability	5
1.4 Applications of Ionic Liquids as Gas Chromatography Stationary Phases.....	6
1.5 Ionic Liquids in Synthesis	7
1.5 Organization of Dissertation	8
Chapter 2 SYNTHESIS OF THERMALLY STABLE GEMINAL DICATIONIC IONIC LIQUIDS AND RELATED IONIC COMPOUNDS: AN EXAMINATION OF PHYSICOCHEMICAL PROPERTIES BY STRUCTURAL MODIFICATION	9
2.1 Abstract.....	9
2.2 Introduction	9
2.3 Experimental Section.....	11
2.3.1 Materials:	11

2.3.2 Methods of Analysis:	11
2.3.3 Synthesis of monocationic ILs:	12
2.3.4 Synthesis of dicationic ionic liquids:	13
2.3.5 Preparation of IL columns:	16
2.4 Results and Discussion	17
2.4.1 Melting Point:	19
2.4.3 Density:.....	27
2.4.4 Solubility:	27
2.4.5 Thermal Stability:.....	27
2.4.6 Thermal stability with inverse GC-FID:.....	30
2.4.7 Performance testing of ILs as GC stationary phases:.....	31
2.5 Conclusions	33
 Chapter 3 EXAMINATION OF SELECTIVITIES OF THERMALLY STABLE GEMINAL DICATIONIC IONIC LIQUIDS BY STRUCTURAL MODIFICATION	
3.1 Abstract.....	35
3.2 Introduction	35
3.3 Experimental Section:.....	37
3.3.1. Materials	37
3.3.2 Instrumentation:.....	39
3.4 Results and Discussion	39
3.4.1 FAME Test Mix	41
3.4.2 Equivalent chain length (ECL) values	45
3.4.3 Grob Test Mix	47
3.4.4 Polar Plus test mix.....	48
3.4.5 PAM-HC test mix.....	50

3.4.6 Custom-PAM mix.....	51
3.4.7 Ionic Liquid test mix:	53
3.5 Conclusions	55
Chapter 4 DICATIONIC IONIC LIQUID THERMAL DECOMPOSITION	
PATHWAYS	57
4.1 Abstract.....	57
4.2 Introduction	57
4.3 Materials and Methods	60
4.3.1 Instruments.....	60
4.3.2 Materials	60
4.3.3 Experimental Design	61
4.4 Results and Discussion	63
4.4.1 Analysis of straight chain linkage ILs	63
4.4.2 Analysis of branched chain linkage ILs	78
4.5 Conclusions	84
Chapter 5 GC SELECTIVITY OF NEW PHOSPHONIUM-BASED	
DICATIONIC IONIC LIQUID STATIONARY PHASES	86
5.1 Abstract.....	86
5.2 Introduction	86
5.3 Materials and methods.....	88
5.3.1 Chemicals.....	88
5.3.2 Phosphonium dicationic ionic liquid synthesis.....	88
5.3.3 Capillary column preparation	89
5.3.4 Gas chromatography instrumentation:	90
5.3.5 Dicationic ionic liquid characterization	90

5.4 Results and discussion	91
5.4.1 Physicochemical properties of the new phosphonium-based DILs.....	91
5.4.2 Analysis of 12 regulated phthalates.....	93
5.4.3 Analysis of a selection of polycyclic aromatic hydrocarbons (PAHs)	97
5.4.4 Separation of chlorinated aromatics	100
5.5 Conclusions	105
Chapter 6 RAPID, EFFECTIVE DEPROTECTION OF TERT- BUTOXYCARBONYL (BOC) AMINO ACIDS AND PEPTIDES AT HIGH TEMPERATURES USING A THERMALLY STABLE IONIC LIQUID	
6.1 Abstract.....	106
6.2 Introduction	106
6.3 Materials and Methods	108
6.3.1 Materials and method of analysis.....	108
6.3.2 Synthesis Procedures	108
6.4 Results and Discussion	110
6.5 Conclusions	114
Chapter 7 CONCLUSIONS	115
Appendix 1 ^1H NMR AND ^{13}C NMR OF $\text{C}_6(\text{bmim})_2\text{-NTf}_2$	117
Appendix 2 ^1H NMR AND ^{13}C NMR OF $\text{C}_6(\text{mzim})_2\text{-NTf}_2$	120
Appendix 3 ^1H NMR AND ^{13}C NMR OF $\text{C}_6(\text{bpy})_2\text{-NTf}_2$	123
Appendix 4 ^1H NMR AND ^{13}C NMR OF $\text{C}_6(\text{mpy})_2\text{-NTf}_2$	126
Appendix 5 ^1H NMR AND ^{13}C NMR OF $\text{C}_6(\text{pr}_3\text{p})_2\text{-NTf}_2$	129
Appendix 6 ^1H NMR AND ^{13}C NMR OF $\text{C}_6(\text{ph}_3\text{p})_2\text{-NTf}_2$	132

Appendix 7 ^1H NMR AND ^{13}C NMR OF $\text{C}_6(\text{bmim})_2\text{-PFOS}$	135
Appendix 8 ^1H NMR AND ^{13}C NMR OF $\text{C}_6(\text{m}_2\text{im})_2\text{-PFOS}$	138
Appendix 9 ^1H NMR AND ^{13}C NMR OF $\text{C}_6(\text{bpy})_2\text{-PFOS}$	141
Appendix 10 ^1H NMR AND ^{13}C NMR OF $\text{C}_6(\text{mpy})_2\text{-PFOS}$	144
Appendix 11 ^1H NMR AND ^{13}C NMR OF $\text{C}_6(\text{pr}_3\text{p})_2\text{-PFOS}$	147
Appendix 12 ^1H NMR AND ^{13}C NMR OF $\text{C}_6(\text{ph}_3\text{p})_2\text{-PFOS}$	150
Appendix 13 ^1H NMR AND ^{13}C NMR OF $\text{C}_9(\text{bmim})_2\text{-NTf}_2$	153
Appendix 14 ^1H NMR AND ^{13}C NMR OF $\text{C}_9(\text{m}_2\text{im})_2\text{-NTf}_2$	156
Appendix 15 ^1H NMR AND ^{13}C NMR OF $\text{C}_9(\text{bpy})_2\text{-NTf}_2$	159
Appendix 16 ^1H NMR AND ^{13}C NMR OF $\text{C}_9(\text{mpy})_2\text{-NTf}_2$	162
Appendix 17 ^1H NMR AND ^{13}C NMR OF $\text{C}_9(\text{pr}_3\text{p})_2\text{-NTf}_2$	165
Appendix 18 ^1H NMR AND ^{13}C NMR OF $\text{C}_9(\text{ph}_3\text{p})_2\text{-NTf}_2$	168
Appendix 19 ^1H NMR AND ^{13}C NMR OF $\text{C}_9(\text{bmim})_2\text{-PFOS}$	171
Appendix 20 ^1H NMR AND ^{13}C NMR OF $\text{C}_9(\text{m}_2\text{im})_2\text{-PFOS}$	174
Appendix 21 ^1H NMR AND ^{13}C NMR OF $\text{C}_9(\text{ph}_3\text{p})_2\text{-PFOS}$	177
Appendix 22 ^1H NMR AND ^{13}C NMR OF $\text{C}_{12}(\text{m}_2\text{im})_2\text{-NTf}_2$	180
Appendix 23 ^1H NMR AND ^{13}C NMR OF $\text{C}_{12}(\text{mpy})_2\text{-NTf}_2$	183
Appendix 24 ^1H NMR AND ^{13}C NMR OF $\text{C}_{12}(\text{pr}_3\text{p})_2\text{-NTf}_2$	186
Appendix 25 ^1H NMR AND ^{13}C NMR OF $\text{C}_{12}(\text{m}_2\text{im})_2\text{-PFOS}$	189
Appendix 26 ^1H NMR AND ^{13}C NMR OF $\text{C}_9(\text{ph}_2\text{tIP})_2\text{-2NTf}_2$	192
Appendix 27 ^1H NMR AND ^{13}C NMR OF $\text{C}_9(\text{pr}_2\text{phP})_2\text{-2NTf}_2$	195
Appendix 28 ^1H NMR AND ^{13}C NMR OF $\text{C}_9(\text{ph}_2\text{prP})_2\text{-2NTf}_2$	198
Appendix 29 PUBLICATION INFORMATION OF THE DISSERTATION.....	201

Appendix 30 RIGHTS AND PERMISSIONS.....	203
References.....	213
Biographical Information	222

List of Illustrations

Figure 1-1 Different types of ionic liquids.....	2
Figure 1-2 General structure of dicationic ionic liquids	3
Figure 1-3 Isothermal gravimetric analyses of [C ₄ mim] [Br] IL at different temperatures, nitrogen-atmosphere.	5
Figure 1-4 Thermal Stability of five different ILs measured with Inverse GC-FID.	6
Figure 2-1 Structure and abbreviations of monocationic ILs synthesized in this study.	20
Figure 2-2 Structure and abbreviations of dicationic ILs synthesized in this study	21
Figure 2-3 Thermal stability comparison of ILs synthesized in this study.....	28
Figure 2-4 Thermal stability diagram with GC-FID for nine dicationic ILs.	32
Figure 2-5 Separation of structural isomers of benzofluoranthene by GC on C ₉ -(m ₂ im) ₂ -NTf ₂ IL column	33
Figure 3-1 Structures and abbreviations of dicationic ILs studied in this analysis.....	40
Figure 3-2 Separation of FAME test mix.....	42
Figure 3-3 Separation of Grob test mix.....	48
Figure 3-4 Separation of Polar Plus test mix.	49
Figure 3-5 Separation of PAM-HC test mix.....	51
Figure 3-6 Separation of Custom-PAM test mix.	53
Figure 3-7 Separation of Ionic Liquid test mix.	54
Figure 4-1 The Experimental setup for the collection of volatile fragments.....	61
Figure 4-2 The volatiles collected in collection flask after heating IL1 C ₉ (m ₂ im) ₂ -NTf ₂ ,	62
Figure 4-3 The pictures of IL1 C ₉ (m ₂ im) ₂ -NTf ₂ taken after heating at different temperatures.	63

Figure 4-4 Mass spectra of IL1	65
Figure 4-5 Mass spectra of IL5.	66
Figure 4-6 Postulated mechanism for the decomposition of ILs. A) Imidazolium based ILs. B) Phosphonium based ILs.	67
Figure 4-7 ESI Mass spectrum of the volatile fraction of IL6 C ₉ (ph ₃ p) ₂ -NTf ₂ collected after heating at 400 °C for 30 min.	69
Figure 4-8 ESI mass spectrum of residue of IL2 C ₉ (bzmim) ₂ -NTf ₂ collected after heating up to 400 °C	70
Figure 4-9 ESI mass spectrum of residue of IL5 C ₉ (pr ₃ p) ₂ -NTf ₂ collected after heating at 440 °C for 30 min in air	70
Figure 4-10 ESI mass spectrum of residue of IL8 C ₉ (mpy) ₂ -NTf ₂ collected after heating up to 400°C.	71
Figure 4-11 ESI Mass spectrum of the volatile fraction of IL2 C ₉ (bzmim) ₂ -NTf ₂ collected after heating at 400 °C for 30 min.....	71
Figure 4-12 ESI mass spectrum of residue of IL5 C ₉ (pr ₃ p) ₂ -NTf ₂ collected after heating at 440 °C for 30 min in argon atmosphere	72
Figure 4-13 ESI Mass spectrum of the volatile fraction of IL8 C ₉ (mpy) ₂ -NTf ₂ collected after heating at 400 °C for 30 min.....	72
Figure 4-14 Postulated mechanism for the thermal decomposition of PEG linked ILs.	76
Figure 4-15 ESI mass spectrum of residue of IL1 C ₉ (m ₂ im) ₂ -NTf ₂ collected after heating at 440 °C for 30 min in argon atmosphere.	77
Figure 4-16 ESI mass spectrum of residue of IL1 C ₉ (m ₂ im) ₂ -NTf ₂ collected after heating at 440 °C for 30 min in air.	77

Figure 4-17 ESI Mass spectrum of the volatile fraction of IL9 1mC ₃ (m ₂ im) ₂ -NTf ₂ collected after heating at 400 °C for 30 min.....	80
Figure 4-18 ESI Mass spectrum of the volatile fraction of IL10 2mC ₃ (m ₂ im) ₂ -NTf ₂ collected after heating at 400 °C for 30 min.....	81
Figure 4-19 ESI Mass spectrum of the volatile fraction of IL11 i-eneC ₄ (m ₂ im) ₂ -NTf ₂ collected after heating at 400 °C for 30 min.....	81
Figure 4-20 ESI Mass spectrum of the volatile fraction of IL12 C ₅ (m ₂ im) ₂ -NTf ₂ collected after heating at 400 °C for 30 min.....	83
Figure 4-21 ESI Mass spectrum of the volatile fraction of IL13 3mC ₅ (m ₂ im) ₂ -NTf ₂ collected after heating at 400 °C for 30 min.....	83
Figure 4-22 ESI Mass spectrum of the volatile fraction of IL14 3m ₂ C ₅ (m ₂ im) ₂ -NTf ₂ collected after heating at 400 °C for 30 min.....	84
Figure 4-23 ESI Mass spectrum of the volatile fraction of IL15 3t-buC ₅ (m ₂ im) ₂ -NTf ₂ collected after heating at 400 °C for 30 min.....	84
Figure 5-1 Inverse GC following the thermal decomposition of the 3 m × 250 μm DIL-coated capillary columns.....	93
Figure 5-2 Chromatograms of the phthalate mix EPA8106 on the three phosphonium-based DIL-coated 30 m columns	96
Figure 5-3 Selectivity on four critical phthalate pairs observed on the three phosphonium DIL-coated capillary columns.....	97
Figure 5-4 Separations of the 16 PAHs of the EPA-610 mix.....	98
Figure 5-5 Selectivity observed on the three phosphonium DIL-coated capillary columns for four critical PAH pairs of the EPA-610 mix.	99
Figure 5-6 Separation of PCBs on phosphonium-based DIL columns.....	102

Figure 5-7 Separation of six pollutant tetrachlorodibenzodioxin isomers on a
phosponium-based DIL column 104

List of Tables

Table 2-1 Physicochemical Properties of monocationic ILs	18
Table 2-2 Physicochemical Properties of C ₆ alkane linkage chain ILs	22
Table 2-3 Physicochemical Properties of C ₉ alkane linkage chain ILs	23
Table 2-4 Physicochemical Properties of C ₁₂ alkane linkage chain ILs.....	24
Table 2-5 Melting points of mixtures of ILs	26
Table 3-1 ECL values of unsaturated fatty acid methyl esters on IL columns at 180 °C..	46
Table 4-1 MS peaks of residual (non-volatile) dicationic NTf ₂ ionic liquids seen after heating at 400 °C for 30 min under argon flow.	73
Table 4-2 MS peaks of the volatiles emitted by dicationic NTf ₂ ionic liquids after heating at 400 °C for 30 min under argon flow.	75
Table 4-3 MS peaks of volatile dicationic NTf ₂ branched ionic liquids seen after heating at 400 °C for 30 min under argon flow.	79
Table 5-1 Structure and physicochemical properties of phosphonium-based bis(trifluoromethyl sulfonyl) imide dicationic ionic liquids.....	92
Table 5-2 Physicochemical properties of the phthalates of the EPA 8106 list.....	95
Table 6-1 Deprotection of N-Boc amino acid and peptide substrates	112

List of Schemes

Scheme 2-1 Synthesis of bromide salt of dication	14
Scheme 2-2 Metathesis of bromide salts to synthesize dicationic ILs.....	15
Scheme 6-1 Boc deprotection of amino acids using phosphonium ionic liquids.	111

Chapter 1

INTRODUCTION

1.1 Introduction to Ionic Liquids

Simple inorganic salts have very high melting points, and this limits their applications as solvents for chemical applications. Salts with bulky organic cations and inorganic or organic anions generally melt at lower temperatures, and those with melting points less than 100 °C are known as ionic liquids (ILs).¹ Salts which are liquid at room temperature (~25 °C) are known as “room temperature ionic liquids (RTILs).”² The history of ionic liquids is a relatively recent one. Walden first reported the room temperature molten salt, ethylammonium nitrate with a melting temperature of 12 °C in 1914.³⁻⁴ However, it was not recognized that chemistry in such solvents could become of widespread use. Organic chloroaluminates were first reported in 1951 and were studied in detail from the 1970s onwards, and were often referred to as molten salts.^{1, 5-6} However, these were not moisture stable, were reactive, and had other shortcomings. In the 1990s, ILs with tolerance to water were reported.⁷⁻⁹ Since then ILs with different combinations of ions have become increasingly popular in different areas of science. The term “neoteric solvents” has recently been used to represent ionic liquids as they have been known for a while, but are now being considered as process solvents.⁴

ILs have “unique” properties such as low volatility, non-flammability, huge liquidus range, wide solubility range, and high thermal stability which gives them advantages over non-ionic solvents.⁶ These diverse properties make them versatile compounds useful in academia and industry.¹ ILs can be designed with a particular interest in mind and hence they are denoted as “functionalized” or “task-specific” ionic liquids.¹⁰

1.2 Structure-Property Relationship of Ionic Liquids

ILs consist of a cation with single charge or multiple charges. The cation is paired with an anion or multiple anions with a single charge; or an anion with multiple charges. Figure 1-1 gives examples and structures of different types of ionic liquids. The simplest ionic liquids with a single cation and anion are known as monocationic or traditional ionic liquids. Monocationic ILs are the most popular and their

physicochemical properties can be modified by using different cations or anions. The cations can have different substituents which can also have strong influence on the physicochemical properties of ILs.

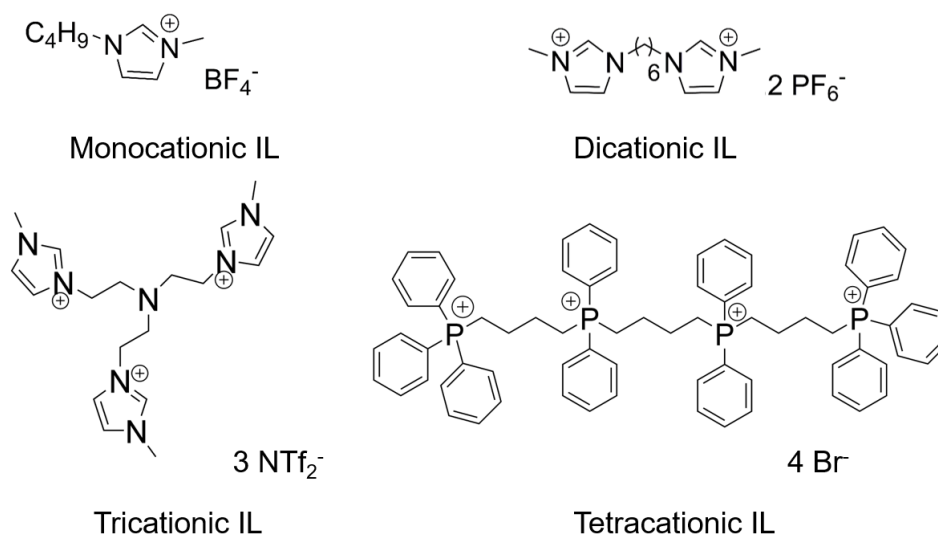


Figure 1-1 Different types of ionic liquids

For example, monocationic ILs with halides as anions can have higher viscosity, but they often show lower thermal stabilities.¹¹ Use of anions such as hexafluorophosphate (PF_6^-) and bis(trifluoromethylsulfonyl)-imide (NTf_2^-) decrease viscosity and provide higher thermal stabilities compared to the halide anions.¹¹ Increasing the length of the alkyl chain on the 1-alkyl-3-methylimidazolium cation increases the viscosity of ILs.¹¹ Dicationic ILs were introduced recently and had some advantages such as high thermal stability and viscosity compared to monocationic ionic liquids.¹¹⁻¹³ A comparison shows that, compared to monocationic ILs, dicationic and polycationic ILs generally have high melting points, and the melting points increase with a number of charges on the cation.^{11, 14-16} The higher melting points or solid nature at room temperature limits applications of most of the multiply charged cationic ILs at room temperature. Hence, more research is focused on the development and applications of monocationic and dicationic ILs.

Compared to monocationic ILs, dicationic ILs provide more opportunities for structural tuning. Dicationic ILs can be considered as a combination of three structural moieties: 1) cationic head groups, 2) a linker or spacer chain and 3) the associated anions. The typical structure of dicationic ILs is shown in Figure 1-2.

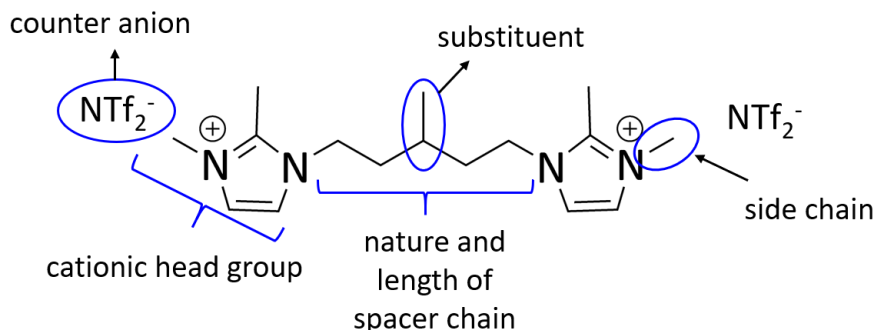


Figure 1-2 General structure of dicationic ionic liquids

The terminal cationic head groups often consist of imidazolium, phosphonium or pyrrolidinium groups. The cationic head groups can have different side chain substituents. Different cationic head groups can be used at two ends of linkage chains, and such ILs are known as “unsymmetrical” ILs.¹² Dicationic ILs with same terminal cationic groups are known as “symmetrical” or “geminal” dicationic ILs.¹¹ The two cationic head groups can be connected by linkage chains of different lengths.¹¹⁻¹² Different linkages such as polyethylene glycol, partially fluorinated chains can be used to connect two cations.¹⁷⁻¹⁸ Instead of straight chain linkage, branched linkage chains can be used as a “tether,” and they can have different substituents.¹⁹ Hence, Different cations can be synthesized by using different combinations of these structural moieties and then these cations can be paired with different anions; bis(trifluoromethane)sulfonimide (NTf₂), perfluorooctanesulfonate (PFOS), triflate (OTf), hexafluorophosphate (PF₆), etc. The structure-property relationship of ILs is studied by systematic variation of structural moieties and examining their physicochemical properties. Understanding the effects of different structural modifications on physicochemical properties is essential if one wants to introduce or enhance the desired property into an IL. The structure-property relationship of ionic liquids will be discussed in detail in the second chapter of this thesis.

1.3 Thermal Stability of Ionic Liquids

One of the important properties of ILs, high thermal stability, makes them useful in a myriad of high temperature applications such as solvents for high temperature reactions,²⁰⁻²¹ gas chromatography (GC) stationary phases,^{13, 22} solvents for headspace GC,²³⁻²⁴ liquid thermal storage media,²⁵ heat transfer

fluids in solar thermal plants,²⁵ high temperature lubricants,²⁶ lubricant additives,²⁷ high temperature non-flammable electrolyte for batteries,²⁸ and high vacuum environments (high-performance lubricating greases for space²⁹ and high vacuum lubricants³⁰).

ILs have a non-boiling character and so, their upper temperature limit is given by their thermal degradation point.³¹ In order to determine the temperatures which allow for a precise and safe application, it is important to study the behavior of ILs at higher temperatures. These studies can provide important information about maximum operating temperatures, the speeds of decomposition, and the nature of IL decomposition products. The information about thermal stability is obtained via various methodologies, and they are discussed in the following sections.

1.3.1 Short term thermal stability

Thermal stability measurements of ILs can be performed by using thermogravimetric analysis (TGA). Ramped temperature analysis at heating rates such as 10 °C/min and 20 °C/min is generally used for such measurements, and this method is also known as a step-tangent method.³¹ Thermal stability is represented by a temperature of T_{onset} , and it is known as short term thermal stability. T_{onset} is a value determined from the translation of the intercept of two linear functions: the baseline of zero weight loss and the tangent of weight vs. temperature upon decomposition.³¹⁻³²

Another method involves ramped temperature analysis with a 10 °C/min temperature ramp and determining temperatures of 5% and 10% mass loss.¹² The temperature of 5% mass loss (T_d) and in some cases of 10% mass loss is considered as the measurements of short term thermal stability.¹² The mass loss can be due to the decomposition and/or evaporation of ILs.³¹ Evaporation of ILs is dependent on the type and flow rate of inert gas flowing over the sample.^{31, 33} Nevertheless, the thermal stability also is affected by the mass of the sample and temperature ramp rate.³⁴ Hence, the temperature profile of ILs is dependent on numerous factors. Also, the actual degradation starts at temperatures lower than T_{onset} or T_d , and hence short thermal stability measurements give an overestimation of thermal stability.

1.3.2 Long-term thermal stability

Ramped temperature TGA analysis pose limitations on the stability measurements, and more profound information can be obtained by long term thermal stability measurements. Long term thermal stability can be evaluated by isothermal (static) TGA measurements³⁴⁻³⁶ or inverse gas chromatography experiments.^{11, 13, 17}

Isothermal TGA experiments are performed by heating ILs at temperatures lower than T_{onset} for prolonged times, and weight loss is monitored as a function of time.³¹ An example isothermal gravimetric analysis of an ionic liquid is shown in Figure 1-3. Isothermal analyses show that in 10 hours over 10% of mass loss can be observed at temperatures lower than T_{onset} . Long term thermal stability determined by measuring weight loss by isothermal TGA experiments, provides detailed information on the stabilities and/or rates of decomposition of ILs.³¹

Inverse GC is another tool to determine long term thermal stability of ILs, especially for their applications as GC stationary phases. In inverse GC, capillary columns coated with ILs are heated in GC oven at temperature ramp as low as 1 °C/min and column bleed is monitored by highly sensitive detectors as a function of temperature.^{11, 13} The temperature at which baseline starts to change or increase is indication of the long term thermal stability of a IL and denoted by T_{IGC} . An example of GC chromatograms for measurement of thermal stability is shown in Figure 1-4.

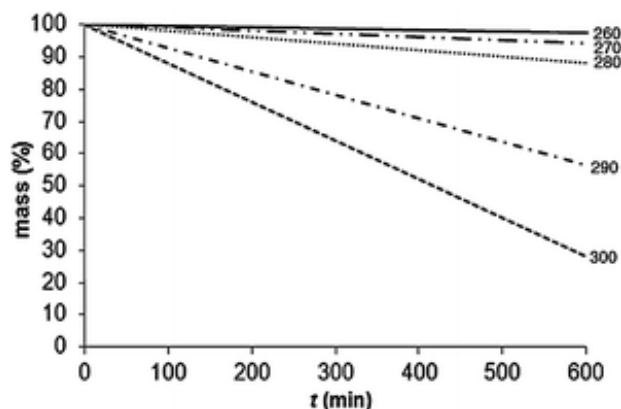


Figure 1-3 Isothermal gravimetric analyses of [C₄mim][Br] IL at different temperatures, nitrogen-atmosphere.³¹

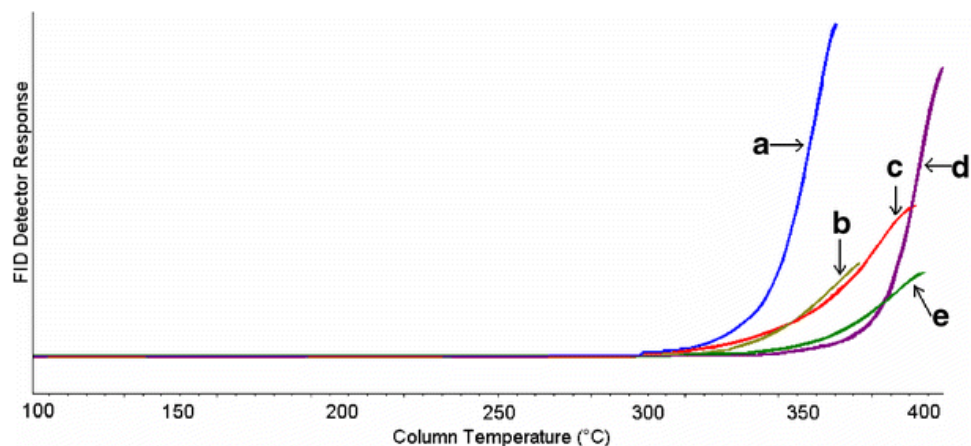


Figure 1-4 Thermal Stability of five different ILs measured with Inverse GC-FID.¹⁷

Different methodologies are designed and used for determining thermal stabilities of ILs. These methods are useful to compare thermal stabilities of different ILs, study their rates of decomposition, etc. However, the answers to the questions “how do they degrade, what are the degradation products, and is intact volatilization possible at high temperatures?” remain unanswered. A study focusing on understanding the thermal breakdown products of ILs at high temperatures, and their decomposition pathways is discussed in Chapter 4 of this thesis.

1.4 Applications of Ionic Liquids as Gas Chromatography Stationary Phases

The unique properties of ILs, i.e., high viscosity, high thermal stability, and good wetting abilities make them attractive material to be used as stationary phases for gas chromatography.^{13, 17, 22, 37-39} On addition, ILs show multiple solvation interactions while traditional stationary phases often show one dominant type of interaction.⁴⁰ ILs show an unusual dual nature behavior, separating both polar and nonpolar compounds.^{37, 41} They perform like nonpolar stationary phases while separating nonpolar compounds and at the same time retain polar analytes showing polar behavior. These properties provide them unique selectivities towards separation of various compounds.

Molten salts which were stearate salts of bivalent metals were used as GC stationary phases for the first time by Barber et al. in 1959.⁴² Later ILs such as ethylammonium nitrate, ethylpyridinium bromide, and tetraalkyl phosphonium salts were used as GC stationary phases.⁴³⁻⁴⁵ However, these ILs showed narrow liquid ranges, low column efficiencies, and poor thermal stabilities. Hence, they were not adapted

as stationary phases for GC. Around 2000, monocationic ILs with imidazolium based cation were developed and evaluated as GC stationary phases.^{22, 37} These stationary phases showed improved performance compared to the previously reported molten salt stationary phases. These ILs were studied in detail, and some fundamental understanding was developed during these studies.⁴⁰ Recently, a new class of highly stable dicationic and tricationic IL stationary phases was developed.^{13, 17, 39} These stationary phases showed very high thermal stabilities and more opportunities for structural modification. The improved performance of these stationary phases compared to other ILs and traditional GC stationary phases led to their commercialization.^{13, 17, 39}

As discussed previously, dicationic ILs provide opportunities for the modification of their physicochemical properties. Similarly, selectivities of dicationic ILs can be modified by their structural modification. However, a fundamental understanding about the effect of structural modification on the selectivities of IL stationary phases is needed. The information can be useful for developing an IL for specific separations. Chapter 3 and 5 will focus on modifying selectivities of dicationic IL stationary phases.

1.5 Ionic Liquids in Synthesis

ILs have emerged as a new class of solvents in synthesis because of their advantages over traditional solvents due to high thermal stability, low volatility, and non-flammability.^{6, 20-21} ILs can solubilize different organic and inorganic compounds, so different reagents and compounds can be brought into a homogeneous solution.⁶ ILs are immiscible with several organic solvents and can form a two phase system with other, which is useful for the extraction of products from ILs.⁶ They can play the dual role of a solvent and a catalyst in a number of organic reactions.⁶ Compared to ammonium based ILs, phosphonium based ILs are more stable, and this gives them advantages in high temperature reactions.³¹ Also, tetralkylphosphonium ILs lack the acidic proton compared to the imidazolium ILs and hence can be considered as comparatively inert towards solutes.⁴⁶ The numerous advantages of phosphonium ILs can be useful in synthetic applications and will be discussed in Chapter 6 of this thesis.

1.6 Organization of Dissertation

Chapter 2 focuses on designing thermally stable ionic liquids and understanding their structure-property relationships. This study presents synthesis of a series of monocationic and dicationic ILs and characterization of their physicochemical properties such as density, viscosity, melting points, and thermal stability. Effect of modification of each dicationic structural moiety on the physicochemical properties of dicationic ILs is discussed.

Chapter 3 discusses the applications of newly developed thermally stable dicationic ionic liquid GC stationary phases in the separation of different classes of compounds. A comparison of the separation patterns of these different compounds on nine different IL columns is discussed. The study elaborates on the effects of structural modifications on the selectivities and polarities of dicationic IL GC stationary phases.

Chapter 4 examines the thermal breakdown products of dicationic ILs at high temperatures. The observations of thermal decomposition study performed on a variety of dicationic ILs with diverse cations connected by straight alkane, branched alkane or polyethylene glycol linkages are presented. The decomposition study provides the information about the structural moieties, i.e. bonds, atoms or linkages of ILs most susceptible to thermally induced changes.

Chapter 5 discusses the development of thermally stable phosphonium based dicationic IL GC stationary phases using different combinations of aromatic and alkyl substituents on phosphonium cation. The advantages of high thermal stability of phosphonium dicationic ILs in the separation of structural isomers high molecular weight environmental pollutants such as polynuclear aromatic hydrocarbons (PAHs), phthalates and polychlorinated biphenyls (PCBs) are presented. The novel selectivities of new phosphonium ILs compared to polysiloxane based GC stationary phases is discussed.

Chapter 6 extends the application of thermally stable phosphonium IL as a solvent in rapid deprotection of *tert*-butoxycarbonyl (Boc) amino acids and peptides.

Chapter 2

SYNTHESIS OF THERMALLY STABLE GEMINAL DICATIONIC IONIC LIQUIDS AND RELATED IONIC COMPOUNDS: AN EXAMINATION OF PHYSICOCHEMICAL PROPERTIES BY STRUCTURAL MODIFICATION

2.1 Abstract

Geminal dicationic ionic liquids (ILs) often display higher thermal stabilities, viscosities, and densities compared to traditional monocationic ILs. Also, dicationic ILs have advantages in terms of tuning of their physicochemical properties by different structural modifications. They can be considered as a combination of three structural moieties: 1) cationic head groups, 2) an alkane linker chain and 3) the associated anions. Two types of each imidazolium, pyrrolidinium and phosphonium cations were joined by different alkane linkages (C6, C9, and C12) to develop eighteen different dications. These dications were paired with two different anions (NTf_2^- and PFOS^-) to synthesize thirty-six different dicationic ILs. The effect of variations in the structural moieties of these related ILs on their physicochemical properties; including melting points, densities, viscosities, solubilities, and thermal stabilities; were evaluated. ILs synthesized in this study displayed TGA thermal stabilities in the range of 330 to 467 °C. Also, nine ILs with high TGA stability and low melting points were tested with inverse gas chromatography and some of them displayed stabilities up to 400 °C.

2.2 Introduction

Ionic liquids (ILs) are salts with melting point generally less than 100 °C.^{6, 47-48} The unique physical and chemical properties of ILs makes them a versatile class of materials for numerous applications.^{6, 13, 22, 47, 49-63} Most of their properties can be tuned to meet the needs of specific applications by employing different combinations of cations and anions or by suitable structural modification of those entities.¹² Some of the properties that makes them suitable for high temperature applications (like; gas chromatography stationary phases^{13, 22}, solvents for high temperature reactions^{20-21, 64-65}, high temperature lubricants²⁶, liquid thermal storage media²⁵ and heat transfer fluids in solar thermal plants²⁵) includes high thermal stability, high density, wide liquid temperature range, tunable viscosity, high chemical stability, non-volatility, and non-flammability. Very few studies have examined the structural effects of dicationic

ILs on their physicochemical properties. In order to design ILs for specific applications, one must understand their structure property relationship. Within ionic liquids, monocationic ILs often display lower thermal stabilities and viscosities compared to geminal dicationic and some polycationic ILs.¹¹⁻¹⁴ Even at high temperatures dicationic ILs show higher viscosities and this property makes them attractive as lubricants and stationary phases. The higher molecular weights, charge and greater intermolecular interactions of dicationic ILs can provide even lower volatility and also alters their stability.^{11, 17, 31} Geminal dicationic ILs were often found to have higher melting points than monocationic ILs with the same anion and sometimes are solids at room temperature.^{11, 13} Recently, many different dicationic ILs were synthesized and the effect of anion type, symmetry of the dications, substituents and the nature of the linkage chain on thermal stability and melting point were studied.¹¹⁻¹² These studies indicated some advantages of dicationic ILs over monocationic ILs with respect to tailoring of physicochemical properties. In addition, structurally they provide a modular approach to fine tune desired properties.

Anderson et al. showed that some imidazolium and pyrrolidinium based dicationic ILs have good thermal stabilities.¹¹ The high thermal stability of phosphonium dicationic ILs was demonstrated by Breitbach et al.¹³ In the case of imidazolium ILs, substitution of the acidic C(2) hydrogen with a methyl group leads to an increase in thermal stability.⁶⁶ In addition it is known that the nature and length of the linkage chain or “tether” coupling two cationic moieties; affects stability, melting point and the viscosity of dicationic ILs.¹¹

According to the limited literature on this subject, ILs with short alkane linkage chains (C₃) tend to have higher melting points and ILs with longer alkane linkage up to C₉-C₁₆, tend to have comparatively lower melting points.¹¹⁻¹³ Viscosity tends to increase with chain length as expected. The thermal stability and density can be highly variable though.

In order to investigate the role of anions on the physicochemical properties of ILs, especially thermal stabilities and viscosities, eight different anions were paired with a tributyltetradecylphosphonium cation. Based on the higher thermal stability of bis(trifluoromethane)sulfonimide (NTf₂⁻) and perfluorooctanesulfonate (PFOS⁻) anions, they were paired with imidazolium, pyrrolidinium and phosphonium based dications. This resulted in the synthesis of thirty-six different ILs. The effect of each

structural modification, i.e. variations in the alkane linker, nature of dication and nature of the counter anion on the physical properties were evaluated.

By varying these structural features, we were able to synthesize ILs with high thermal stability. There have been extensive reports of ILs with NTf_2^- anions. However, IL literature involving the PFOS^- counter anion is limited. The use of PFOS^- anion for the synthesis of thermally stable ionic liquids is demonstrated in this study. The current study presents and discusses the synthesis and structure–property relationships of geminal dicationic ionic liquids.

2.3 Experimental Section

2.3.1 Materials:

1-benzyl-2-methylimidazole (90%), 1,2-dimethylimidazole (98%), N-methylpyrrolidine (97%), 1-butylpyrrolidine (98%), tripropylphosphine (97%), triphenylphosphine (99%), 1,6-dibromohexane (96%), 1,9-dibromononane (97%), 1,12-dibromododecane (98%), bis(trifluoromethane)sulfonimide lithium salt (99.95%), heptadecafluorooctanesulfonic acid potassium salt (98%), bis(pentafluoromethane)sulfonimide lithium salt (98%), Iron(III) chloride (97%), bis(2-ethylhexyl) sulfosuccinate sodium salt (96%), 1-octanesulfonic acid sodium salt (98%), potassium dodecafluoro-closo-dodecaborate (97%) and N,N-dimethylformamide(99.8%) were purchased from sigma-Aldrich (St. Louis, MO, USA). 1-hexyl-3-methylimidazolium tris(pentafluoroethyl)trifluorophosphate was obtained from Millipore Corp. (Bedford, MA, USA). It was converted to tris(pentafluoroethyl)trifluorophosphate hydride through ion-exchange resin prior to use. Tributyltetradecylphosphonium chloride was purchased from Cytec (Woodland Park, NJ, USA). Acetonitrile, methanol, dichloromethane and heptane were purchased from Fisher Scientific (Fair Lawn, NJ, USA). Salt treated fused silica capillary tubing (0.25 mm i.d.) and C9-(m2im)2-NTf2 IL coated column (30 m x 0.25 mm i.d.) were provided by Supelco (Bellefonte, PA, USA). Deionized water was from Synergy 185 water purification system (Millipore, Billerica, Massachusetts, USA).

2.3.2 Methods of Analysis:

The monocationic ionic liquids and dicationic ionic liquids were characterized by electrospray ionization mass spectrometry (ESI-MS) for molecular weight. ESI-MS spectra were acquired by using a Finnigan LXQ (Thermo Fisher Scientific, San Jose, CA). ^1H NMR, ^{13}C NMR and ^{31}P NMR experiments

were performed on 500 MHz JEOL Eclipse Plus 500 instrument for spectral analysis. Thermogravimetric analysis were performed using Shimadzu TGA-51 Thermogravimetric Analyzer (Kyoto, Kyoto Prefecture, Japan) for the stability testing. Samples (~10 mg) were placed in the platinum pans, and heated at 10 °C min⁻¹ from room temperature to 600 °C in a nitrogen atmosphere (flow – 30mL min⁻¹). The decomposition temperature were determined at 1%, 5% and 15% weight loss. 5% weight loss of the sample which corresponds to 95% w value was considered as measure of thermal stability. The GC thermal stability measurements were made using Agilent 6890N Gas Chromatograph equipped with flame ionization detector (FID). The studies were performed ramping the column oven temperature from 100 to 450 °C at 1 °C min⁻¹ and using helium as carrier gas at flow rate of 1 mL min⁻¹. The injector and FID temperatures were set at 250 °C and 400 °C respectively. The DSC measurements were carried out on a Shimadzu DSC-60 (Kyoto, Kyoto Prefecture, Japan) differential scanning calorimeter (DSC). The samples (~ 10 mg) were sealed in aluminum pans, and then heated at rate of 10 °C min⁻¹ up to 500 °C. Melting points were determined using a *Mel-Temp* apparatus (Laboratory Devices, Cambridge, MA). Density was measured using 10 mL Kimble specific gravity pycnometer at 22 °C. Heptane was used as an immiscible solvent for these measurements. Kinematic viscosity was determined using a Cannon-Manning semi-micro viscometer at 30 °C and 50 °C. All compounds synthesized in this study were tested for solubility with polar (water) and non-polar (heptane) solvent. This study was performed by placing a small amount (60-100 mg) of the compound in the solvent (15 mL) and through observation of whether the solute was miscible or immiscible in the solvent.

2.3.3 Synthesis of monocationic ILs:

Compounds **IL1**, **IL2**, **IL3**, **IL4**, **IL5**, **IL6**, **IL7**, and **IL8** were made through metathesis reactions of 1 molar equivalents of tributyltetradecylphosphonium chloride salt with 1 molar equivalents of bis(trifluoromethane)sulfonimide lithium (LiNTf₂), bis(pentafluoromethane)sulfonimide lithium (LiNPF₂), heptadecafluorooctanesulfonic acid potassium salt (KPFOS), Iron (III) chloride(FeCl₃), tris(pentafluoroethyl)trifluorophosphate hydride (FAP), bis(2-ethylhexyl) sulfosuccinate sodium (NaAOT), 1-octanesulfonic acid sodium salt (NaOS), and potassium dodecafluoro-closo-dodecaborate (KB₁₂F₁₂), respectively. The reactions for all ILs were performed in water at room-temperature for 12 h with the exception of heptadecafluorooctanesulfonic acid potassium salt (KPFOS), which was performed at

elevated temperature (110 °C) with oil-bath. Dichloromethane was added to the resulting solution to dissolve the target product. The aqueous layer was then removed and the organic layer washed three times with water to remove any starting material. Dichloromethane was then removed by rotary evaporation followed by vacuum drying over phosphorous pentoxide at 40 °C for 24 h. The procedure resulted in the pure monocationic ionic liquid.

2.3.4 Synthesis of dicationic ionic liquids:

Synthesis of dicationic ionic liquids involved two steps. First step involved a nucleophilic substitution reaction of imidazoles / pyrrolidones / phosphines with corresponding terminal dibromoalkanes to obtain bromide salt of dication. Second step was metathesis dibromodicationic salt with LiNTf₂ and KPFOS. In metathesis step bromide ions were exchanged by NTf₂⁻ or PFOS⁻ anions to obtain final product ILs and LiBr and KBr as side products.

2.3.4.1 Synthesis of imidazolium based Ionic Liquids

Procedure 1:

Step 1) IL9, IL21 and IL 33 were made by refluxing 2 molar equivalents of 1-butyl-2-methylimidazole with 1 molar equivalent of 1, 6-dibromohexane, 1, 9-dibromononane and 1, 12-dibromododecane respectively in acetonitrile at 80 °C for 72 h.(Scheme 1) Rotary evaporation of solvent yielded the crude dibromodicationic salt. The salt was then dissolved in water and transferred to a separatory funnel and washed with dichloromethane (3x50 ml) to remove excess starting material. The aqueous layer containing dibromodications was then dried by rotary evaporation of water. Further, vacuum drying over phosphorous pentoxide at 40 °C for 24h resulted in the pure dibromodicationic salts. The products were then verified by mass spectrometry analysis.

Step 2) For the synthesis of final products, the dibromodications synthesized in the first step were dissolved in water and reacted with 2 molar equivalents of (LiNTf₂)(Scheme 2). The solution was stirred for 24 h at room temperature. The metathesis process resulted in exchange of bromide anions with NTf₂⁻ anions. Following that, dichloromethane (40 mL) was added to the solution to extract NTf₂⁻ salt of the ionic liquid that has phase separated from the water. The lithium bromide and excess NTf₂⁻ were removed from the dichloromethane phase with successive extraction with water (3x40mL). Removal of

dichloromethane through rotary evaporation followed by vacuum drying over P_2O_5 at 40 °C for 24 h resulted in the pure dicationic 1-butyl-2-methylimidazolium ILs with NTf_2^- counter anion.

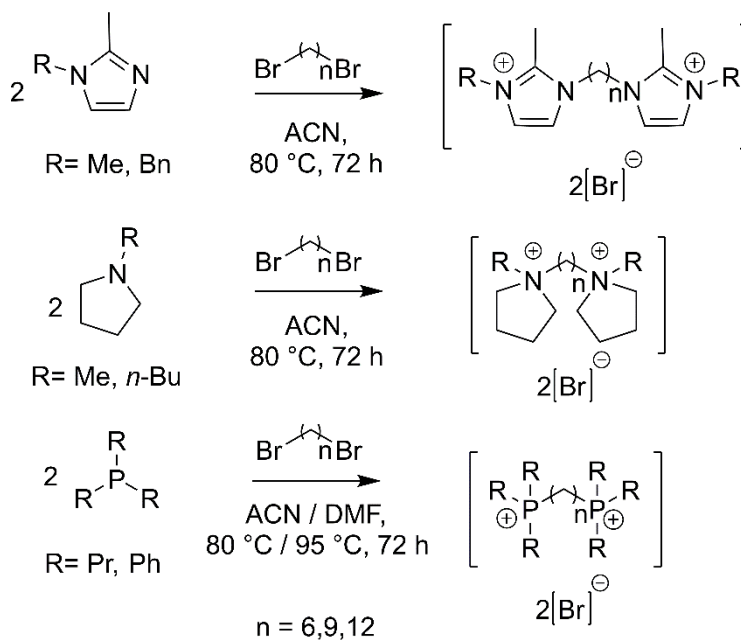
Procedure 2:

For the synthesis of **IL15**, **IL27** and **IL 39** with $PFOS^-$ anion; dibromodications and heptadecafluorooctanesulfonic acid potassium salt (KPFOS) were dissolved in a mixture of methanol and water (1:1) and stirred for 12 h.(Scheme 2) The solvents were evaporated using rotary evaporation method and similar protocol as mentioned in Step 2 of procedure 1 was followed for the rest of the reaction workup.

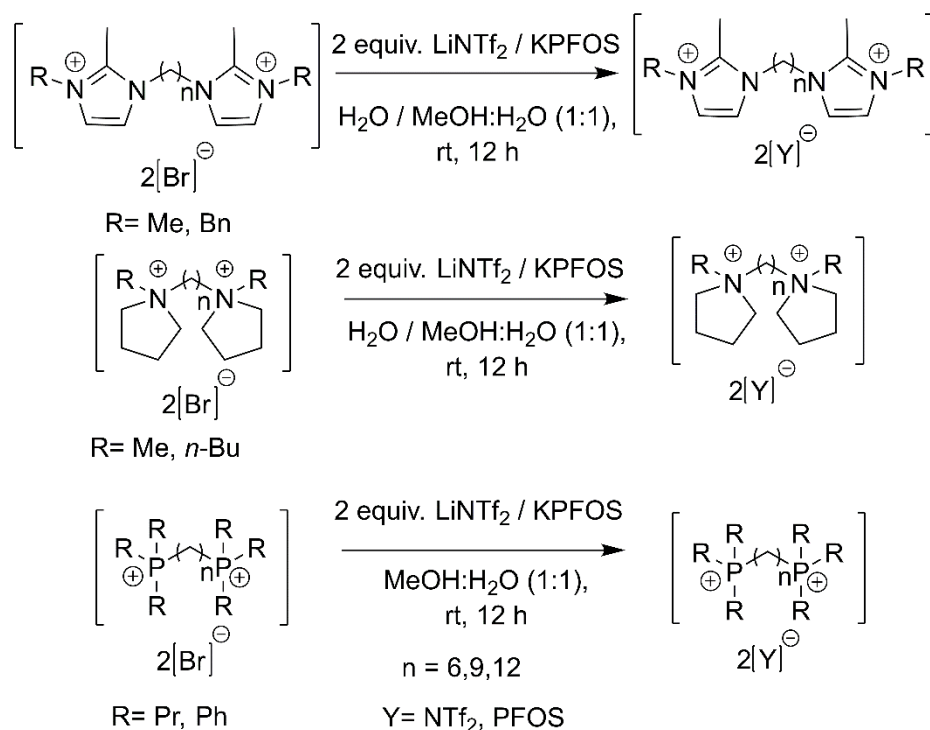
Procedure 3:

For the synthesis of **IL10**, **IL22**, **IL34**, **IL15**, **IL28** and **IL40** similar protocol as procedure 1 and 2 was followed except 2 moles of 1, 2-dimethylimidazole used instead of 1-butyl-2-methylimidazole.

Scheme 2-1 Synthesis of bromide salt of dication



Scheme 2-2 Metathesis of bromide salts to synthesize dicationic ILs



2.3.4.1 Synthesis of pyrrolidinium based Ionic Liquids:

Procedure 4:

For the synthesis of **IL11**, **IL23**, **IL35**, **IL17**, **IL29** and **IL41** similar protocol as procedure 1 and 2 was followed except 2 moles of 1-butylpyrrolidine was used instead of 1-butyl-2-methylimidazole.

Procedure 5:

For the synthesis of **IL12**, **IL24**, **IL36**, **IL18**, **IL30** and **IL42** similar protocol as procedure 1 and 2 was followed except 2 moles of N-methylpyrrolidine was used instead of 1-butyl-2-methylimidazole.

2.3.4.2 Synthesis of phosphonium based ionic liquids:

Procedure 6:

Step 1) **IL13**, **IL25**, **IL37**, **IL19**, **IL31** and **IL43** were made by refluxing 2 molar equivalents of tripropylphosphine with 1 molar equivalent of 1,6-dibromohexane, 1,9-dibromononane and 1,12-dibromododecane respectively in acetonitrile at 80 °C for 72 h. (Scheme 1) The reaction was performed under inert argon condition to prevent oxidation of tripropylphosphine. Rotary evaporation of solvent yielded the crude dibromodicationic salt. Similar protocol as mentioned in Procedure 1 and 2 was followed for the rest of the reaction workup.

Procedure 7:

Step 1) Compounds **IL14**, **IL26** and **IL38** were synthesized by refluxing 2 molar equivalents of triphenylphosphine with 1 molar equivalent of 1,6-dibromohexane, 1,9-dibromononane and 1,12-dibromododecane respectively in N,N-Dimethylformamide at 95 °C for 72 h.(Scheme 1) Rotary evaporation of solvent yielded the crude dibromodicationic salt. The salt was then washed with five aliquots of ethyl acetate (3x50 mL) to remove unreacted starting material. The rotary evaporation of solvent and further vacuum drying over phosphorous pentoxide resulted in the pure dibromodicationic salts. Obtained products then verified by mass spectrometry analysis.

Step 2) For the synthesis of final products, the dibromodications synthesized in the first step were dissolved in methanol and water (1:1) and reacted with 2 molar equivalents of (LiNTf₂). The solution was stirred for 24 h at room temperature.(Scheme 2) This metathesis process resulted in final IL with bromide anions exchanged with NTf₂⁻ anions. The solvents were evaporated using rotary evaporation method. The crude NTf₂⁻ salt was dissolved in dichloromethane. The lithium bromide and excess NTf₂⁻ were removed from the dichloromethane phase with successive extractions with water (3x40 mL). Removal of dichloromethane through rotary evaporation followed by vacuum drying over P₂O₅ at 40 °C for 24 h resulted in the pure dicationic triphenylphosphonium ILs with NTf₂⁻ counter anion.

Procedure 8:

To synthesize compounds **IL20**, **IL32** and **IL44**; dibromodications and heptadecafluorooctanesulfonic acid potassium salt (KPFOS) were dissolved in a mixture of methanol and water (1:1) and stirred for 24 h. The solvents were evaporated using rotary evaporation method and similar protocol as mentioned in Step 2 of Procedure 7 was followed for the rest of the reaction workup.

2.3.5 Preparation of IL columns:

All IL columns were prepared by using static coating method at 40-60 °C using a 0.20% (w/v) coating solution of IL in dichloromethane or methanol. Methanol was used as a coating solvent for PFOS anionic IL to improve the solubility of these IL. ILs were coated on inner walls of salt treated fused silica capillary with dimensions 3 m x 0.25 mm i.d. After coating process columns were conditioned at 250 °C for 12 h. The efficiency of column was tested using naphthalene at 100 °C. The columns showed efficiency ranging from 2000 to 2500 plates m⁻¹.

2.4 Results and Discussion

Eight different anions were screened using thermogravimetric analysis (TGA) after pairing them with the same cation of known high thermal stability. The cation used was tributyltetradecylphosphonium (TBTD-P). This cation was selected because phosphonium ILs have high thermal stabilities while the anions evaluated were bis[(trifluoromethyl)sulfonyl] imide (NTf_2^-), bis[(pentafluoroethyl)sulfonyl] imide (NPf_2^-), perfluorooctanesulfonate (PFOS^-), iron tetrachloride (FeCl_4^-), tris(pentafluoroethyl)trifluorophosphate (FAP^-), dioctyl sulfosuccinate (docusate $^-$), 1-octanesulfonate (1-oct-sulf $^-$) and dodecafluoro-closo-dodecaborate ($\text{B}_{12}\text{F}_{12}^-$). The structures of these monocationic ILs are shown in Figure 2-1. The physicochemical data obtained from the analysis of these monocationic ILs is compiled in Table 2-1. All monocationic ILs were liquids at room temperature. **IL1, IL2, IL3** and **IL4** appeared to be stable under the TGA experimental conditions to temperatures ≥ 400 °C (see Experimental Section). Thermal stabilities (via TGA) of **IL5, IL6, IL7** and **IL8** were lower than 350 °C. Based on this study, the NTf_2^- , NPf_2^- and PFOS^- anions provided the best thermal stability (Table 2-1). The structural similarity of NPf_2^- and NTf_2^- anions led us to select NTf_2^- for our study due to its lower cost. NTf_2^- and PFOS^- were chosen as counter anions for the synthesis of “high stability ILs”.

Monocationic ILs with PFOS^- (IL3), FeCl_4 (IL4) and AOT (IL6) anions displayed higher viscosities compared to other monocationic ILs. The observed densities for monocationic ILs were in the range of 0.89 to 1.23 g/cm³ and highest densities were observed for ILs with FAP (IL5) and PFOS^- (IL3) anions. All the synthesized monocationic ILs were insoluble in water but the ILs with NTf_2^- , NPf_2^- , PFOS^- , AOT $^-$ and OS $^-$ anions were soluble in heptane.

Three general classes of dications were chosen for examination: (1) imidazolium (2) pyrrolidinium and (3) phosphonium. These dications were chosen based on previous research which indicated that they had good thermal stabilities.^{11, 13} The presence of methyl or benzyl substituents at the C(3) position of the imidazolium ring was shown to enhance stability and/or decrease volatility.¹¹⁻¹² Replacement of the acidic C(2) hydrogen with a methyl group appeared to confer additional stability to imidazolium ILs due to inhibition of reaction leading to the formation of carbenes.⁶⁶ So, the dications

Table 2-1 Physicochemical Properties of monocationic ILs

	ionic liquid	MW (g/mol)	Physical state at rt ^e	thermal stability ^a (°C)			density ^b (g/cm ³)	viscosity ^c (cSt)		miscibility with heptane ^d	miscibility with water ^d
				99%w	95%w	85%w		30°C	50°C		
IL1	TBTD-P-NTf ₂	679.8	liquid	330	405	454	1.10	202	73	M	I
IL2	TBTD-P-NPf ₂	779.9	liquid	379	418	440	1.13	311	91	M	I
IL3	TBTD-P-PFOS	898.8	liquid	380	426	455	1.22	1672	350	M	I
IL4	TBTD-P-FeCl ₄	597.4	liquid	311	401	450	0.98	1364	397	I	I
IL5	TBTD-P-FAP	844.7	liquid	241	303	336	1.23	327	130	I	I
IL6	TBTD-P-AOT	821.3	liquid	288	330	355	0.94	1393	387	M	I
IL7	TBTD-P-OS	593.0	liquid	93	194	369	0.89	125	53	M	I
IL8	TBTD-P-B ₁₂ F ₁₂	757.4	liquid	194	298	432	0.90	-	-	I	I

^a Thermogravimetric analysis (TGA) conditions: temperature program= 10 °C/min from room temperature (22 °C) to 600 °C, atmosphere= nitrogen, 99% w= temperature of 1% mass decrease of sample, 95% w= temperature of 5% mass decrease of sample, 85% w= temperature of 15% mass decrease of sample.

^b Measured using pycnometer.

^c Measured using capillary viscometer.

^d I= immiscible, M= miscible.

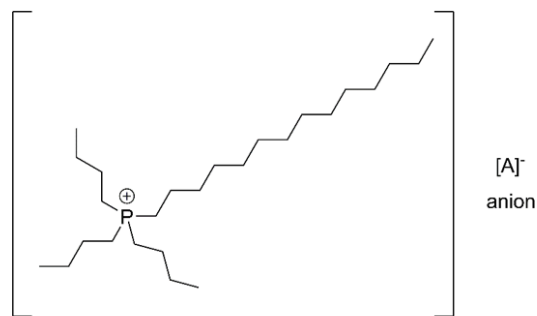
^e physical state at room temperature.

chosen had methyl groups at the C(2) position and the C(3) position had either a benzyl or methyl substituent (see Figure 2-2). High stability dicationic ILs with N-substituted methyl and butyl groups on the pyrrolidinium ring were synthesized previously and shown to have good thermal stability and/or low volatility.¹¹ The same dications were selected for this study. However, the effect of short and long alkyl chains on pyrrolidinium stability was studied. Likewise, tripropyl and triphenyl substituted phosphonium dicationic salts were evaluated. The two cationic moieties were linked with six carbon (C₆), nine carbon (C₉) and twelve carbon (C₁₂) alkane chains (see Experimental Section). Thus, eighteen different symmetrical dications were evaluated. These dications were paired with the selected NTf₂⁻ and PFOS⁻ anions. The dication and anion combinations resulted in thirty-six different dicationic ionic liquids. The structure of these ionic liquids are shown in Figure 2-2. The physicochemical data of all these ionic liquids is combined in Table 2-2 (C₆), Table 2-3 (C₉) and Table 2-4 (C₁₂).

2.4.1 Melting Point:

The melting point of an ionic liquid depends on the crystal lattice energy between the cation and anion.⁶⁷ The crystal lattice energy depends on interionic forces, molecular symmetry and conformational degrees of freedom of the molecule.⁶⁸ ILs with PFOS⁻ anions have higher melting point than ILs with NTf₂⁻ anions. The NTf₂⁻ anion has more charge delocalization than PFOS⁻ anion. More charge delocalization generally leads to a decrease in melting point.⁶⁹ Also, the PFOS⁻ anion has a higher molar mass than NTf₂⁻ which can also raise the melting point. The only exception to this trend were the ph₃p⁺- dicationic ILs in which the NTf₂⁻ ILs have higher melting point than PFOS⁻ ILs.

In general the melting points of dicationic ILs with NTf₂⁻ anions are dependent on the length of the alkyl linkage chain. ILs with C₆ linkage chains have higher melting points than analogous ILs with C₉ and C₁₂ linkage chains. Also, C₉ ILs with NTf₂⁻ anions have



tributyltetradecyl phosphonium (TBTD-P) cation

cation	anion (A)	ionic liquid abbreviation	ionic liquid
tributyltetradecyl phosphonium (TBTD-P)	bis(trifluoromethane)sulfonimide (NTf ₂)	TBTD-P-NTf ₂	IL1
	bis(pentafluoromethane)sulfonimide (NPF ₂)	TBTD-P-NPF ₂	IL2
	perfluorooctanesulfonate (PFOS)	TBTD-P-PFOS	IL3
	iron tetrachloride (FeCl ₄)	TBTD-P-FeCl ₄	IL4
	tris(pentafluoroethyl)trifluorophosphate (FAP)	TBTD-P-FAP	IL5
	bis(2-ethylhexyl) sulfosuccinate (AOT)	TBTD-P-AOT	IL6
	1-octanesulfonate (OS)	TBTD-P-OS	IL7
	dodecafluoro-closo-dodecaborate (B ₁₂ F ₁₂)	TBTD-P-B ₁₂ F ₁₂	IL8

structures of anions:

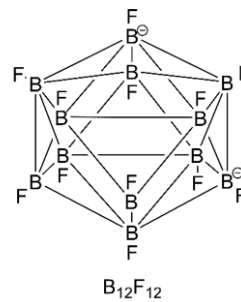
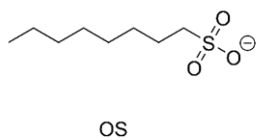
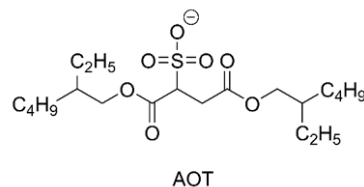
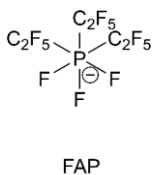
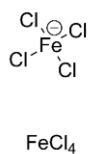
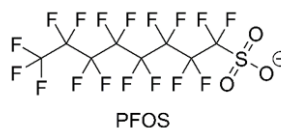
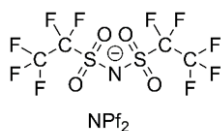
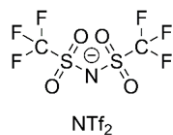
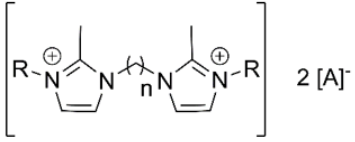


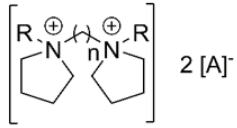
Figure 2-1 Structure and abbreviations of monocationic ILs synthesized in this study. (Eight different ILs synthesized by pairing eight different anions with the same cation.)

Base structure



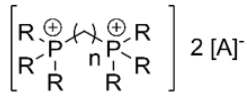
Imidazolium

substituent (R)	anion (A)	linker chain length (n)	ionic liquid abbreviation	ionic liquid
benzyl	NTf ₂	6	C ₆ (bmim) ₂ -NTf ₂	IL9
		9	C ₉ (bmim) ₂ -NTf ₂	IL21
		12	C ₁₂ (bmim) ₂ -NTf ₂	IL33
	PFOS	6	C ₆ (bmim) ₂ -PFOS	IL15
		9	C ₉ (bmim) ₂ -PFOS	IL27
		12	C ₁₂ (bmim) ₂ -PFOS	IL39
methyl	NTf ₂	6	C ₆ (m ₂ im) ₂ -NTf ₂	IL10
		9	C ₉ (m ₂ im) ₂ -NTf ₂	IL22
		12	C ₁₂ (m ₂ im) ₂ -NTf ₂	IL34
	PFOS	6	C ₆ (m ₂ im) ₂ -PFOS	IL16
		9	C ₉ (m ₂ im) ₂ -PFOS	IL28
		12	C ₁₂ (m ₂ im) ₂ -PFOS	IL40



Pyrrolidinium

substituent (R)	anion (A)	linker chain length (n)	ionic liquid abbreviation	ionic liquid
n-butyl	NTf ₂	6	C ₆ (bpy) ₂ -NTf ₂	IL11
		9	C ₉ (bpy) ₂ -NTf ₂	IL23
		12	C ₁₂ (bpy) ₂ -NTf ₂	IL35
	PFOS	6	C ₆ (bpy) ₂ -PFOS	IL17
		9	C ₉ (bpy) ₂ -PFOS	IL29
		12	C ₁₂ (bpy) ₂ -PFOS	IL41
methyl	NTf ₂	6	C ₆ (mpy) ₂ -NTf ₂	IL12
		9	C ₉ (mpy) ₂ -NTf ₂	IL24
		12	C ₁₂ (mpy) ₂ -NTf ₂	IL36
	PFOS	6	C ₆ (mpy) ₂ -PFOS	IL18
		9	C ₉ (mpy) ₂ -PFOS	IL30
		12	C ₁₂ (mpy) ₂ -PFOS	IL42



Phosphonium

substituent (R)	anion (A)	linker chain length (n)	ionic liquid abbreviation	ionic liquid
propyl	NTf ₂	6	C ₆ (pr ₃ p) ₂ -NTf ₂	IL13
		9	C ₉ (pr ₃ p) ₂ -NTf ₂	IL25
		12	C ₁₂ (pr ₃ p) ₂ -NTf ₂	IL37
	PFOS	6	C ₆ (pr ₃ p) ₂ -PFOS	IL19
		9	C ₉ (pr ₃ p) ₂ -PFOS	IL31
		12	C ₁₂ (pr ₃ p) ₂ -PFOS	IL43
phenyl	NTf ₂	6	C ₆ (ph ₃ p) ₂ -NTf ₂	IL14
		9	C ₉ (ph ₃ p) ₂ -NTf ₂	IL26
		12	C ₁₂ (ph ₃ p) ₂ -NTf ₂	IL38
	PFOS	6	C ₆ (ph ₃ p) ₂ -PFOS	IL20
		9	C ₉ (ph ₃ p) ₂ -PFOS	IL32
		12	C ₁₂ (ph ₃ p) ₂ -PFOS	IL44

Figure 2-2 Structure and abbreviations of dicationic ILs synthesized in this study

Table 2-2 Physicochemical Properties of C₆ alkane linkage chain ILs

ionic liquid	MW (g/mol)	melting point (°C)	thermal stability ^a (°C)			viscosity ^b (cSt)	miscibility with heptane ^c	miscibility with water ^c	
			99%w	95%w	85%w	80°C			
IL9	C ₆ (bmim) ₂ -NTf ₂	989.0	85-86	263	412	434	-		
IL10	C ₆ (m ₂ im) ₂ -NTf ₂	836.8	82-84	377	437	454	-		
IL11	C ₆ (bpy) ₂ -NTf ₂	899.0	99-101	351	403	421	-		
IL12	C ₆ (mpy) ₂ -NTf ₂	814.8	64-66	404	433	454	100		
IL13	C ₆ (pr ₃ p) ₂ -NTf ₂	965.0	95-96	396	408	422	-		
IL14	C ₆ (ph ₃ p) ₂ -NTf ₂	1169.1	146-148	367	405	443	-		
IL15	C ₆ (bmim) ₂ -PFOS	1444.9	100-102	376	405	429	-		
IL16	C ₆ (m ₂ im) ₂ -PFOS	1274.7	101-103	387	425	453	-		
IL17	C ₆ (bpy) ₂ -PFOS	1336.9	155-157	369	391	407	-		
IL18	C ₆ (mpy) ₂ -PFOS	1252.8	138-140	347	382	397	-		
IL19	C ₆ (pr ₃ p) ₂ -PFOS	1403.0	121-123	368	401	417	-		
IL20	C ₆ (ph ₃ p) ₂ -PFOS	1605.0	62-64	311	395	424	-		

^a Thermogravimetric analysis (TGA) conditions: temperature program= 10 °C/min from room temperature (22 °C) to 600 °C, 99% w= temperature of 1% mass decrease of sample, 95% w= temperature of 5% mass decrease of sample, 85% w= temperature of 15% mass decrease of sample.

^b Measured using capillary viscometer.

^c I= immiscible, M= miscible.

Table 2-3 Physicochemical Properties of C₉ alkane linkage chain ILs

	ionic liquid	MW (g/mol)	melting point (°C)	thermal stability ^a (°C)			density ^b (g/cm ³)	viscosity ^c (cSt)		miscibility with heptane ^d	miscibility with water ^d
				99%w	95%w	85%w		30°C	50°C		
IL21	C ₉ (bmim) ₂ -NTf ₂	1031.0	>-76, <-22 ^e	166	437	453	1.42	3132	568		
IL22	C ₉ (m ₂ im) ₂ -NTf ₂	878.8	>-76, <-22 ^e	185	467	485	1.47	690	198		
IL23	C ₉ (bpy) ₂ -NTf ₂	941.0	87-89	344	426	449	-	-	-		
IL24	C ₉ (mpy) ₂ -NTf ₂	856.8	>-22, <4 ^e	310	447	461	1.46	1040	290		
IL25	C ₉ (pr ₃ p) ₂ -NTf ₂	1007.0	89-91	366	464	480	-	-	-		
IL26	C ₉ (ph ₃ p) ₂ -NTf ₂	1211.1	82-84	378	424	457	-	-	-		
IL27	C ₉ (bmim) ₂ -PFOS	1468.9	147-148	409	416	451	-	-	-		
IL28	C ₉ (m ₂ im) ₂ -PFOS	1316.7	133-135	428	450	473	-	-	-		
IL29	C ₉ (bpy) ₂ -PFOS	1378.9	214-216	317	353	391	-	-	-		
IL30	C ₉ (mpy) ₂ -PFOS	1294.8	157-159	332	373	421	-	-	-		
IL31	C ₉ (pr ₃ p) ₂ -PFOS	1445.0	78-80	368	412	423	-	-	-		
IL32	C ₉ (ph ₃ p) ₂ -PFOS	1649.0	56-58	301	407	420	-	-	-		

^a Thermogravimetric analysis (TGA) conditions: temperature program= 10 °C/min from room temperature (22 °C) to 600 °C, 99% w= temperature of 1% mass decrease of sample, 95%w= temperature of 5% mass decrease of sample, 85%w= temperature of 15% mass decrease of sample.

^b Measured using pycnometer.

^c Measured using capillary viscometer.

^d I= immiscible, M= miscible.

^e Liquid at room temperature, melting point is in the given range.

Table 2-4 Physicochemical Properties of C₁₂ alkane linkage chain ILs

ionic liquid	MW (g/mol)	melting point (°C)	thermal stability ^a (°C)			density ^b (g/cm ³)	viscosity ^c (cSt)			miscibility with heptane ^d	miscibility with water ^d	
			99% w	95% w	85% w		30°C	50°C	80°C			
IL33	C ₁₂ (bmim) ₂ -NTf ₂	1085.0	>-76, <-22 ^e	182	394	419	1.36	2970	612.5	-		
IL34	C ₁₂ (m ₂ im) ₂ -NTf ₂	932.8	55-56	418	442	455	-	-	-	90		
IL35	C ₁₂ (bpy) ₂ -NTf ₂	995.0	53-54	352	398	425	-	-	-	115		
IL36	C ₁₂ (mpy) ₂ -NTf ₂	910.8	>-76, <-22 ^e	400	422	434	1.38	930	282.5	-		
IL37	C ₁₂ (pr ₃ p) ₂ -NTf ₂	1061.0	40-45	234	392	422	-	-	-	82.5		
IL38	C ₁₂ (ph ₃ p) ₂ -NTf ₂	1265.1	118-119	352	385	403	-	-	-	-		
IL39	C ₁₂ (bmim) ₂ -PFOS	1540.9	99-101	354	385	410	-	-	-	-		
IL40	C ₁₂ (m ₂ im) ₂ -PFOS	1370.7	98-100	387	412	429	-	-	-	-		
IL41	C ₁₂ (bpy) ₂ -PFOS	1432.9	165-167	243	329	369	-	-	-	-		
IL42	C ₁₂ (mpy) ₂ -PFOS	1348.8	136-137	343	369	383	-	-	-	-		
IL43	C ₁₂ (pr ₃ p) ₂ -PFOS	1499.0	86-87	232	387	419	-	-	-	-		
IL44	C ₁₂ (ph ₃ p) ₂ -PFOS	1701.0	71-73	346	381	401	-	-	-	-		

^a Thermogravimetric analysis (TGA) conditions: temperature program= 10 °C/min from room temperature (22 °C) to 600 °C, 99%w= temperature of 1% mass decrease of sample, 95%w= temperature of 5% mass decrease of sample, 85%w= temperature of 15% mass decrease of sample.

^b Measured using pycnometer.

^c Measured using capillary viscometer.

^d I= immiscible, M= miscible.

^e Liquid at room temperature, melting point is in the given range.

have higher melting points than C₁₂ ILs with the same cationic groups. As the length of spacer alkane chain length increases, melting points decrease due to the added conformational degrees of freedom.⁶⁸ Some exceptions were observed to this trend. The (m₂m) and (ph₃ph) dicationic ILs with C₁₂ linkages had slightly higher melting points than the analogous dicationic ILs with C₉ linkers. In the case of pyrrolidinium based ILs, the butyl substituted ILs (bpy) have higher melting point than the methyl substituted ILs (see Tables 2-2 to 2-4).¹¹

The melting points of PFOS⁻ ILs were found to exhibit a different behavior. The imidazolium and pyrrolidinium based ILs with C₉ linkages had higher melting points and the C₆ and C₁₂ linked ILs had lower, but comparable melting points. Conversely, the phosphonium based ILs with C₉ linkers had lower melting points than those with C₆ and C₁₂ linkage chains (Table 2-2 to 2-4). All the synthesized ILs were symmetrical and most of them were solids at room temperature. The ILs which were liquid at room temperature were C₉(bmim)₂-NTf₂, C₁₂(bmim)₂-NTf₂, C₉(m₂m)₂-NTf₂, C₉(mpy)₂-NTf₂ and C₁₂(mpy)₂-NTf₂. ILs with PFOS⁻ anion were all solids at room temperature.

Some analogous solid ILs with high thermal stabilities were combined to lower the melting points of the resulting IL mixture. The ILs with same cation and anion but different alkane linkage chains (C₉ and C₁₂) were mixed in different weight percentages (Table 2-5). Thus, thirteen different mixtures of ILs (IL45 to IL57) were synthesized from four groups of analogous ILs which are (bpy)₂-NTf₂, (pr₃p)₂-NTf₂, (bmim)₂-PFOS and (pr₃p)₂-PFOS. A significant decrease in melting points was achieved with the mixtures. The mixtures with lowest melting points from every group were selected and used for coating on GC columns (more details in 'thermal stability with GC-FID' section).

Table 2-5 Melting points of mixtures of ILs

	ionic liquid A (IL-A) (C ₉ linkage chain)	weight percentage of IL-A	ionic liquid B (IL-B) (C ₁₂ linkage chain)	weight percentage of IL-B	final ionic liquid ^a (IL-A + IL-B)	melting point (°C)
IL45 mix	C ₉ (bpy) ₂ -NTf ₂	30	C ₁₂ (bpy) ₂ -NTf ₂	70	C _{mix} (bpy) ₂ -NTf ₂	43-55
IL46 mix	C ₉ (bpy) ₂ -NTf ₂	50	C ₁₂ (bpy) ₂ -NTf ₂	50	-	49-65
IL47 mix	C ₉ (bpy) ₂ -NTf ₂	70	C ₁₂ (bpy) ₂ -NTf ₂	30	-	69-73
IL48 mix	C ₉ (pr ₃ p) ₂ -NTf ₂	30	C ₁₂ (pr ₃ p) ₂ -NTf ₂	70	-	58-62
IL49 mix	C ₉ (pr ₃ p) ₂ -NTf ₂	40	C ₁₂ (pr ₃ p) ₂ -NTf ₂	60	C _{mix} (pr ₃ p) ₂ -NTf ₂	55-62
IL50 mix	C ₉ (pr ₃ p) ₂ -NTf ₂	50	C ₁₂ (pr ₃ p) ₂ -NTf ₂	50	-	58-69
IL51 mix	C ₉ (pr ₃ p) ₂ -NTf ₂	70	C ₁₂ (pr ₃ p) ₂ -NTf ₂	30	-	73-79
IL52 mix	C ₉ (bmim) ₂ -PFOS	30	C ₁₂ (bmim) ₂ -PFOS	70	-	69-78
IL53 mix	C ₉ (bmim) ₂ -PFOS	50	C ₁₂ (bmim) ₂ -PFOS	50	-	65-76
IL54 mix	C ₉ (bmim) ₂ -PFOS	70	C ₁₂ (bmim) ₂ -PFOS	30	C _{mix} (bmim) ₂ -PFOS	59-70
IL55 mix	C ₉ (pr ₃ p) ₂ -PFOS	30	C ₁₂ (pr ₃ p) ₂ -PFOS	70	-	72-85
IL56 mix	C ₉ (pr ₃ p) ₂ -PFOS	50	C ₁₂ (pr ₃ p) ₂ -PFOS	50	-	70-81
IL57 mix	C ₉ (pr ₃ p) ₂ -PFOS	70	C ₁₂ (pr ₃ p) ₂ -PFOS	30	-	63-74

^a Naming was done only to mixtures with low melting points and were selected for GC-FID study

2.4.2 Viscosity:

The viscosities were determined at 30 °C and 50 °C for the five ILs that were liquids at room temperature (Table 2-2 to 2-4). Viscosities were also determined at 80 °C for ILs which were solids at room temperature but having melting points less than 80 °C (Table 2-2 and 2-4). Imidazolium ILs containing benzyl groups have considerably higher viscosities than pyrrolidinium and dimethyl imidazolium ILs. The presence of benzyl group adds extra intermolecular π - π interactions which may be a factor leading to higher viscosity.¹² Methylpyrrolidine ILs had higher viscosities than dimethylimidazolium ILs of the same connecting chain lengths.

2.4.3 Density:

Similar to viscosity, density measurements were done for the ILs that were liquid at room temperature. Densities for dicationic ILs were found to be higher than monocationic ILs (Tables 2-1 to 2-4). ILs with C₉ alkane linkages have somewhat higher densities than ILs with C₁₂ linkages (Table 2-3 and 2-4). The decrease in density with increase in alkane linkage for dicationic ILs has been reported previously.¹¹

2.4.4 Solubility:

All the dicationic ILs synthesized in this study were insoluble in both water and heptane (Table 2-2 to 2-4). All the monocationic ILs were insoluble in water but some of these ILs, with NTf₂⁻, NPf₂⁻, PFOS⁻, AOT⁻ and OS⁻ anions, were soluble in heptane (Table 2-1).

2.4.5 Thermal Stability:

Thermal stability of ILs was determined using thermogravimetric analysis (TGA). For dicationic ILs the thermal stability data is compiled in Tables 2-1, 2-2 and 2-3 and specific data compared in Figure 2-3 at the 5% weight loss level. Geminal dicationic ILs can be considered as a combination of three main structural moieties: 1) a cation

head group, 2) an alkane linker chain and 3) the anions. The effect of each component on the physical and chemical properties was studied by single variable modifications.

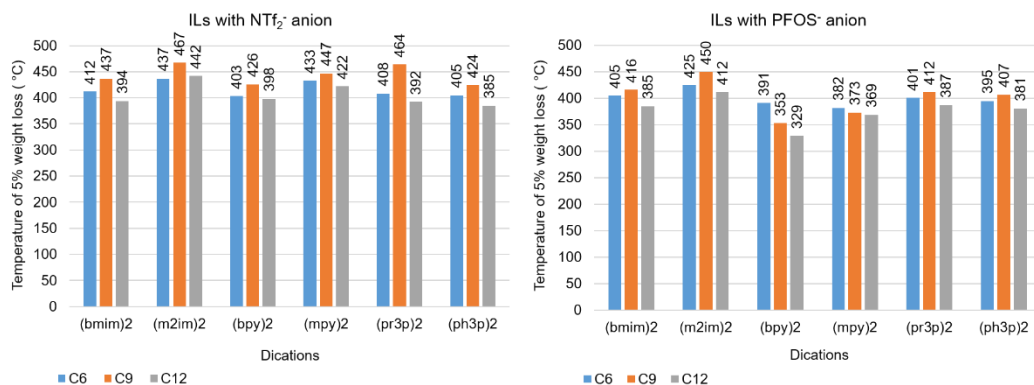


Figure 2-3 Thermal stability comparison of ILs synthesized in this study

Effect of the anion:

NTf₂⁻ based ILs were observed to have somewhat greater thermal stability compared to analogous ILs with PFOS⁻ counter anions. This is may be attributed to the higher nucleophilicity of PFOS⁻ anion than NTf₂⁻ anion, as NTf₂⁻ shows greater negative charge delocalization. The decrease in IL thermal stability with increasing nucleophilicity of the anion was previously reported by Bonhote et al.⁹

Effect of linker chain length:

The thermal stability of dicationic ILs with C₉ linkage chains were observed to be higher than the analogous C₆ and C₁₂ ILs. In addition, it can be seen the densities and viscosities of the C₉ ILs are generally greater than those of their C₆ and C₁₂ analogues (Table 2-3). Higher densities, meaning smaller free volumes between molecules and higher shear viscosities may favor reversibility of breakdown reactions or recombination of fragments. The reversibility leading to recombination of fragments, also known as the 'cage effect', can lead to higher thermal stabilities.¹⁶ ILs with C₆ linkage

chains have higher thermal stabilities than those analogous dications with C₁₂ linkage chains. Therefore, an increase in the alkane linkage from C₆ to C₉ leads to an increase in thermal stability while further increases in chain length lead to a decrease in thermal stability (C₁₂<C₆<C₉).

In case of ILs with the PFOS⁻ anion, imidazolium and phosphonium based ILs with the C₉ linker chains were found to be more stable than C₆ and C₁₂ linked ILs thereby following a similar trend to the NTf₂⁻ ILs. Conversely, pyrrolidinium based dicationic ILs with C₆ linkages showed higher thermal stability than the analogous C₉ and C₁₂ ILs. C₆(bpy)₂-PFOS is more stable than C₉(bpy)₂-PFOS and C₁₂(bpy)₂-PFOS and C₆(mpy)₂-PFOS is more stable than C₉(mpy)₂-PFOS and C₁₂(mpy)₂-PFOS (Table 2-2 to 2-4).

Effect of cationic head groups:

In case of imidazolium based ILs, the C(3) methylated (m₂im) dicationic ILs are more stable than the corresponding (bmim) dicationic ILs. The presence of methyl groups at the C(3) positions of the imidazole ring conferred more stability than did benzyl groups at the same position (Table 2-2 to 2-4 and Figure 2-3). The TGA experiments indicated that the ILs containing the dimethylimidazolium dications usually showed slightly higher thermal stabilities (Table 2-2 to 2-4). In case of the pyrrolidinium based ILs, those substituted with methyl groups (mpy) were more stable than those substituted with butyl groups (bpy) (Table 2-2 to 2-4 and Figure 2-3). Increasing the length of the alkyl chain substituent on the pyrrolidinium nitrogen leads to a decrease in the IL thermal stability. The stability of linear, aliphatic carbocations and carbon radicals increases with increasing chain length.⁷⁰ This stability means that longer chains can be better leaving groups during heating processes and this infers a more facile disconnection of the C-N bond. Overall this effect tends to decrease the thermal stability of analogous compounds with longer alkyl chains.⁷⁰

For phosphonium based ILs, the thermal stability of the tripropylphosphonium ILs (pr₃p) was higher than of the analogous triphenylphosphonium ILs (ph₃p). Obviously, (ph₃p) dications are bulkier than (pr₃p) due to presence of three phenyl rings on a single phosphorus atom (Cone angle of ph₃p > cone angle of pr₃p).⁷¹ Breaking of the (ph₃p) C-P bond may be accentuated at higher temperatures to lower the steric strain, which in turn, would lead to lower thermal stabilities. C₉(m₂im)₂-NTf₂ (467 °C) and C₉(pr₃ph)₂-NTf₂ (464 °C) showed the best TGA stability (at the 95% weight loss level) of all the synthesized ILs. Other ILs which displayed high TGA stability were; C₉(m₂im)₂-PFOS (450 °C), C₉(mpy)₂-NTf₂ (447 °C) and C₁₂(m₂im)₂-NTf₂ (442 °C). TGA is not the only way to measure thermal stability/volatility. Indeed, depending on the analysis program used, its results can sometime differ from those of other tests (see following section).

2.4.6 Thermal stability with inverse GC-FID:

Nine different dicationic ILs with TGA thermal stabilities higher than 400°C and having low melting points were selected and coated on GC capillary columns. Some ILs having high thermal stability but melting points around 60 °C were mixed with an analogous IL with a different alkane linkage but same cations and anions. This was done to lower the melting point of mixture. Low melting ILs can act as good GC stationary phases.^{13, 17, 22, 37} For example, C₉(pr₃p)₂-NTf₂, C₁₂(pr₃p)₂-NTf₂, C₉(bpy)₂-NTf₂, C₁₂(bpy)₂-NTf₂, C₉(bmim)₂-PFOS and C₁₂(bmim)₂-PFOS ILs have high thermal stabilities (> 400 °C) but also high melting points. In order to lower melting points, analogous ILs with C₉ and C₁₂ alkane linkage were mixed together in different ratios. (Table 2-5). The mixtures with lowest melting points were chosen to coat on the inner surface of capillary GC columns.

Inverse gas chromatography with FID can be more sensitive method than TGA when examining the thermal stability of ILs.¹¹ In a reverse GC experiment the IL coated columns were heated from room temperature (22 °C) to 450 °C at temperature ramp of 1

°C/min, which is much slower than the temp ramp used in TGA (10 °C/min). FID is very sensitive detector and allows sensitive detection of even trace volatile/decomposed products from ILs. Consequently, stability testing with GC-FID can sometimes give a more accurate indication of the stability of ILs depending on the experimental conditions. The data collected with GC-FID is shown in Figure 2-4. The Highest thermal stabilities were observed for $C_{mix}(pr_3ph)_2-NTf_2$ and $C_{12}(m_2im)_2-NTf_2$ (first bleeding at 400 °C), followed by $C_9(mpy)_2-NTf_2$ (bleeding at 390 °C) and the $C_{12}(m_2im)_2-NTf_2$ (bleeding at 380 °C). $(bmim)_2-NTf_2$ with C_9 and C_{12} linkage were stable up to 300 °C (lower than observed with TGA). $C_{12}(mpy)_2-NTf_2$ and $C_{mix}(bpy)_2-NTf_2$ started bleeding at 320 °C. $C_{mix}(bmim)_2-PFOS$ IL was the least stable and started bleeding at 260 °C.

2.4.7 Performance testing of ILs as GC stationary phases:

One of the synthesized ILs; $C_9-(m_2im)_2-NTf_2$, which showed GC-FID stability up to 350 °C was further evaluated for performance as GC stationary phase. The selected IL was coated on a 30 m capillary column (internal diameter of 0.25mm) and the column was used for the separation of polycyclic aromatic hydrocarbons (PAHs). PAHs are ubiquitous environmental pollutants derived mainly from incomplete combustion of organic materials.⁷² “Benzo-fluoranthenes” are PAHs with three structural isomers; benzo[b]-fluoranthene, benzo[j]-fluoranthene and benzo[k]-fluoranthene. The separation and detection of these structural isomers is difficult due to high degree of overlap in the boiling points of these compounds.⁷³ Typically, the separation of PAHs is performed on methyl and phenyl substituted polysiloxanes stationary phases.⁷⁴ The traditional polysiloxanes based stationary phases are not efficient for the separation of these structural isomers and they typically coelute.⁷⁴ However, the thermally stable $C_9-(m_2im)_2-NTf_2$ IL based column effectively separated the structural isomers at temperature of

280°C. The separation is shown in Figure 2-5.

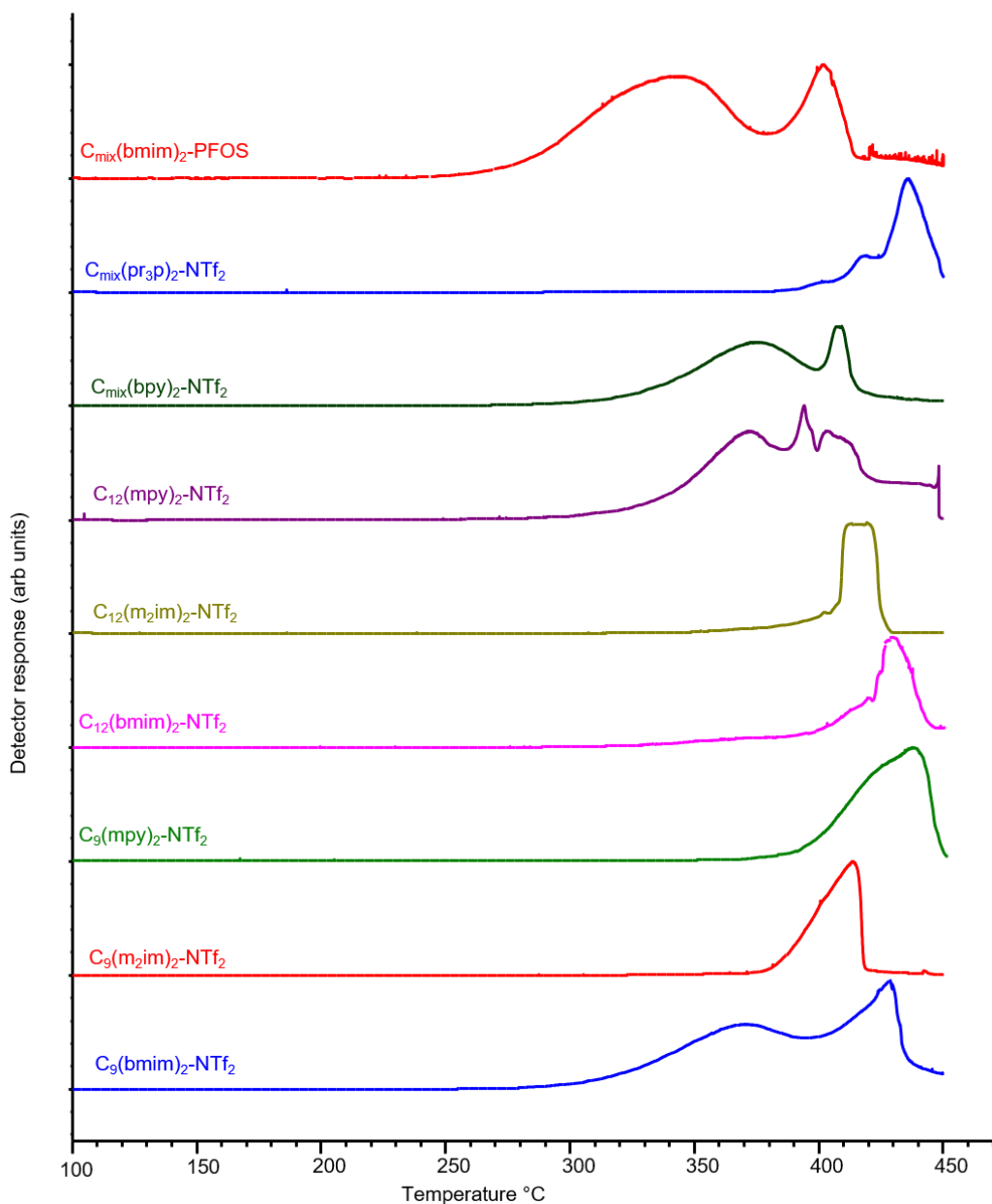


Figure 2-4 Thermal stability diagram with GC-FID for nine dicationic ILs. Plot shows the bleeding temperature of ILs as GC stationary phases. The study was done with oven temperature ramp of 1 °C/min with helium as carrier gas and flow 1 ml/min.

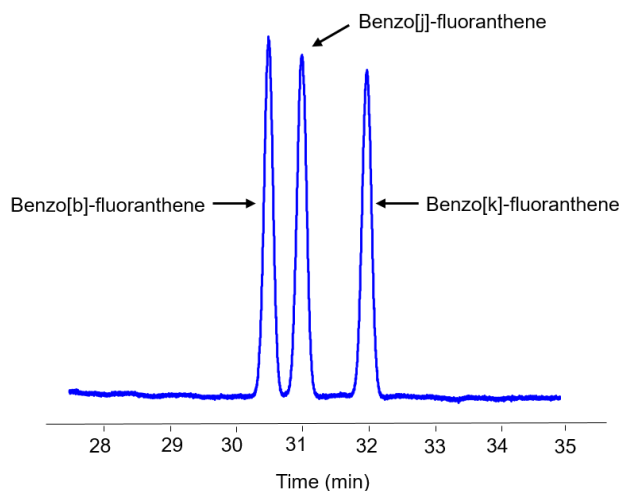


Figure 2-5 Separation of structural isomers of benzofluoranthene by GC on C_9 -(*m*₂im)₂-NTf₂ IL column (30 m x 0.25 mm i.d.). GC separation conditions: 150-250 °C at 20 °C/min, hold 2 min, 20 °C/min to 280 °C, 1 mL/min He; FID

2.5 Conclusions

In this study, we have demonstrated the effect of different structural modifications including alkane linkage chain, substituents and type of dications and anions on the physicochemical properties of ILs. The new series of synthesized dicationic ILs with different structural moieties displayed excellent TGA thermal stabilities up to 460 °C. A correlation between the physicochemical properties of analogous ILs and their unique structural features was observed. In general, ILs with C_9 linkage chains had higher stability than C_6 and C_{12} linkage chain ILs. They also had higher viscosities and densities. Within the three different classes of dications, comparison of stabilities of analogous ILs lead to following observations, Imidazolium group: (*m*₂im) > (*b*mim), pyrrolidinium group: mpy > bpy and phosphonium group: (pr₃p) > (ph₃p). Also, some ILs tested with GC-FID showed stability up to 400 °C (C_{mix} (pr₃p)₂- NTf₂ and C_{12} (*m*₂im)₂- NTf₂).

The thermal stability of ILs with NTf₂⁻ anions was higher than those with PFOS⁻ anions. Also NTf₂⁻ anions tended to lower the melting points of ILs. Dicationic ILs with PFOS⁻ anions were all solids at room temperature and had higher melting points compared to NTf₂⁻ based ILs. The melting points of ILs found to decrease with length of alkane linkage chain due to added conformational degrees of freedom. N-butyl substituted pyrrolidinium dicationic ILs have higher melting points than N-methyl substituted pyrrolidinium ILs. The densities of dicationic ILs were higher than monocationic ILs and dicationic ILs with C₉ alkane linkages had higher densities than analogous ILs with C₁₂ linkers. Benzyl substituted imidazolium ILs displayed the highest viscosities of all the dicationic ILs studied. Performance testing of C₉-(m₂im)₂-NTf₂ IL as GC stationary phase at high temperatures provided an exceptional separation of the benzo-fluoranthene isomers.

Chapter 3

EXAMINATION OF SELECTIVITIES OF THERMALLY STABLE GEMINAL DICATIONIC IONIC LIQUIDS BY STRUCTURAL MODIFICATION

3.1 Abstract

Dicationic ionic liquids (ILs) are widely used as gas chromatography (GC) stationary phases as they show higher thermal stabilities, variety of polarities and unique selectivities towards certain compounds. An important aspect contributing to them is that they show multiple solvation interactions compared to traditional GC stationary phases. Dicationic ILs are considered as combination of three structural moieties: 1) cationic head groups, 2) a linkage chain, and 3) the counter anions. Modifications in these structural moieties can alter the chromatographic properties of IL stationary phases. In this study a series of nine thermally stable ionic liquid stationary phases were synthesized by the combination of five different cations, two different linkage chains, and two different anions. Different test mixtures composed of a variety of compounds having different functional groups and polarities were analyzed on these columns. A comparison of the separation patterns of these different compounds on nine different IL columns provided some insights about the effects of structural modifications on the selectivities and polarities of dicationic ionic liquids.

3.2 Introduction

Ionic Liquids (ILs) are salts with melting points generally less than 100 °C.^{6, 48} ILs generally consist of nitrogen or phosphorus containing organic cations and an inorganic or organic anion.⁴¹ ILs are of interest to researchers due to their many fascinating properties such as high thermal stabilities, low volatilities (negligible vapor pressure), non-flammability, tunable viscosities, high densities, wide liquid temperature

range, adjustable miscibility, conductivity, high chemical stability and so on.^{13, 39} These unique physical and chemical properties are the reasons for their usefulness in many different areas of chemistry such as solvents for organic synthesis reactions,^{6, 20-21, 64-65, 75-77} gas chromatographic stationary phases,^{13, 17, 22, 37-40, 78} high temperature lubricants,²⁶ solvents for liquid-liquid extractions,⁷⁹⁻⁸² matrices for MALDI-MS,⁸³⁻⁸⁷ and electrochemical studies.^{15, 88-92}

The best performance of ILs as gas chromatography (GC) stationary phases is obtained when they are liquids at room temperature.³⁹ The specific properties of RTILs such as low volatility, high thermal stability, excellent selectivities for certain compounds and good wetting abilities have made them suitable and popular as GC stationary phases.^{13, 17, 22, 37-38, 40, 78, 93} Generally, traditional stationary phases show one dominant type of chemical interaction, while IL phases show multiple solvation interactions and this is the origin of their unique selectivity toward a variety of molecules with many different functional groups.⁴⁰ As ILs provide different selectivities, IL stationary phases have been used in different applications. They are popular in the separation of fatty acid methyl esters (FAMEs), flavors, fragrances, aromatic hydrocarbons and environmental pollutants.⁹⁴⁻¹⁰¹ Most of the ILs are air and moisture stable, they have been used in the analysis of water content in pharmaceuticals, petroleum products, and foods.¹⁰²⁻¹⁰⁶ ILs with higher thermal stabilities and a variety of polarities have opened new exciting possibilities in the field of multidimensional gas chromatography.^{93, 107-109} Currently more research is being done towards the improvement of the thermal stabilities of ILs and producing even greater variations in their selectivities.

Geminal dicationic ILs often display higher thermal stabilities compared to traditional monocationic ILs.^{11-13, 110} Also, dicationic ionic liquids have advantages in terms of tuning their physicochemical properties by structural modifications. The geminal

dicationic ILs are considered as a combination of three structural moieties: 1) cationic head groups, (2) a linkage chain and (3) the counter anions. Modifications in these structural moieties can alter their physicochemical properties such as thermal stabilities, viscosities, densities, and melting points.^{11-12, 110} Also, such structural modifications can modify the chromatographic properties of IL stationary phases.^{13, 17} Since the selectivities of dicationic ILs vary with their structure, a systematic study showing the effects of modification of each structural moiety on the polarities and selectivities of dicationic ILs is needed.

We recently synthesized a series of thirty-six thermally stable geminal dicationic ionic liquids.¹¹⁰ The thermogravimetric analysis (TGA) stabilities of these ILs were in the range of 330 – 467 °C. Nine ILs with high TGA stability and low melting points were tested for stability with inverse gas chromatography – flame ionization detector (GC-FID) and they displayed short term stability up to 400 °C.¹¹⁰ The current study focuses on the further evaluation of these nine thermally stable ILs as GC stationary phases. The selected dicationic ILs are combinations of five different cations, two different alkane linker chains and two different anions. Different test mixtures composed of a variety of compounds with different polarities and functional groups were injected on these IL columns. A comparison of separation patterns of different compounds on the IL columns provided insights into the effects of structural modifications on the polarities and selectivities of dicationic ILs.

3.3 Experimental Section:

3.3.1. *Materials*

1-Benzyl-2-methylimidazole (90%), 1,2-dimethylimidazole (98%), N-methylpyrrolidine (97%), 1-butylpyrrolidine (98%), tripropylphosphine (97%), 1,9-

dibromononane (97%), 1,12-dibromododecane (98%), bis(trifluoromethane)sulfonimide lithium salt (99.95%), and heptadecafluorooctanesulfonic acid potassium salt (98%) were purchased from Sigma-Aldrich (St. Louis, MO). The detailed procedures for synthesis of ILs are reported in the literature.¹¹⁰ The structures of synthesized IL stationary phases are given in Fig. 1. The ILs were coated on fused silica capillary columns with dimensions 30m x 0.25 mm i.d. and film thickness of 0.20 μm . All the IL coated columns were provided by Supelco (Bellefonte, PA). The commercial SLB IL111 column and all test mixes used to characterize the stationary phases were provided by MilliporeSigma (Bellefonte, PA).

FAME test mix is a mixture of 11 compounds; methyl myristate (C14:0), methyl palmitate (C16:0), methyl stearate (C18:0), methyl oleate (C18:1n9), methyl linoleate (C18:2n6), methyl linolenate (C18:3n3), methyl arachidate (C20:0), cis-11-Eicosenoic acid methyl ester (C20:1), methyl behenate (C22:0), erucic acid methyl ester (C22:1), and methyl tetracosanoate (C24:0) at different concentrations in dichloromethane. Grob test mix is a mixture of 12 compounds; dicyclohexylamine, methyl decanoate, methyl undecanoate, methyl laurate, decane, undecane, 1-nonanal, 1-octanol, 2-ethylhexanoic acid, 2,3-butanediol, 2,6-dimethylaniline, and 2,6-dimethylphenol at different concentrations in dichloromethane. Polar Plus test mix is a mixture of 13 compounds; 2-octanone, 1-octanol, 2,6-dimethylaniline, 2,6-dimethylphenol, pentadecane, hexadecane, heptadecane, octadecane, icosane, heneicosane, docosane, tetracosane, and pentacosane at concentrations of 500 ppm each in dichloromethane. PAM-HC test mix is a mixture of 15 compounds; naphthalene, acenaphthylene, acenaphthene, fluorene, phenanthrene, anthracene, fluoranthene, pyrene, triacontane, dotriacontane, tetratriacontane, hexatriacontane, octatriacontane, tetracontane, and tetratetracontane at concentrations of 100 ppm each in dichloromethane. Custom-PAM test mix is a mixture

of 9 compounds; naphthalene, phenanthrene, anthracene, benzo(a)anthracene, chrysene, triphenylene, benzo(b)fluoranthene, benzo(k)fluoranthene, and benzo(j)fluoranthene (MW- 252) S) at concentrations of 100 ppm each in dichloromethane. Ionic Liquid test mix is a mixture of 14 compounds; toluene, camphene, tridecane, 2,6-di-t-butyl-4-methylene-2,5 cyclohexadiene-1-one, naphthalene, 2,6-dimethylaniline, dimethylsulfoxide, methyl linolenate, methyl arachidate, cis-11-Eicosenoic acid methyl ester, coumarin, dioctyladipate, tetracosane, and tetracontane at different concentrations in dichloromethane.

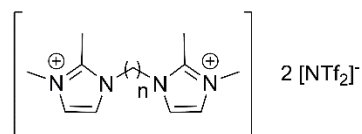
The identification of different compounds of the test mixtures was done by analyzing individual standards of each compound.

3.3.2 Instrumentation:

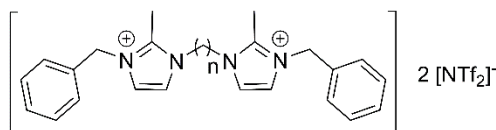
The gas chromatographic analyses were made using Agilent 6890N gas chromatograph equipped with flame ionization detector. Helium was used as a carrier gas. Efficiencies of all the IL columns were determined by using naphthalene at 110 °C and were ~4000 plates m⁻¹.

3.4 Results and Discussion

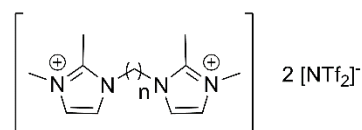
Nine different geminal dicationic ILs which are combination of different cationic groups, alkane linkage chains and anions were chosen for analysis (see Figure 3-1). The three general classes of dications were; (1) Imidazolium: benzylmethylimidazolium and dimethylimidazolium, (2) pyrrolidinium: methylpyrrolidinium and butyl pyrrolidinium, and (3) phosphonium: tripropylphosphonium. The two cationic moieties were linked together by two different alkane linkage chains; 9 carbon (C₉) and 12 carbon (C₁₂). The resulting dications were paired with NTf₂⁻ and PFOS⁻ anions.



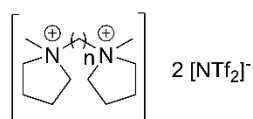
IL1: n=5, C₅(m₂im)₂-NTf₂, **SLB IL 111**



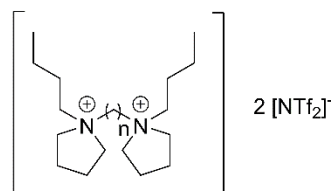
IL2: n=9, C₉(bmim)₂-NTf₂,
IL3: n=12, C₁₂(bmim)₂-NTf₂



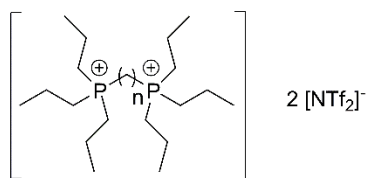
IL4: n=9, C₉(m₂im)₂-NTf₂,
IL5: n=12, C₁₂(m₂im)₂-NTf₂



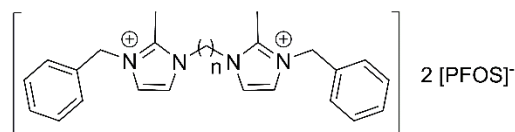
IL6: n=9, C₉(mpy)₂-NTf₂,
IL7: n=12, C₁₂(mpy)₂-NTf₂



IL8: n=mix*, C_{mix}(bpy)₂-NTf₂: C₉(bpy)₂-NTf₂ (30%)
+ C₁₂(bpy)₂-NTf₂ (70%)

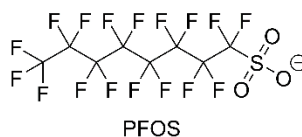
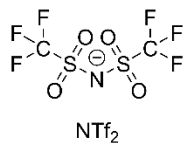


IL9: n=mix*, C_{mix}(pr₃p)₂-NTf₂: C₉(pr₃p)₂-NTf₂ (40%)
+ C₁₂(pr₃p)₂-NTf₂ (60%)



IL10: n=9, C₉(bmim)₂-PFOS,

structures of anions:



*The ionic liquids with the same cation and anion but different alkane linkage chains (C₉ and C₁₂) were mixed in the given weight percentages

Figure 3-1 Structures and abbreviations of dicationic ILs studied in this analysis

IL8 and IL9 are mixtures of analogous ILs with the same cation and anion but different alkane linkage chains (C_9 and C_{12}) with a specific weight percentages (IL8: mixture of $C_9(\text{bpy})_2\text{-NTf}_2$ (30%) and $C_{12}(\text{bpy})_2\text{-NTf}_2$ (70%); IL9: mixture of $C_9(\text{pr}_3\text{p})_2\text{-NTf}_2$ (40%) and $C_{12}(\text{pr}_3\text{p})_2\text{-NTf}_2$ (60%)) (see Figure 3-1). This was necessary in order to decrease the melting points of the resulting mixtures to a level that was amenable for gas-liquid chromatography. The individual ILs had good thermal stabilities but high melting points.¹¹⁰

The chromatographic properties and selectivities of the IL coated capillary columns were investigated by using different compound test mixtures. The FAME test mix was injected on all the nine new IL columns along with the commercial SLB IL 111 which is currently the most polar commercially available column. The thermal stability evaluation of ILs using inverse GC-FID showed that only four ILs; $C_9(\text{m}_2\text{im})_2\text{-NTf}_2$, $C_{12}(\text{m}_2\text{im})_2\text{-NTf}_2$, $C_9(\text{mpy})_2\text{-NTf}_2$, and $C_{\text{mix}}(\text{pr}_3\text{p})\text{-NTf}_2$ were stable at temperatures greater than 350 °C (refer to Figure 2-4). The other high temperature test mixes Grob, Polar Plus, PAM-HC, Custom-PAM, and Ionic Liquid mix were analyzed only on these four IL columns.

3.4.1 FAME Test Mix

The FAME test mix is based on rapeseed oil which has a mixture of eleven fatty acid methyl esters. The isothermal chromatographic profiles obtained from the analysis of the FAME test mix is shown in Figure 3-2. This test mix was used to compare the polarities of the newly synthesized ILs. Also, the elution patterns of eleven FAMEs were helpful in understanding the effects of cations, alkane linkage chains, and anions on the selectivities of ILs. The most important compounds in the test mix are methyl linolenate ($C_{18:3n3}$) (6), methyl arachidate ($C_{20:0}$) (7), and cis-11-eicosenoic acid methyl ester

(C20:1) (8). Compounds C18:3 (6), C20:1 (8), and C20:0 (7) contain three, one, and zero double bonds respectively. So, the C18:3 FAME is more polarizable compared to C20:1 and C20:0. In general, the relative retention of compound 6 increases while compound 7 decreases with increases in the polarity of the stationary phase.

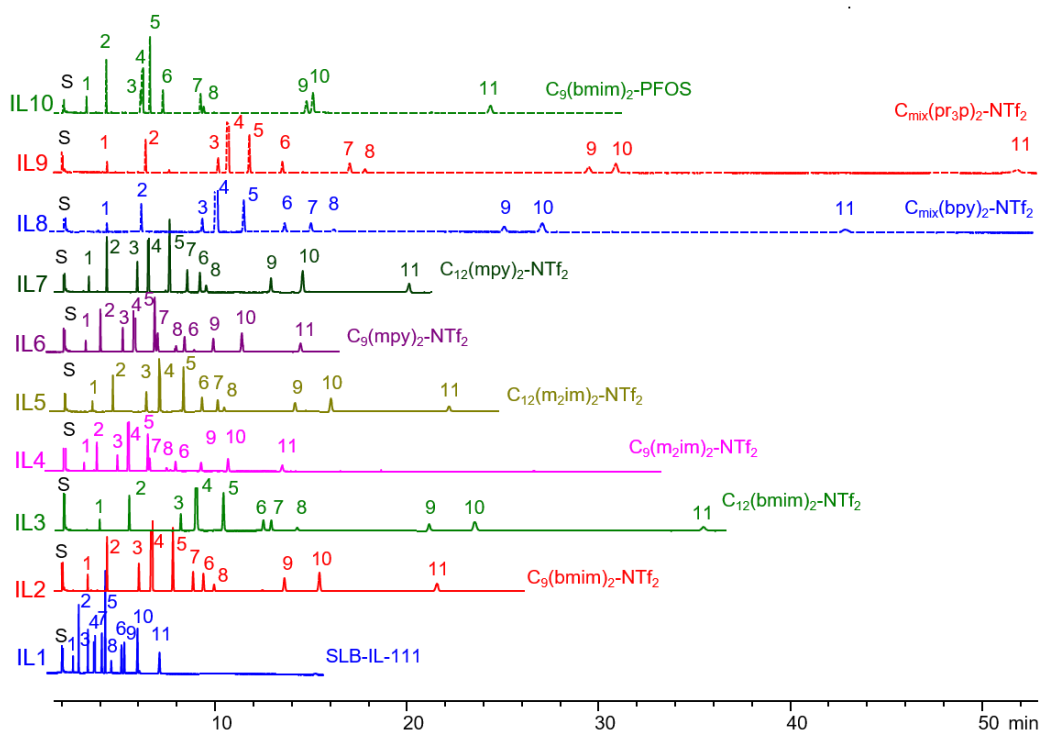


Figure 3-2 Separation of FAME test mix. 1) methyl myristate (C14:0) 2) methyl palmitate (C16:0) 3) methyl stearate (C18:0) 4) methyl oleate (C18:1n9) 5) methyl linoleate (C18:2n6) 6) methyl linolenate (C18:3n3) 7) methyl arachidate (C20:0) 8) cis-11-Eicosenoic acid methyl ester (C20:1) 9) methyl behenate (C22:0) 10) erucic acid methyl ester (C22:1) 11) methyl tetracosanoate (C24:0) S: dichloromethane. GC separation conditions: 180 °C isothermal; 1 mL min⁻¹ He; FID

Effect of linker chain length:

The synthesized ILs contain three pairs (**IL2** and **IL3**, **IL4** and **IL5**, and **IL6** and **IL7**) of analogous ILs with two different linker chain lengths (C₉ and C₁₂). Comparison of

bmim-dicationic ILs with NTf₂⁻ anion (**IL2** and **IL3**) showed that C18:3n3 (6) was retained longer on the C₉ linkage chain IL (**IL2**) than the C₁₂ linkage chain IL (**IL3**). C18:3n3 (6) was retained longer compared to both compounds C20:0 (7) and (C20:1) (8) on C₉(m₂im)₂-NTf₂ (**IL4**) while C18:3n6 (6) showed shorter retention than both C20:0 (7) and (C20:1) (8) on C₁₂(m₂im)₂-NTf₂ (**IL5**). In case of mpy-dicationic ILs with NTf₂⁻ anions (**IL6** and **IL7**), C18:3n3 (6) was more retained on the C₉ linkage chain IL (**IL6**) as compared to the C₁₂ linkage chain IL (**IL7**). The C₉ linked ILs (**IL2** and **IL4**) showed different selectivities to compounds C18:3n6 (6) and C20:0 (7) (reversal of elution order) compared to analogous C₁₂ linked ILs (**IL3** and **IL5**). The compounds C18:3n3 (6) and (C20:1) (8) also showed different selectivities (reversal of elution order) on C₉ and C₁₂ linked (mpy) ILs, **IL6** and **IL7**. Methyl tetracosanoate (C24:0) (11) is the most nonpolar compound in the FAME test mix. The relative retention of (C24:0) (11) was longer on C₁₂ linkage chain ILs than the analogous ILs with C₉ linkages. The selectivity (k_{11}/k_{10}) for **IL4** was 1.33 while for **IL5** it was 1.58; the C₁₂ linked IL showed higher selectivity to C24:0 compared to analogous C₉ IL. Hence, from the above results it can be concluded that the C₉ linked ILs are more polar than their C₁₂ analogues. The FAME test mix also was analyzed on the commercially available SLB-IL111 (**IL1**) column which is the most polar known IL stationary phase. SLB IL111 can be abbreviated as C₅(m₂im)₂-NTf₂ based on its structure. This shorter linkage chain (C₅) IL column showed the least retention of the FAMEs as compared to the IL columns used in this study. From the elution patterns of FAMEs on all these ILs it can be concluded that the polarity of stationary phase increases with decrease in length of alkane linkage chain.

Effect of the anion:

To understand the effect of anions on the polarities of ILs, we compared the relative retention of FAMEs on **IL2** and **IL10** which are analogous ILs with different

anions (NTf_2^- and PFOS^-). C18:3n3 (6) was retained longer than C20:0 (7) on $\text{C}_9(\text{bmim})_2\text{-NTf}_2$ (**IL2**) while the order of elution was reversed on $\text{C}_9(\text{bmim})_2\text{-PFOS}$ (**IL10**). The selectivities (k_{10}/k_9 and k_8/k_7) for unsaturated and saturated analogues of same chain length FAMES were also higher for **IL2** ($k_{10}/k_9 = 1.15$ and $k_8/k_7 = 1.16$) compared to **IL3** ($k_{10}/k_9 = 1.03$ and $k_8/k_7 = 1.02$). This shows that the ILs with NTf_2^- anion are more polar as compared to the analogous ILs with PFOS^- anions and also they have different selectivities.

Effect of the cation

The synthesized groups of the ILs contain two types of each imidazolium and pyrrolidinium dications and one type of phosphonium dication. The relative retention of C18:3n3 (6) was longer compared to C20:0 (7) and (C20:1) (8) on $\text{C}_9(\text{m}_2\text{im})_2\text{-NTf}_2$ (**IL4**) IL, while C18:3n3 (6) eluted before (C20:1) (8) on the $\text{C}_9(\text{bmim})_2\text{-NTf}_2$ (**IL2**) IL. Substitution of benzyl group instead of methyl group on the imidazolium ring leads to a decrease in the polarity of the IL. The elution order of compounds C18:3n3 (6), C20:0 (7), and (C20:1) (8) on the $\text{C}_{\text{mix}}(\text{bpy})_2\text{-NTf}_2$ (**IL8**) column was $6 < 7 < 8$ while C18:3n3 (6) was retained longer than C20:0 (7) on both $\text{C}_9(\text{mpy})_2\text{-NTf}_2$ (**IL6**) and $\text{C}_{12}(\text{mpy})_2\text{-NTf}_2$ (**IL7**). Replacement of a methyl group by a butyl group on the pyrrolidinium nitrogen may significantly decrease the polarity of an IL. This was also supported by the longer retention of the C24:0 (11) FAME on the bpy-dicationic column compared to the mpy-dicationic columns. The relative polarities of mpy and m_2im dications were compared by observing the relative elution of C18:3n3 (6) and C20:0 (7) on $\text{C}_{12}(\text{m}_2\text{im})_2\text{-NTf}_2$ (**IL5**) and $\text{C}_{12}(\text{mpy})_2\text{-NTf}_2$ (**IL7**) ILs. C18:3n3 (6) eluted later than C20:0 (7) on $\text{C}_{12}(\text{mpy})_2\text{-NTf}_2$ (**IL7**) while the order was reversed on $\text{C}_{12}(\text{m}_2\text{im})_2\text{-NTf}_2$ (**IL5**). This shows that pyrrolidinium dicationic ILs are more polar as compared to the imidazolium dicationic ILs. The IL $\text{C}_{\text{mix}}(\text{pr}_3\text{p})_2\text{-NTf}_2$ (**IL9**) displayed longest retention of C24:0 (11) compared to the tested IL

stationary phases. Also, the phosphonium IL (**IL9**) showed longer retention of compounds C20:0 (7), C20:1 (8), C22:0 (9), and C22:1 (10) as compared to imidazolium (**IL2**, **IL3**, **IL4**, and **IL5**) and pyrrolidinium (**IL6**, **IL7**, and **IL8**) ILs. This makes the phosphonium IL less polar than both the imidazolium and pyrrolidinium ILs. The overall comparison showed that $C_9(\text{mpy})_2\text{-NTf}_2$ (**IL6**) is the most polar while $C_{\text{mix}}(\text{prf}_3\text{p})_2\text{-NTf}_2$ (**IL9**) is the least polar of all the ILs analyzed in this study.

3.4.2 Equivalent chain length (ECL) values

The ECL values can be used for the quantitative comparison of selectivities and retention indices of FAMEs on different IL columns.¹¹¹⁻¹¹² The ECL values for unsaturated fatty acid methyl esters were calculated at 180 °C and they are reported in Table 3-1. The FAMEs with higher degree of unsaturation showed higher ECL values on all the IL columns. The ECL values increased with increase in the length of the unsaturated FAMEs. The ECL values for unsaturated FAMEs were also observed to increase with an increase in the polarity of the IL stationary phases; consistent with the polarity trends discussed in the previous section. The ECL values for all the FAMEs were higher on SLB-IL111 (**IL1**) column compared to all other IL columns (**IL2** to **IL10**). The $C_9(\text{m}_2\text{im})_2\text{-NTf}_2$ (**IL4**) and $C_9(\text{mpy})_2\text{-NTf}_2$ (**IL6**) showed comparable ECL values and their ECL values were higher than all the other newly synthesized IL columns (**IL2**, **IL3**, **IL5**, and **IL7** to **IL10**) analyzed in this study.

Table 3-1 ECL values of unsaturated fatty acid methyl esters on IL columns at 180 °C

FAME No.	FAME Abbreviation	ECL Values									
		IL1	IL2	IL3	IL4	IL5	IL6	IL7	IL8	IL9	IL10
4	C18:1n9	19.02	18.56	18.43	18.78	18.46	18.76	18.55	18.32	18.19	18.10
5	C18:2n6	20.34	19.34	19.06	19.90	19.15	19.86	19.37	18.88	18.58	18.38
6	C18:3n3	21.76	20.27	19.86	21.09	19.64	21.06	20.36	19.59	19.11	18.84
8	C20:1	20.91	20.54	20.41	20.76	20.19	20.74	20.53	20.30	20.17	20.07
10	C22:1	22.85	22.55	22.41	22.75	22.55	22.75	22.54	22.29	22.17	22.09

3.4.3 Grob Test Mix

Grob test mix is a mixture of twelve different components at varied concentrations in dichloromethane as a solvent (all compounds are at concentrations less than 500 ppm). The test mix contains saturated alkanes, FAMES, acid/base pairs, alcohols, and an aldehyde. The Grob test mix is used to evaluate the capillary column chromatographically and each compound gives a specific information about the column.¹¹³⁻¹¹⁴ The test mix is useful to evaluate the separation efficiency, adsorptive activity, hydrogen bonding interactions, and inertness (acid/base characteristic) of the column.³⁹ Figure 3-3 shows the analysis of the Grob test mix on four highest stability IL columns.

The symmetrical peaks of decane (5) and undecane (6) means that all the columns were properly produced and installed in the GC system.³⁹ The FAMES (compounds 2, 3, and 4) were well separated on all columns with symmetrical peaks and showed good separation efficiencies. The alcohols; 1-octanol (8) and 2,3-butanediol (10) are used for the evaluation of H-bonding interactions. The asymmetric peak shapes of 1-octanol (8) on **IL3**, **IL4** and **IL5** showed presence of H-bonding sites. 1-octanol (8) and 2,3-butanediol (10) co-eluted on **IL8** column with high tailing showing the presence of strong H-bonding interactions. The acid/base pair 2-ethylhexanoic acid (9), dicyclohexylamine (1) and 2,3-butanediol (10) were either irreversibly adsorbed or eluted with high peak tailing as they were indistinguishable from the base line. 1-nonanal (7) shows adsorptive interactions independent of H-bonding and it eluted with minor tailing on all the four IL columns. 2-ethylhexanoic acid (9) and 2,3-butanediol (10) were retained longest on C₉(mpy)₂-NTf₂ (**IL5**) compared to the other ILs.

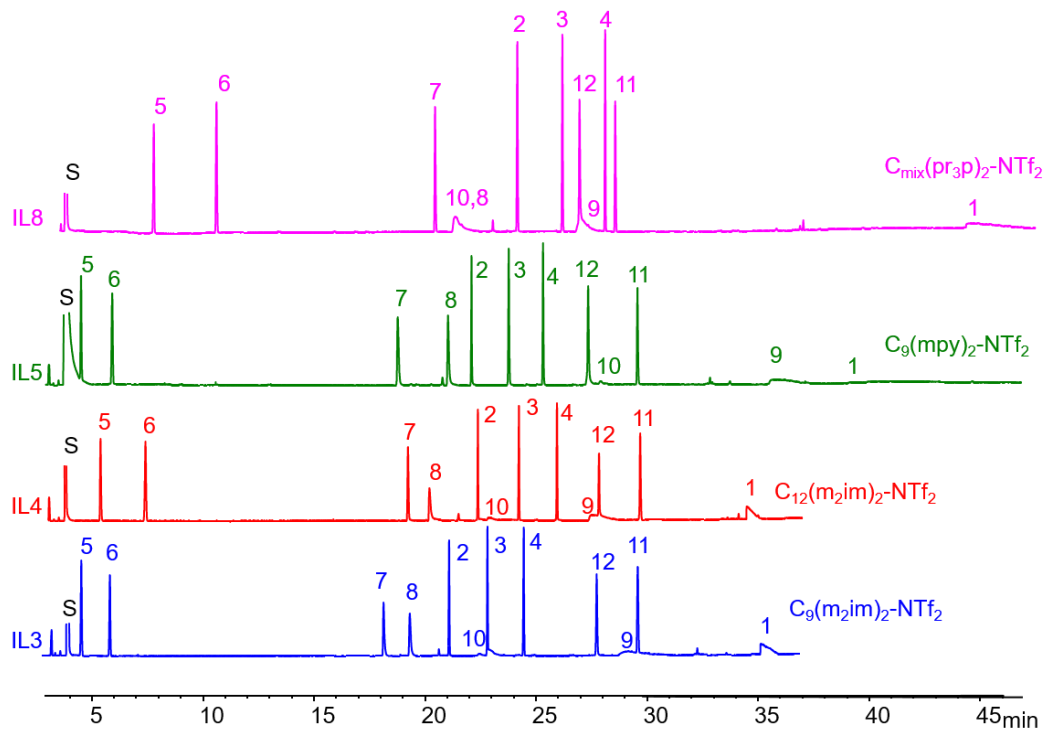


Figure 3-3 Separation of Grob test mix. 1) dicyclohexylamine 2) methyl decanoate (C10:0) 3) methyl undecanoate (C11:0 FAME) 4) methyl laurate (C12:0 FAME) 5) decane (C10) 6) undecane (C11) 7) 1-nonanal 8) 1-octanol 9) 2-ethylhexanoic acid 10) 2,3-butanediol 11) 2,6-dimethylaniline 12) 2,6-dimethylphenol S) dichloromethane. GC separation conditions: 40 °C for 5 min, 5 °C min⁻¹ to 200 °C; 1 mL min⁻¹ He; FID

3.4.4 Polar Plus test mix

Polar Plus test mix is a mixture of thirteen different polar and non-polar compounds at concentrations of 500 ppm each. The significance of the test mix is to understand the elution of polar compounds with respect to the nonpolar compounds (alkanes). The relative chromatographic behavior obtained from the analysis of Polar Plus test mix under identical conditions is shown in Figure 3-4.

2-octanone (1) showed variation in relative elution on all the stationary phases.

2-octanone (1) was less retained compared to alkanes on the phosphonium column (**IL8**).

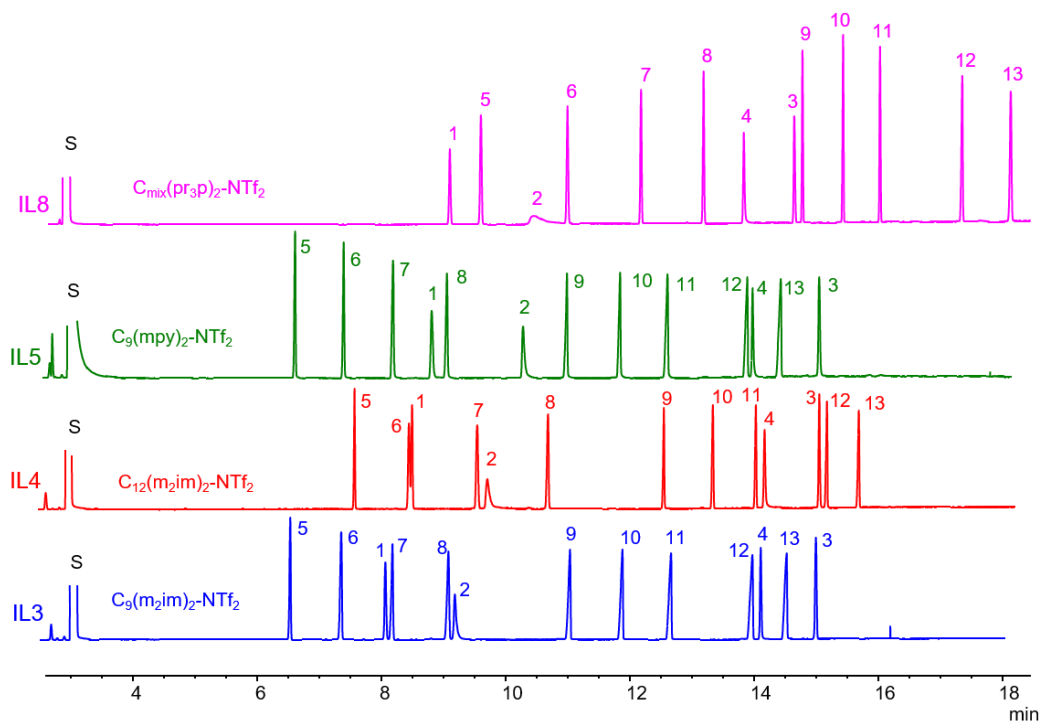


Figure 3-4 Separation of Polar Plus test mix. 1) 2-octanone 2) 1-octanol 3) 2,6-dimethylaniline 4) 2,6-dimethylphenol 5) pentadecane (C15) 6) hexadecane (C16) 7) heptadecane (C17) 8) octadecane (C18) 9) icosane (C20) 10) heneicosane (C21) 11) docosane (C22) 12) tetracosane (C24) 13) pentacosane (C25) S) dichloromethane. GC separation conditions: 60 °C for 3 min, 15 °C min⁻¹ to 120 °C, hold for 3 min, 15 °C min⁻¹ to 200 °C; 1 mL min⁻¹ He; FID

Also, the homologous series of alkanes were retained relatively longer on the phosphonium column compared to other ILs; supporting the nonpolar nature of the phosphonium IL. The order of elution of 2-octanone (1) and 1-octanol (2) with respect to the alkanes on all the columns was in accordance with the relative polarities of stationary phases (**IL5 > IL3 > IL4 > IL8**) (Refer to section 3.1 for relative polarities). Also, 2,6-

dimethylaniline (3) was retained longer than the highest alkane, C₂₅ (13), on the relatively polar C₉(mpy)₂-NTf₂ (**IL5**) and C₉(m₂im)₂-NTf₂ (**IL3**) ILs. Alkane C₂₅ (13) was retained longer than 2,6-dimethylaniline (3) on relatively nonpolar columns C₁₂(m₂im)₂-NTf₂ (**IL4**) and C_{mix}(pr₃p)₂-NTf₂ (**IL8**). All the IL columns showed reasonable retention for both polar and nonpolar compounds. This test mix is a good example of the “dual nature” behavior of ILs; which means they can act as a polar medium to retain polar compounds and a nonpolar medium to retain nonpolar compounds.

3.4.5 PAM-HC test mix

The PAM-HC test mix is a mixture of eight polynuclear aromatic hydrocarbons (PAHs) and seven saturated higher alkanes at concentrations of 100 ppm each. The test mix was used to evaluate the relative retention of aromatic and aliphatic hydrocarbons. This test mix contains low molecular weight PAHs. The chromatograms obtained from the analysis of PAM-HC test mix are shown in Figure 3-5.

Fluoranthene (7) and pyrene (8) are structural isomers and were well separated on all the IL columns. The C₄₄ alkane (15) (bp 547 °C) has a higher boiling point than fluoranthene (7) (bp 375 °C) and pyrene (8) (bp 404 °C). But, compounds 7 and 8 were retained longer than compound 15 on all IL columns. The alkanes were relatively less retained on the **IL3**, **IL4** and **IL5** columns, while they were retained longer on **IL8**. In general, alkanes with higher boiling points eluted earlier than the low boiling PAHs. This shows the stronger interaction of PAHs with the IL stationary phases. Compound 2 (bp 280 °C) and 3 (bp 279 °C) have similar boiling points, but the relative retention of compound 2 was longer compared to compound 3. The presence of additional double bond in compound 2 could be the reason for its longer retention. Fluorene (4) showed different selectivities towards different ILs mainly affected by the polarities of ILs. The

structural isomers, phenanthrene (5) and anthracene (6), were not separated on any of the four columns at the given temperature conditions (Figure 3-5).

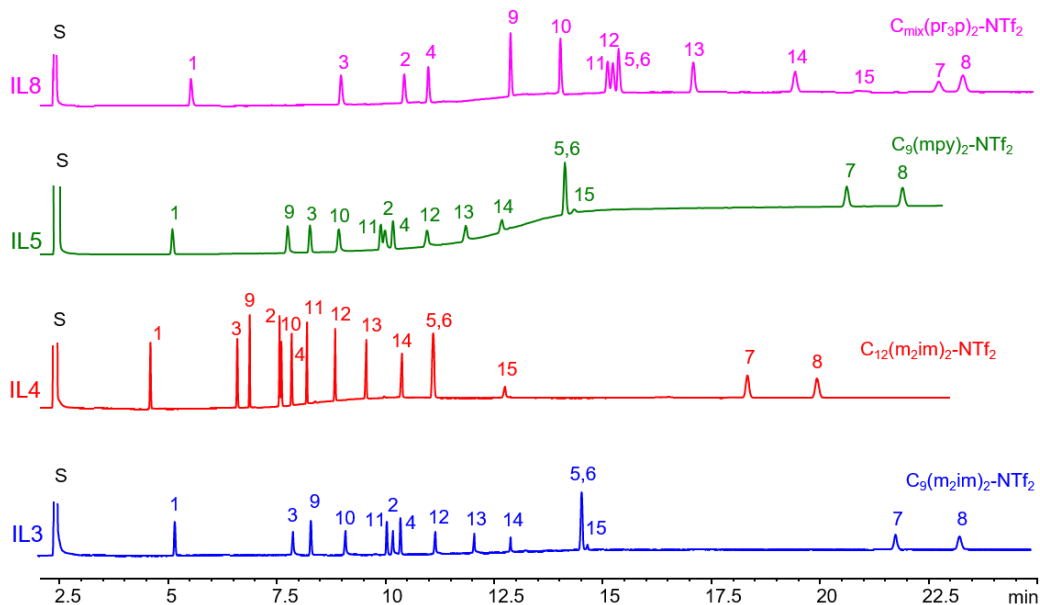


Figure 3-5 Separation of PAM-HC test mix. 1) naphthalene (MW- 128) (bp- 218 °C) 2) acenaphthylene (MW- 152) (bp- 280 °C) 3) acenaphthene (MW- 154) (bp- 279 °C) 4) fluorene (MW- 166) (bp- 295 °C) 5) phenanthrene (MW- 178) (bp- 340 °C) 6) anthracene (MW- 178) (bp- 340 °C) 7) fluoranthene (MW- 202) (bp- 375 °C) 8) pyrene (MW- 202) (bp- 404 °C) 9) triacontane (C30) (bp- 450 °C) 10) dotriacontane (C32) (bp- 467 °C) 11) tetratriacontane (C34) (bp- 483 °C) 12) hexatriacontane (C36) (bp- 497 °C) 13) octatriacontane (C38) (bp- 511 °C) 14) tetracontane (C40) (bp- 524 °C) 15) tetratetracontane (C44) (bp- 547 °C) S) dichloromethane. GC separation conditions: 160 °C for 4 min, 10 °C min⁻¹ to 250 °C; 1 mL min⁻¹ He; FID

3.4.6 Custom-PAM mix

Custom-PAM mix is another test mix of nine polycyclic aromatic hydrocarbons (PAHs) at concentration of 100 ppm each. It contains the high molecular weight PAHs (compared to PAM-HC test mix) and three different groups of structural isomers. One

group of structural isomers is: phenanthrene (2) and anthracene (3); the second group is: benz[a]anthracene (4), chrysene (5), and triphenylene (6); and the third group of structural isomers is: benzo(b)-fluoranthene (7), benzo[k]-fluoranthene (8) and benzo[j]-fluoranthene (9). The PAHs are generated due to incomplete combustion of organic matter and they are toxic environmental pollutants.⁷² The structural isomers of PAHs are difficult to separate and detect due to the high degree of overlap in their boiling points.⁷³ The analysis of test mix was significant to check the separation efficacy of ILs towards the high boiling structural isomers of PAHs. The analysis requires high temperatures and hence the test mix is also significant in evaluating the performance of IL stationary phases at higher temperatures (analysis done at 280 °C). The chromatograms obtained from the separation of the Custom-PAM test mix is shown in Figure 3-6.

Only the phosphonium column (**IL8**) was successful in the baseline separation ($R_s = 1.6$) of two structural isomers; phenanthrene (2) and anthracene (3) under the given analysis conditions (Figure 3-6). The other structural isomers; compounds 4, 5, and 6 were well separated on all of the IL columns. The separation of the benzofluoranthene structural isomers is difficult on the traditional polysiloxane based stationary phases and they typically coelute (generally, separation is carried out on phenyl and methyl substituted polysiloxanes).⁷⁴ But, the three benzofluoranthene isomers (compounds 7, 8 and 9) were well separated on all four dicationic IL columns.

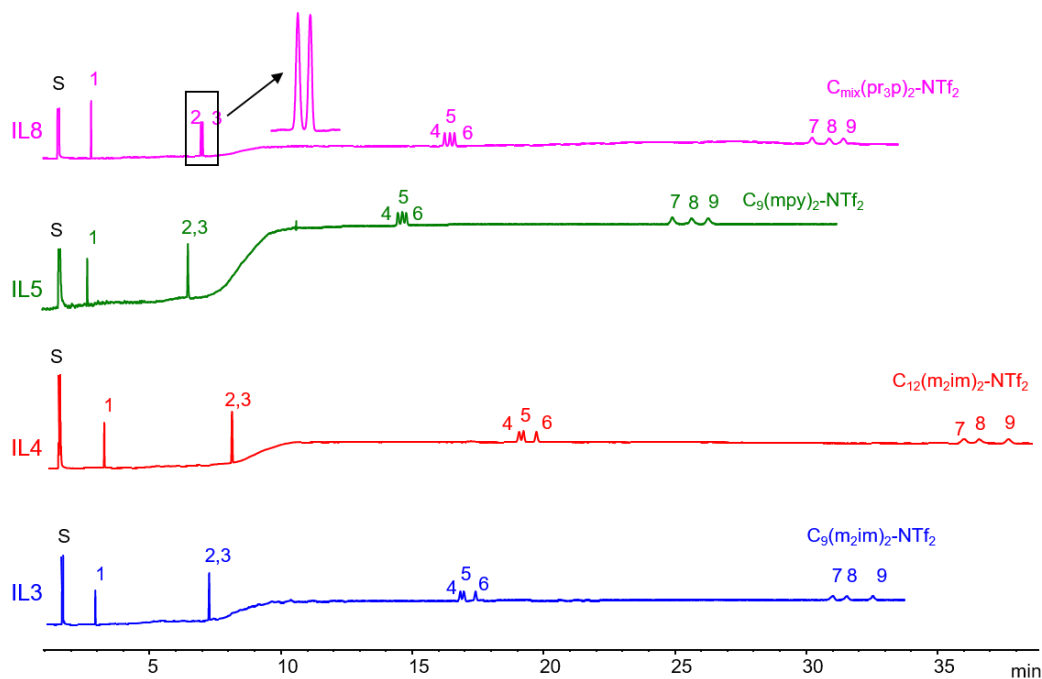


Figure 3-6 Separation of Custom-PAM test mix. 1) naphthalene (MW- 128) 2) phenanthrene (MW-178) 3) anthracene (MW- 178) 4) benzo(a)anthracene (MW- 228) 5) chrysene (MW- 228) 6) triphenylene (MW- 228) 7) benzo(b)fluoranthene (MW- 252) 8) benzo(k)fluoranthene (MW- 252) 9) benzo(j)fluoranthene (MW- 252) S) dichloromethane. GC separation conditions: 150 °C to 250 °C at 15 °C min⁻¹, hold for 2 min, 20 °C min⁻¹ to 280 °C; 1.5 mL min⁻¹ He; FID

3.4.7 Ionic Liquid test mix:

The Ionic Liquid test mix is a mixture of fourteen compounds with various functional groups. It contains aromatics, alkanes, FAMEs, a ketone, a sulfoxide, a lactone, an ester, and an amine. The function of this test mix is to compare the retention and selectivities of compounds with different functional groups. The separations obtained from the analysis of Ionic Liquid test mix is shown in Figure 3-7.

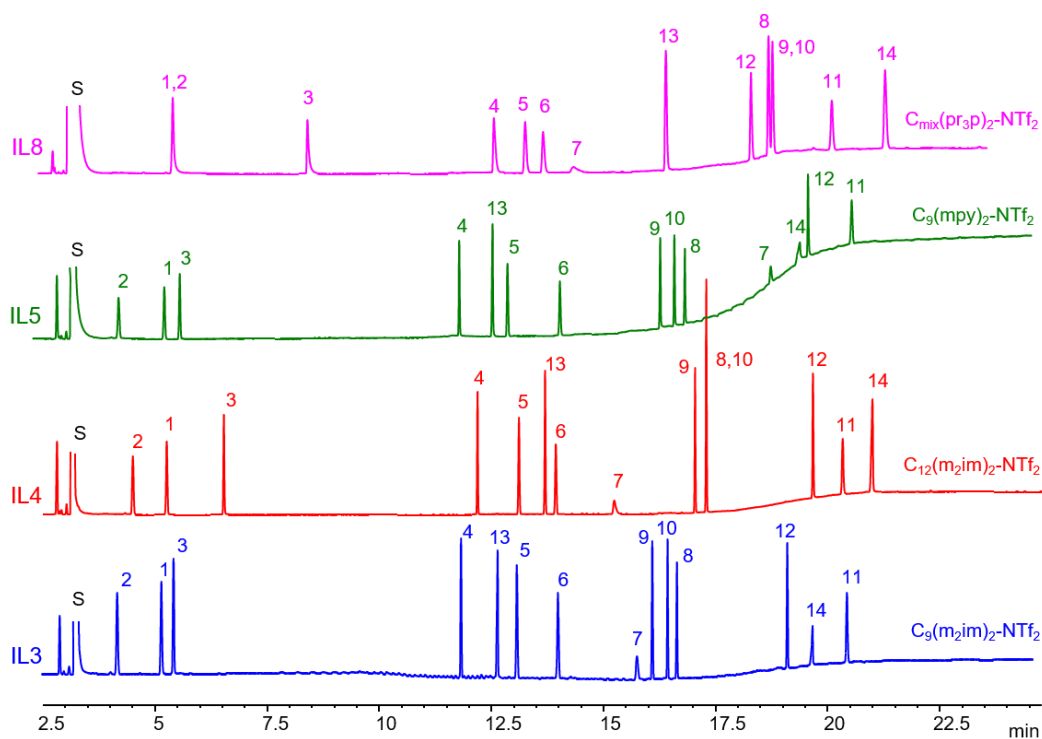


Figure 3-7 Separation of Ionic Liquid test mix. 1) toluene (bp- 110 °C) 2) camphene (bp- 159 °C) 3) tridecane (C13) (bp- 234 °C) 4) 2,6-di-*t*-butyl-4-methylene-2,5 cyclohexadiene-1-one (bp- 306 °C) 5) naphthalene (bp- 218 °C) 6) 2,6-dimethylaniline (bp- 216 °C) 7) dimethylsulfoxide (bp- 189 °C) 8) methyl linolenate (C18:3 FAME) 9) methyl arachidate (C20:0 FAME) 10) *cis*-11-Eicosenoic acid methyl ester (C20:1 FAME) 11) coumarin (bp- 301 °C) 12) dioctyladipate (bp- 405 °C) 13) tetracosane (C24) (bp- 391 °C) 14) tetracontane (C40) (bp- 524 °C) S) dichloromethane. GC separation conditions: 60 °C for 4 min, 15 °C min⁻¹ to 180 °C, hold for 2 min, 15 °C min⁻¹ to 250 °C; 1 mL min⁻¹ He; FID

The relative retention of non-polar compounds camphene (2) and tridecane (3) was observed with respect to toluene (1). Camphene (2) was less retained and elutes before toluene on nitrogen containing ILs (IL3, IL4, and IL5). The relative retention of tridecane (3) with respect to toluene (1) increased as the polarity of the stationary phase decreased (higher relative retention on IL4 and IL8 compared to IL3 and IL5). The ILs

$C_9(\text{mpy})_2 \text{NTf}_2$ (**IL5**) and $C_9(\text{m}_2\text{im})_2\text{-NTf}_2$ (**IL3**) displayed almost similar elution patterns for all the previously analyzed test mixes (see Figures 3-3 to 3-7). However, two ILs (**IL3** and **IL5**) displayed different selectivity towards dimethylsulfoxide (7). Compound 7 (DMSO) was retained much longer on $C_9(\text{mpy})_2 \text{NTf}_2$ (**IL5**) ($k = 4.50$) compared to $C_9(\text{m}_2\text{im})_2\text{-NTf}_2$ (**IL3**) ($k = 3.78$). The methylpyrrolidinium cationic IL displayed increased retention for the sulfoxide ($-\text{S}=\text{O}$) group containing compound relative to the imidazolium and phosphonium cationic ILs. A lactone coumarin (11) (bp 301 °C) and a diester dioctyladipate (12) (bp 405 °C) displayed retention independent of their boiling points even though they both contain carbonyl groups. High boiling compound 12 (dioctyladipate) eluted before the low boiling compound 11 (coumarin) on all the IL stationary phases. The same retention pattern independent of the boiling point but dependent on polarity was observed for coumarin (11) (bp 301 °C) and C40 alkane (14) (bp 524 °C). Compound 14 was retained longer on nonpolar **IL4** and **IL8** columns while it eluted earlier than (11) on the relatively polar **IL3** and **IL5** columns.

The four IL columns displayed good performance at higher temperatures (250 °C and 280 °C) for the analyses of the Ionic Liquid test mix and both the test mixes containing PAHs (Figures 3-5 to 3-7). The phosphonium column $C_{\text{mix}}(\text{pr}_3\text{p})_2\text{-NTf}_2$ (**IL8**) was observed to be the most stable and among the four ILs (showed least bleeding at 280 °C; Figure 3-6). The pyrrolidinium IL (**IL5**) was observed to be the most polar but displayed the least thermal stability (high bleeding at 280 °C; Figure 3-6). Both the imidazolium ILs displayed similar bleeding and stabilities at 280 °C (Figure 3-6).

3.5 Conclusions

In this study, we have demonstrated the effect of different IL structural features such as cation types, alkane linkage chains and anions on the polarities and selectivities

of geminal dicationic ILs. The polarities of IL stationary phases were observed to increase with a decrease in the length of alkane linkage chain. Benzyl-imidazolium cationic ILs were observed to be less polar than the methyl-imidazolium ILs. The presence of an aromatic substituent (benzyl group) on position 3 of the imidazole ring lead to decrease in polarity. N-methyl substituted pyrrolidinium dicationic ILs were more polar than N-butyl substituted pyrrolidinium dicationic IL. Within the three different types of dications following trends were observed for polarity of ILs: pyrrolidinium > imidazolium > phosphonium. The comparison of analogous ILs with different anions showed that NTf_2^- anionic ILs were more polar than the PFOS^- anionic ILs. The overall comparison of FAME test mix showed that $\text{C}_9(\text{mpy})_2\text{-NTf}_2$ was the most polar while the $\text{C}_{\text{mix}}(\text{pr}_3\text{p})_2\text{-NTf}_2$ was the least polar among all the ILs analyzed in this study.

Compounds do not elute relative to their boiling points on IL stationary phases. Also, IL columns were successful in the separation of the structural isomers of PAHs. The $\text{C}_9(\text{m}_2\text{im})_2\text{-NTf}_2$, $\text{C}_{12}(\text{m}_2\text{im})_2\text{-NTf}_2$, $\text{C}_9(\text{mpy})_2\text{-NTf}_2$, and $\text{C}_{\text{mix}}(\text{pr}_3\text{p})_2\text{-NTf}_2$ IL columns displayed good performance at high temperatures (280 °C) by separating the three benzofluoranthene isomers. The $\text{C}_{\text{mix}}(\text{pr}_3\text{p})_2\text{-NTf}_2$ was the highlight of this study which displayed the efficient separation of anthracene and phenanthrene isomers and also displayed better thermal stability compared to other ILs. The pyrrolidinium IL $\text{C}_9(\text{mpy})_2\text{-NTf}_2$ displayed lowest thermal stability among the four ILs. $\text{C}_9(\text{mpy})_2\text{-NTf}_2$ and $\text{C}_9(\text{m}_2\text{im})_2\text{-NTf}_2$ showed almost similar elution pattern for all the compounds analyzed except for dimethylsulfoxide. The pyrrolidinium column displayed higher interaction towards the sulfoxide group compared to other ILs. The IL with pyrrolidinium dication displayed stronger hydrogen bonding interactions compared to the analogous ILs with imidazolium and phosphonium dications.

Chapter 4

DICATIONIC IONIC LIQUID THERMAL DECOMPOSITION PATHWAYS

4.1 Abstract

The rapid expansion in the study and use of ionic liquids (ILs) is a result of their unique properties including negligible volatility, high thermal stability and ability to dissolve disparate compounds. However, because ILs have infinitely variable structures (often referred to as “tunability”), these properties can differ considerably. Herein, we focus on the thermal stability of fifteen bis/dicationic ionic liquids. Specifically, their thermal breakdown products are examined to determine the structural linkages, bonds or atoms most susceptible to thermally induced changes and whether such changes occur before possible volatilization. In most cases, the heteroatom carbon single bonds were susceptible to thermolytic decomposition.

4.2 Introduction

Salts with melting points lower than 100°C are referred to as ionic liquids (ILs) ⁶. Since their rediscovery at the end of the last century, these innovative fluids found applications in different branches of chemistry such as liquid-liquid extraction ¹¹⁵, microextractions ^{2, 116}, solvents for extraction of DNA ¹¹⁷⁻¹¹⁸, mass spectrometry ^{83-85, 119}, electrochemistry ^{89, 91}, spectroscopy ^{2, 120}, high performance liquid chromatography ¹²¹⁻¹²², and capillary electrophoresis ¹²³⁻¹²⁴. Thanks to their extremely low vapor pressure, nonflammability, wide liquid temperature range, and high thermal stability, ILs have been successfully applied in high temperature environments (such as liquid thermal storage media ²⁵, high temperature lubricants ^{26, 125}, lubricant additives ^{27, 126}, solvents for high temperature reactions ^{20-21, 65}, gas chromatography (GC) stationary phases ^{13, 22, 127}, solvents for headspace GC ^{23-24, 103-104}, high temperature non-flammable electrolytes for

batteries ²⁸, etc.) and high vacuum environments (high performance lubricating greases for space ²⁹ and high vacuum lubricants ^{30, 128}). In fact, the IL thermal stability can vary considerably depending on the nature of the IL anion and cation. Bis- or di-cationic, imidazolium based or phosphonium based ILs, often show decomposition temperatures higher than traditional monocationic ILs ^{11, 110}. The anion also can play a significant role in the IL thermal stability, e.g., nucleophilic halogens can attack the cation moiety ^{11, 31}.

The most striking features of ILs are their low volatilities and high thermal stabilities, compared to common organic solvents. There are several methods reported for determining thermal stabilities of ILs. The short-term IL thermal stability is determined by thermogravimetric analysis (TGA) using temperature ramps of 5-10 °C/min and measuring the temperatures of 5% weight loss (T_d) ^{12, 31, 110}. The T_d temperatures are useful to compare the thermal stabilities of different ILs ¹¹⁰. Since thermal stability is a time-dependent process, different results may be obtained when ILs are exposed to thermal stress for longer periods ⁶⁷. The long term thermal stability; determined by monitoring weight loss by isothermal TGA experiments, provides detailed information on the stabilities/volatilities and/or rates of decomposition of ILs ³¹. In kinetic studies, determination of frequency factor and activation energies, using the Arrhenius equation, provides information about the frequency of molecular collisions (collisions between cations and anions) and the proportion of collisions resulting in decomposition reactions respectively ¹²⁹. The long term thermal stability is also determined by inverse gas chromatography, in which the column bleed is monitored by highly sensitive detectors as a function of temperature ^{11, 13, 110}. The observed mass loss upon heating can be due to volatilization (formation of neutral ion pairs (NIPs)) or to real thermal decomposition (TD) ^{31, 130}. Along with mass loss, ILs also can show color changes after heating at high

temperatures, long storage times, and wear/ friction in tribological applications which can be related to decomposition and formation of side products ^{20, 129, 131}.

Most IL literature focuses on the determination of thermal stabilities, methods to determine thermal stabilities, rates of decomposition, etc. Little attention has been paid to the analysis of decomposition products, the reasons for weight loss, and color changes in ILs at higher temperatures. Recent reports have shown that the thermal stabilities of ILs can be altered by structural modifications ^{12, 127, 132}. These reports compile trends of the “structure-thermal stability” relationships of ILs but do not provide any detailed explanation about the effects of various structural moieties on the IL decomposition. There are only a few reports on the thermal degradation products of some imidazolium and pyrrolidinium monocationic ILs ^{129, 133-135}, and no reports on the analysis of decomposition products of dicationic ILs. The degradation studies of imidazolium-based monocationic ILs were done by pyrolysis GC-MS and established that the decomposition started by the removal of alkyl substituents on the imidazole ring ¹³³⁻¹³⁴, while the monocationic pyrrolidinium-based ILs with cyano anions were observed to polymerize at higher temperatures ¹³⁵.

Considering the popularity of dicationic ILs in high temperature applications, the results of a degradation study can be helpful for their optimal use, determining their changes at high temperatures and for providing information on possible structural modifications to further improve stability. The present work summarizes the results of a systematic and comprehensive thermal decomposition study performed on fifteen bis-(trifluoromethylsulfonyl) imide (NTf₂) dicationic imidazolium, pyrrolidinium, and phosphonium-based ILs at 400-440 °C. The effect of different linkages such as straight alkane chains, polyethylene glycol chains, and branched alkane chains on the thermal behavior of ILs also was evaluated via these degradation studies. The soft ionization

technique, electrospray ionization mass spectrometer (ESI-MS) was used to avoid the further fragmentation of decomposition fragments and to identify them, in contrast to what can be accomplished with pyrolysis GC-MS.

4.3 Materials and Methods

4.3.1 Instruments

The analyses were performed on a mass spectrometer Finnigan LXQ ESI-MS (Thermo Fisher Scientific, San Jose, CA). The ESI analysis conditions: spray voltage - 4.5 kV, sheath gas flow rate - 35, aux gas flow rate - 6, capillary temperature - 275 °C, capillary voltage - 16 V, tube lens - 110 V, scan range - 50-1000 m/z, positive mode.

4.3.2 Materials

1-Benzyl-2-methylimidazole (90%), 1,2-dimethylimidazole (98%), N-methylpyrrolidine (97%), tripropylphosphine (97%), 1-(2-hydroxyethyl) imidazole (97%), 1,9-dibromononane (97%), 1,5-dibromopentane (97%), 3-bromo-2-bromomethyl-1-propene (97%), 1-bromo-3-(2-bromoethyl)-4,4-diethylpentane, 1,3-dibromobutane (97%), tetraethylene glycol (99%), phosphorus tribromide (99%), and bis(trifluoromethane)sulfonyl imide lithium salt (99.95%) were purchased from MilliporeSigma (ex-Sigma-Aldrich, St. Louis, MO). 1,5-Dibromo-3-methylpentane (98+%) was purchased from Alfa Aesar (Haverhill, MA). 1,5-dibromo-3,3-dimethylpentane (95%) was obtained from Alfa Chemistry (Holtsville, NY). 1,3-dibromo-2-methylpropane (95+%) was purchased from Oakwood Chemicals (Estill, SC). The detailed procedures for synthesis of ILs are reported in the literature^{17, 110, 136}.

4.3.3 Experimental Design

4.3.3.1 Analysis of vapor phase decomposition products:

Approx. one gram of ionic liquid was placed in a 25 mL clean and dry three neck round bottom flask fitted with a thermometer and short condenser. A flask was attached at the other end of the condenser which was kept in a dry ice/acetone bath at $-78\text{ }^{\circ}\text{C}$. An argon line was inserted in to the flask through one of the necks (Figure 4-1). The assembly was purged with argon for 15 minutes before starting the experiment. The temperature of flask was raised gradually at a rate of about $5\text{-}8\text{ }^{\circ}\text{C}/\text{min}$ from room temperature to $400\text{ }^{\circ}\text{C}$ and hold for 30 minutes. During heating, argon was flowing over the ILs carrying the volatile products along with it to the other flask kept in dry ice/acetone bath. Different volatile fractions were collected at $300\text{ }^{\circ}\text{C}$, $350\text{ }^{\circ}\text{C}$, $400\text{ }^{\circ}\text{C}$, and after 30 minutes of heating at $400\text{ }^{\circ}\text{C}$. The collection flask was rinsed with methanol. The solution was further diluted with methanol/water (50/50). The samples were analyzed by ESI/MS.



Figure 4-1 The Experimental setup for the collection of volatile fragments

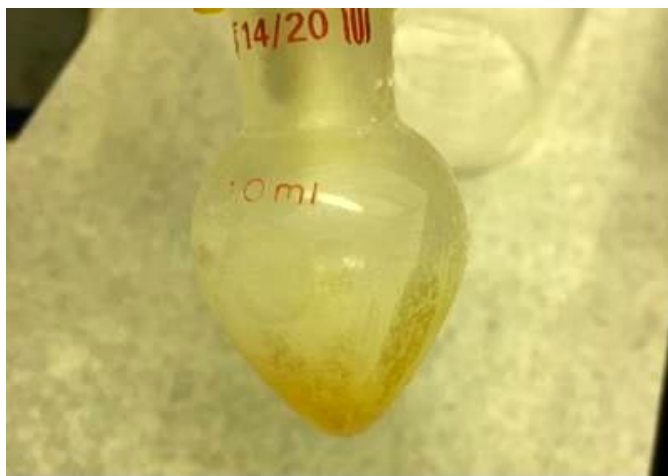


Figure 4-2 The volatiles collected in collection flask after heating IL1 $C_9(m_2im)_2-NTf_2$, 400 °C, 30 min.

4.3.3.2 Analysis of residual decomposition products:

In argon atmosphere:

0.2 mL of ionic liquid was placed in a 1 mL ampoule. The ampoule was purged with argon and then sealed. The sealed ampoule was then heated in a GC oven at 440 °C for 30 min. After heating a charred residue was obtained that was further dissolved in methanol. The solubility of all heated IL was low and most of the charred black residue was insoluble. The solution was filtered and further diluted with methanol/water (50/50). The sample was then analyzed by direct infusion in the electrospray ionization mass spectrometer (ESI/MS).

In air:

0.2 mL of ionic liquid was placed in a 1 mL ampoule. The ampoule was sealed in air and then heated in a GC oven at 440 °C for 30 min. After heating, a charred residue was obtained. The charring was more severe compared to the samples analyzed under argon atmosphere. The residue had very low solubility in methanol and most of the charred black residue was insoluble. The solution was filtered and further diluted with

methanol/water (50/50). The sample was then analyzed by ESI/MS. As the air sealed ILs showed severe charring and low solubility in methanol, the degradation study was performed by purging the vials with argon before sealing. The decomposition studies in air were performed only with some ILs when more information was needed.

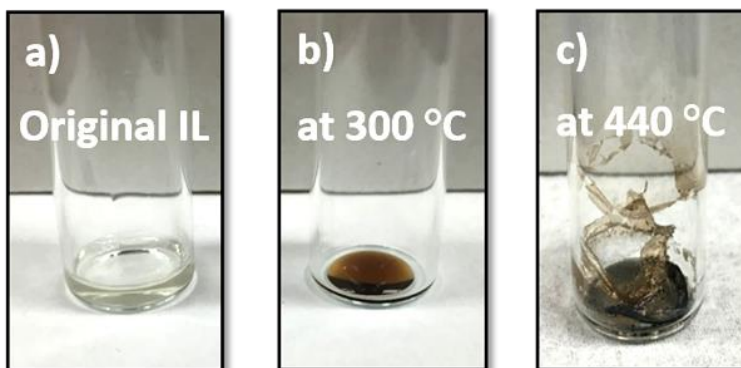


Figure 4-3 The pictures of IL1 $C_9(m_2im)_2-NTf_2$ taken after heating at different temperatures. a) The original IL1; b) The IL1 collected from the flask of vapor decomposition products analysis at 300 °C. c) The IL1 after heating at 440 °C for 30 min under air.

4.4 Results and Discussion

Fifteen different dicationic ILs (**IL1** to **IL15**), either di-imidazolium, di-pyrrolidinium, or di-phosphonium paired with bis-(trifluoromethylsulfonyl)imide (NTf_2) anions were synthesized. Five dicationic ILs were made with a nonane (C_9) alkyl spacer, three with a polyethylene glycol (PEG, three units) spacer, three with branched C_3 spacers, one with a C_5 linkage spacer, and three with branched C_5 spacers^{17, 110}. Their thermal behavior was tested as per the procedure outlined in the Experimental Design.

4.4.1 Analysis of straight chain linkage ILs

Table 4-1 lists the structure of the eight ILs, coded **IL1** to **IL8**, along with, the three major peaks seen in the mass spectra of the residual ILs after 30 min heating at

400°C, in decreasing intensity order. The mass spectra of the collected volatiles were much richer in peaks than those of the residual heated ILs. **Table 4-2** lists similarly the four major peaks seen in the spectra of the collected volatiles along with the bonds broken to form these fragments. **Figure 4-4** compared the mass spectrum of the **original IL1 (Figure 4-4A)** with that of the 400°C heated **IL1 residue (Figure 4-4B)**, and the corresponding spectrum of the **collected IL1 volatiles** after 30 min of heating at 400 °C (**Figure 4-4C**).

On visual inspection, apart from some darkening, **IL1** is practically unchanged after heating at 400°C for 30 min. The mass spectrum of the heated **IL1** is practically identical to the initial spectrum showing a very small 152 m/z peak, likely the result of N-methyl elimination (**Figures 4-4A and 4-4B**). A color change is observed (see **Figure 4-3**), and trace amounts of volatiles were collected giving the **Figure 4-4C** mass spectrum. As listed in **Table 4-2**, the 207 m/z peak corresponds to the loss of a dimethylimidazole group plus a methylene group. The possible mechanism for the loss of alkyl substituents on the imidazole ring is shown in **Figure 4-6**. The loss of alkyl substituents on the imidazole ring due to the nucleophilicity of an anion, known as the “reverse Menshutkin reaction” was observed in case of ammonium and imidazolium cations paired with halide ions^{31, 66, 133, 137}. Since halides being more nucleophilic, the reaction can occur at lower temperatures (<100 °C), decreasing the thermal stability of ILs.³¹ The NTf₂ anion is less nucleophilic compared to the halides, which provides higher thermal stabilities and the reverse Menshutkin reaction occurs at higher temperatures (> 350 °C). Further fragmentation was observed with loss of methylene groups from the alkyl chain with intervals of m/z 14 (**Figure 4-4C**). The sequential loss of CH₂ groups is a characteristic feature of alkanes observed under electron ionization experiments¹³⁸.

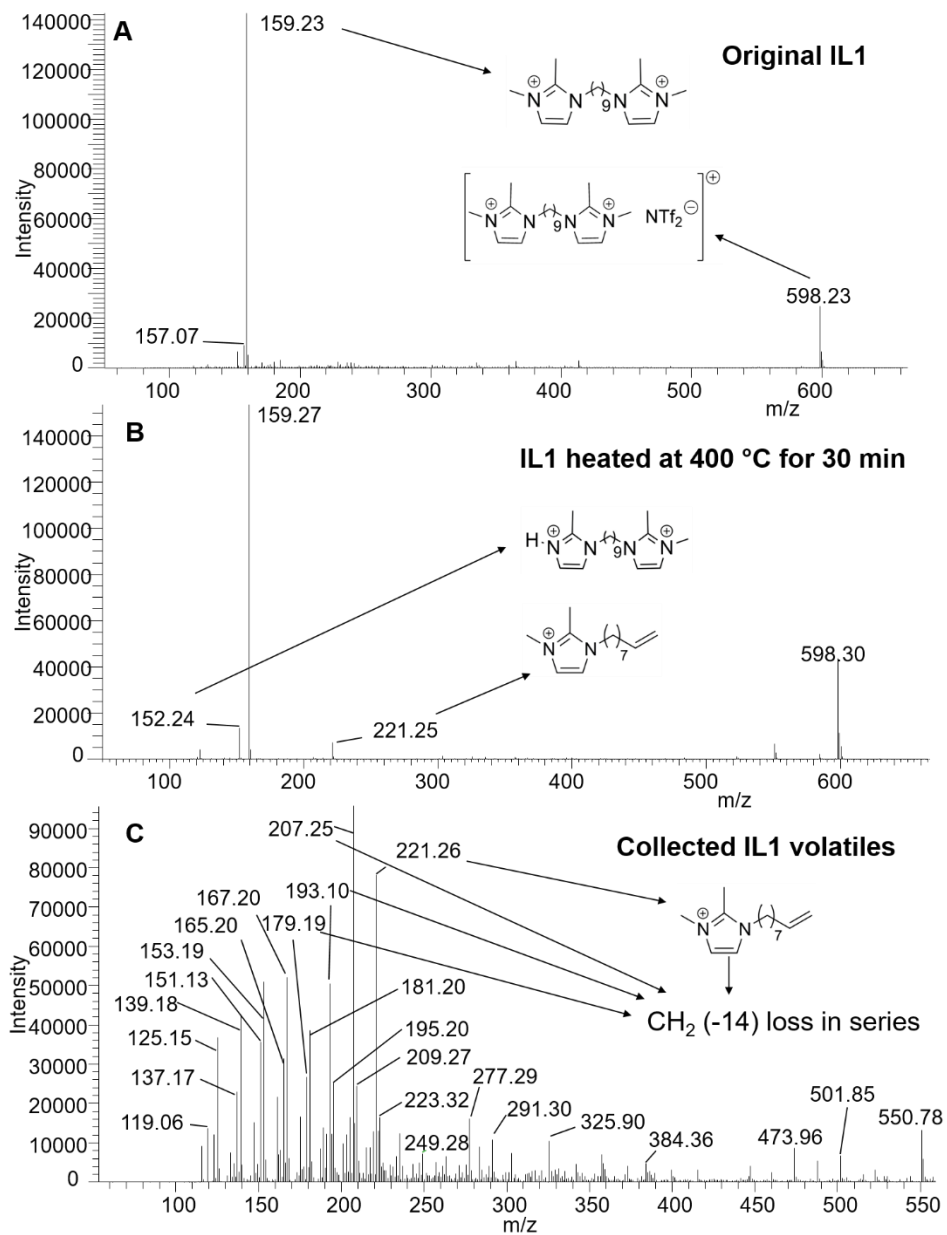


Figure 4-4 Mass spectra of IL1. A- original IL; B-residual IL1 after heating at 400°C for 30 min; C- methanolic solution of collected IL1 volatiles after heating at 400°C for 30 min.

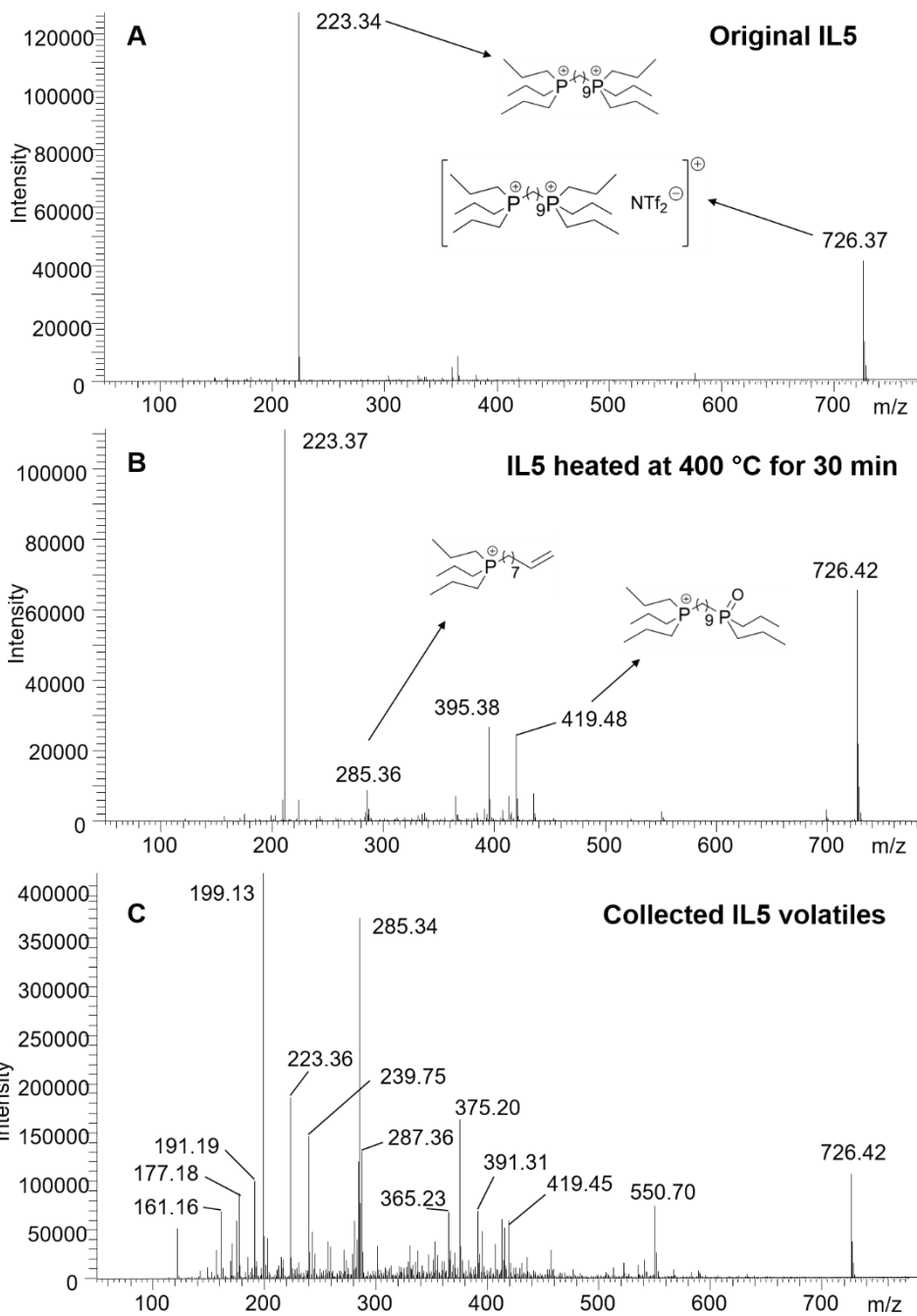


Figure 4-5 Mass spectra of IL5. A- original IL; B-residual IL5 after heating at 400°C for 30 min; C- methanolic solution of collected IL5 volatiles after heating at 400°C for 30 min.

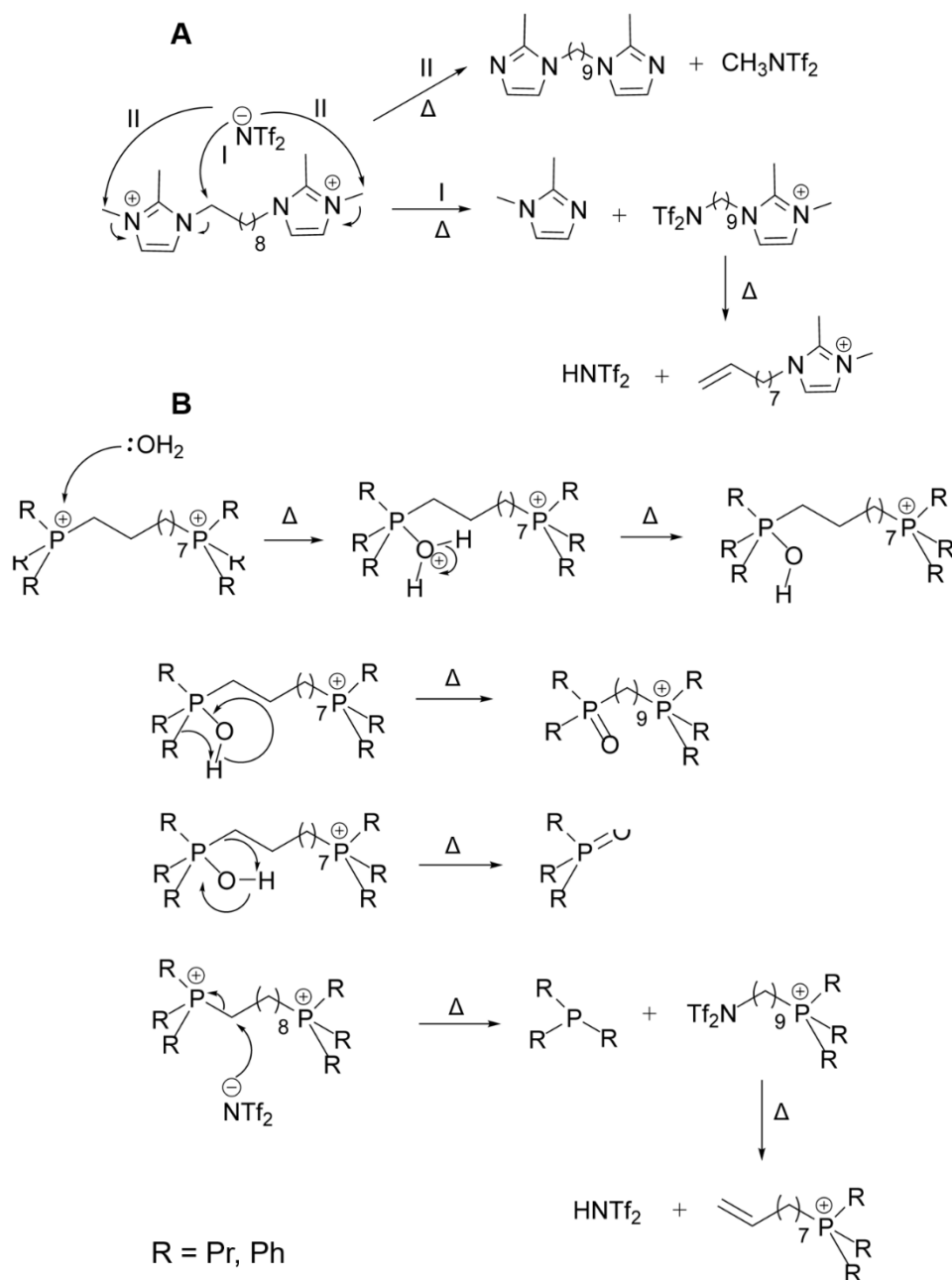


Figure 4-6 Postulated mechanism for the decomposition of ILs. A) Imidazolium based ILs.
B) Phosphonium based ILs.

Figure 4-5 shows the mass spectra of the **original IL5 (Figure 4-5A)**, the **IL5 residue (Figure 4-5B)** collected after heating at 400°C, and the **collected IL5 volatiles** after 30 min of heating at 400 °C (**Figure 4-5C**). An important point to note is that the mass spectra of the collected volatiles of phosphonium ILs with alkyl (C₉) linkage, **IL5**, and **IL6**, showed small peaks at respectively m/z 223 and 325 (**Figure 4-5C**). They correspond to the intact dicationic IL demonstrating the possibility of volatile NIP formation for these two ILs. The mass spectrum of the collected volatiles was more complex compared to the residual IL and showed multiple fragments due to the breaking of C-P bonds and C-C bonds (**Table 4-2, Figure 4-5**). The mass spectra of residual **IL5** and collected volatiles showed peaks at m/z 419 and 199. The peaks were of interest, as they belonged to the formation of oxides by **IL5** at high temperatures. The possible mechanism for the formation of phosphine oxides is shown in **Figure 4-6**. Despite the inert atmosphere, trace moisture content of the argon may have led to the oxide formation. The formation of phosphine oxides was also observed during the thermal degradation study of quaternary phosphonium based montmorillonites¹³⁹⁻¹⁴⁰. Like **IL5**, **IL6** also showed the formation of oxides at high temperatures (see **Figure 4-7**). The results for **IL6** were similar to **IL1**, with a practically unchanged mass spectrum compared to the original IL, and a spectrum of the trace collected volatiles showing phosphorus oxidation and some thermal breakings (**Table 4-2**) (see **Figure 4-7**).

The six other ILs had different behaviors. For **IL2**, **IL5**, and **IL8** the original IL peak, observed before heating, was still visible in the spectrum of the heated residual IL (see **Figures 4-8, 4-9, and 4-10**). However, it was not the highest peak and was accompanied by several peaks denoting partial but significant thermal decomposition. Indeed, the corresponding spectra of the collected fumes showed a wealth of IL thermal fragments (**Table 2**) (see **Figures 4-11, 4-12, and 4-13**).

IL3, **IL4**, and **IL7**, the ILs with a three-unit PEG spacer, were completely destroyed by 30 min heating at 400°C. **Table 4-1** lists the m/z values of major peaks seen in the crowded MS spectra obtained by infusing the methanol solution that washed the black carbonaceous material remaining in the vial. The PEG linked ILs started decomposing at about 300 °C as fragments due to the breaking of C-O bonds (possible mechanism shown in the **Fig 4-14**) were observed in the mass spectra of collected volatiles at 300 °C. The decomposition at lower temperatures can also be seen with lower T_d temperatures of all three PEG ILs (**Table 4-2**).

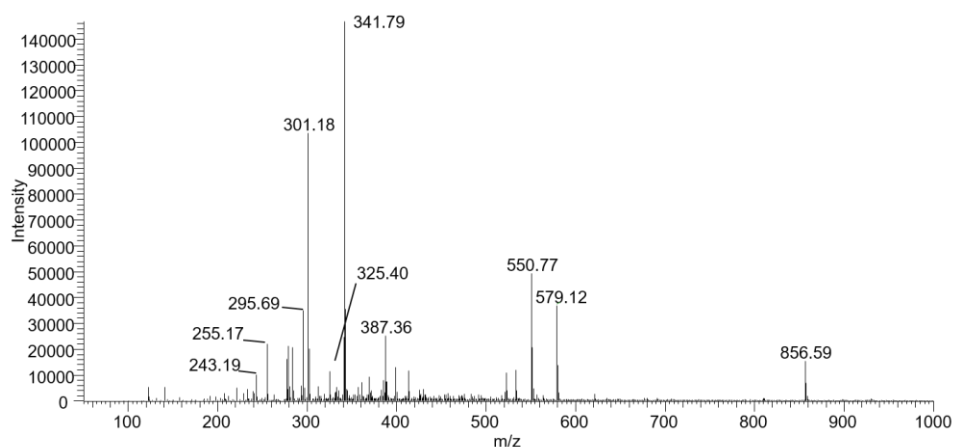


Figure 4-7 ESI Mass spectrum of the volatile fraction of IL6 $C_9(ph_3p)_2-NTf_2$ collected after heating at 400 °C for 30 min.

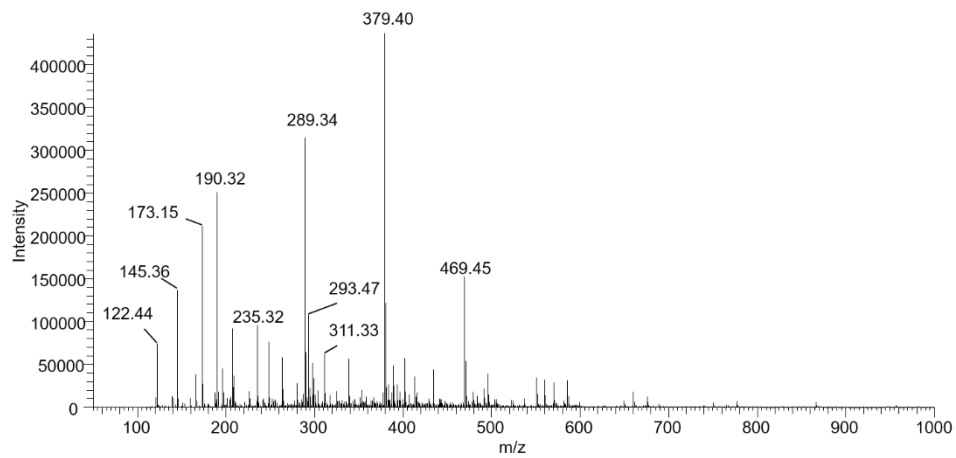


Figure 4-8 ESI mass spectrum of residue of IL2 $C_9(\text{bzmim})_2\text{-NTf}_2$ collected after heating up to 400 °C

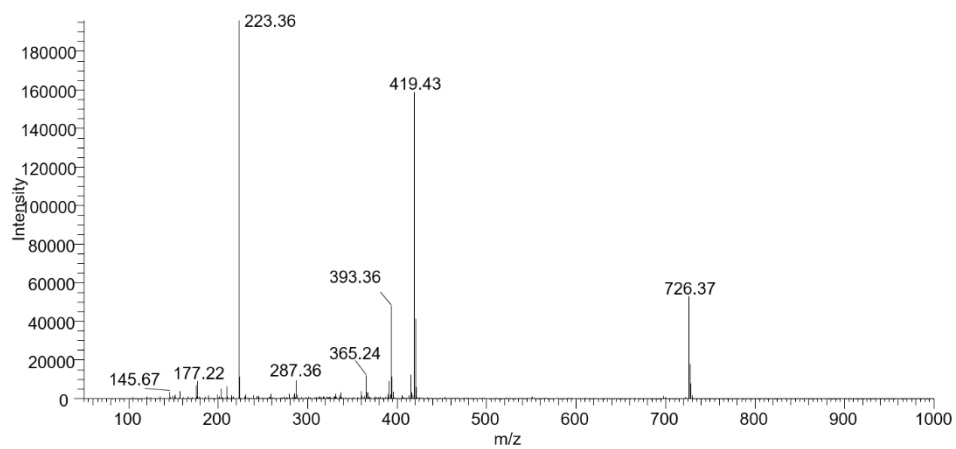


Figure 4-9 ESI mass spectrum of residue of IL5 $C_9(\text{pr}_3\text{p})_2\text{-NTf}_2$ collected after heating at 440 °C for 30 min in air

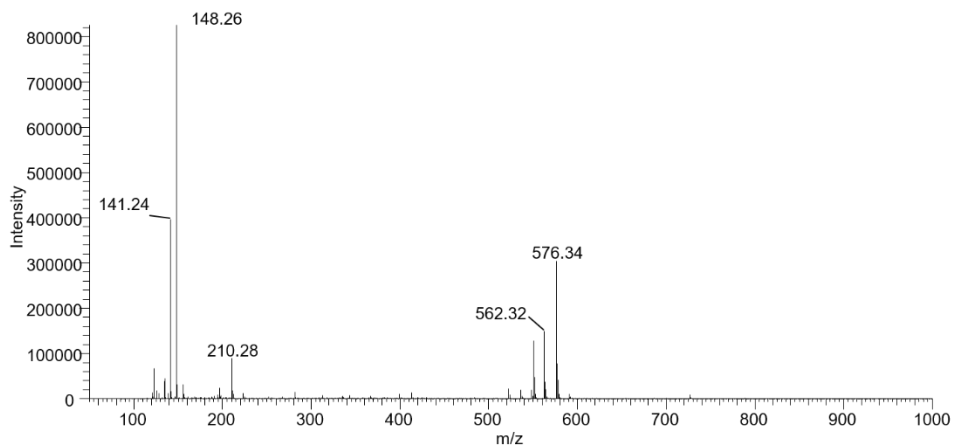


Figure 4-10 ESI mass spectrum of residue of IL8 $C_9(\text{mpy})_2\text{-NTf}_2$ collected after heating up to 400°C.

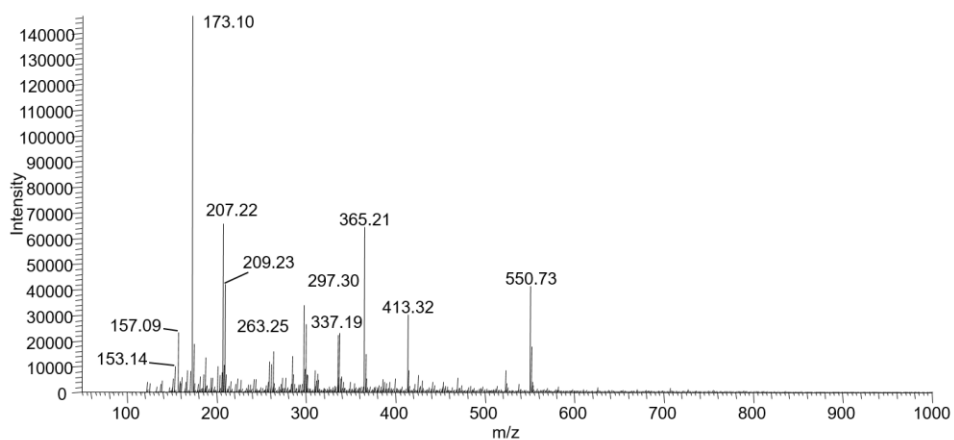


Figure 4-11 ESI Mass spectrum of the volatile fraction of IL2 $C_9(\text{bzmim})_2\text{-NTf}_2$ collected after heating at 400 °C for 30 min.

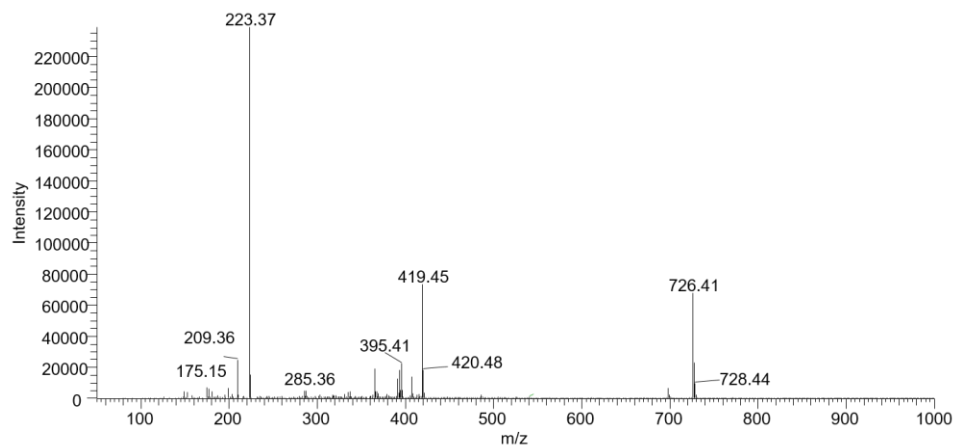


Figure 4-12 ESI mass spectrum of residue of IL5 $C_9(pr_3p)_2-NTf_2$ collected after heating at 440 °C for 30 min in argon atmosphere

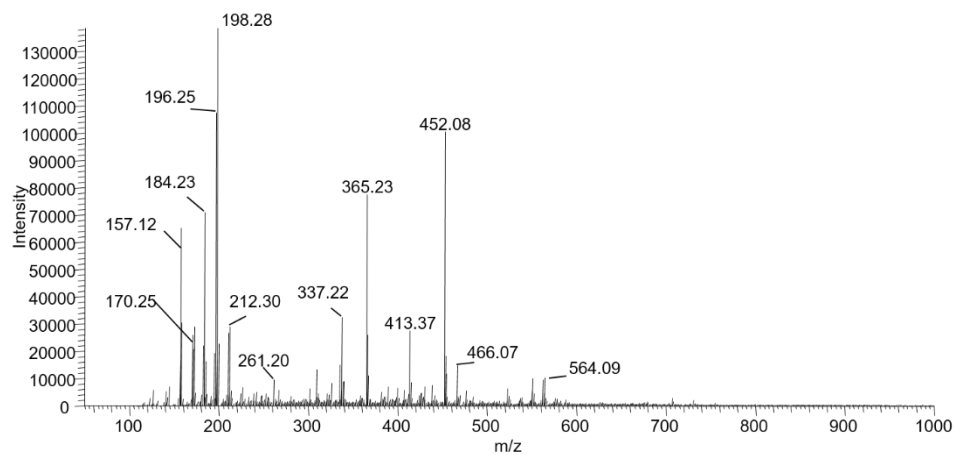
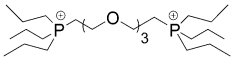
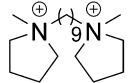


Figure 4-13 ESI Mass spectrum of the volatile fraction of IL8 $C_9(mpy)_2-NTf_2$ collected after heating at 400 °C for 30 min.

Table 4-1 MS peaks of residual (non-volatile) dicationic NTf₂ ionic liquids seen after heating at 400 °C for 30 min under argon flow.

IL Code	Dication structure	Dication m.w.	T _d ^a °C	Peak 1		Peak 2		Peak 3	
				Mass	Broken bond	Mass	Broken bond	Mass	Broken bond
IL1		318.54	467 ^b	intact 318 (m/z 159)	none	dication + NTf ₂ 598	none	loss of methyl 304 (m/z 152)	C-N
IL2		470.34	437 ^b	loss N- benzyl 379	C-N	loss of 2 benzyls 289	C-N	loss of linkage 173	C-N
IL3		352.25	362	141	C-O	139	C-O	125	C-O
IL4		384.24	340	139	C-O	complete degradation			
IL5		446.42	464 ^b	intact 446 (m/z 223)	none	dication + NTf ₂ 726	none	loss of propyl, gain O 419	C-P oxidation
IL6		650.83	424 ^b	intact 650 (m/z 325)	none	dication + NTf ₂ 930	none	NA	

Table 4-1 – continued

IL7		480.39	398	187	C-O	complete degradation			
IL8		296.32	373 ^b	intact 296 (m/z 148)	none	loss of methyl 282 (m/z 141)	C-N	dication + NTf ₂ 576	none

^a Temperature of 5% weight loss determined with thermogravimetric analysis (TGA). Conditions: 10 °C/min from room temperature (22 °C) to 600 °C.
^b T_d temperatures taken from reference 14.

Table 4-2 MS peaks of the volatiles emitted by dicationic NTf₂ ionic liquids after heating at 400 °C for 30 min under argon flow.

IL Code	Peak 1		Peak 2		Peak 3		Peak 4	
	Mass	Broken bond	Mass	Broken bond	Mass	Broken bond	Mass	Broken bond
IL1	207	C-N imidazole C-C methylene	221	C-N imidazole	193	C-N imidazole + 2 C-C methylene	167	C-N imidazole + 4 C-C methylene
IL2	173	C-N benzyl imidazole	207	as 1 + C-N benzyl	209	as 2 + C-C methylene	297	C-N loss of benzyl-imidazole
IL3	125	C-N and C-O bonds	139	C-N and C-O bonds	141	C-N, C-C and C-O bonds	153	C-N, C-O
IL4	244	C-N and C-O bonds	322 (m/z 161)	C-C bonds	139	C-N and C-O bonds	125	C-N and C-O bonds
IL5	199	C-P + oxidation	285	C-P	223	none	375	C-P + oxidation
IL6	683 (m/z 341)	dioxidized IL	387	C-P	373	C-P + C-C methylene	301	C-P + oxidation
IL7	453	C-P + oxidation	187	C-P and C-O bonds	161	C-P, tripropyl phosphonium	199	C-P
IL8	198	C-N pyrrolidine + C-C methylene	196	C-N pyrrolidine + C-C methylene	184	C-N pyrrolidine + 2 C-C methylene	170	C-N pyrrolidine + 3 C-C methylene

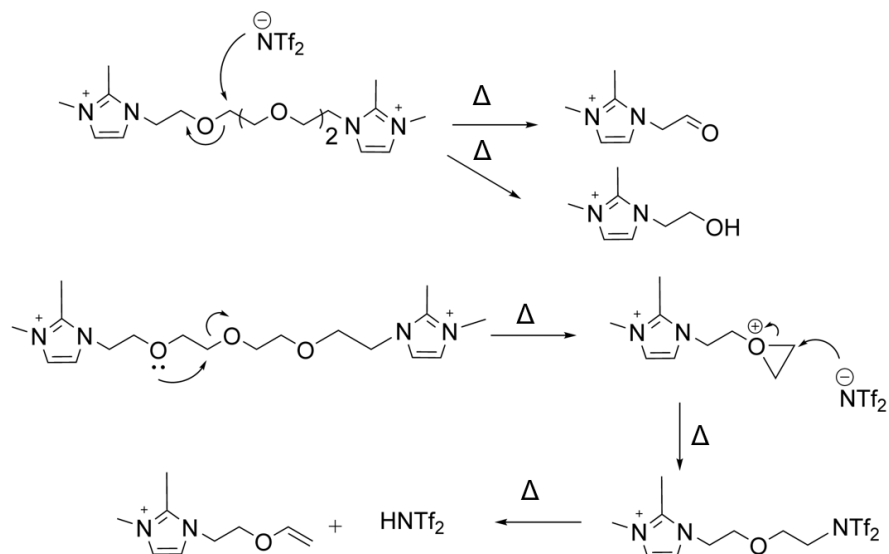


Figure 4-14 Postulated mechanism for the thermal decomposition of PEG linked ILs.

To complete this study, the 400°C-resistant ILs, i.e., **IL1**, **IL2**, **IL5**, **IL6**, and **IL8**, were submitted to a 440°C test. For each IL, an ampoule containing 0.2 mL of IL was sealed under argon and placed in an oven able to generate a 440°C regulated temperature. A second ampoule was similarly prepared in the air (no argon purging) and 440°C heating. **IL2** and **IL8** were completely decomposed by heating at 440°C for 30 min leaving black solid material in the vials. The **IL5** and **IL6** MS base peaks, corresponding to the intact phosphonium dicationic ILs with C₉ spacer were observed (see **Figure 4-12**). The intensity of the m/z 419 (**IL5**) peak (oxidized IL) was, not surprisingly, much higher under air than under argon heating (see **Figures 4-9** and **4-12**). **IL1** showed some darkening color but seemed to mostly withstand the 440°C temperature both under argon and air (see **Figures 4-15** and **4-16**). There was more degradation under air than under argon as seen by the darker color of heated **IL1** and the lower solubility of the residual material in methanol. However, the two mass spectra of

the extracted methanolic solutions still showed the intact **IL1** peak and some degradation fragments (see **Figures 4-15** and **4-16**).

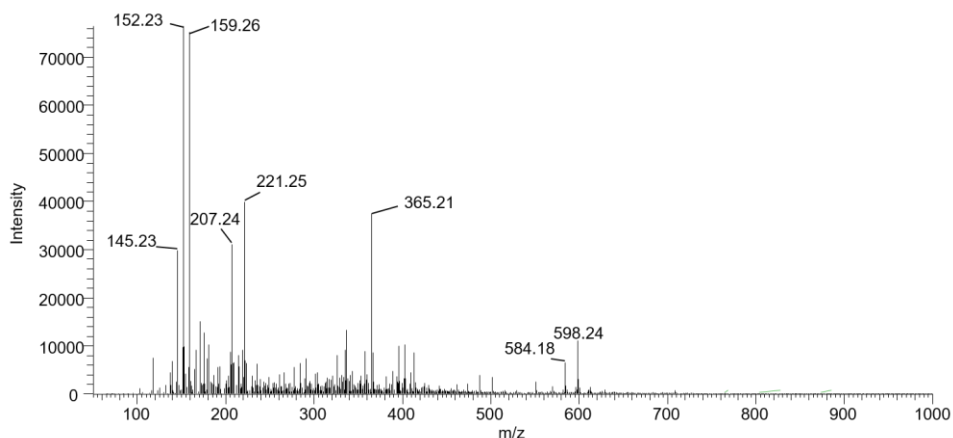


Figure 4-15 ESI mass spectrum of residue of IL1 $C_9(m_2im)_2-NTf_2$ collected after heating at 440 °C for 30 min in argon atmosphere.

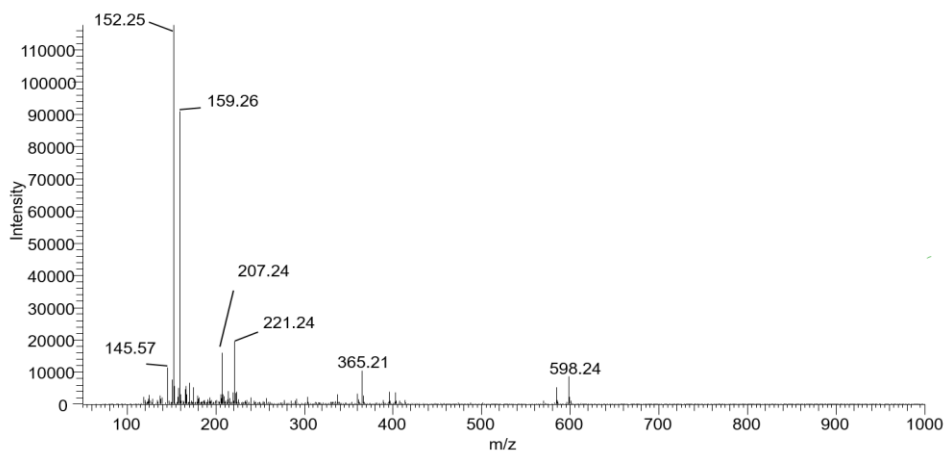


Figure 4-16 ESI mass spectrum of residue of IL1 $C_9(m_2im)_2-NTf_2$ collected after heating at 440 °C for 30 min in air. The m/z 152 (demethylated IL) is significantly increased compared to Figure 4-15.

The decomposition studies on dicationic ILs led to some specific observations: the ether bond present in the PEG linkage is the most thermally fragile. The next bond that seems to break under thermal stress is the C-N bond followed by C-C bonds. This order does not follow the strength of chemical bonds that is: 358 kJ/mol, 348 kJ/mol and 293 kJ/mol for the C-O, C-C and C-N bond, respectively ¹⁴¹. The listed strength of the C-P bond, 264 kJ/mol, is even weaker than the C-N bond. However, it seems that the phosphorus-based dicationic ILs are thermally stable, being able to form NIPs with two NTf₂ anions. The probability of cleavage of a particular bond not only depends on the bond strengths but also on the stability of the fragments formed in the fragmentation process ¹³⁸. The rupture of the C-P bond may be initiated by oxidation by trace amounts of oxygen present in our set-up, inducing the thermal breakdown of phosphonium-based dicationic **IL5** and **IL6**. It is worth mentioning that, the thermal decomposition temperature is the upper limit of the liquid range of ILs and is much higher than the boiling points and decomposition temperatures of starting materials (N-methyl pyrrolidine: bp= 81 °C, tripropyl phosphine: bp= 187.5 °C, dibromoalkanes: bp range= 167 to 286 °C, tetraethylene glycol: bp= 330 °C with extreme decomposition) ^{11, 110, 142}. The lower volatilities of ionic liquids (salts) are due to the increased electrostatic and intermolecular interactions as is well known ^{11, 31, 143}.

4.4.2 Analysis of branched chain linkage ILs

To understand the effect of substituted linkage chains on the thermal stabilities of dicationic ILs, the degradation study was extended to a selection of C₃, and C₅ branched chain dicationic ILs. **Table 4-3** summarizes the data obtained by the degradation study of six branched chain ILs and one linear analog, **IL9** to **IL15**.

Table 4-3 MS peaks of volatile dicationic NTf₂ branched ionic liquids seen after heating at 400 °C for 30 min under argon flow.

IL Code	Dication structure	Dication m.w.	T _d ^a °C	Peak 1		Peak 2		Peak 3	
				Mass	Broken bond	Mass	Broken bond	Mass	Broken bond
IL9		248.37	406	151	C-N imidazole	137	C-N imidazole + C-C methylene	NA	NA
IL10		248.37	438	151	C-N imidazole	137	C-N imidazole + C-C methylene	NA	NA
IL11		246.36	437	137	C-C methylene	151	C-N imidazole	NA	NA
IL12		262.40	438	165	C-N imidazole	151	C-N imidazole + C-C methylene	NA	NA
IL13		276.43	440	179	C-N imidazole	165	C-N imidazole + C-C methylene	151	C-N imidazole + 2 C-C methylene
IL14		290.45	423	193	C-N imidazole	179	C-N imidazole + C-C methylene	NA	NA
IL15		318.51	429	207	C-C methylene	221	C-N imidazole	165	C-N imidazole + C-C tert-butyl

^a Temperature of 5% weight loss determined with thermogravimetric analysis (TGA). Conditions: 10 °C/min from room temperature (22 °C) to 600 °C

4.4.2.1 C₃- branched ILs

The α - (**IL9**) and β - (**IL10**) substituted C₃ linked branched ILs showed similar mass spectra for the collected volatiles at 400 °C (see **Figures 4-17** and **4-18**). The peak at m/z 151 was the highest in intensity and belonged to the fragment formed from breaking of C-N bonds. The m/z 151 peak was also present in the mass spectrum obtained from the analysis of volatile fragments of **IL9** collected at 300 °C. However, the same fragment was absent in the mass spectrum of collected volatiles of **IL10** at 300 °C. This shows that the presence of methyl group on the α -carbon provided extra stability to the carbocation of the broken fragment. This is also supported by the decreased T_d temperature of **IL9** (406 °C) compared to **IL10** (438 °C). In the case of **IL11** with an external double bond on the C2 carbon, the fragment with m/z 137 was the base peak, and the fragment due to breaking of C-N bond (m/z 151) was about one third the intensity of the base peak (see **Figure 4-19**). The double bond on the C2 carbon may have accelerated the breaking of the C1-C2 bond.

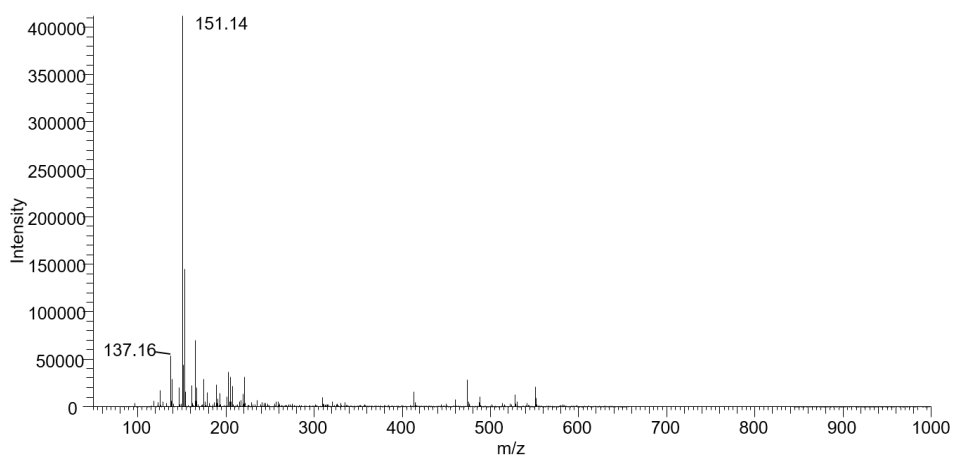


Figure 4-17 ESI Mass spectrum of the volatile fraction of **IL9** 1mC₃(m₂im)₂-NTf₂ collected after heating at 400 °C for 30 min.

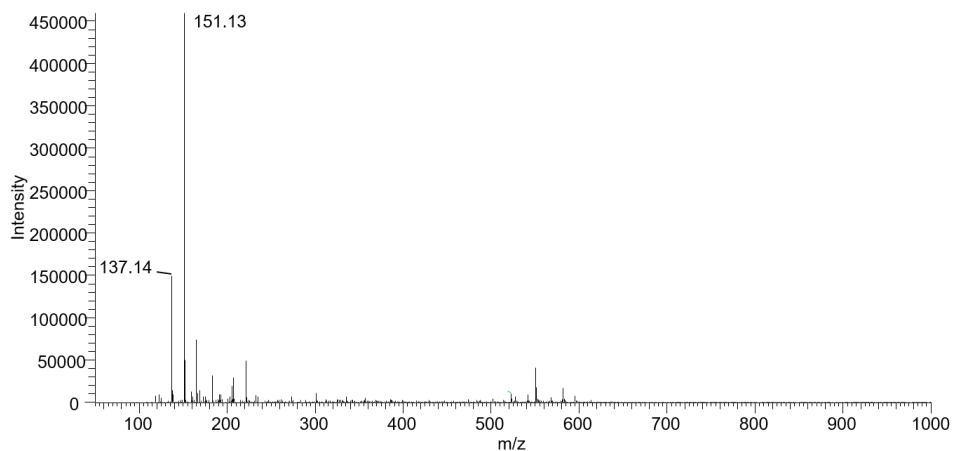


Figure 4-18 ESI Mass spectrum of the volatile fraction of IL10 2mC₃(m₂im)₂-NTf₂ collected after heating at 400 °C for 30 min.

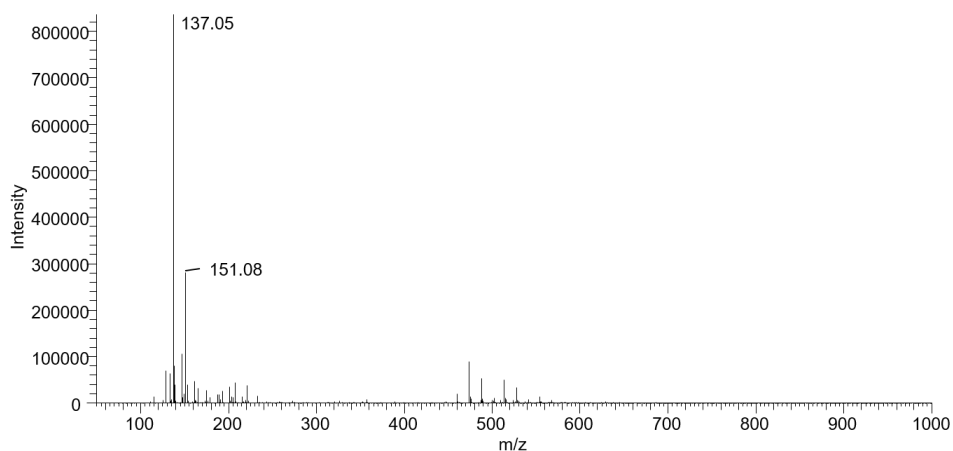


Figure 4-19 ESI Mass spectrum of the volatile fraction of IL11 i-eneC₄(m₂im)₂-NTf₂ collected after heating at 400 °C for 30 min.

4.4.2.2 C₅ branched ILs

Four ILs with different substitutions patterns on the C₅ branched linkages were analyzed. **IL13**, **IL14**, and **IL15** contain a methyl, dimethyl, and a tert-butyl substituent on the central carbon (C3) of the C₅ linkage, respectively. The fragmentation pattern of **IL12** was similar to **IL1** (both straight chain linked ILs), with the breaking of the C-N bond

(base peak at m/z 165) and further loss of $-CH_2$ groups in series (see **Figure 4-20**). **IL13** and **IL15** (both with single substituents on the C3 carbon) showed similar fragmentation pattern with major peaks belonging to the breaking of the C-N bond, C1-C2 bond, and C2-C3 bond (see **Figures 4-21** and **4-23**). The presence of methyl and *tert*-butyl substituent on the C3 carbon may have accelerated the breaking of the C2-C3 bond as fragments at m/z 165, and 207 were base peaks (see **Figures 4-21** and **4-23**). These fragments must be the daughter fragments of a parent fragment obtained by the breaking of a C-N bond (fragments at m/z 179, and 221) of the intact IL. The T_d temperatures of **IL12** and **IL13** are close (438°C and 440°C, respectively) which means that the C2-C3 bond must have broken after the cleavage of the C-N bond. The breaking of *tert*-butyl substituent was also observed in the case of **IL15** as it is a good leaving group, and this might be the reason for the lower T_d temp of **IL15** (429°C) compared to **IL12**. Interestingly **IL14** showed a different degradation pattern compared to the **IL13**, and **IL15**. The mass spectrum of the volatiles of **IL14** ($T_d = 423^\circ\text{C}$) was cleaner than the mass spectra of **IL13** and **IL15** (see **Figure 4-22**). The base peak observed at the m/z 193 was due to the breaking of C-N bond and a less intense peak observed at m/z 179 was may be due to the breaking of one of the methyl substituents on the C3 carbon. Removal of one methyl group leads to the formation of stable tertiary carbocation which might be the reason for its cleavage and the lower T_d temperature of **IL14** compared to **IL13**.

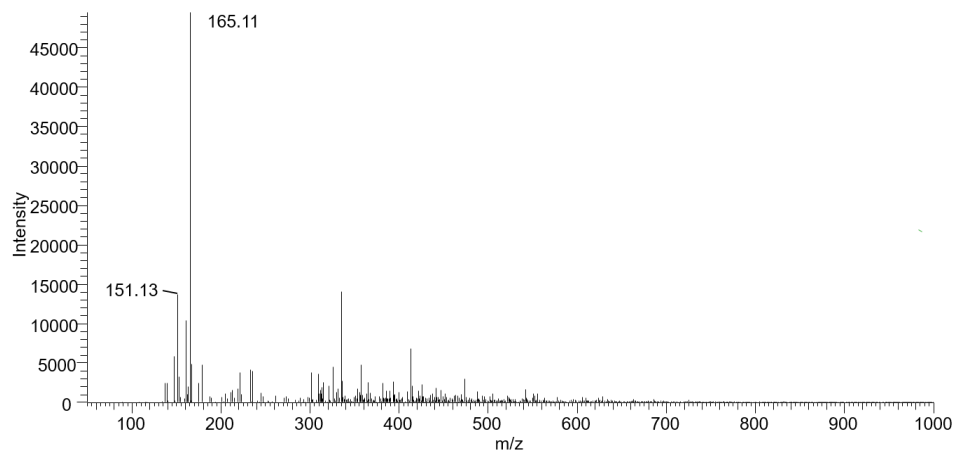


Figure 4-20 ESI Mass spectrum of the volatile fraction of IL12 $C_5(m_2im)_2-NTf_2$ collected after heating at 400 °C for 30 min.

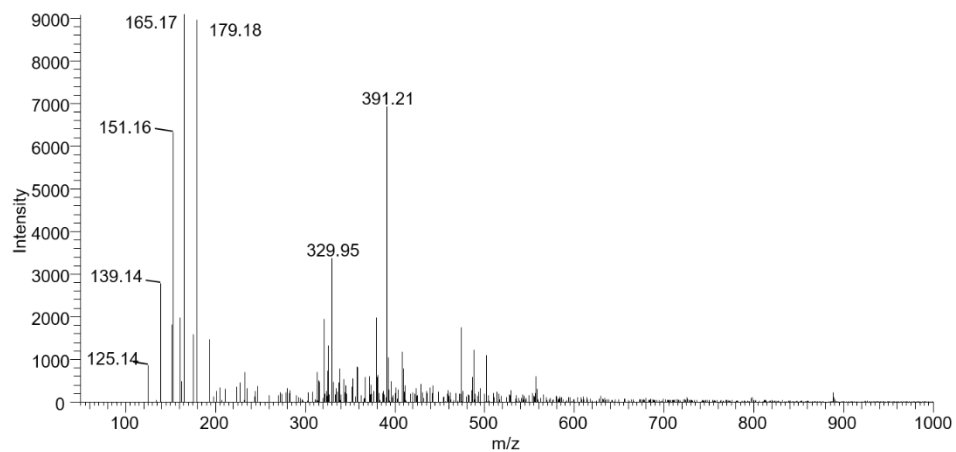


Figure 4-21 ESI Mass spectrum of the volatile fraction of IL13 $3mC_5(m_2im)_2-NTf_2$ collected after heating at 400 °C for 30 min.

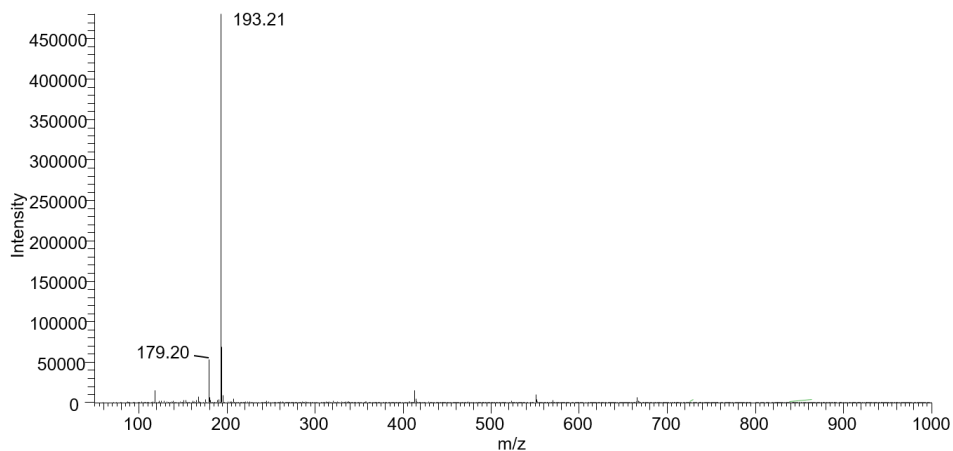


Figure 4-22 ESI Mass spectrum of the volatile fraction of IL14 $3m_2C_5(m_2im)_2-NTf_2$ collected after heating at 400 °C for 30 min.

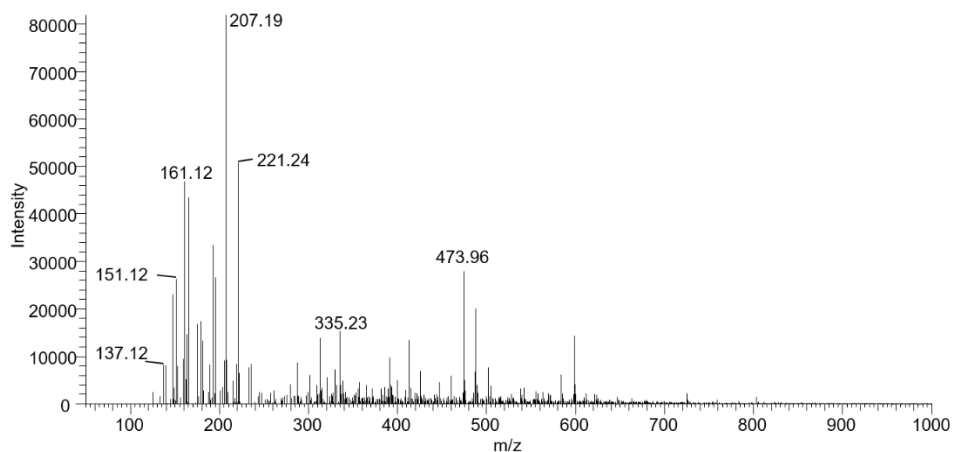


Figure 4-23 ESI Mass spectrum of the volatile fraction of IL15 $3t-buC_5(m_2im)_2-NTf_2$ collected after heating at 400 °C for 30 min.

4.5 Conclusions

The results of the degradation study led to the following observations: 1) only the phosphonium based ILs formed volatile NIPs found in the collected “volatile fractions.” All other tested dicationic ILs have undetectable volatility at 400°C with no NIP formation. 2) All the studied ILs show at least some decomposition at 400°C, but with

considerable differences in magnitude. The dicationic ILs decompose even when their observed TGA temperature (T_d) is much higher than 400°C (e.g., 467°C and 464°C for IL1 and IL5, respectively, Table 1). 3) All three studied dicationic ILs with a PEG spacer were completely destroyed in less than 30 min at 400°C with the prolific breaking of C-O bonds. 4) The phosphonium based dicationic ILs are sensitive to P-oxidation at higher temperatures. 5) The bis-dimethylimidazolium **IL1** with a nonyl (C₉) spacer was remarkably thermally resistant even in the presence of oxygen. 6) The position and number of substituents on the linkage chain affects the degradation pattern and stabilities of ILs, as the presence of one substituent on the central carbon of the C-5 linkage accelerated the breaking of the C2-C3 bond. Whereas, the presence of two substituents on the C3 carbon leads to removal of one of the substituents and a further decrease in thermal stability. 7) The breaking of bonds under thermal stress studies did not follow the order of bond strengths and may be dependent on other factors such as the stability of fragments and the influence of substituents. 8) The heteroatom-carbon single bonds were more prone to thermal decomposition, and the order of thermal breaking was observed to be C-O<C-N<C-P in the studied ILs. In high temperature applications, to be sure that dicationic ILs are stable and remain in a condensed state, it is recommended that their maximum working temperature be at least 100°C or in some cases even lower than their experimental TGA decomposition temperatures.

Chapter 5

GC SELECTIVITY OF NEW PHOSPHONIUM-BASED DICATIONIC IONIC LIQUID STATIONARY PHASES

5.1 Abstract

Three phosphonium based dicationic ionic liquids (DILs) were synthesized as bis(trifluoromethylsulfonyl) imide salts. The three dications had a nonyl spacer between two identical phosphonium substituted groups. The three phosphonium moieties were dipropyl(phenyl), diphenyl(propyl) and diphenyl(tolyl). The physicochemical properties of the DILs were appropriate to prepare 30-m capillary columns that were tested in GC. A unique selectivity compared to different polysiloxane or polar cyanosiloxane commercial columns was observed for selected mixes of phthalates, polyaromatic hydrocarbons, polychlorobiphenyls, and dioxins. Only minor selectivity variations were observed with the three DILs. The different number of aromatic rings on the positively charged phosphonium group did not influence the DIL selectivity significantly.

5.2 Introduction

The new class of non-molecular solvents, ionic liquids, has been found to be particularly useful as stationary phases for gas chromatography (GC).^{37, 48, 78, 93, 144-145} Dicationic ionic liquids (DILs) have demonstrated high thermal stabilities and can be engineered to have a wide range of polarities.^{11, 22, 38, 40} Although DIL-based GC stationary phases were developed with a large range of polarities, their selectivities often were different when compared to classical GC stationary phases having similar polarities.

^{96, 111, 146}

The molecular structure of the DILs dictates their properties. It was found that longer linkage "chain" between the two positive charges and alkyl chain branching in the

spacer were beneficial for physicochemical properties needed for GC stationary phase such as low melting points, high viscosities, and high thermal stabilities.^{19, 110, 147}

Variations in the counter anions also affect the DILs physicochemical properties¹⁴⁸⁻¹⁵⁰

Most of the developed DILs are nitrogen-based, and they especially focus on imidazolium-based cations.^{48, 93, 96, 111, 144-145} Compared to simple imidazolium cations, phosphonium cations lack an acidic proton which can be thermally lost, making phosphonium-based ILs more thermally stable than nitrogen-based ILs.^{13, 45, 151}

Viscosities of phosphonium ILs are also somewhat higher than analogous ammonium ILs.¹⁵² Phosphonium-based DIL GC stationary phases were commercialized in 2009 under the trade names of SLB-IL59, SLB-IL61, and SLB-IL76 with the numbers referring to a polarity index.¹⁰⁰ In this polarity scale, the classical polyoxyethylene-based polar columns have indexes around 50 and the most polar tris(2-cyanoethoxy)propane (TCEP) column has the index 100. Since then a SLB-IL111 was introduced as the most polar and thermally stable GC column available. It allowed analytical GC separations not possible before.^{96, 111, 153} However, SLB-IL111 contains an imidazolium-based DIL. Imidazolium ILs are more polar than analogous phosphonium ILs.¹⁵⁴ However, phosphonium-based DILs were found very useful having unique selectivities for a variety of different classes of volatile compounds when compared to traditional GC stationary phases of similar polarities.^{153, 155-156}

Three new phosphonium-based DILs containing different arrangements of aromatic rings and propyl groups were synthesized and used to coat three 30 m × 250 μm capillary columns. The syntheses, physicochemical properties along with the ability of these new DIL-coated capillary columns to separate different classes of compounds are presented and discussed.

5.3 Materials and methods

5.3.1 Chemicals

1,9-Dibromononane, P,P-dichlorophenylphosphine, propyl-magnesium chloride, diphenyl(*o*-tolyl)-phosphine, and lithium bis(trifluoromethylsulfonyl)imide were obtained from MilliporeSigma (St Louis, MO, USA). Diphenyl-*n*-propylphosphine was purchased from Alfa Aesar (ThermoFisher Scientific, Tewksbury, MA, USA). The solvents acetonitrile, dichloromethane, diethyl ether, and ethyl acetate were purchased from Fisher Scientific (Fair Lawn, NJ, USA). Deionized water was obtained from a Synergy 185 water purification system (Millipore, Billerica, MA, USA).

Several commercial test mixes were analyzed on the three phosphonium DIL GC columns. They were two polychlorinated biphenyl (PCB) solutions: the Supelco PCB congener mix with 6 PCBs (MilliporeSigma) and the WHO PCB congener mix with 12 PCBs obtained from AccuStandard (New Heaven, CT, USA); the tetrachlorodibenzo-dioxin (TCDD) mix containing 6 dioxins; and EPA-610 mix containing 16 polyaromatic hydrocarbons (PAHs) were obtained from MilliporeSigma. Also a phthalate mix: EPA method 8061A with 15 phthalates was obtained from Restek (Bellefonte, PA, USA). Individual standards were acquired for identification purposes when the mass spectrometry trace was not definitive.

5.3.2 Phosphonium dicationic ionic liquid synthesis

Synthesis of dipropyl-phenylphosphine:

Dipropyl-phenylphosphine was synthesized by the previously reported procedure.¹⁵⁷

Synthesis of ionic liquids:

The three phosphonium-based DILs were synthesized in a similar way. Briefly, in a sealed flask, 1 equivalent of 1,9-dibromononane was dissolved in 50 mL acetonitrile. Then, 2.5 molar equivalents of the appropriate phosphine was added to the solution. The mixture was heated to 115 °C with stirring. After 48 h, the reacting solution was cooled to room temperature and acetonitrile was removed by roto-evaporation. The bromide salt was solubilized in a minimum amount of methanol and an excess of ethyl acetate was added to induce salt precipitation. The bromide salt was collected by filtration and washed with 2 x 30 mL ethyl acetate. The salt was dried under vacuum at 40°C for 12 h. The bromide salts were converted to NTf₂⁻ salts by simple metathesis with 2 molar equivalents LiNTf₂ in 60 mL methanol solution for 24 h. Methanol was evaporated, and the residue was treated with 30 mL water and 30 mL dichloromethane was added to extract the phosphonium NTf₂ DILs in the lower organic layer phase and the lithium salts in the aqueous solution. The dichloromethane separated phase was washed with three portions of 30 mL water to remove trace of lithium chloride and excess lithium NTf₂. Dichloromethane was evaporated leaving the desired phosphonium DILs that were dried over phosphorus pentoxide for at least a day (global yield 85%).

5.3.3 Capillary column preparation

All IL columns were prepared by using the static coating method at 40 °C with a 0.20% w/v coating solution of DIL in dichloromethane. The DILs were coated on the inner wall of salt treated capillaries with dimensions 30 m x 250 µm i.d. capillary tubing (MilliporeSigma). Following the coating process giving a film thickness of 0.2 µm, the coated columns DIL column were conditioned with helium at 200°C for 12 h. The column efficiencies were tested using naphthalene at 110 °C, and the efficiencies ranged from

3800-4000 plates m^{-1} . Capillary Columns with dimensions 3 m \times 250 μm i.d. (efficiencies 2000 – 2200 plates m^{-1}) were also prepared and used to perform inverse GC to assess the DIL thermal stability.

5.3.4 Gas chromatography instrumentation:

All GC experiments were made using an Agilent GC 6890N apparatus with a flame ionization detector, except for PCBs that were detected with an Agilent 5975 mass spectrometer (Agilent, Santa Clara, CA, USA). Data were handled by the Agilent software Chemstation B.01.04.

5.3.5 Dicationic ionic liquid characterization

The DILs were characterized by electrospray ionization mass spectrometry (ESI-MS) for molecular weight. ESI-MS spectra were acquired by using a Finnigan LXQ (Thermo Fisher Scientific, San Jose, CA). 1H NMR and ^{13}C NMR experiments were performed on 500 MHz JEOL Eclipse Plus 500 (Peabody, MA, USA). The melting point measurements were carried out on a Shimadzu DSC-60 (Kyoto, Kyoto Prefecture, Japan) differential scanning calorimeter. The DIL sample (\sim 10 mg) was sealed in an aluminum pan and then heated at a rate of $5\text{ }^\circ C \cdot min^{-1}$ from $-120\text{ }^\circ C$ to $200\text{ }^\circ C$. Thermogravimetric analyses were performed using Shimadzu TGA-51 thermogravimetric analyzer (Kyoto, Kyoto Prefecture, Japan). For the stability testing, the DIL sample (\sim 8 mg) was placed in a platinum pan heated at $10\text{ }^\circ C \cdot min^{-1}$ from room temperature to $600\text{ }^\circ C$ in a nitrogen atmosphere (flow $30\text{ mL } min^{-1}$). The decomposition temperatures were determined at 1%, 5%, and 15% weight loss. The 5% weight loss of the sample which corresponds to 95% w value, was considered as the measure of thermal stability. The GC thermal

stability measurements were made using 3-m DIL columns in the GC chromatograph. The oven temperature was raised from 100 to 450 °C at 1 °C min⁻¹ with helium as carrier gas at 1 mL. min⁻¹. The injector and FID temperatures were both set at 250 °C.

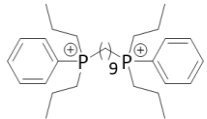
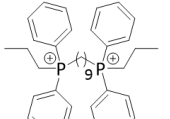
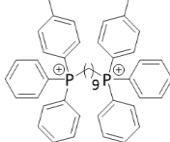
5.4 Results and discussion

5.4.1 Physicochemical properties of the new phosphonium-based DILs

Table 5-1 gives the structures of the three newly synthesized DILs. All three ILs have a nine alkyl carbon (C₉) linkage chain between the two positively charged phosphonium groups. Different numbers of aromatic rings were attached to the phosphorous atoms differentiating these new DILs from previous work and from the SLB-IL 59 and SLB-IL 61 phosphonium-based GC capillary columns that all contain tripropyl phosphonium groups.^{13, 100, 158} All three DILs are symmetrical with two benzene rings (one on each phosphonium group) in C₉(pr₂phP)₂-2NTf₂, four benzene rings (2 × 2) C₉(ph₂prP)₂-2NTf₂, and six benzene rings (2 benzyl + 1 tolyl rings on each phosphonium group) in C₉(ph₂tlP)₂-2NTf₂ (**Table 5-1**). The three DILs were room temperature ionic liquids with melting points well below 15 °C.

The thermal stabilities of the DILs were as high as 300 °C, but the different experimental procedures provided mixed results. According to inverse GC measurements, **Figure 5-1** shows that C₉(pr₂phP)₂-2NTf₂ is the most stable DIL starting to decompose above 370°C. C₉(ph₂tlP)₂-2NTf₂ show the lowest value with a T_{IGC} value of 340 °C only 30 °C lower. The TGA results are somewhat different, indicating that C₉(ph₂prP)₂-2NTf₂ is the most thermally stable DILs of the set (**Table 5-1**). All results considered, it seems that the three DILs have similar high thermal stabilities, greater than 300 °C.

Table 5-1 Structure and physicochemical properties of phosphonium-based bis(trifluoromethyl sulfonyl) imide dicationic ionic liquids.

DIL Structure	Cation name	DIL code	Melting Point (°C)	thermal stability (°C)				
				TGA ^a			GC ^b	
				T _{1%}	T _{5%}	T _{15%}	T _{IGC}	
	2NTf ₂ ⁻	1,9-bis[dipropyl(phenyl)-phosphonium]nonane	C ₉ (pr ₂ phP) ₂ -2NTf ₂	-12	280	396	437	370
	2NTf ₂ ⁻	1,9-bis[diphenyl(propyl)-phosphonium]nonane	C ₉ (ph ₂ prP) ₂ -2NTf ₂	-18	412	445	463	360
	2NTf ₂ ⁻	1,9-bis[diphenyl(o-tolyl)-phosphonium]nonane	C ₉ (ph ₂ tIP) ₂ -2NTf ₂	4	291	392	455	340

^a Thermogravimetric analysis (TGA) conditions: temperature program = 1 °C/min from room temperature (22 °C) to 600 °C, T_{1%} = temperature of 1% decrease of sample mass, T_{5%} = temperature of 5% decrease of sample mass, T_{15%} = temperature of 15% decrease of sample mass

^b Determined by inverse gas chromatography with flame ionization detector (see Figure 4-1). Temperature program = 1 °C/min from 100 °C to 450 °C, 1 mL/min Helium.

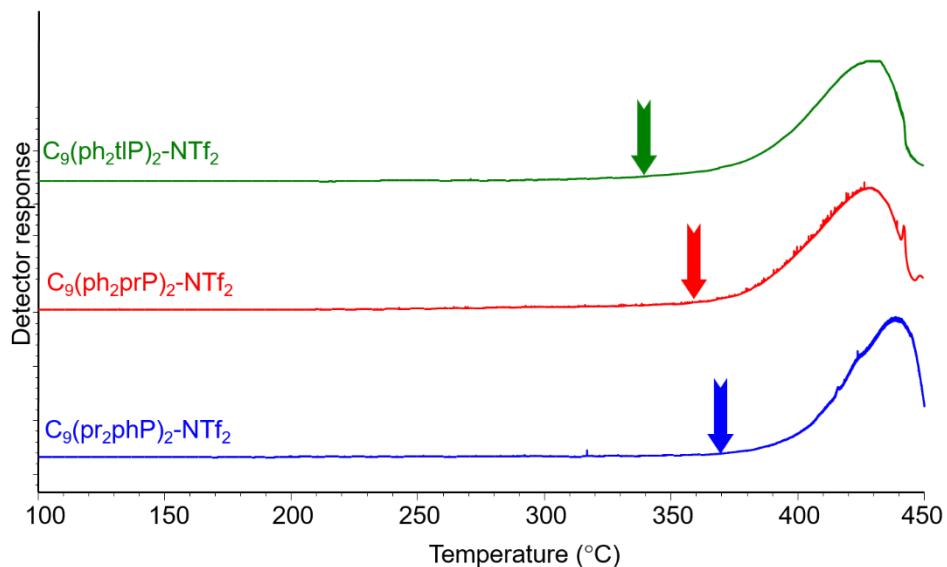


Figure 5-1 Inverse GC following the thermal decomposition of the 3 m × 250 μm DIL-coated capillary columns. Temperature gradient: 1 °C/min. Helium flow rate: 1 mL/min. The vertical arrows point the temperature at which the FID baseline starts to change and considered as T_{IGC} (Table 5-1).

5.4.2 Analysis of 12 regulated phthalates

The main use of phthalates is as plasticizers in a wide variety of man-made industrial products. For a variety of reasons, phthalate esters are ubiquitous in the environment. Their potential adverse effects on human health have been reported¹⁵⁹. Six dialkyl *ortho*-phthalates were permanently banned in 2008.¹⁵⁹ The Restek EPA method 8061A mix contains the 6 banned phthalates plus 9 more that are listed as regulated by US and European agencies (**Table 5-2**).

Fig. 2 shows the chromatograms of the EPA8601 mix analyzed on the three phosphonium DIL-coated columns at identical experimental conditions and compared with the separation obtained on a classical polydimethylsiloxane 5% phenyl capillary column of the same geometry. A dramatic selectivity change is obvious between the 5% phenyl and

the DIL-coated columns. The ether containing phthalates #5 (methoxy), #7 (ethoxy), and #11 (butoxy) were relatively retained longer on the DIL columns than the alkyl phthalates of similar weight. Similarly, #10 with a benzene ring and #12 with a cyclohexyl ring are also retained longer on the DIL columns than on the 5% phenyl column (arrows in **Figure 5-2**). The stereoisomeric pair of #6 starts to show separation on all columns. Three pairs of compounds #6/#7 (methyl pentyl/ethoxy), #9/#10 (hexyl/butylbenzyl), and #12/#13 (ethyl hexyl/cyclohexyl) are hard to separate on the 5% phenyl column, but they are several minutes apart on the DIL coated columns.

Considering the three different DIL-coated columns, the phthalate chromatograms are very similar with minor selectivity variations between phthalate pairs. **Figure 5-3** shows the measured selectivity factors of the four closely eluting pairs: #4/#6 (butyl/methylpentyl), #13/#9 (hexyl/ethylhexyl), #7/#5 (ethoxyhexyl/methoxyhexyl), and #15/#12 (cyclohexyl/nonyl). There is no emerging clear trend. The dipropylphenyl phosphonium $C_9(\text{pr}_2\text{phP})_2\text{-2NTf}_2$ is slightly better for pairs #13/#9 and #15/#12 and worst for pair #4/#6. The $C_9(\text{ph}_2\text{prP})_2\text{-2NTf}_2$ is slightly better for pairs #4/#6 and #7/#5 and worst for pair #4/#6 (**Figure 5-3**). **Figure 5-2** shows that, in all cases, the four pairs are baseline separated even with a selectivity factor as low as 1.008. No particular retention changes were observed on phthalate #10 which is the only ester containing an aromatic ring. The increasing number of aromatic rings between $C_9(\text{pr}_2\text{phP})_2\text{-NTf}_2$ (2 phenyl rings), $C_9(\text{ph}_2\text{prP})_2\text{-NTf}_2$ (4 phenyl rings), and $C_9(\text{pr}_2\text{phP})_2\text{-NTf}_2$ (6 phenyl rings) lead to minor increases in the retention time of di(butylbenzyl)phthalate #10.

Table 5-2 Physicochemical properties of the phthalates of the EPA 8106 list.

#	phthalates	m.w.	b.p. °C	Log P	Water solubility mg/L	remarks
1	Dimethyl	194.2	283	1.90	4000	
2	Diethyl	222.2	295	2.50	1080	
3	Diisobutyl	278.3	320	4.11	5	
4	Di- <i>n</i> -butyl	278.3	340	4.60	13	
5	Bis(2-methoxyethyl)	282.3	340	1.11	1730	Higher retention on DILs
6	Bis(4-methyl-2-pentyl)*	334.4	356	6.28	0.033	Less retained than <i>n</i> -hexyl
7	Bis(2-ethoxyethyl)	310.3	362	2.10	173	Less retained than methoxy on DILs
8	Di- <i>n</i> -pentyl	306.4	342	5.60	0.18	
9	Di- <i>n</i> -hexyl	334.5	377	6.82	0.011	
10	Butyl benzyl	312.4	370	4.73	0.95	Higher retention on DILs
11	Bis(2- <i>n</i> -butoxyethyl)	366.4	408	4.05	1.7	
12	Dicyclohexyl	330.4	395	6.10	0.041	No coelution with 13 on DILs
13	Bis(2-ethylhexyl)	390.6	384	7.5	0.3	Lower retention on DILs
14	Di- <i>n</i> -octyl	390.6	390	8.1	0.0004	
15	Dinonyl	418.6	400	8.8	<0.001	

* Bis(4-methyl-2-pentyl) phthalate has two asymmetric centers, hence four enantiomers in two diastereoisomeric pairs that could be separated on achiral columns.

Log P and water solubilities are data calculated by ACD/Labs, EPISuite or ChemAxon softwares.

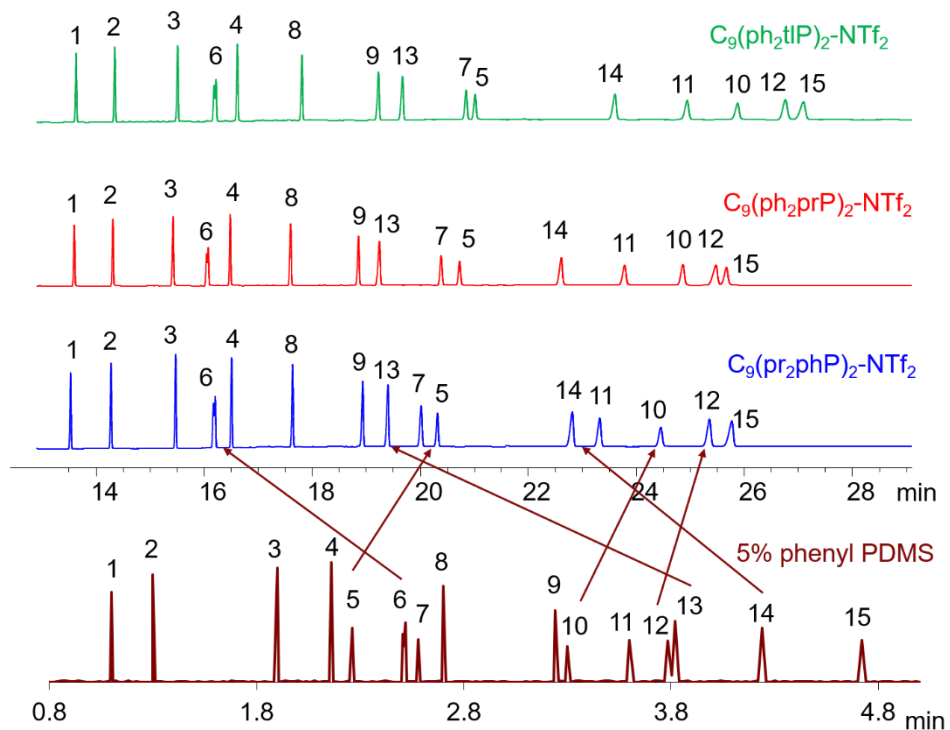


Figure 5-2 Chromatograms of the phthalate mix EPA8106 on the three phosphonium-based DIL-coated 30 m columns (top chromatograms) and a 30 m Restek Rxi-5ms, 5%diphenyl-95%dimethylpolysiloxane coated column (bottom chromatogram). The arrows point at the selectivity changes. Compound codes are listed in Table 2.

Chromatographic conditions: He carrier gas: 2 mL/min, 66 cm/s average gas velocity. Temperature program for the 3 DIL columns: 120 °C for 3 min, 10 °C/min to 260 °C hold for 15 min. Temperature program for Rxi-5ms column: 200 °C for 0.5 min, 30 °C/min to 320 °C hold for 1 min.

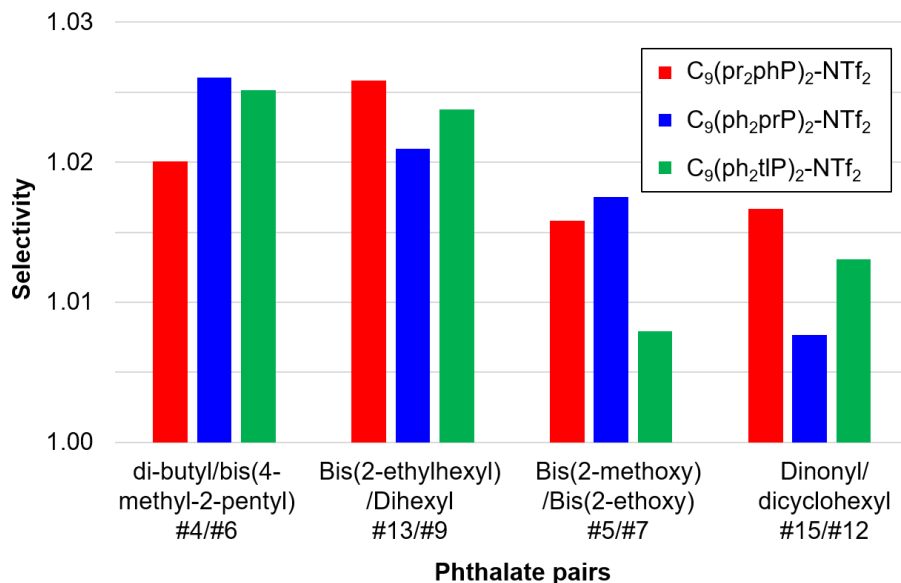


Figure 5-3 Selectivity on four critical phthalate pairs observed on the three phosphonium DIL-coated capillary columns. The numbers refer to the Figure 5-2 peaks with code listed in Table 5-1.

5.4.3 Analysis of selected polycyclic aromatic hydrocarbons (PAHs)

PAHs are pollutants released into the environment due to incomplete combustion of organic substances. PAHs have low acute toxicity. However, in the long term, several PAHs are carcinogens so they must be accurately accessed. PAHs are mostly analyzed by GC-MS.⁷⁴ The EPA-610 mix contains 16 PAHs that are known for their toxicity. Figure 5-4 compares the separation of the EPA-610 mix on the $C_9(\text{pr}_2\text{phP})_2\text{-NTf}_2$ phosphonium DIL and a commercial 50% phenyl polydimethyl siloxane Rxi-PAH columns.¹⁶⁰ The selectivity difference between the two columns is not as marked as it was with the phthalate compounds. The elution order inversion of the early eluting acenaphthene and acenaphthylene (#2 and #3) is indicated by a green arrow in Figure 5-4. The structural isomer pairs: benzo(b) and (k) fluoranthenes (#11 and #12), and dibenz(a,h) anthracene and indeno(1,2,3) pyrene (#14 and #15), were both baseline

separated with the DIL columns (red arrows in Figure 5-4). It must be acknowledged that a very smooth temperature gradient must be used to obtain these two baseline separations. The DIL columns could work at temperature higher than 300 °C, but the 100 min 285 °C isothermal plateau was necessary to obtain the two critical pair baseline separations. The Rxi-PAH separation was done faster at a higher temperature.

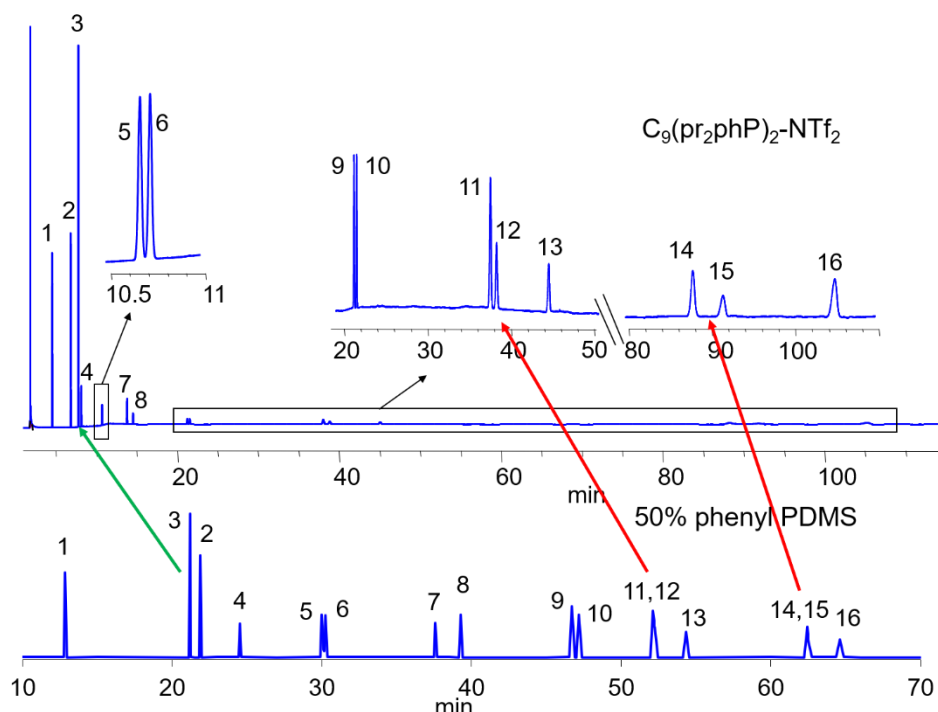


Figure 5-4 Separations of the 16 PAHs of the EPA-610 mix. Chromatographic conditions: column 30 m x 250 μm , 0.2 μm film thickness. Top chromatogram on phosphonium DIL: helium 1.5 mL/min, oven temperature 150 °C for 5 min, 15 °C/min to 285 °C hold for 100 min (hold at 285 °C necessary for baseline separation of 14 and 15). Bottom chromatogram on 30 m x 250 μm Rxi-PAH 50% phenyl dimethylpolysiloxane: helium 1.2 mL/min, 45 cm/s average velocity, oven temperature 60 °C for 2 min, 5 °C/min to 300 °C hold for 50 min. 1-Naphthalene, 2-Acenaphthene, 3-Acenaphthylene, 4-Fluorene, 5-Phenanthrene, 6-Anthracene, 7-Fluoranthene, 8-Pyrene, 9-Benzo(a)anthracene, 10-Chrysene, 11-Benzo(b) fluoranthene, 12-Benzo(k) fluoranthene, 13-Benzo(a) pyrene, 14-Dibenz(a,h) anthracene, 15-Indeno(1,2,3-cd) pyrene, 16-Benzo(g,h,i) perylene.

Comparing the three different DIL-coated columns, the PAH chromatograms were very similar, and there were only minor selectivity variations between the phthalate esters. A small increase of PAH retention times was noted on phosphonium DILs richer in aromatic rings; namely, with identical temperature ramps, benzo(a) pyrene (#13) eluted at 44 min (Fig. 4), 47 min and 53 min on $C_9(pr_2phP)_2-2NTf_2$, $C_9(ph_2prP)_2-2NTf_2$, and $C_9(ph_2tIP)_2-2NTf_2$, respectively. Figure 5-5 shows the measured selectivity factors of the four closely eluting pairs: phenanthrene/anthracene #5/#6, benzo(a)anthracene/chrysene #9/#10, benzo(b) and benzo(k) fluoranthene #11/#12, and dibenzo(a,h)anthracene/indeno(1,2,2-cd) pyrene #14/#15. All critical pairs are baseline separated on all DIL columns with no clear trend. The $C_9(pr_2phP)_2-2NTf_2$ chromatogram was selected for Fig. 4 because it provided the best separation of the #14/#15 critical pair.

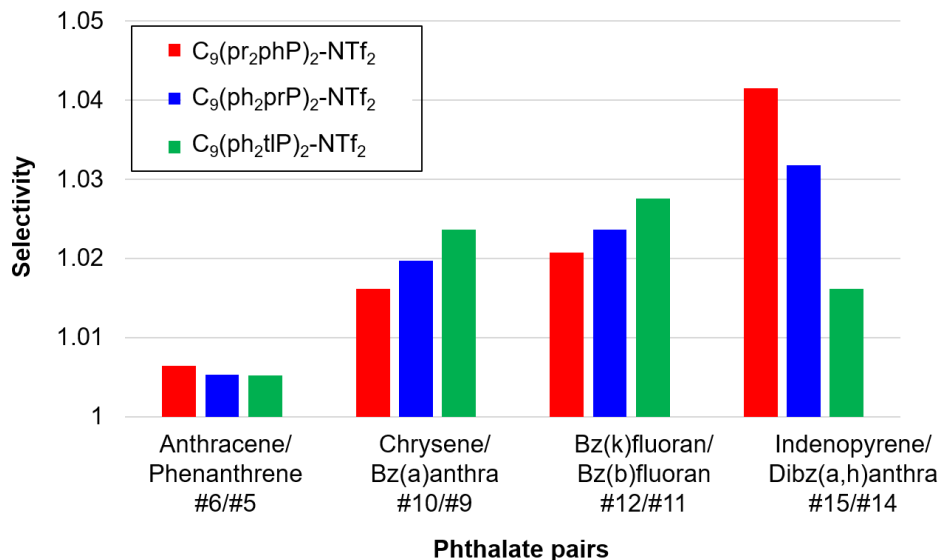


Figure 5-5 Selectivity observed on the three phosphonium DIL-coated capillary columns for four critical PAH pairs of the EPA-610 mix. The numbers refer to the Figure 5-4 peaks with code listed in its caption.

5.4.4 Separation of chlorinated aromatics

Polychlorinated biphenyls (PCBs) were used as a liquid coolant in high voltage transformer throughout the world between the 1930s and 1978, the year of their ban. Considering that the PCBs water solubility is between 2 to 400 pg/L, and that a transformer could contain as much as 200 kg of PCBs, a spill on only 1 kg PCBs in a river would need between 250 millions and 50 billion m³ of water to dissolve it.¹⁶¹ To give an idea of the massive pollution, this amount of water corresponds to the Mississippi river at Saint Louis (average discharge of 7000 m³/s) flowing between 10 h and 83 days. For most common rivers with discharge flows hundreds to thousands of times lower than the Mississippi river, their flow can be polluted for years to centuries if exposed to a PCB source.

There are 209 possible PCBs categorized by the increasing number of chlorine atoms in the molecule: 1-3 chlorobiphenyl; 4-15 dichloro PCBs; 16-39 trichloro PCBs; 40-81 tetrachloro PCBs; 82-127 pentachloro PCBs; 128-169 hexachloro PCBs; 170-193 heptachloro PCBs; 194-205 octachloro PCBs; 206-208 nonachloro PCBs and 209 being the fully chlorinated PCB.¹⁶¹ Out of the 209 PCBs, mainly the non- and mono-*ortho* substituted PCBs show high toxicity. The two test mixes analyzed contain regulated toxic PCBs. The Supelco PCB congener mix #1 with six PCBs, #10, #28, #52, #138, #153, and #180 was tested on the three phosphonium-based DIL columns showing similar baseline separation of the six PCBs on the three DIL columns (**Figure 5-6**, top). The AccuStandard World Health Organization congener mix with 12 PCBs: #77, #81, #105, #114, #118, #123, #126, #156, #157, #167, #169, and #189, was also analyzed on the three DIL columns. Again, similar chromatograms were obtained with the same column geometries and temperature program on the three DIL-columns with a baseline separation of 10 PCBs and overlap of PCBs #81 and #114 (peaks 2 and 4). The

broadened coeluting peak 2/4 suggested that a longer column could separate the two underlying #81 and #114 PCBs. The bottom chromatogram of Figure 5-6 shows the partial separation of peak 2 and 4 obtained on a 60 m $C_9(\text{ph}_2\text{tIP})_2\text{-2NTf}_2$ column.

In a recent work, the commercial columns SLB-IL 59 and SLB-IL 61 were found to have a unique selectivity differing from that of other IL-based and low bleed commercial phases.¹⁵⁸ The stationary phase of these columns is the phosphonium DIL $C_{12}(\text{pr}_3\text{p})_2$ with the NTf_2 (SLB-IL 59) or triflate anions (SLB-IL 61) similar to the three DIL of this work but not carrying any phenyl group for π - π interaction. The #77/#105 and #126/#156 coelutions of toxic PCB congeners commonly encountered on many GC columns are no problem with the three phosphonium DIL GC columns (Peaks 1 and 3, and 7 and 8). The #81/#114 partial overlap observed in this work was not seen with any other columns tested in¹⁵⁸ confirming the unique orthogonal selectivity of the phosphonium-DIL columns for PCBs. The association of phosphonium based DIL columns with other types of stationary phase in 2D-GC should allow for better analyses of PCBs.

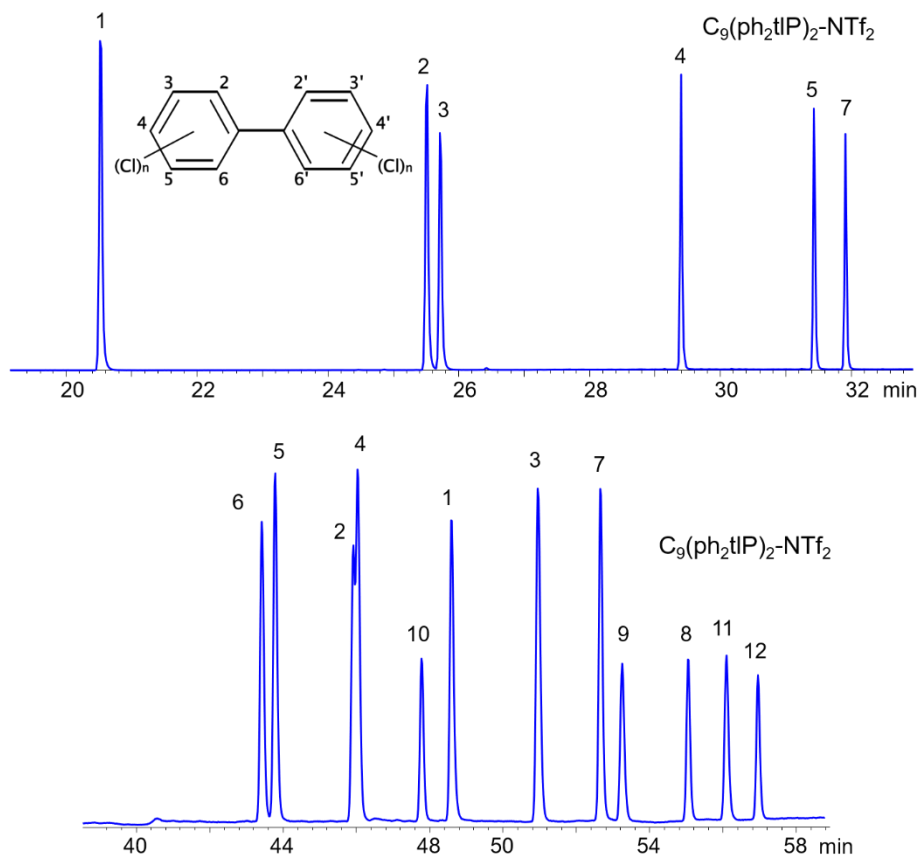


Figure 5-6 Separation of PCBs on phosphonium-based DIL columns. Top chromatogram: separation of the Supelco mix with 6 PCBs: 1: #10 2,6-Dichloro, 2: #28 2,4,4'-trichloro, 3: #52 2,2',5,5'-tetrachloro, 4: #138 2,2',3,4,4',5'-hexachloro, 5: #153 2,2',4,4',5,5'-hexachloro, and 6: #180 2,2',3,4,4',5,5'-heptachlorobiphenyl. Column $C_9(\text{ph}_2\text{tIP})_2\text{-2NTf}_2$ 30 m \times 250 μm , 0.2 μm film; helium: 1 mL/min, average velocity: 37 cm/s @ 100 $^\circ\text{C}$, oven: 100 $^\circ\text{C}$ for 2 min, 5 $^\circ\text{C}/\text{min}$ to 220 $^\circ\text{C}$, 10 $^\circ\text{C}/\text{min}$ to 270 $^\circ\text{C}$ hold for 2 min. Bottom chromatogram: separation of the WHO congener mix with 12 PCBs: 1: #77 3,3',4,4'-Tetrachloro, 2: #81 3,4,4',5-tetrachloro, 3: #105 2,3,3',4,4'-pentachloro, 4: #114 2,3,4,4',5-pentachloro, 5: #118 2,3',4,4',5-pentachloro, 6: #123 2',3,4,4',5-pentachloro, 7: #126 3,3',4,4',5-pentachloro, 8: #156 2,3,3',4,4',5-hexachloro, 9: #157 2,3,3',4,4',5'-hexachloro, 10: #167 2,3',4,4',5,5'-hexachloro, 11: #169 3,3',4,4',5,5'-hexachloro, and 12: #189 2,3,3',4,4',5,5'-heptachlorobiphenyl. Column $C_9(\text{ph}_2\text{tIP})_2\text{-2NTf}_2$ 60 m \times 250 μm , 0.2 μm film; helium: 1 mL/min, average velocity: 27 cm/s @ 150 $^\circ\text{C}$, oven: 150 $^\circ\text{C}$ for 5 min, 5 $^\circ\text{C}/\text{min}$ to 280 $^\circ\text{C}$ hold for 3 min.

Tetrachlorodibenzodioxins (TCDDs) are another class of carcinogenic chlorinated hydrocarbons that are strictly regulated since the 1976 Seveso disaster and must be analyzed at very low levels.¹⁶² The standard mix of 6 TCDD congeners was injected in the three phosphonium DIL 30-m columns producing three similar chromatograms with only four peaks; the three 1,2,3,X-TCDDs were eluting together. Since the peak of the three TCDD congeners was broad, a partial separation was suspected and the 60-m $C_9(\text{ph}_2\text{tIP})_2\text{-NTf}_2$ column was tested showing five peaks (**Figure 5-7** top). 1,2,3,4-TCDD was partly separated from 1,2,3,7 and 1,2,3,8-TCDDs (Peaks 3, and 4-5, respectively). None of the two TCDD-dedicated commercial columns could separate these congeners. However, the phosphonium-DIL columns do show a better selectivity for these TCDD than the two commercial columns SLB-5MS and SP-2331: Peaks 1 and 6 are 5 min apart on the 60-m column compared to 0.8 min on the 60-m SP-2331 (**Figure 5-7**). They were 2 min apart on the 30-m columns (not shown) compared to 40 s on the SLB-5MS. The temperature programs are different, but the partial TCDD separation on the two commercial columns is no match to the baseline separation of four TCDD on the phosphonium DIL columns (**Figure 5-7**).

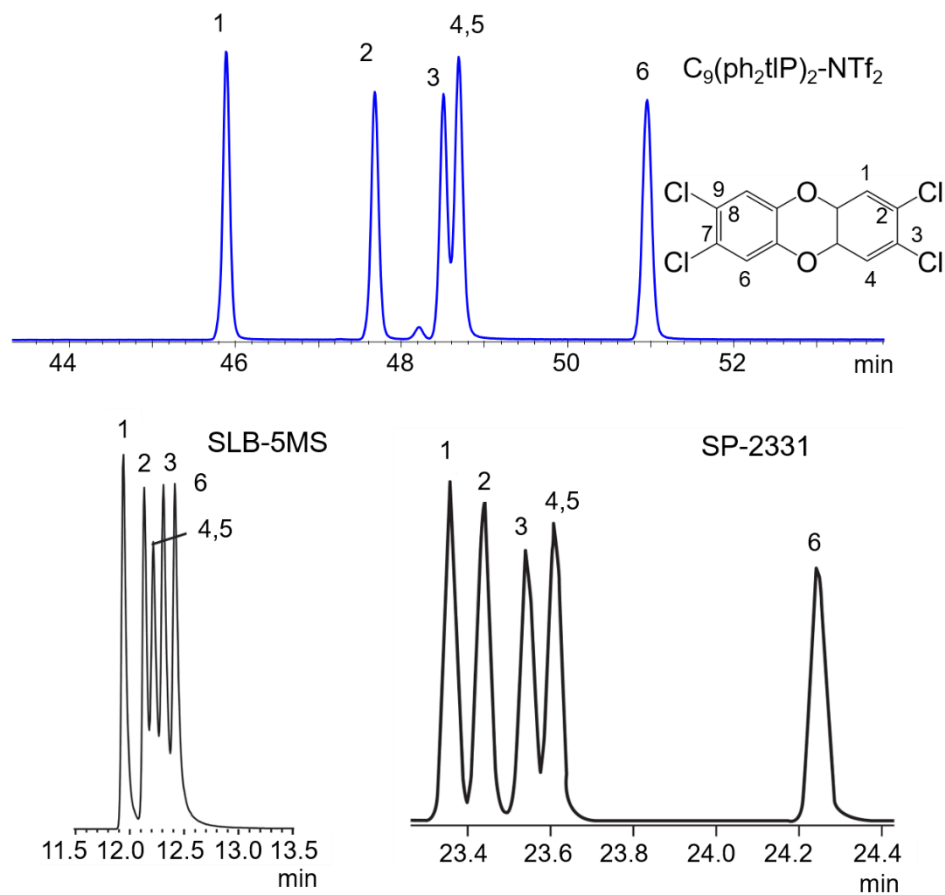


Figure 5-7 Separation of six pollutant tetrachlorodibenzodioxin isomers on a phosphonium-based DIL column (top chromatogram) compared to two commercial columns: a 5% phenyl dimethyl polysiloxane (bottom left) and a polar cyanosilicone (bottom right). Column $C_9(\text{ph}_2\text{tIP})_2\text{-NTf}_2$ 60 m x 250 μm , 0.2 μm film; helium: 1 mL/min, average velocity: 27 cm/s, oven: 180 $^\circ\text{C}$ for 5 min, 2 $^\circ\text{C}/\text{min}$ to 260 $^\circ\text{C}$ hold for 10 min. Column SLB-5MS 30 m x 250 μm , 0.25 μm film; helium: 1 mL/min; oven 170 $^\circ\text{C}$ for 1 min, 8 $^\circ\text{C}/\text{min}$ to 270 $^\circ\text{C}$. Column SP-2331 60 m x 250 μm , 0.25 μm film, helium: 1 mL/min; oven 170 $^\circ\text{C}$ for 1 min, 8 $^\circ\text{C}/\text{min}$ to 265 $^\circ\text{C}$ hold for 12 min. Sample 1.5 $\mu\text{g}/\text{mL}$ TCDD standard in dodecane; 1 μL splitless injection of: 1- 1,4,7,8-TCDD; 2- 2,3,7,8-TCDD; 3- 1,2,3,4-TCDD; 4- 1,2,3,7-TCDD; 5- 1,2,3,8-TCDD; 6- 1,2,7,8-TCDD. Chromatograms for SLB-5MS and SP-2331 obtained from dioxin and PCB analysis handbook from Supelco. https://www.sigmaaldrich.com/content/dam/sigmaaldrich/docs/Supelco/General_Information/dioxin-brochure-jxb.pdf

5.5 Conclusions

The new phosphonium dicationic ionic liquids containing aromatic rings showed a very high thermal stability passing 350 °C. These three DILs have appropriate low melting points and high viscosities allowing to coat well on 250 µm i.d. capillary fused silica to make highly polar, efficient, and thermally stable GC columns.

Testing of the three 30-m phosphonium DIL coated columns returned somewhat similar results. These DIL stationary phases show remarkable original selectivity toward the separation of phthalates, retaining oxygen-containing and phenyl members much longer than polysiloxane-based columns. Problematic coelutions of critical phthalates were not observed on the DIL columns. PAHs, PCBs, and tetrachloro-dioxins were also separated with a unique selectivity very orthogonal to those observed on accepted commercial columns for these separations. These columns should be of great help in 2D-GC for the analysis of a variety of volatile pollutants.

In all studied cases, the three different phosphonium DILs containing a different number of aromatic rings gave very similar separations. No obvious retention differences were observed on the π -electron containing butyl benzyl phthalate, PAHs, PCBs or dioxins even though $C_9(\text{ph}_2\text{tIP})_2\text{-2NTf}_2$ (six rings) is richer in π -electrons than $C_9(\text{pr}_2\text{phP})_2\text{-2NTf}_2$ (only two rings). Since their polarities and selectivities are similar, if one has to be selected, it may be the $C_9(\text{ph}_2\text{prP})_2\text{-2NTf}_2$ given its best thermal stability and the fact that it contains four phenyl aromatic rings in its DIL structure (**Table 5-1**).

Chapter 6

RAPID, EFFECTIVE DEPROTECTION OF TERT- BUTOXYCARBONYL (BOC) AMINO ACIDS AND PEPTIDES AT HIGH TEMPERATURES USING A THERMALLY STABLE IONIC LIQUID

6.1 Abstract

A method for high temperature Boc deprotection of amino acids and peptides in a phosphonium ionic liquid is described. The ionic liquid had low viscosity, high thermal stability and demonstrated a beneficial effect. The study extended the possibility for extraction of water soluble polar organic molecules using ionic liquids. Trace water significantly improved product purity and yield, while only 2 equiv. TFA led to deprotection within 10 min. The trityl group was also deprotected.

6.2 Introduction

The development of simple, effective and environmentally compliant organic transformations are increasingly sought after as a means to drive sustainable processes. Ionic liquids (ILs) have appeared in the literature as a new class of designer solvents and have been found to be attractive for organic synthesis.^{6, 163-166} They offer several advantages over traditional solvents including negligible vapor pressure (safety), recyclability (lowering cost) and modulation of properties (scope).^{20, 167}

Sequential protection and deprotection of amine functional groups play a significant role in organic synthesis.¹⁶⁸ The *tert*-butoxycarbonyl (Boc) group is one of the more widely used amine protecting group.¹⁶⁹⁻¹⁷² The most common method for its deprotection uses TFA and generally requires large excesses (TFA: CH₂Cl₂ (1:1)), reaction times ranging from 2-16 h depending on the substrate and a tedious purification process.¹⁷³ Another well-established method for faster (~10-30 min) and selective

deprotection (in most cases) of Boc group utilizes (4 M) HCl/dioxane.¹⁷⁴ In a classic publication, Wang et al. reported deprotection of *N*-Boc aliphatic, aromatic and heterocyclic amine substrates using boiling water as a reaction medium, indicating the role of water as a dual acid/base catalyst at elevated temperature.¹⁷⁵ However, reaction times with water insoluble substrates could be significantly longer, when water is the only solvent. A few Boc deprotections have also been reported in subcritical water ($150\text{ }^{\circ}\text{C} < T < 370\text{ }^{\circ}\text{C}$, $0.4 < p < 22\text{ MPa}$) to take advantage of the higher dissociation of water.¹⁷⁶ Extraction of water soluble organic molecules using ionic liquids have been explored with the advent of [BMIM]PF₆ ionic liquid.¹⁷⁷ Recently, Majumdar et al. reported deprotection of several *N*-Boc protected aromatic and heteroaromatic compounds using imidazolium based protic ionic liquid and also discussed the selectivity of their approach.¹⁷⁸ Interestingly, use of phosphonium based ionic liquids in organic synthesis has been very limited. This is surprising, given some of their interesting properties like lack of an acidic proton (which may lead to carbene formation), generally lower density than water (helpful in liquid-liquid extraction), tolerance towards air, moisture and high thermal stability.¹³

To the best of our knowledge, this is the first report on a generalized Boc-deprotection of natural amino acids and peptides in ionic liquid media. There are challenges in purification of water soluble compounds involving many ILs traditionally used in organic synthesis (due to their own aqueous solubility). This problem is circumvented by the current approach.

The current work, utilizes trihexyltetradecylphosphonium bis(trifluoromethane)sulfonimide (TTP-NTf₂) ionic liquid as a water insoluble solvent having a relatively low kinematic viscosity of 218.6 cSt @ 30 °C, density of 1.065 g cm⁻³, high thermal stability (~380 °C), broad substrate solubility and thermal range (-22 to 350 °C).¹³

6.3 Materials and Methods

6.3.1 Materials and method of analysis

Compounds were purchased in their purest commercial quality. All materials were used as obtained, unless and otherwise indicated. Column chromatography for recovery of Ionic Liquid was performed using silica gel (300-400 mesh) with Hexane/Ethyl acetate as eluent. ^1H NMR, ^{13}C NMR, ^{19}F NMR and ^{31}P NMR experiments were performed on 500 MHz a JEOL Eclipse Plus 500 instrument. Chemical shifts were recorded with reference to residual solvent peaks (D_2O residue = 4.79 ppm, CDCl_3 residue = 7.26 ppm). ESI Mass spectroscopy was performed with Thermo Finnigan LXQ linear Ion Trap mass spectrometer, when required.

6.3.2 Synthesis Procedures

6.3.2.1 Preparation of TTP-NTf₂

To a solution of (40 g, 77 mmol) trihexyltetradecylphosphonium chloride, (graciously donated by CYTEC, West Paterson, NJ, USA) in methanol (20 mL) was added (24.32 g, 84.71 mmol) LiNTf₂. Additional methanol was added to obtain a clear solution. The solution was slightly warm at the beginning and was stirred overnight. Methanol was removed under reduced pressure and ~200 mL CH_2Cl_2 was added to the round bottom flask. The organic layer containing the ionic liquid was transferred to the separating funnel and LiCl was extracted with (3x100 mL) deionized water. The organic layer was concentrated under reduced pressure and dried in vacuum oven (maintained at 40 °C) over P_2O_5 for at least 36 h before use. The products were characterized by ^1H NMR, ^{13}C NMR, ^{19}F and ^{31}P NMR.

6.3.2.2 Method A (Neat Reaction in TTP-NTf₂)

A mixture of (0.25 g, 0.32-1.43 mmol) N-Boc protected amino acid/peptides and TTP-NTf₂ (7 g, 9.16 mmol) was stirred (~150 rpm) for 5-6 h at 150 °C in a round bottom flask (50 mL) equipped with a reflux condenser. Completion of reaction was monitored by TLC using ethyl acetate/methanol (95:5) and ninhydrin as staining agent. On cooling, the reaction mixture was transferred into separating funnel with 3 x 10 mL (CH₂Cl₂/water 1:1). In addition, CH₂Cl₂ (100 mL) and water (50 – 80 mL, depending on the substrate) was added to the separating funnel. The layers were allowed to separate after shaking and the organic layer (containing the ionic liquid) was removed. To the aqueous layer (containing the amino acids) fresh CH₂Cl₂ (2 x 75mL) was added to ensure removal of any trace of ionic liquid remaining. The aqueous layer was evaporated to dryness to obtain the product. In most of the cases, this gave us the purified amino acid, but otherwise a final washing with ~ 5 mL isopropanol (using centrifuge) proved very effective.

6.3.2.3 Method B (TTP-NTf₂ and water)

To a mixture of (0.25 g, 0.32-1.43 mmol) N-Boc protected amino acid/peptides and TTP-NTf₂ (7 g, 9.16 mmol) was added deionized water 12-14% (based on TTP-NTf₂). The resulting mixture was stirred (~200 rpm) for 2.5-6 h at 150 °C (for amino acids) and 2.5 h at 110 °C (for peptides). The remaining work-up is similar to method A.

L-Histidine and L-lysine tends to form emulsions especially for method B. They were centrifuged for 5 min at around 5000 rpm (the Drucker Co., Model 614 B) to obtain the purified compound. For peptides, the water was generally removed at 40-45 °C under reduced pressure.

6.3.2.4 Method C (TTP-NTf₂ and TFA)

To a stirring mixture of (0.25 g, 0.32-1.43 mmol) N-Boc protected amino acid/peptides and TTP-NTf₂ (7 g, 9.16 mmol) was added TFA (2 equiv, based on substrate). The resulting mixture was stirred (~150 rpm) for 7-10 min at 100 °C (for peptides) and 130 °C (for amino acids). The remaining procedure is similar to method A.

For peptides, the water was removed by either freeze drying, air drying at higher flow in a crystallizing dish using an inverted funnel at room temperature or direct precipitation of amino acid by adding acetone.

6.4 Results and Discussion

Three different methods were employed to liberate the built in gaseous entity in the Boc group (Scheme 6-1 and Table 6-1). Simple thermal treatment of Boc protected amino acids at around 150 °C gave the desired product for selected substrates, however the yields were not satisfactory with incomplete conversions and some product decomposition was observed (Table 6-1, 1A-16A)

Addition of small amount of water led to significant improvement in yield and product purity as evident in (Table 6-1, 1B-16B). Deprotection of Boc-L-aspartic and glutamic acid (having two free acid groups) conversion took the least time. It is well known that quaternary ammonium and phosphonium cations act as phase transfer agents.¹⁷⁹ Therefore, reactions were also performed in tetrabutylammonium NTf₂ (mp 84-85 °C) with *N*-Boc-L-Ala-OH as a substrate under reaction conditions identical to method B, which gave alanine in 97% yield. A similar reaction with butylmethylimidazolium NTf₂ resulted in incomplete conversion with 67% of L-alanine as a product. These observations may indicate the possibility of phosphonium cation acting as a phase transfer catalyst, while acidic pH in the aqueous phase would drive deprotection of Boc

group at high temperature. Lewis acidic type interaction of carbonyl group with imidazolium based ionic liquids have been indicated in earlier reports.¹⁷⁸⁻¹⁷⁹ For phosphonium ionic liquids, especially in the absence of water as a separate phase, similar interactions have been suggested.^{46, 180-181} This however does not appear to be operative in the present case.

In the third method variation, (Table 6-1, 1C-16C) addition of only 2 equiv. TFA resulted in accelerated deprotection within 10 min in almost all the cases studied compared to conventional methods that requires 2-5 h and uses high concentrations of TFA (generally 1:1 TFA:CH₂Cl₂).¹⁷³ The method was extended for the deprotection of Boc groups of dipeptides and two Boc and a trityl group for a tripeptide. However, some condensation products were observed for entry 14B which was avoided by performing the reaction at 110 °C for 2.5 h.

Scheme 6-1 Boc deprotection of amino acids using phosphonium ionic liquids.

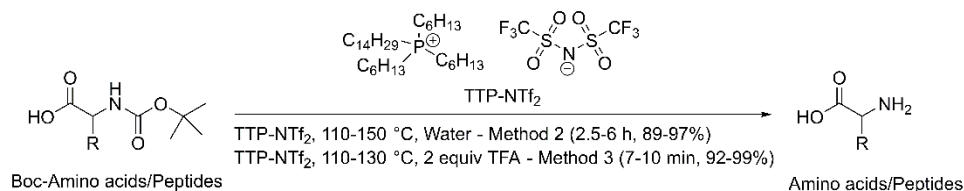


Table 6-1 Deprotection of N-Boc amino acid and peptide substrates

#	Substrate	Method A ^a neat + Δ, yield (%), time (h)	Method A product	Method B ^b H ₂ O + Δ, yield (%), time (h)	Method B product	Method C ^c TFA + Δ, yield (%), time (h)	Method C product
Amino acids ^{a,b,c,d}							
1	<i>N</i> -Boc-L-Gly-OH	71% (5 h)	H-L-Gly-QH	96% (3 h)	H-L-Gly-OH	93% (7 min)	H-L-Gly-OH
2	<i>N</i> -Boc-L-Ala-OH	67% (5 h)	H-L-Ala-OH	91% (3 h)	H-L-Ala-OH	98% (7 min)	H-L-Ala-OH
3	<i>N</i> -Boc-L-Val-OH	29% (6 h)	H-L-Val-OH	92% (6 h)	H-L-Val-QH	93% (10 min)	H-L-Val-OH
4	<i>N</i> -Boc-L-Leu-OH	D ^d (6h)	NA	89% (6 h)	H-L-Leu-QH	98% (10 min)	H-L-Leu-OH
5	<i>N</i> -Boc-L-Ile-OH	D ^d (6 h)	NA	94% (6 h)	H-L-Ile-OH	98% (10 min)	H-L-Ile-OH
6	<i>N</i> -Boc-L-Phe-OH	20% (6 h)	H-L-Phe-OH	93%(5 h)	H-L-Phe-OH	95% (10 min)	H-L-Phe-OH
7	<i>N</i> -Boc-L-Pro-OH	D ^d (6 h)	NA	95% (5 h)	H-L-Pro-OH	96% (10 min)	H-L-Pro-OH
8	<i>N</i> -Boc-L-Met-OH	D ^d (6 h)	NA	92% (5 h)	H-L-Met-OH	97% (10 min)	H-L-Met-OH
9	<i>N</i> -Boc-L-Thr-OH	D ^d (6 h)	H-L-Thr-DH	90% (5 h)	H-L-Thr-OH	92% (10 min)	H-L-Thr-OH
10	<i>N</i> -Boc-L-His-OH	D ^d (6 h)	NA	92% (6 h)	H-L-His-OH	92% (10 min)	H-L-His-OH
11	Boc-L-Lys(Boc)-OH	D ^d (6 h)	NA	91% (6 h)	H-L-Lys-OH	93% (11 min)	H-L-Lys-OH
12	<i>N</i> -Boc-L-Asp-OH	87% (5 h)	H-L-Asp-OH	97% (2.5 h)	H-L-Asp-OH	99% (10 min)	H-L-Asp-OH
13	<i>N</i> -Boc-L-Glu-OH	27% (5 h)	H-L-Glu-OH	93% (4 h)	H-L-Glu-OH	96% (10 min)	H-L-Glu-OH

Table 6-1- *Continued*

Peptides ^{e,f,g}							
14	<i>N</i> -Boc-Ala-Ala-OH	13%	-	92% (2.5 h) ^f	H-Ala-Ala-OH	94% 10 min ^g	H-Ala-Ala-OH
15	<i>N</i> -Boc-Gly-Val-OH	IC ^e	-	94% (2.5 h) ^f	H-Gly-Val-OH	95% 10 min ^g	H-Gly-Val-OH
16	Boc-Gly-His(Trt)-Lys(Boc)-OH	IC ^e	NA	92% (2.5 h) ^f	H-Gly-His-Lys-OH	95% 7-8 min ^g	H-Gly-His-Lys-OH

^a TTP-NTf₂, 150 °C, 5-6 h (incomplete reaction with unreacted starting material for entry 1, 2, 3, 6, 12 and 13. For entry 14A, trace condensation by product observed along with unreacted starting material).^b TTP-NTf₂, 12-14% water as additive (based on TTP-NTf₂), 150 °C, 2.5-6 h. ^c TTP-NTf₂ 2 equiv. TFA as additive (based on substrate), 130 °C, ~10 min. ^dD (decomposed), TTP-NTf₂ 150 °C, 6 h. ^e IC (trace product with unreacted starting material and some decomposition observed), TTP-NTf₂, 120 °C, 3 h. ^f TTP-NTf₂, 110 °C, 12-14% water as additive (based on TPP-NTf₂), 2.5 h. ^gTTP-NTf₂, 2 equiv. TFA as additive based on substrate, 110 °C, 7-10 min. Yields reported are isolated.

6.5 Conclusions

In summary, the current work provides a simple and convenient procedure for Boc-deprotection reaction in ionic liquid media. The lower viscosity, broad substrate solubility and thermal stability of the ionic liquid provide scope for carrying out high temperature organic reactions and opens up the possibility of extraction and purification for water soluble organic compounds using ionic liquids. The rapid deprotection; using only two equivalent of TFA (little excess of which is mostly removed during the water distillation under reduced pressure) allowed the whole process to be very efficient. The various amino acids were extracted without any chromatographic purification (as it can be challenging to separate ionic liquid and water miscible organic compounds in the normal phase mode using silica gel chromatography). Also, the said ionic liquid from all batches was pooled together and recycled for further use by column purification using silica gel Chromatography (ethyl acetate/hexane 70:30 to ethyl acetate 100%). Reactions performed with the recycled ionic liquid, (92% recovery and characterized by NMR spectroscopy) gave similar efficiencies.

Chapter 7

CONCLUSIONS

Chapter 2 discussed the effects of various structural modifications including cation, alkane linkage chain, and anions on the physicochemical properties of ILs. This study presented the designing of dicationic ILs with high thermal stabilities, and dicationic ILs with TGA thermal stabilities up to 460 °C were reported. Considering the popularity of ILs in academia and industry, understanding of the structure-property relationship is essential to design “task-specific” ionic liquids. Applications of ILs are feasible when they are liquids at room temperature, and the results of this study will be useful to choose proper structural moieties to obtain room temperature ionic liquids.

The thermal decomposition study was useful to identify the thermal degradation products of ILs at high temperatures. The results provided information about the structural moieties, i.e., bonds, atoms or linkages of ILs most susceptible to thermally induced changes. The heteroatom carbon single bonds were most prone to thermal decomposition, and phosphonium ILs formed oxides at high temperatures. The results of thermal degradation study will be useful for optimal use of ILs and providing information on possible structural modifications to further improving their stability.

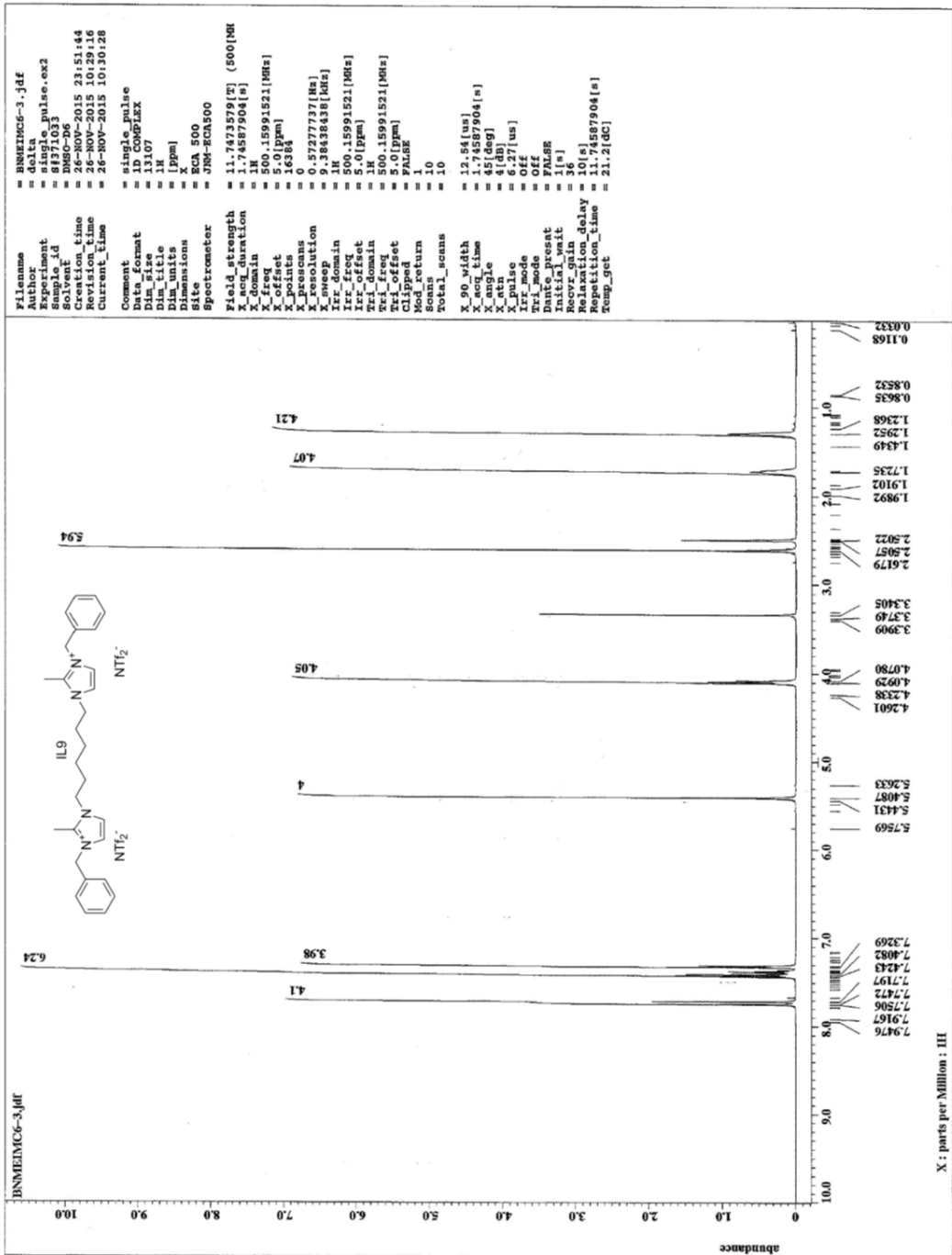
Chapter 3 discussed the effect of different IL structural moieties such as cation type, alkane linkage chain, and anion on the polarities and selectivities of dicationic IL GC stationary phases. Chapters 3 and 5 presented the applications of thermally stable IL stationary phases in high temperature GC separations. Phosphonium based dicationic IL GC stationary phases showed excellent selectivities in the separation of structural isomers of different toxic environmental pollutants. The structural isomers of pollutants are difficult to quantify by mass spectrometer as they have same mass spectrum but, can

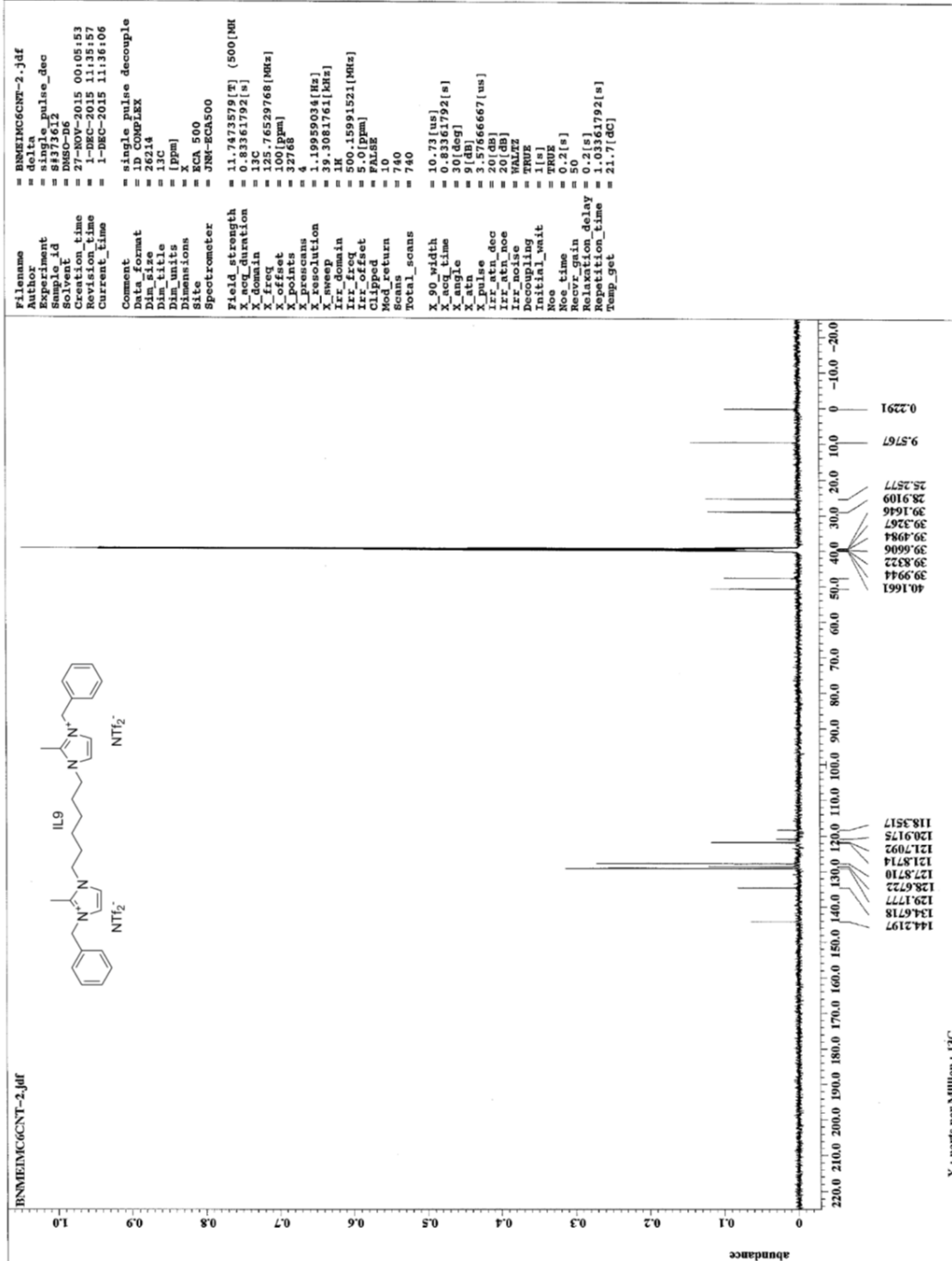
be easily quantified due to their chromatographic separation on the phosphonium based column. The newly designed phosphonium ILs showed improved performance in the separation of tetrachlorodibenzodioxin isomers compared to the other stationary phases. The selectivities of new IL GC stationary phases were different than most of the commercially available traditional GC stationary phases and few of the IL stationary phases. The understanding of structure-selectivity relationship ILs provides endless opportunities for modifying selectivities of IL GC stationary phases.

Chapter 6 discussed the report on the application of thermally stable phosphonium IL for the rapid and efficient deprotection tert-butoxycarbonyl (Boc) protected amino acids and peptides. The phosphonium IL acted as a phase transfer catalyst during the deprotection reaction. The reaction was carried out in IL at higher temperatures and deprotection was completed in 10 min (with TFA) to 2-3 h (with water) with easy purification processes compared to traditional Boc-deprotection reactions.

Appendix 1

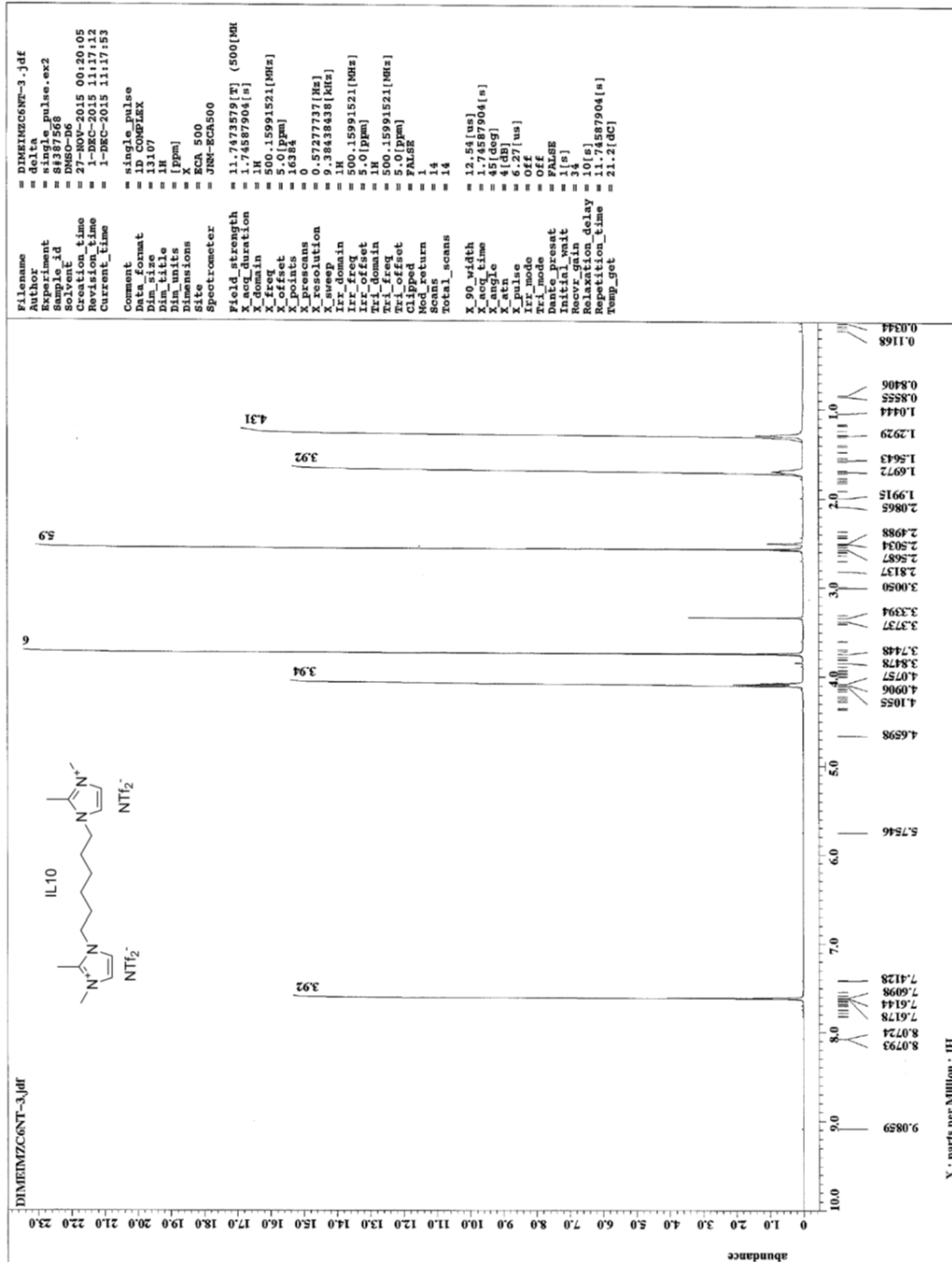
^1H NMR AND ^{13}C NMR OF $\text{C}_6(\text{bmim})_2\text{-NTf}_2$

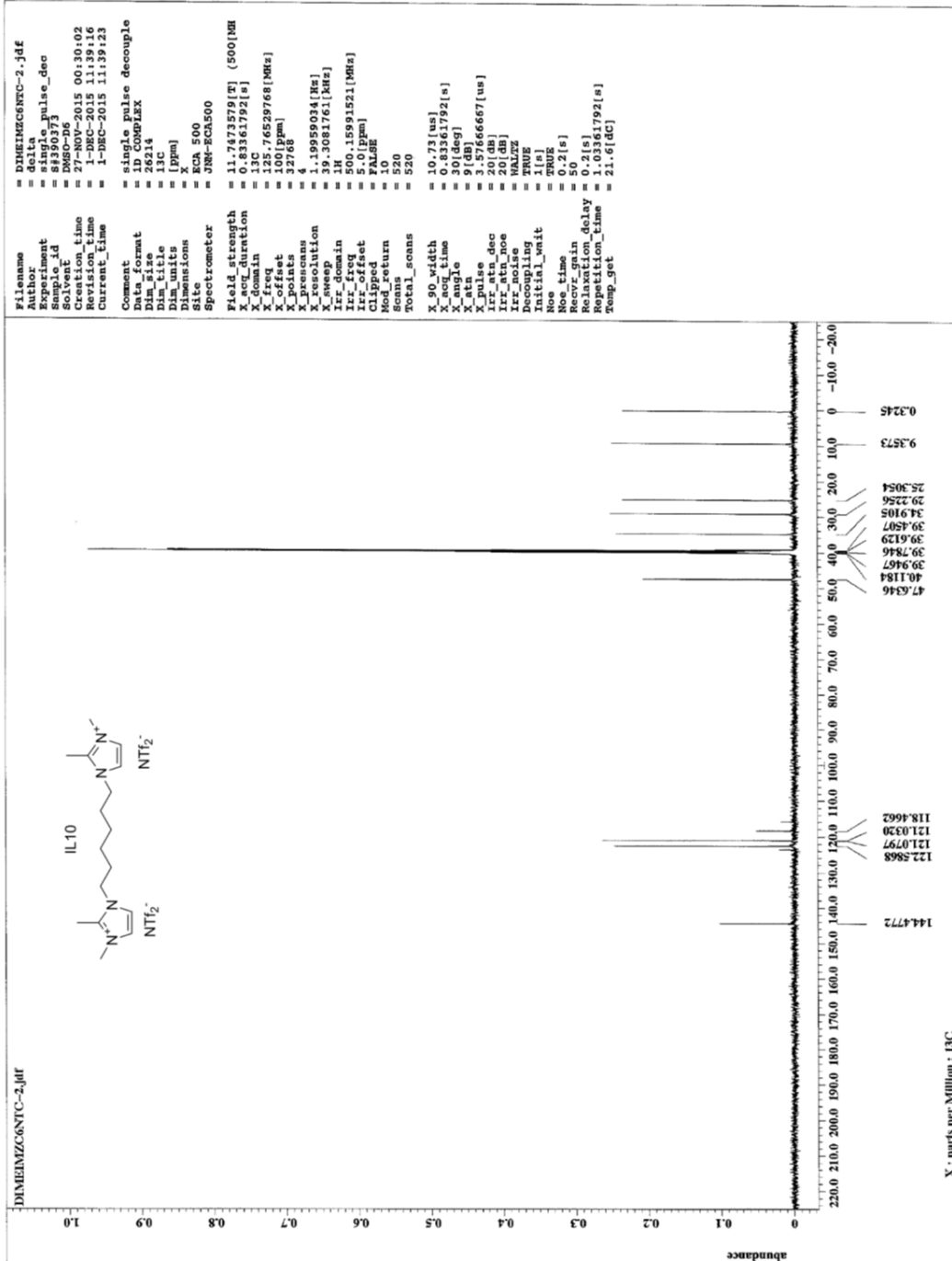




Appendix 2

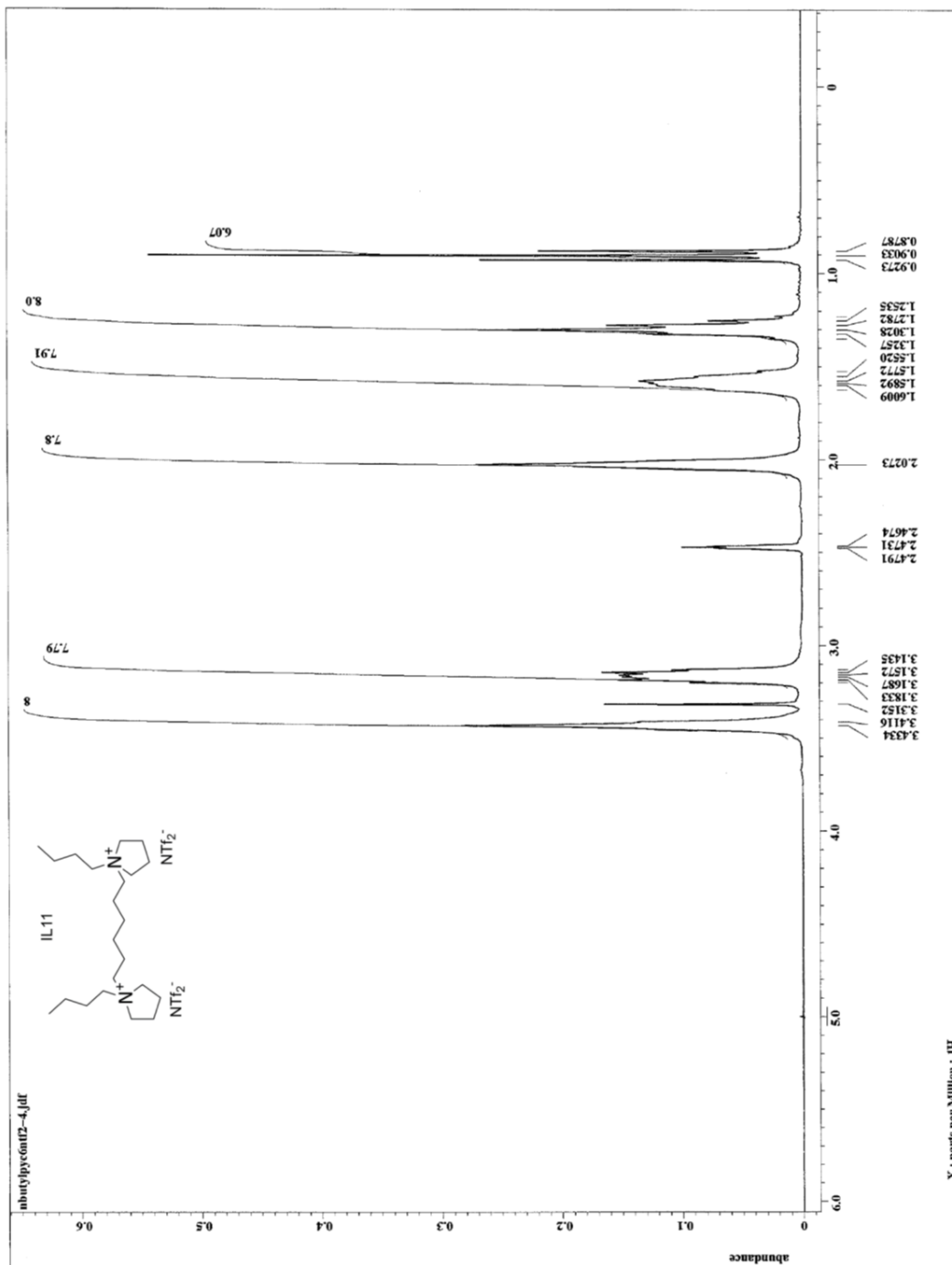
^1H NMR AND ^{13}C NMR OF $\text{C}_6(\text{mzim})_2\text{-NTf}_2$

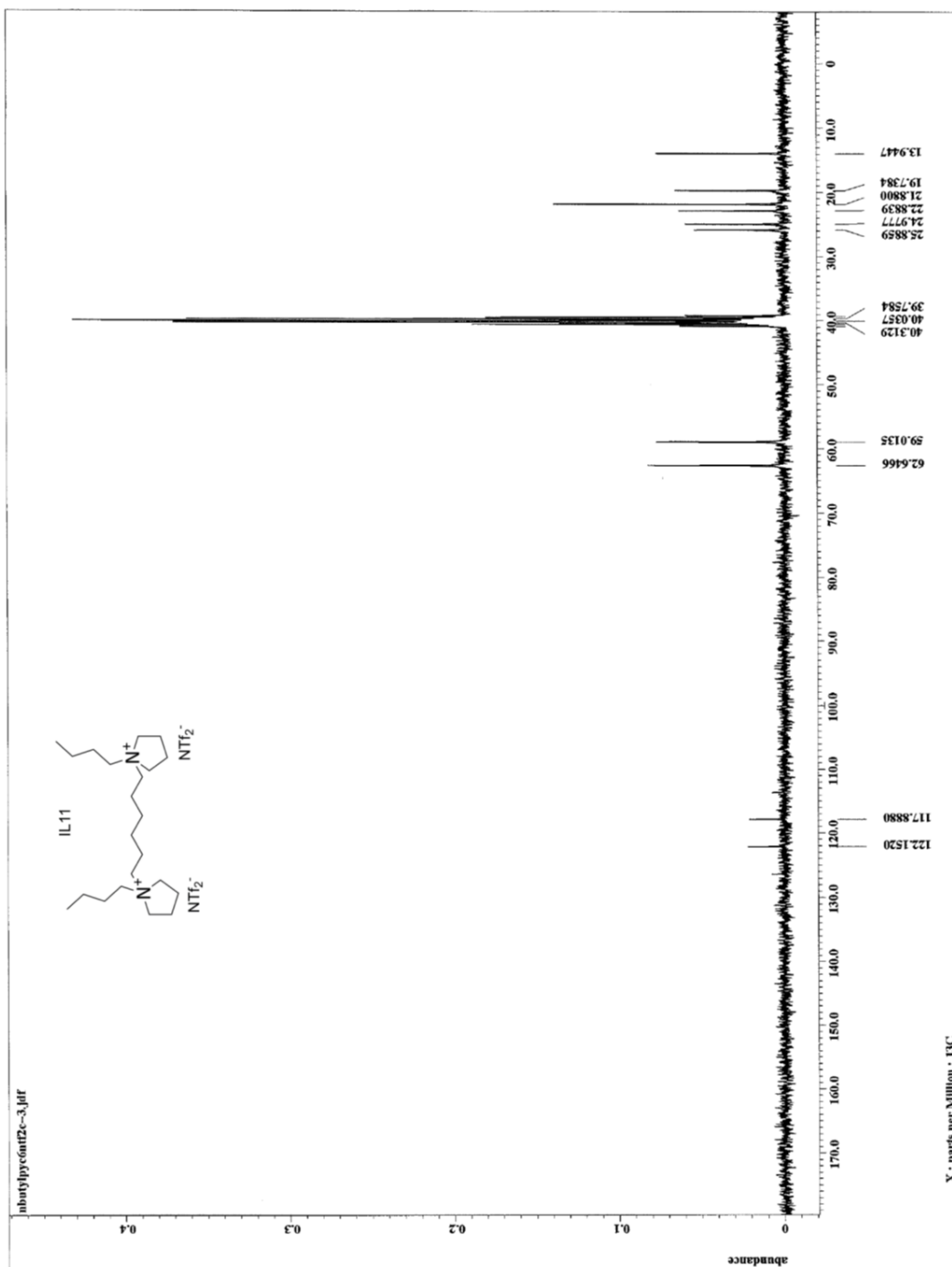




Appendix 3

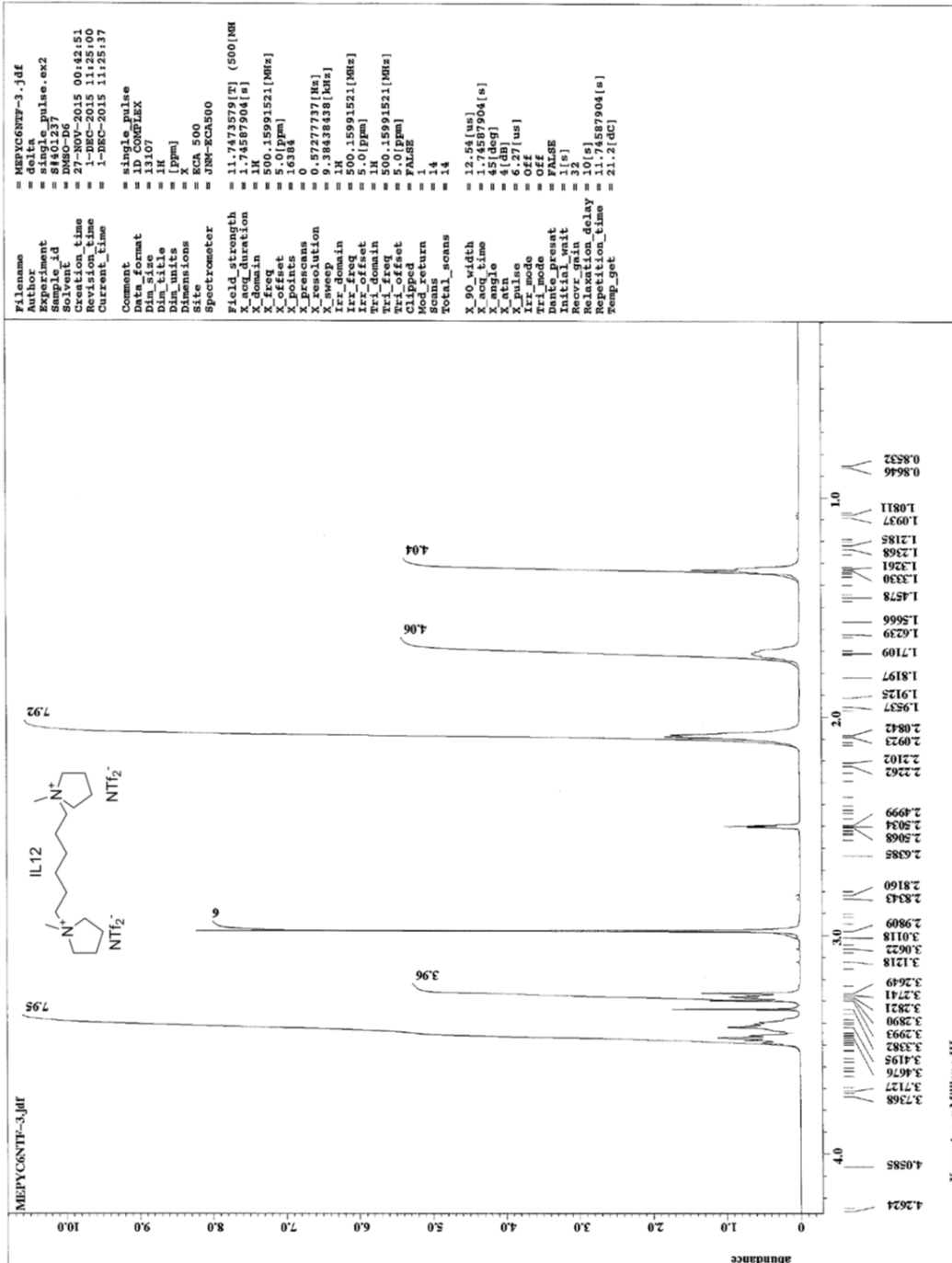
^1H NMR AND ^{13}C NMR OF $\text{C}_6(\text{bpy})_2\text{-NTf}_2$

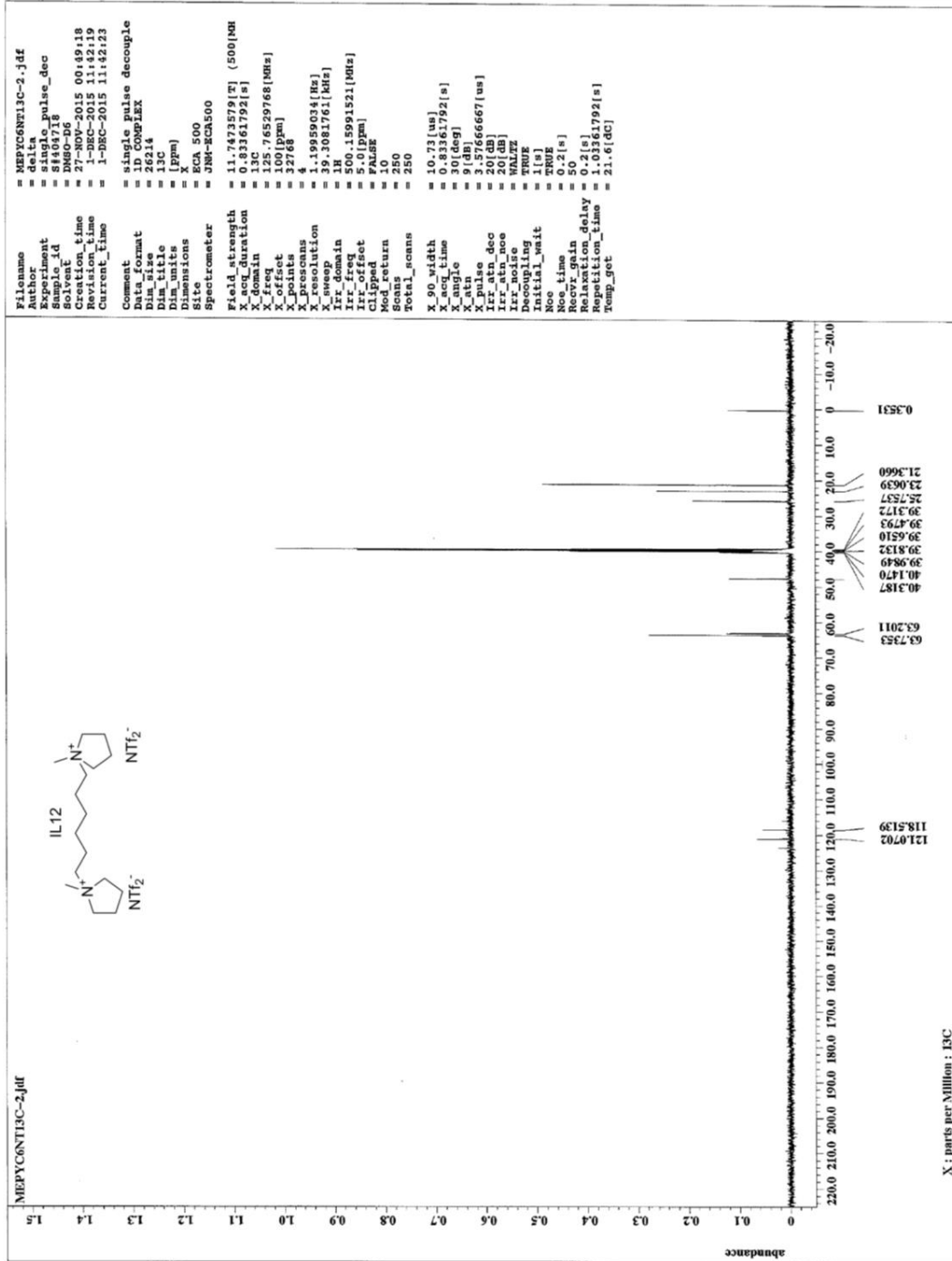




Appendix 4

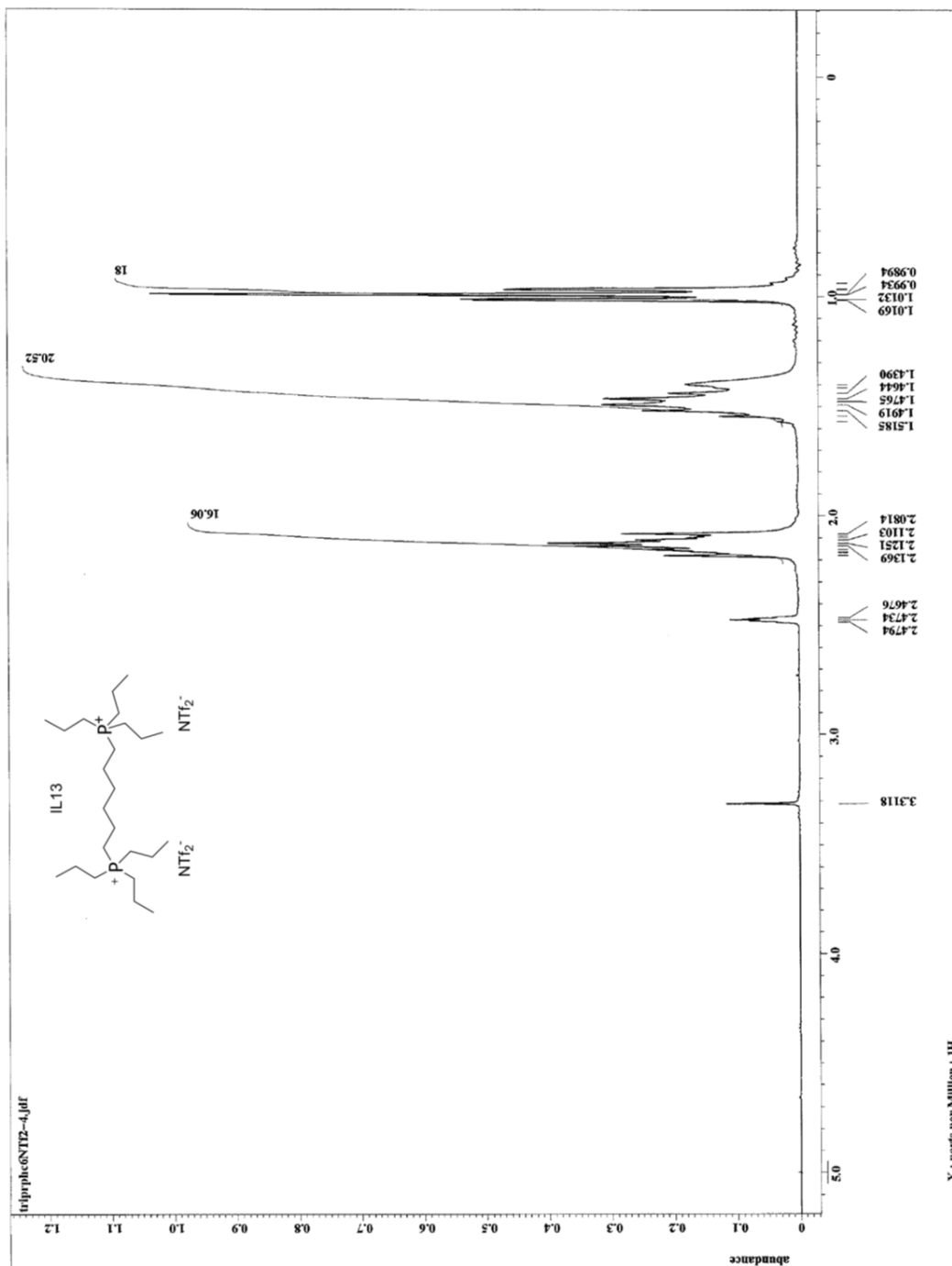
^1H NMR AND ^{13}C NMR OF $\text{C}_6(\text{mpy})_2\text{-NTf}_2$

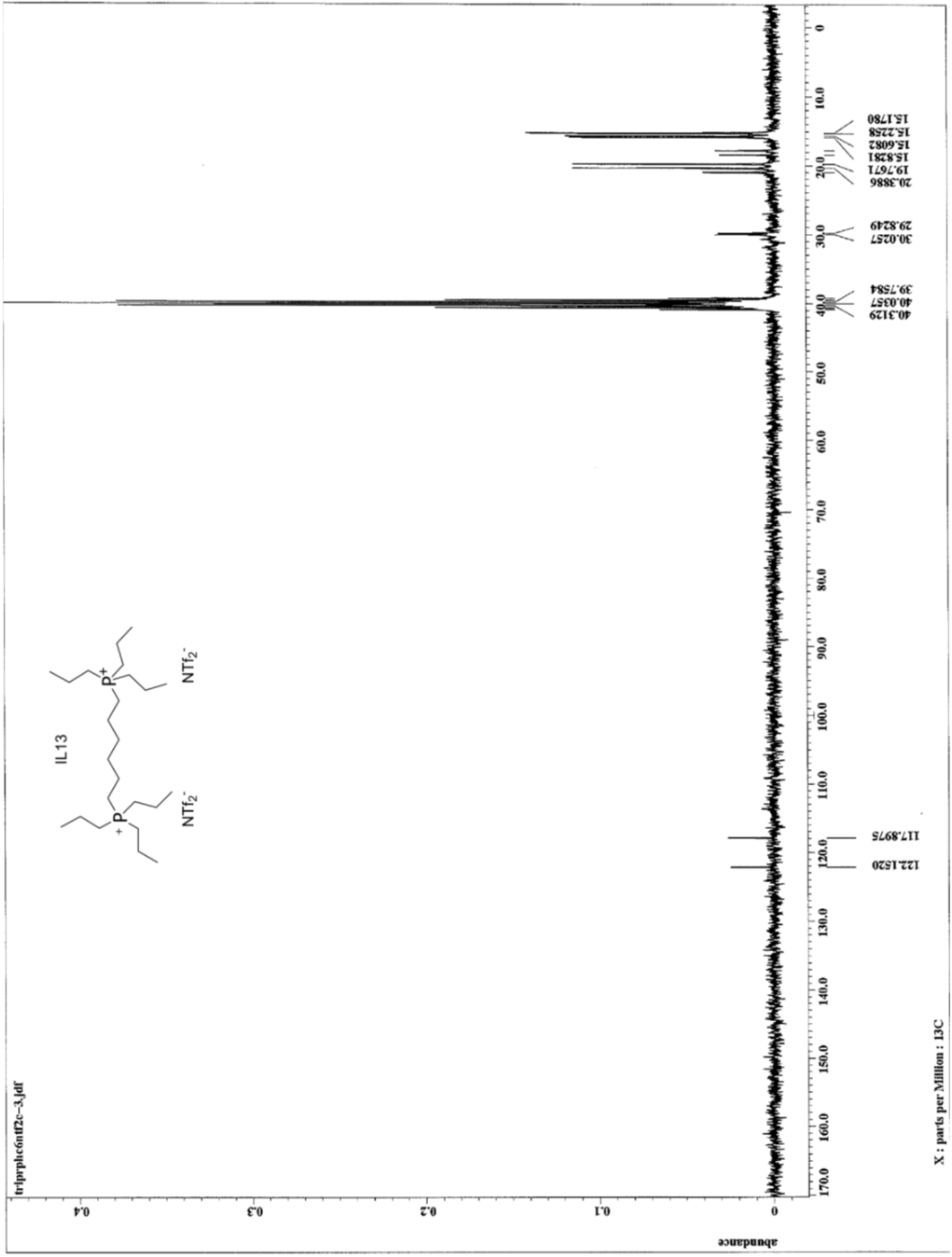




Appendix 5

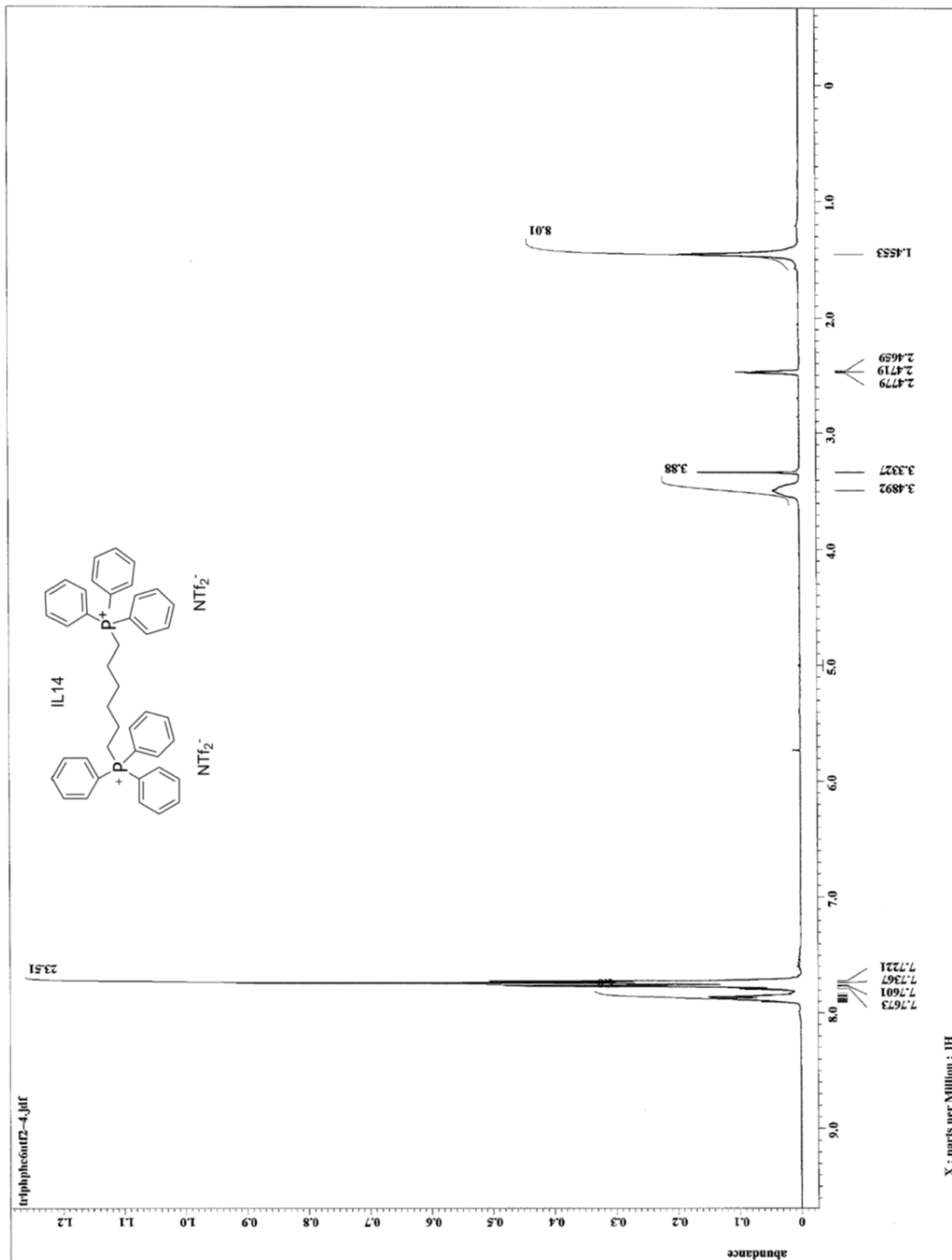
^1H NMR AND ^{13}C NMR OF $\text{C}_6(\text{pr}_3\text{p})_2\text{-NTf}_2$

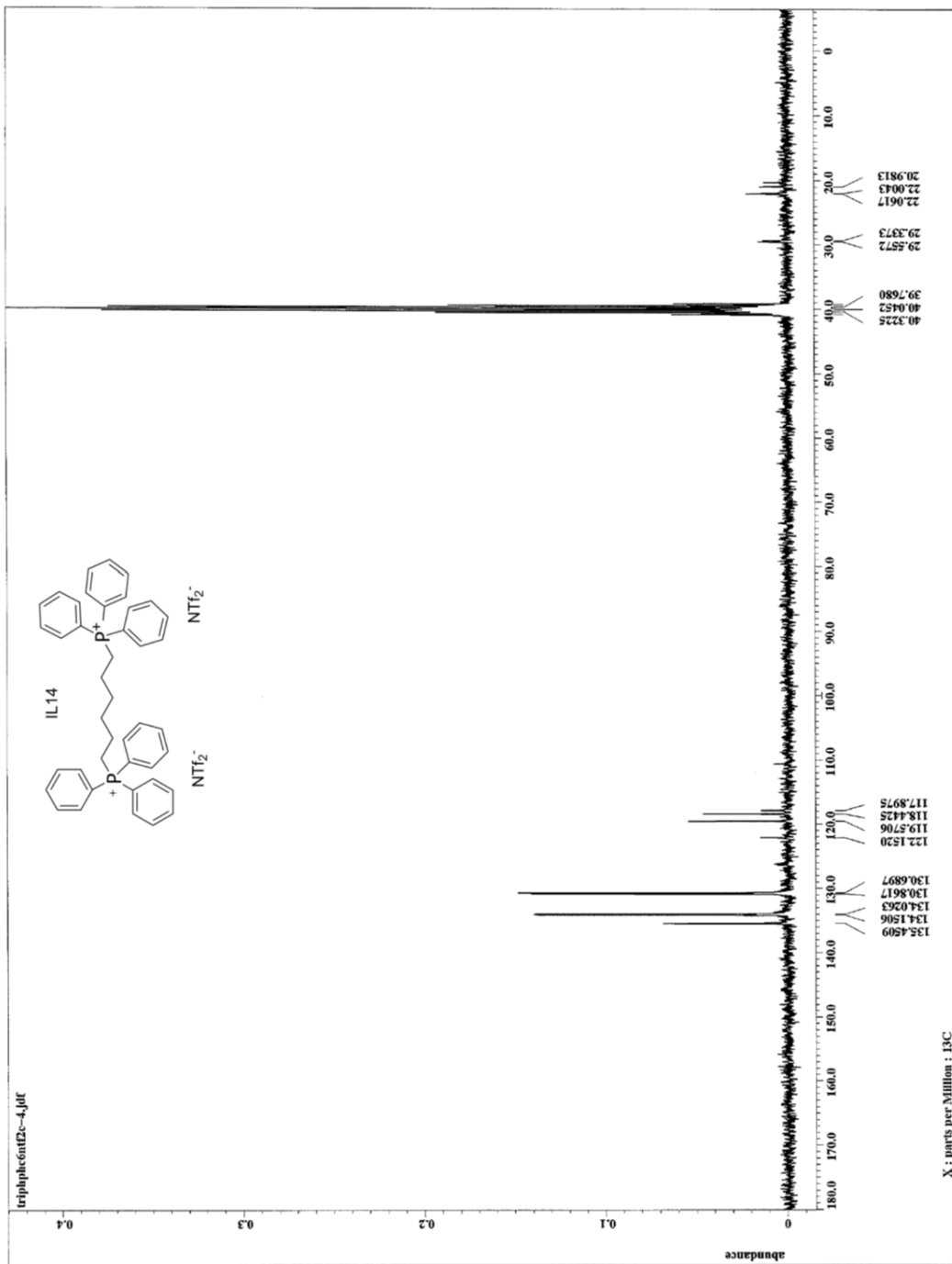




Appendix 6

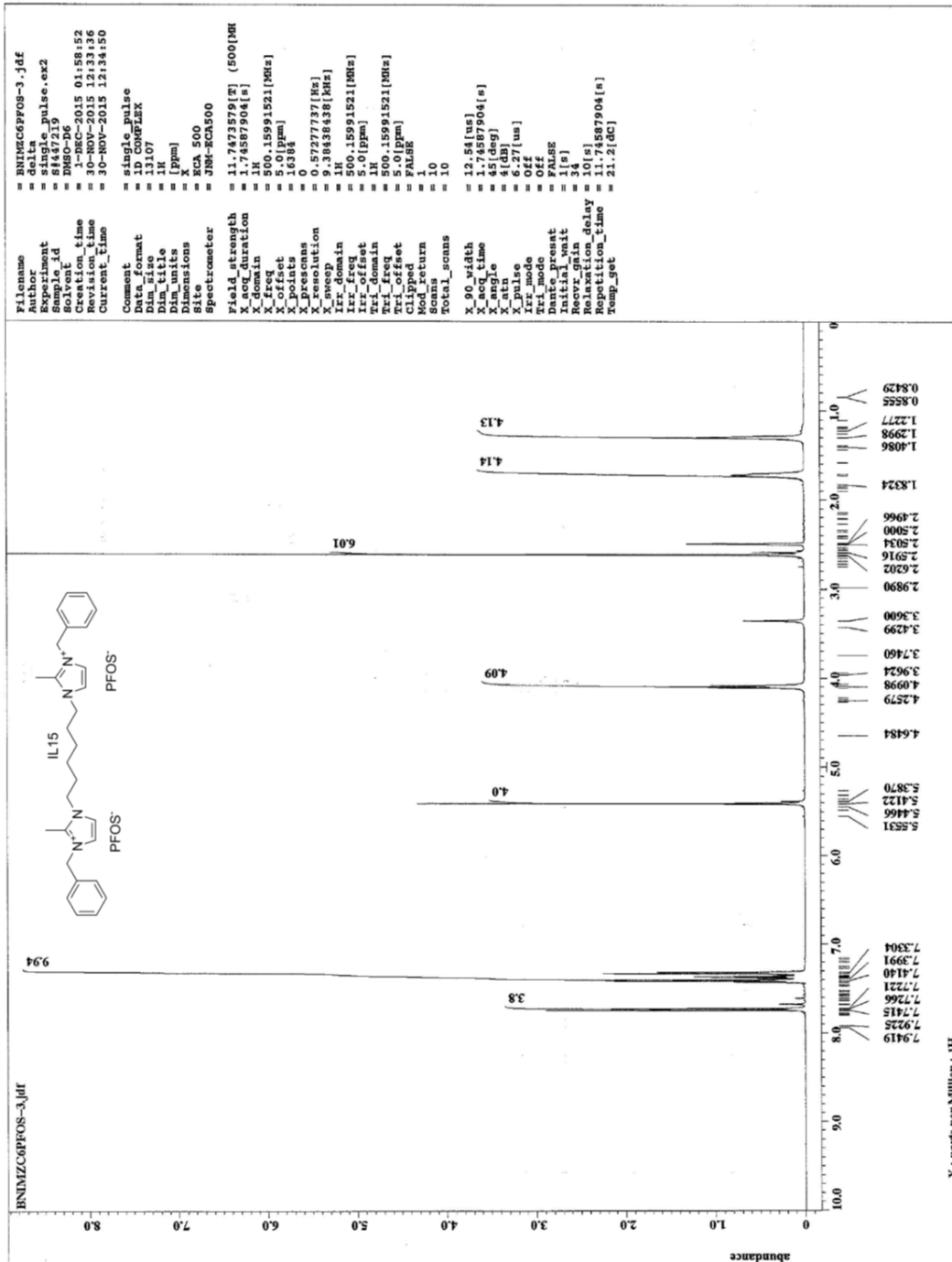
^1H NMR AND ^{13}C NMR OF $\text{C}_6(\text{ph}_3\text{p})_2\text{-NTf}_2$

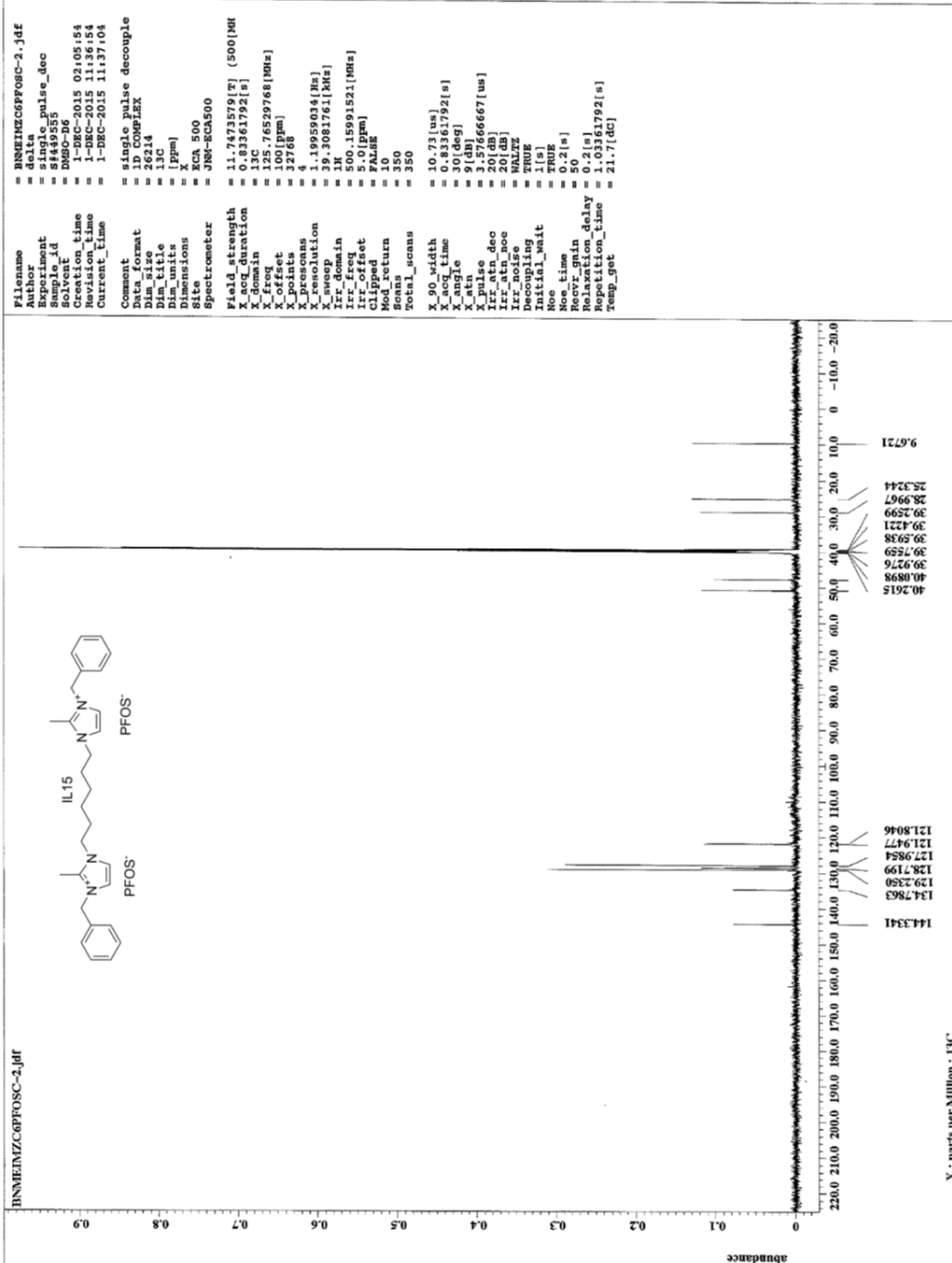




Appendix 7

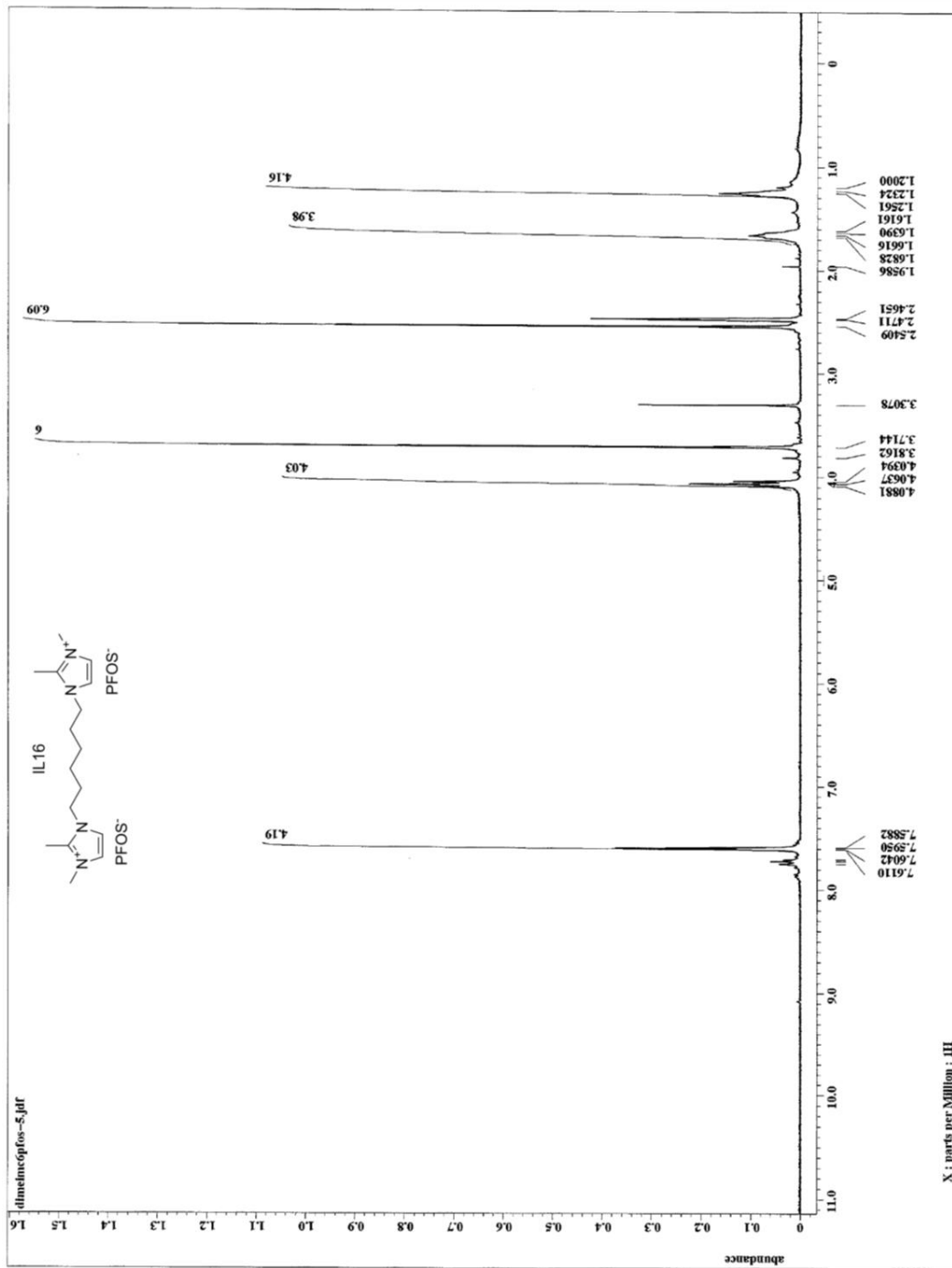
^1H NMR AND ^{13}C NMR OF $\text{C}_6(\text{bmim})_2\text{-PFOS}$

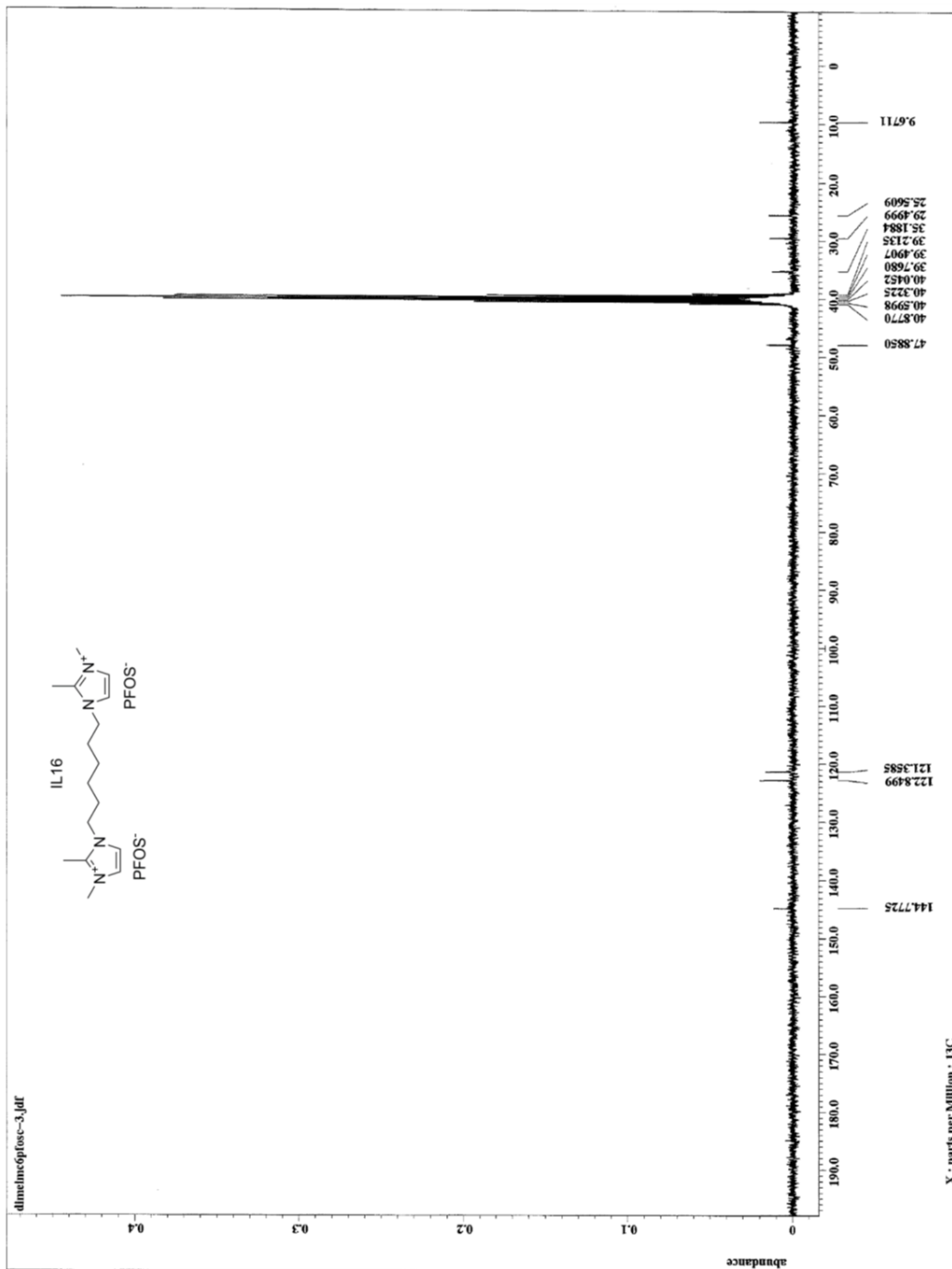




Appendix 8

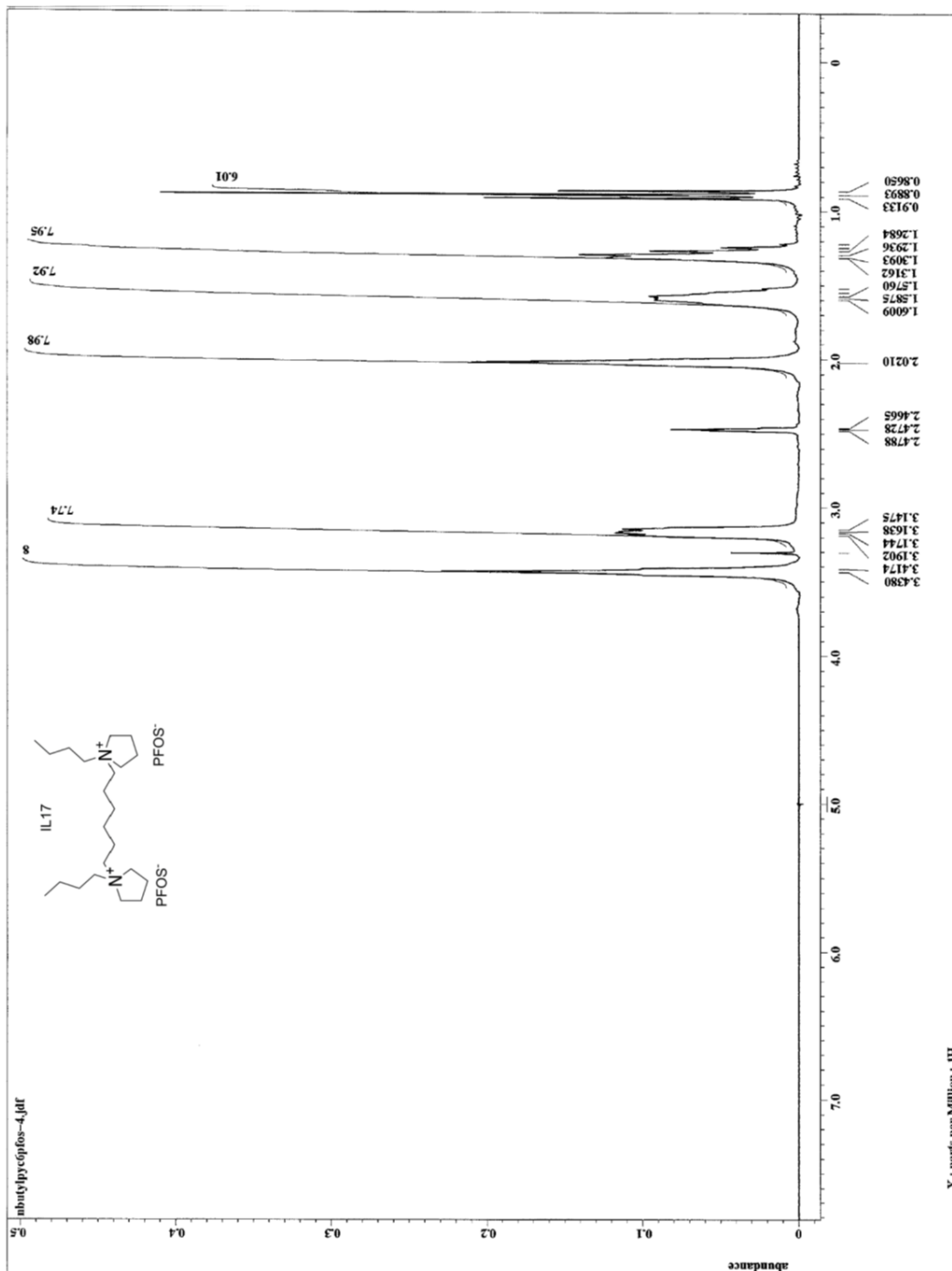
^1H NMR AND ^{13}C NMR OF $\text{C6}(\text{m}_2\text{im})_2\text{-PFOS}$

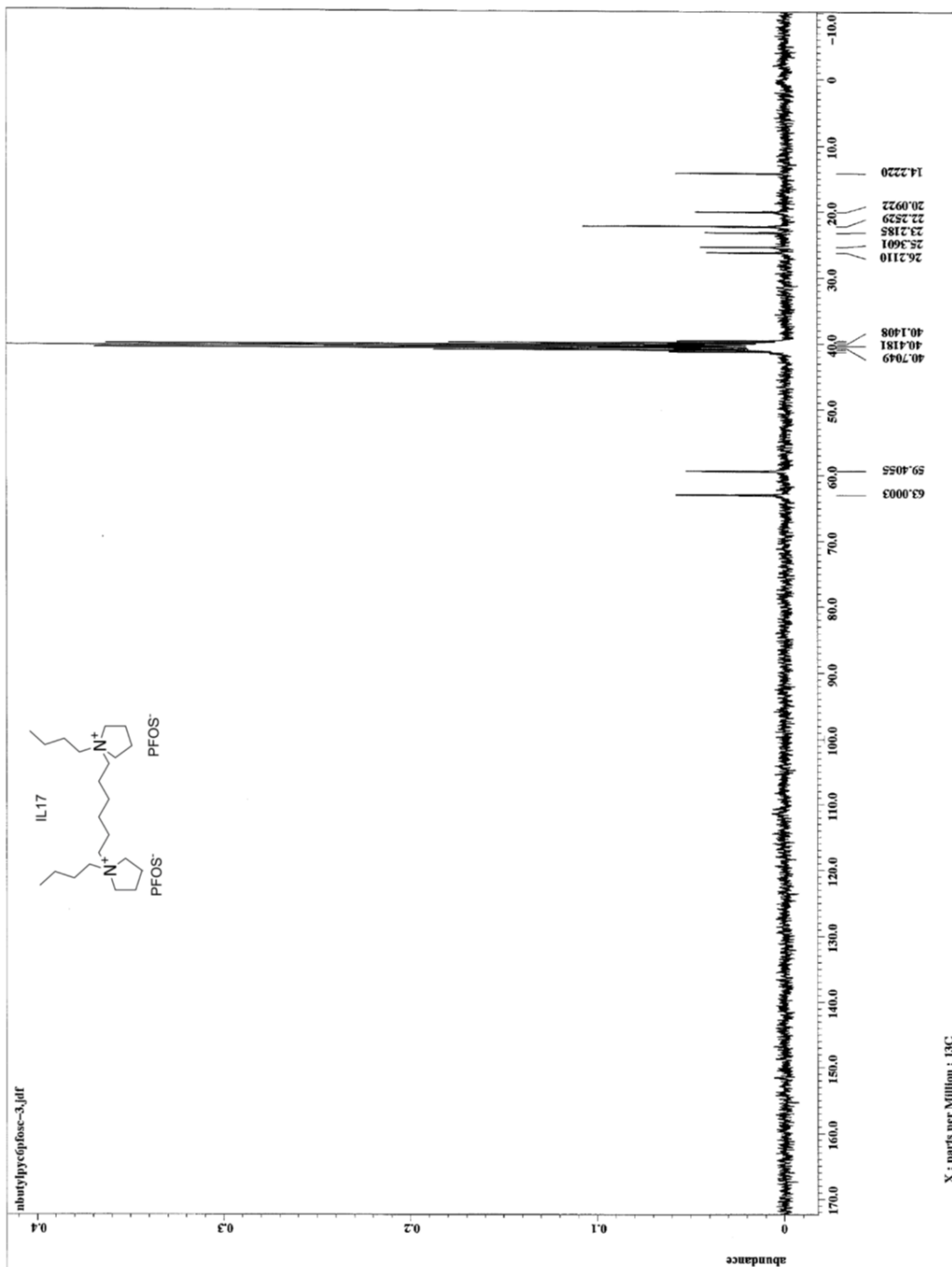




Appendix 9

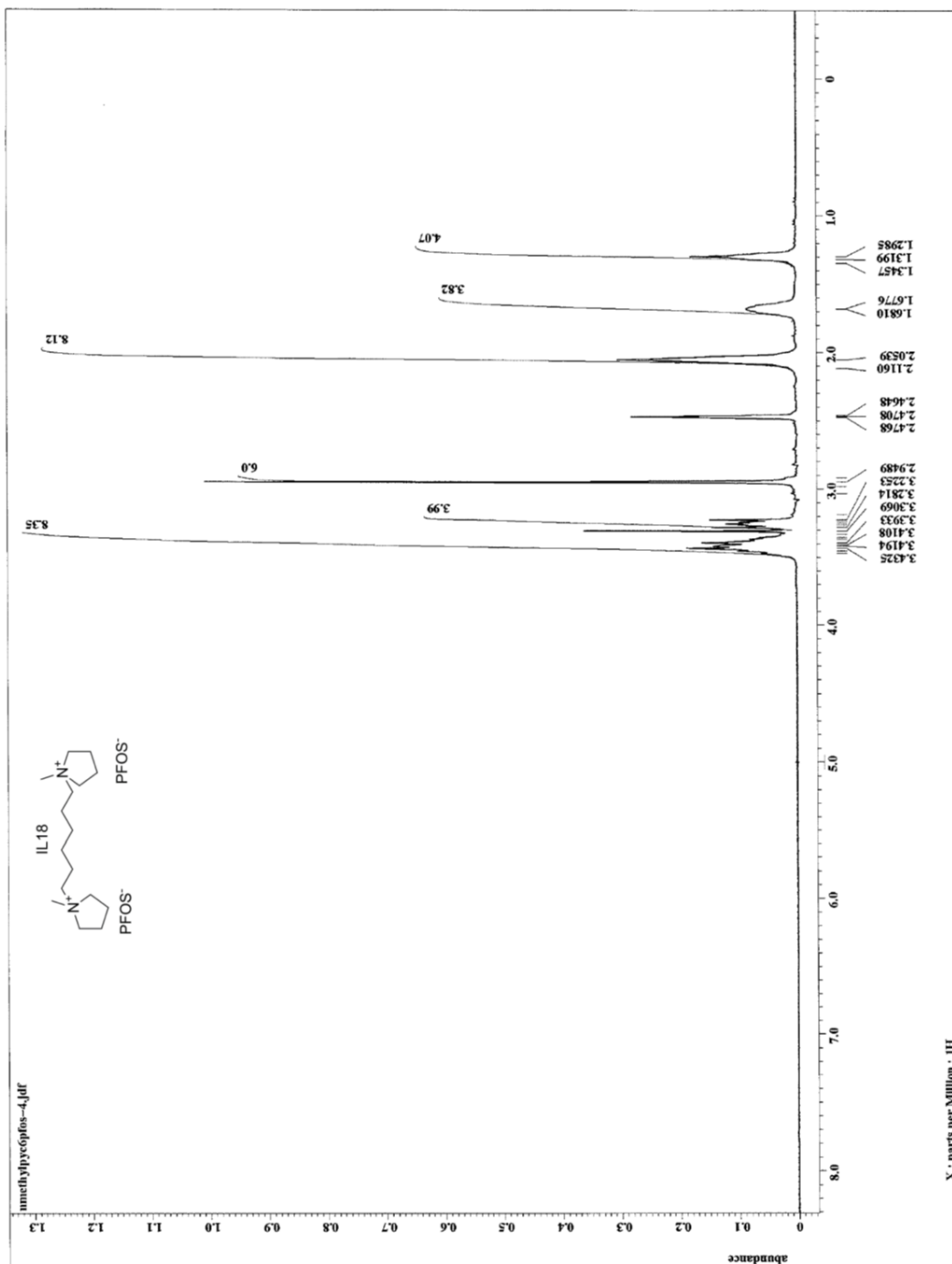
^1H NMR AND ^{13}C NMR OF $\text{C}_6(\text{bpy})_2\text{-PFOS}$

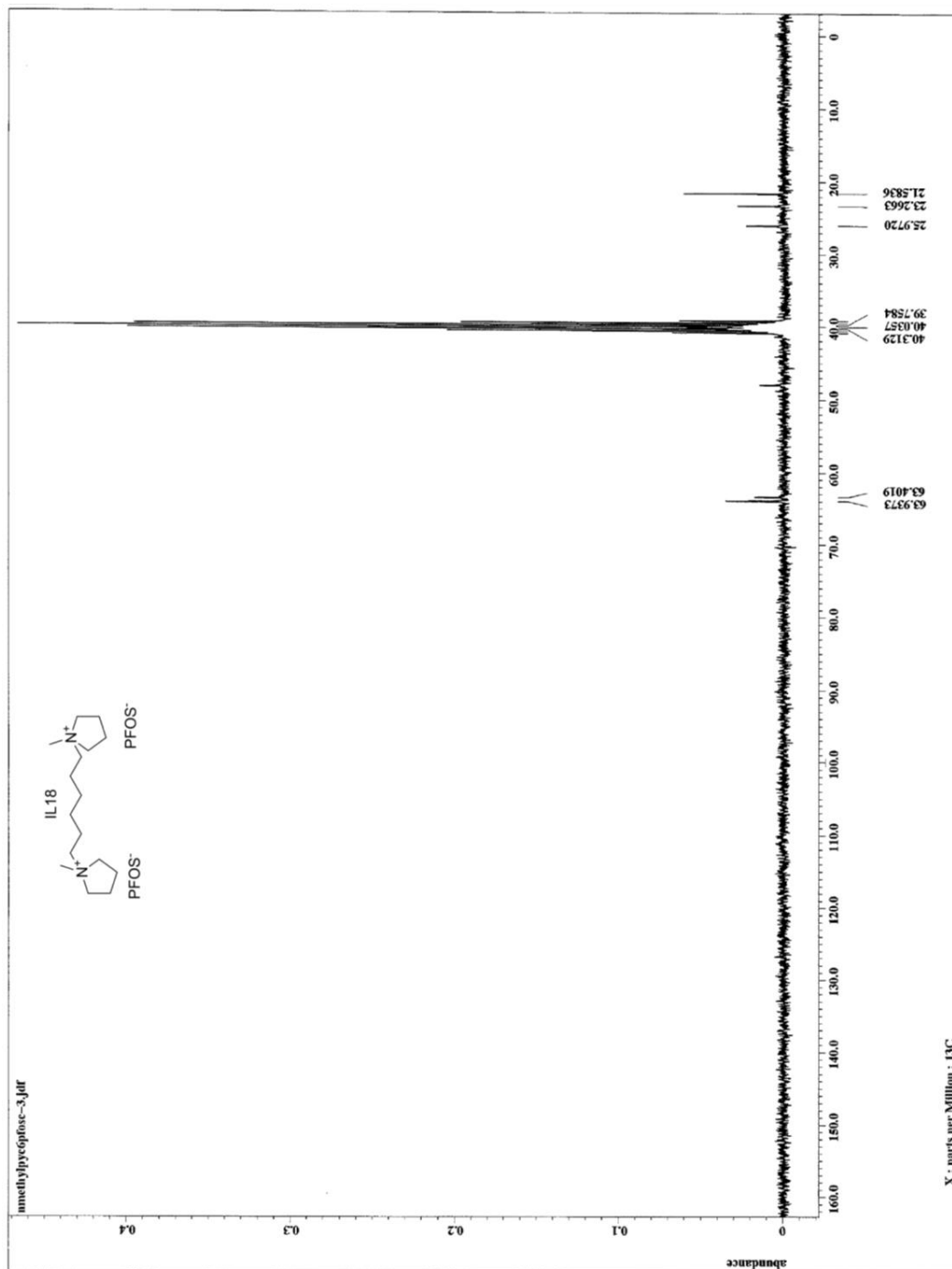




Appendix 10

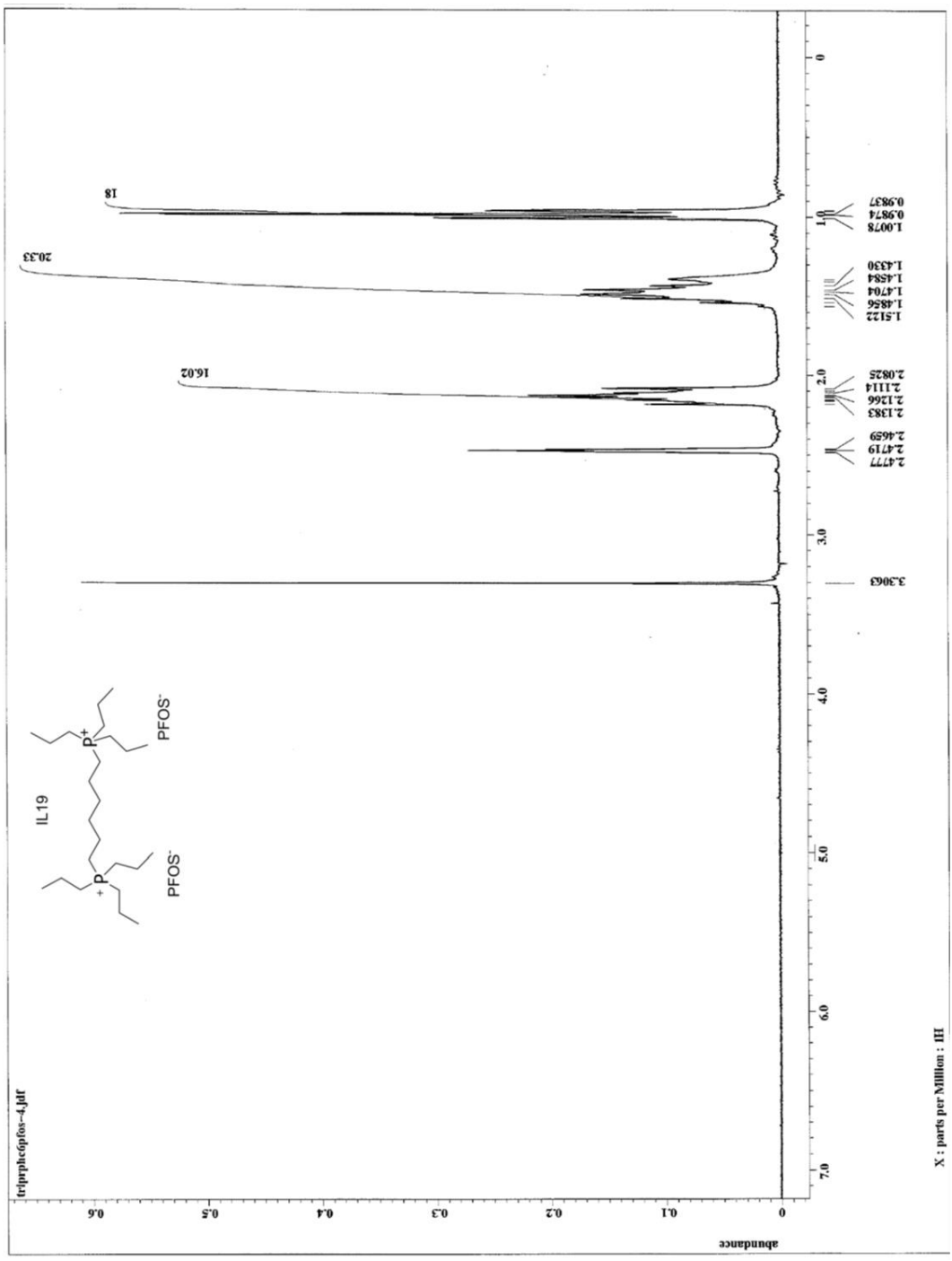
^1H NMR AND ^{13}C NMR OF $\text{C}_6(\text{mpy})_2\text{-PFOS}$

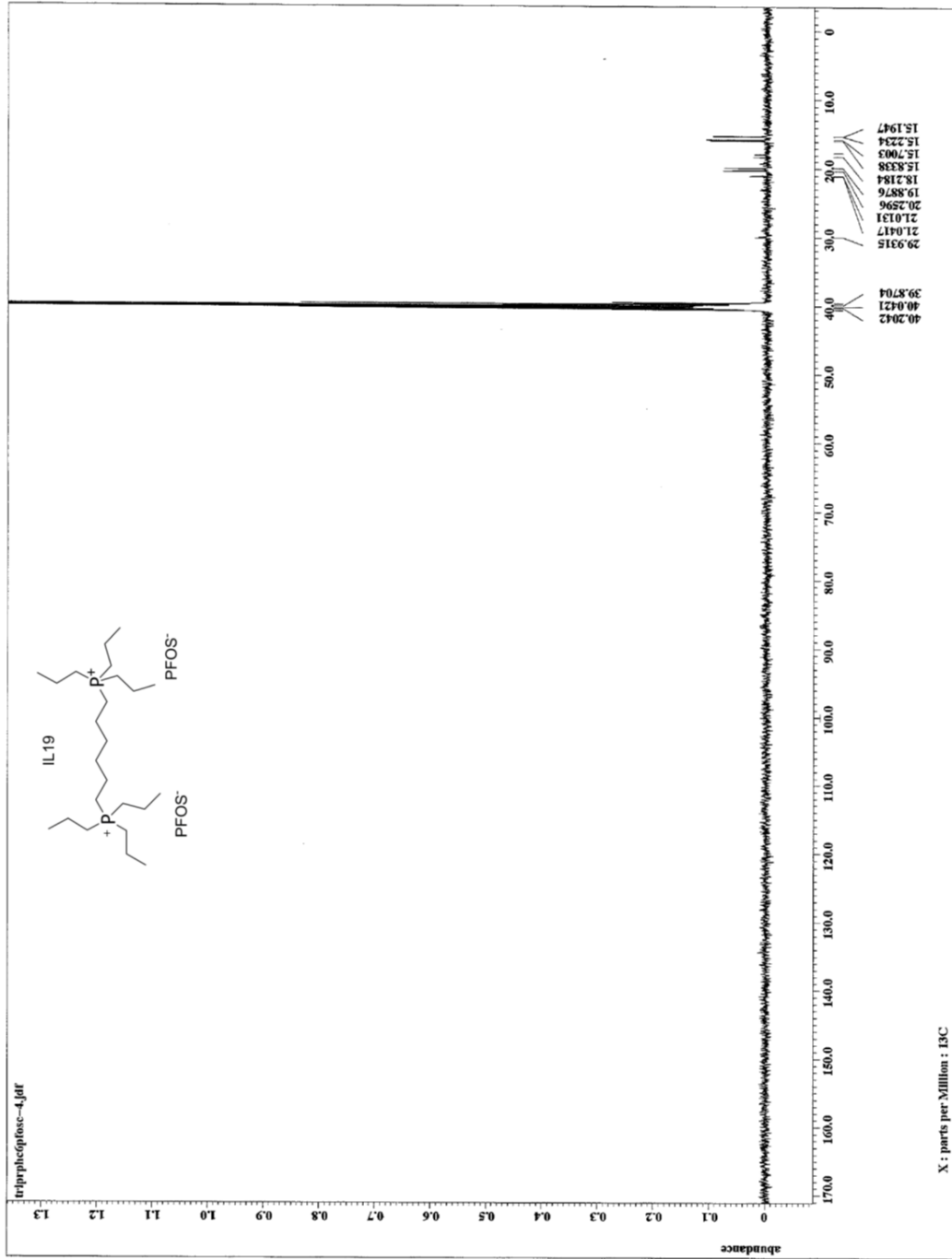




Appendix 11

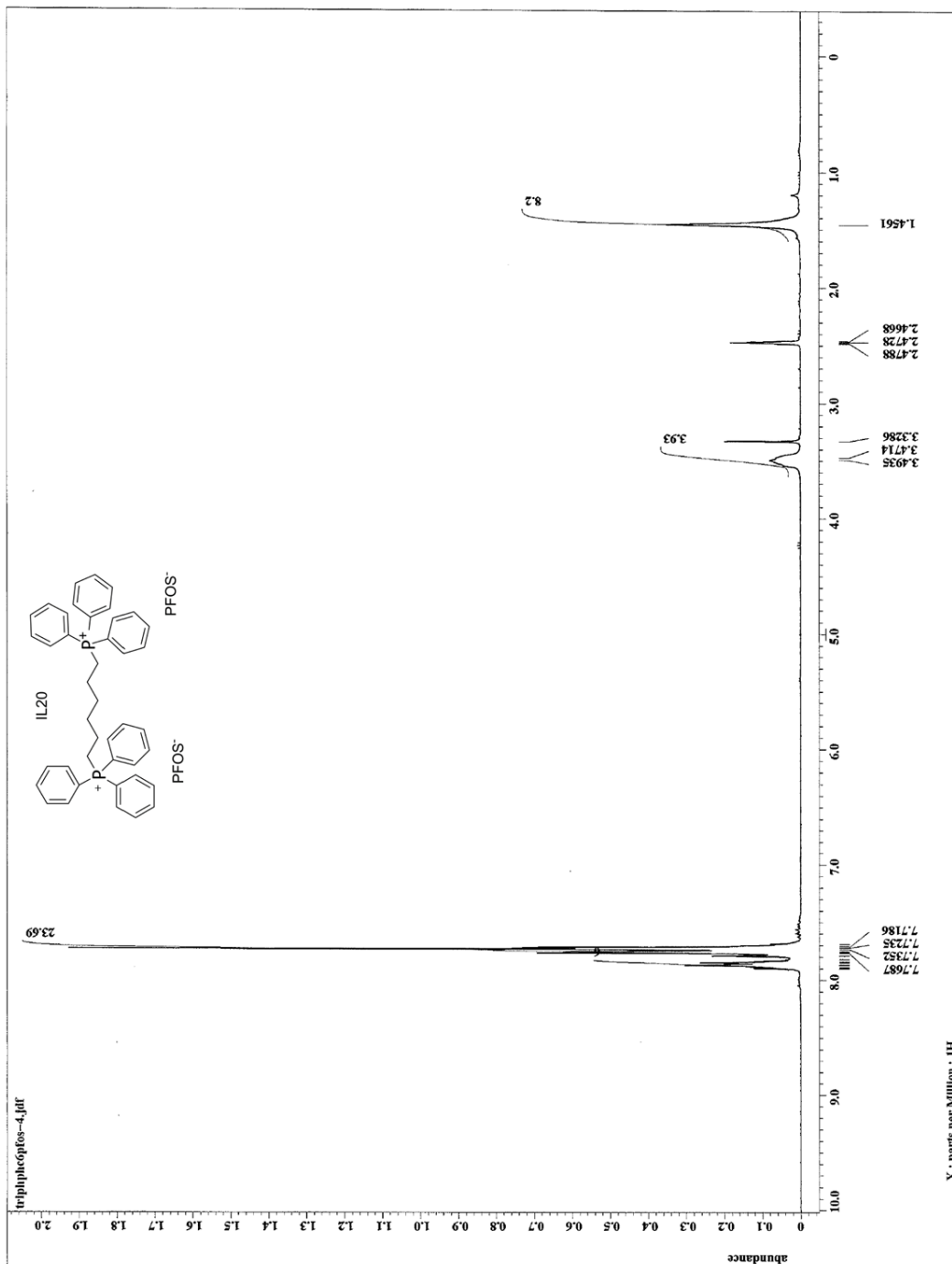
^1H NMR AND ^{13}C NMR OF $\text{C}_6(\text{pr}_3\text{p})_2\text{-PFOS}$





Appendix 12

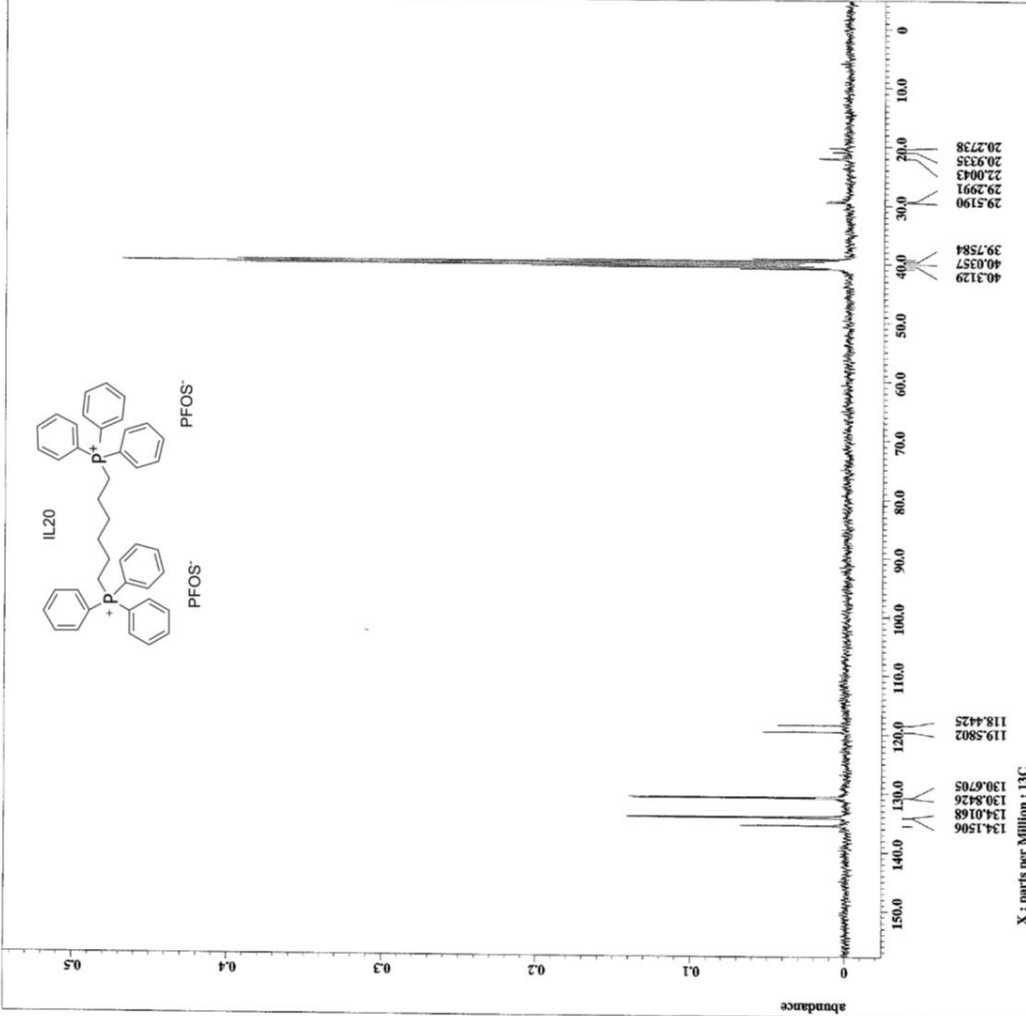
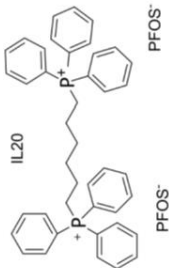
^1H NMR AND ^{13}C NMR OF $\text{C}_6(\text{ph}_3\text{p})_2\text{-PFOS}$





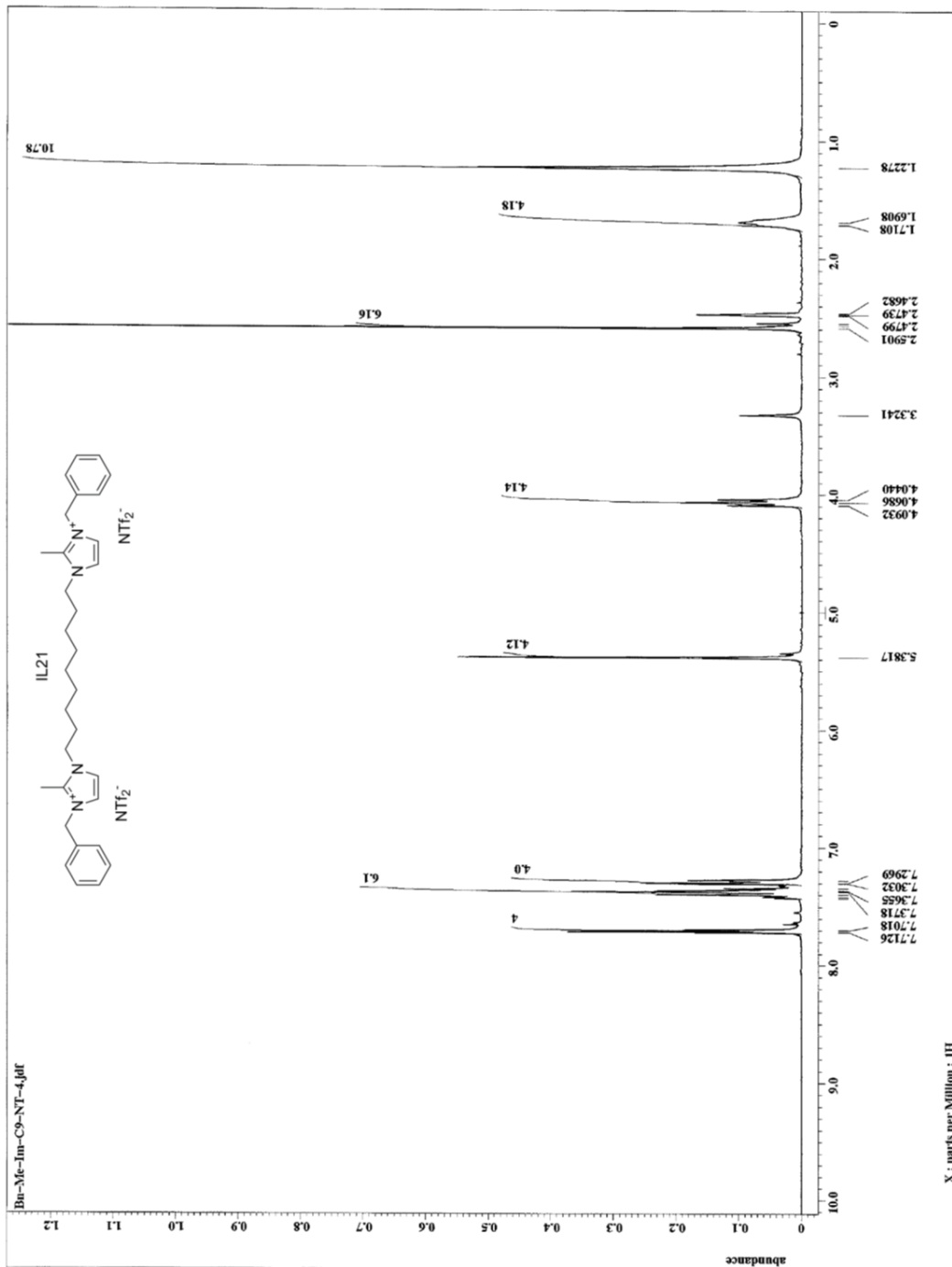
```

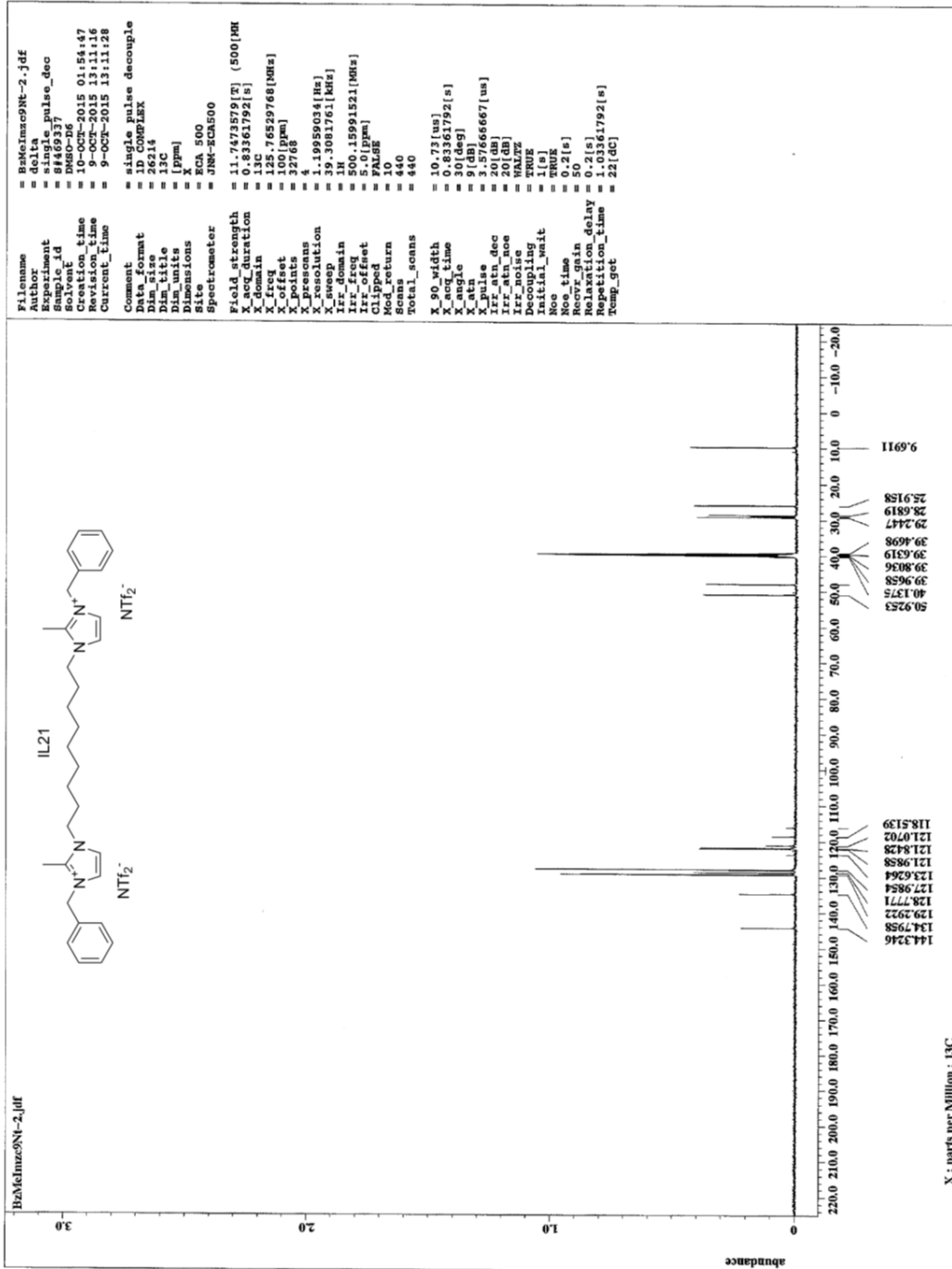
Filename = triphpc6pfonc-4.jcf
Author = delta
Experiment = single_pulse_dec
Date_ymd = 20160309
Solvent = DMSO-d6
Creation_time = 21-MAR-2016 20:30:58
Revision_time = 25-MAR-2016 16:47:34
Current_time = 25-MAR-2016 16:49:21
Comment = single pulse decouple
Data_format = 1D COMPLEX
Dir_size = 26214
Dir_title = 13C
Dimensions = 1[ppm]
Spectrometer = ECKX 300
Site = DELTA2_NMR
Field_strength = 7.0586031[G] (300[MHz]
X_acq_duration = 1.38412032[s]
X_domain = 13C
X_freq = 75.56823426[MHz]
X_offset = 100[ppm]
X_prescans = 32768
X_swept = 4
X_resolution = 0.72248054[Hz]
X_sweep = 23.67424242[MHz]
IR_domain = 1H
IR_freq = 500.53965892[MHz]
IR_offset = 51[ppm]
Clipped = FALSE
Mod_return = 10
Scans = 310
Total_scans = 310
X_90_width = 9.75[us]
X_acq_time = 1.38412032[s]
X_angle = 30[deg]
X_pulse = 3.25[us]
IR_atn_dec = 25[dB]
IR_atn_noe = 25[dB]
IR_pulse = WALTZ
IR_wait = 1[s]
Initial_wait = 1[s]
Noe_time = TRUE
Noe_gain = 2[s]
Revr_gain = 0
Revr_delay = 2[s]
Repetition_delay = 3.38412032[s]
Repetition_time = 3.38412032[s]
Temp_set = 21.5[degC]
  
```



Appendix 13

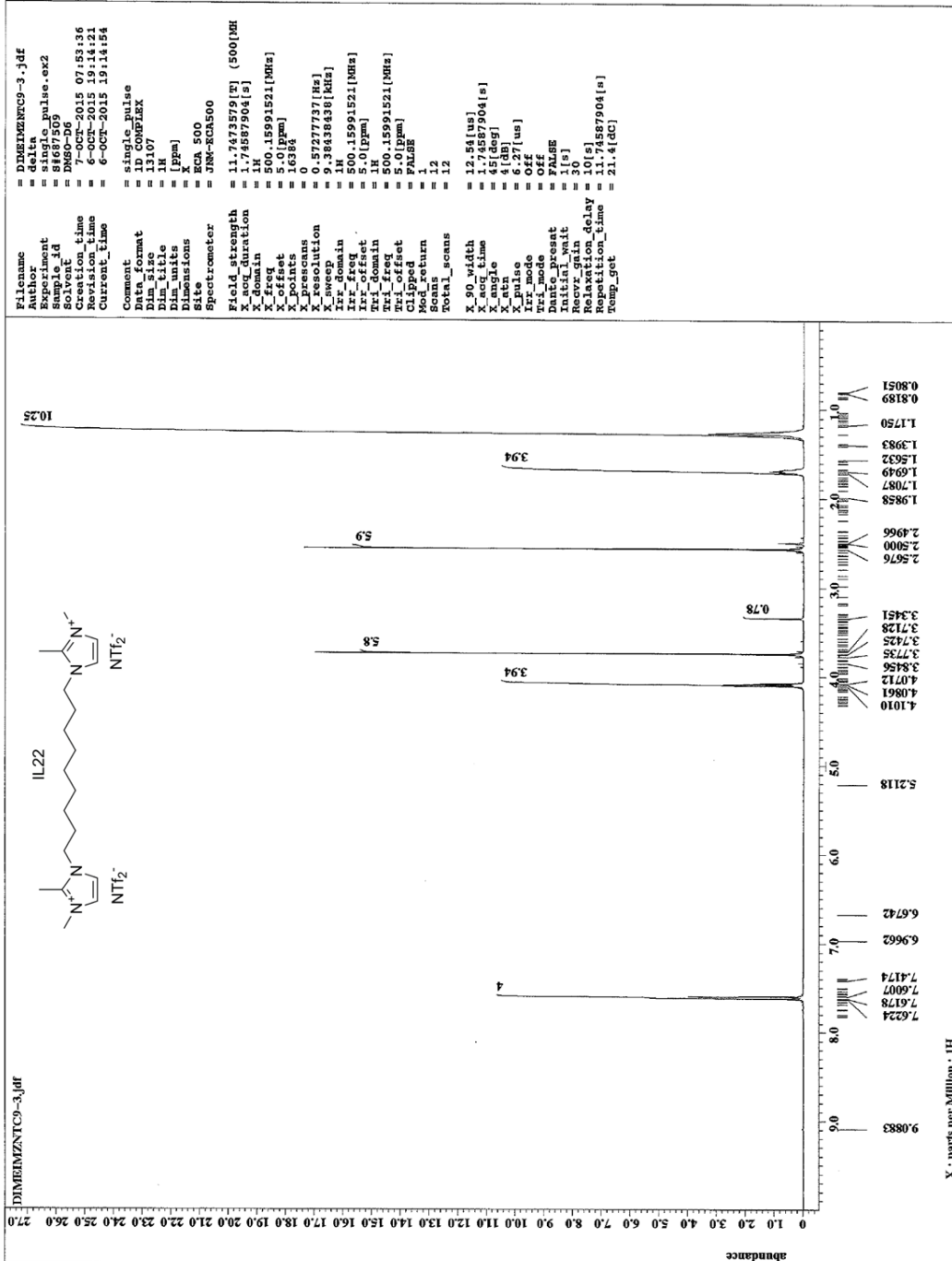
^1H NMR AND ^{13}C NMR OF $\text{C}_9(\text{bmim})_2\text{-NTf}_2$

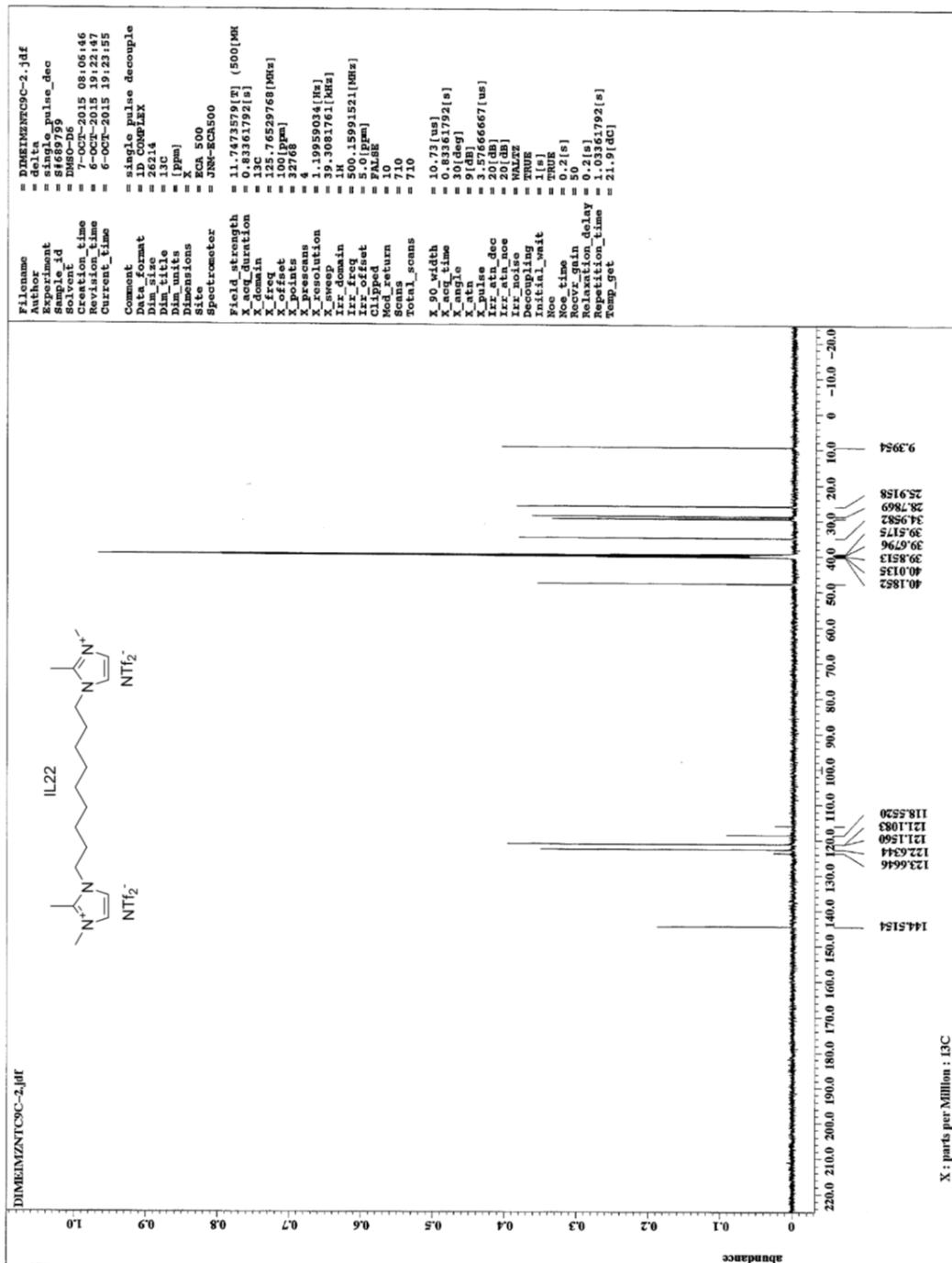




Appendix 14

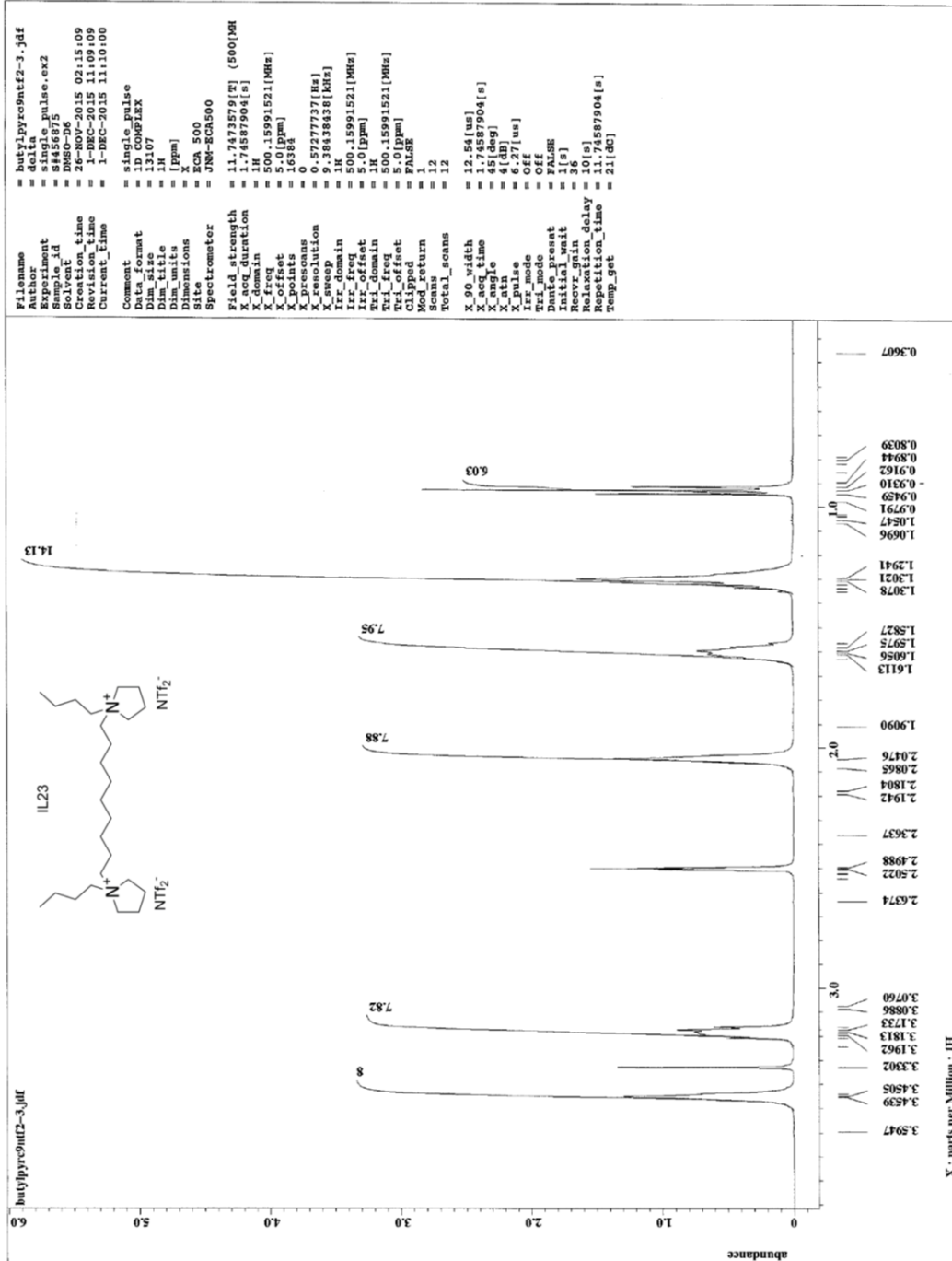
^1H NMR AND ^{13}C NMR OF $\text{C}_9(\text{mzim})_2\text{-NTf}_2$

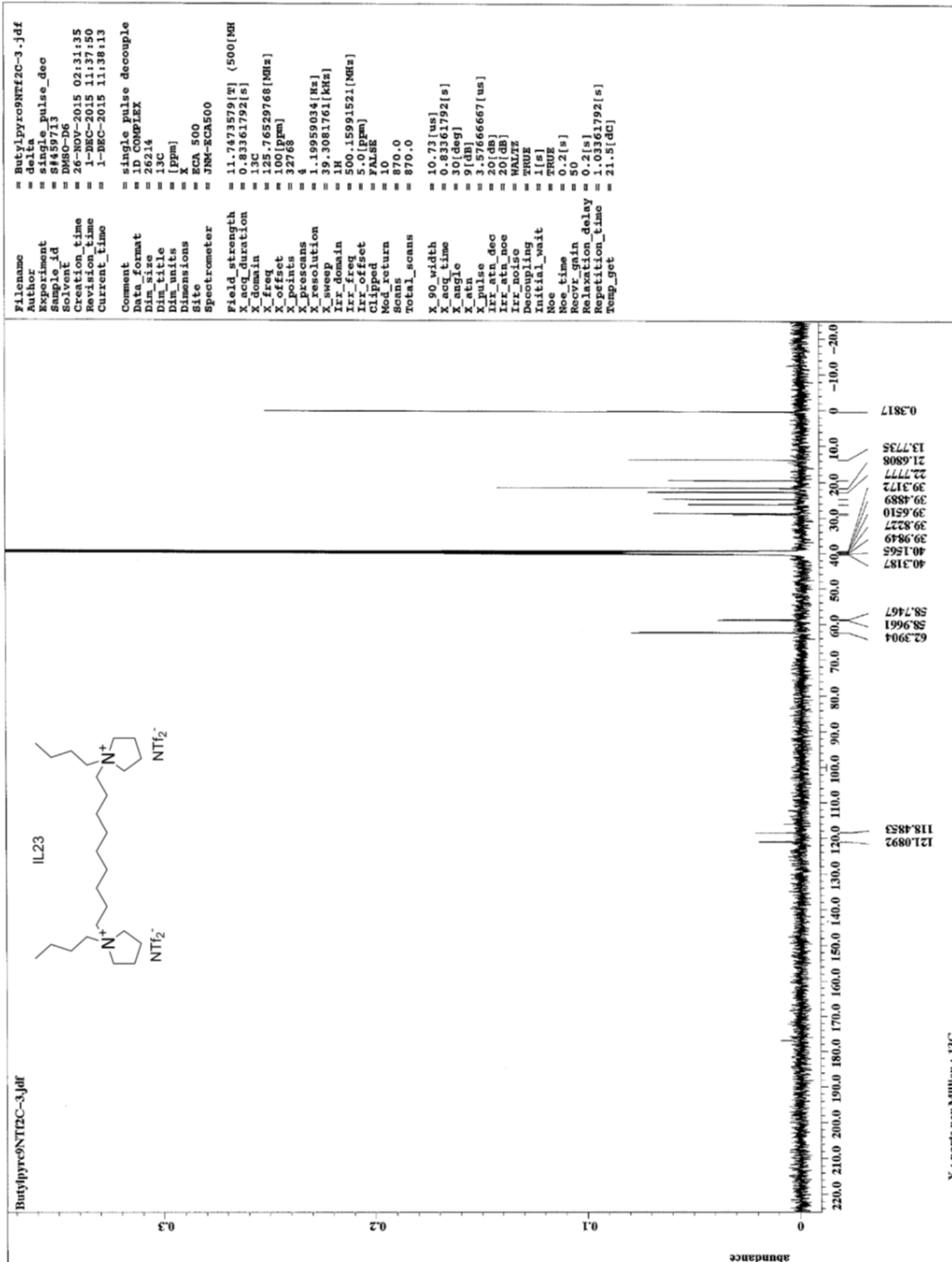




Appendix 15

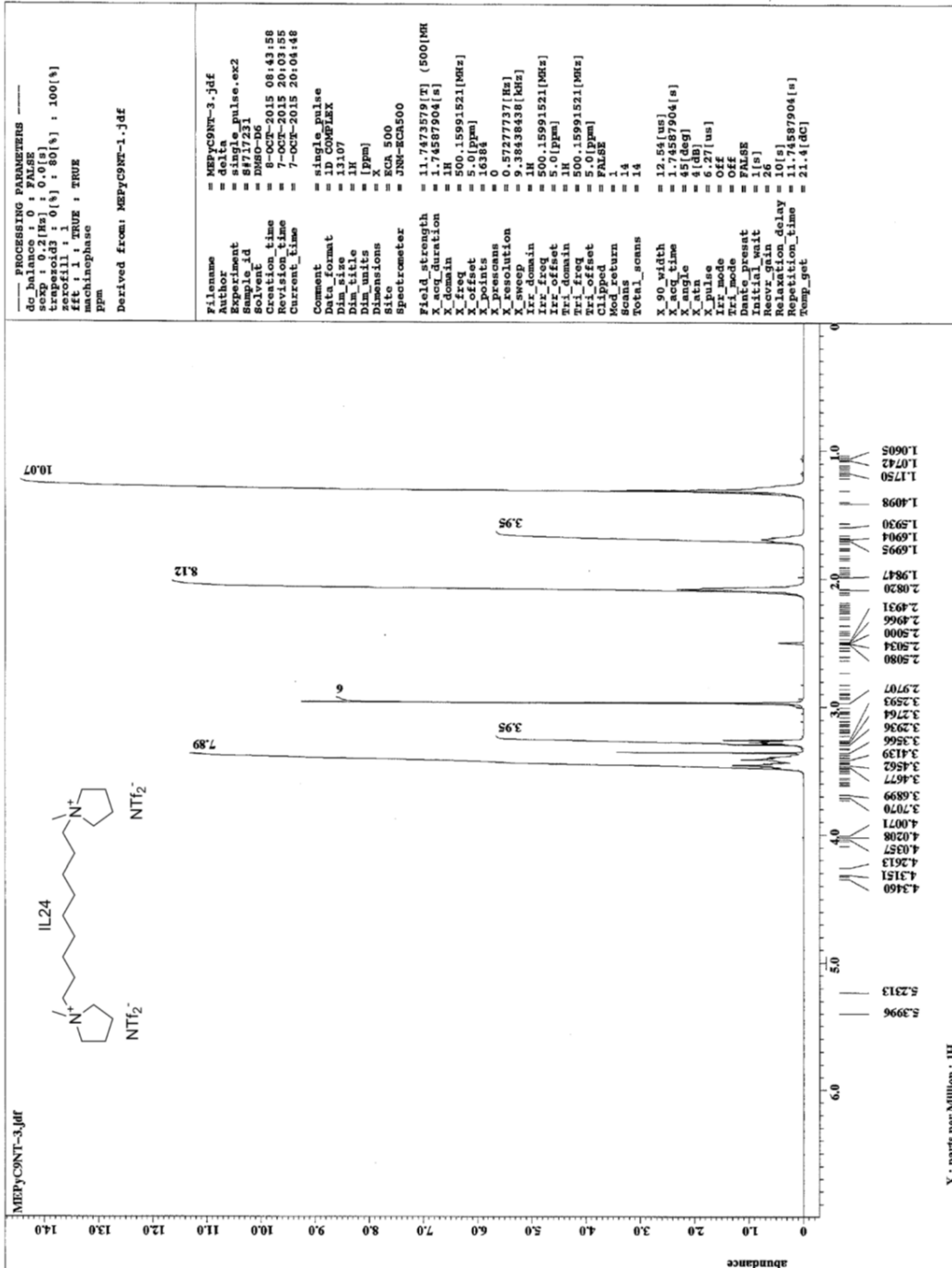
^1H NMR AND ^{13}C NMR OF $\text{C}_9(\text{bpy})_2\text{-NTf}_2$

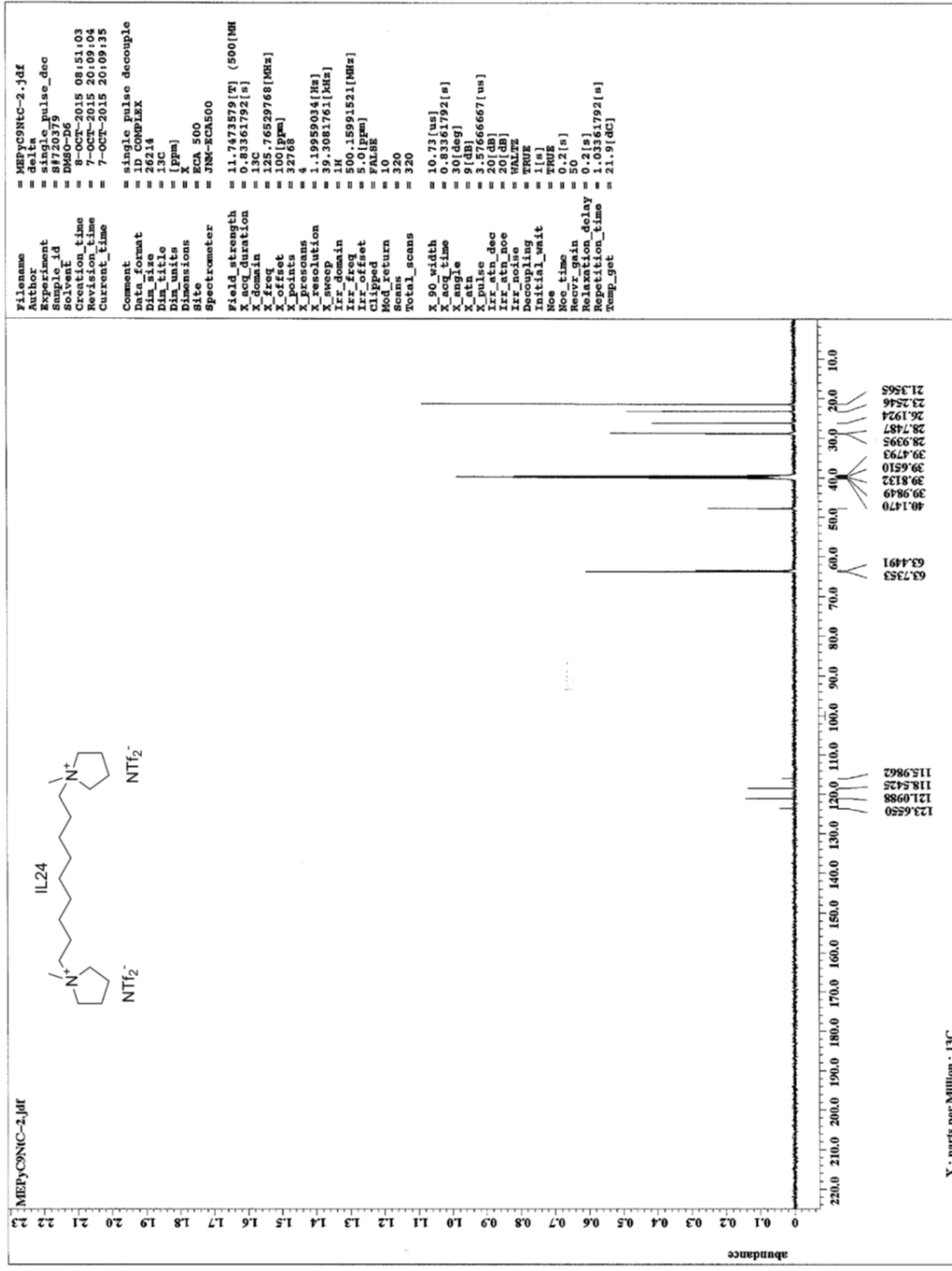




Appendix 16

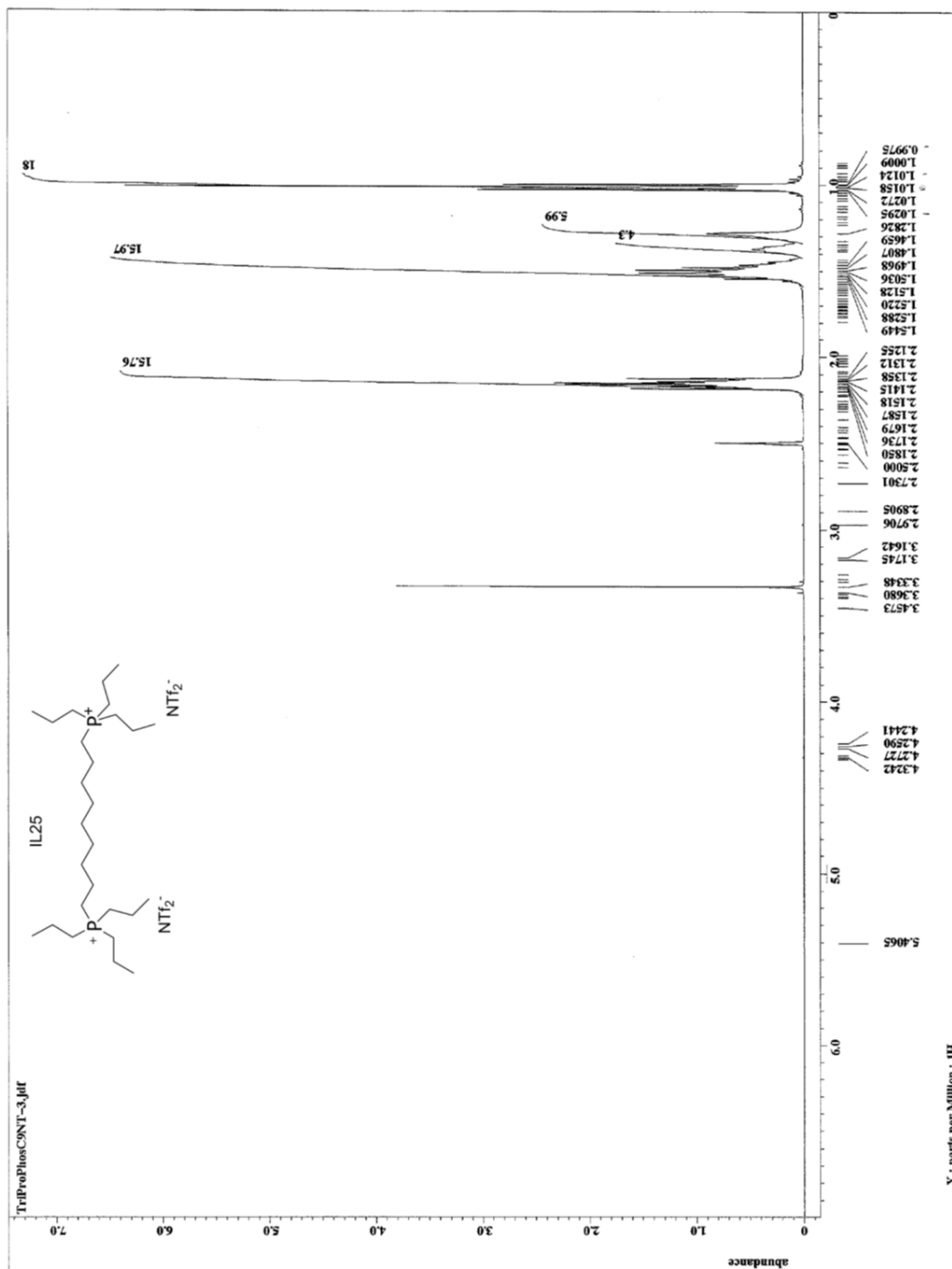
^1H NMR AND ^{13}C NMR OF $\text{C}_9(\text{mpy})_2\text{-NTf}_2$

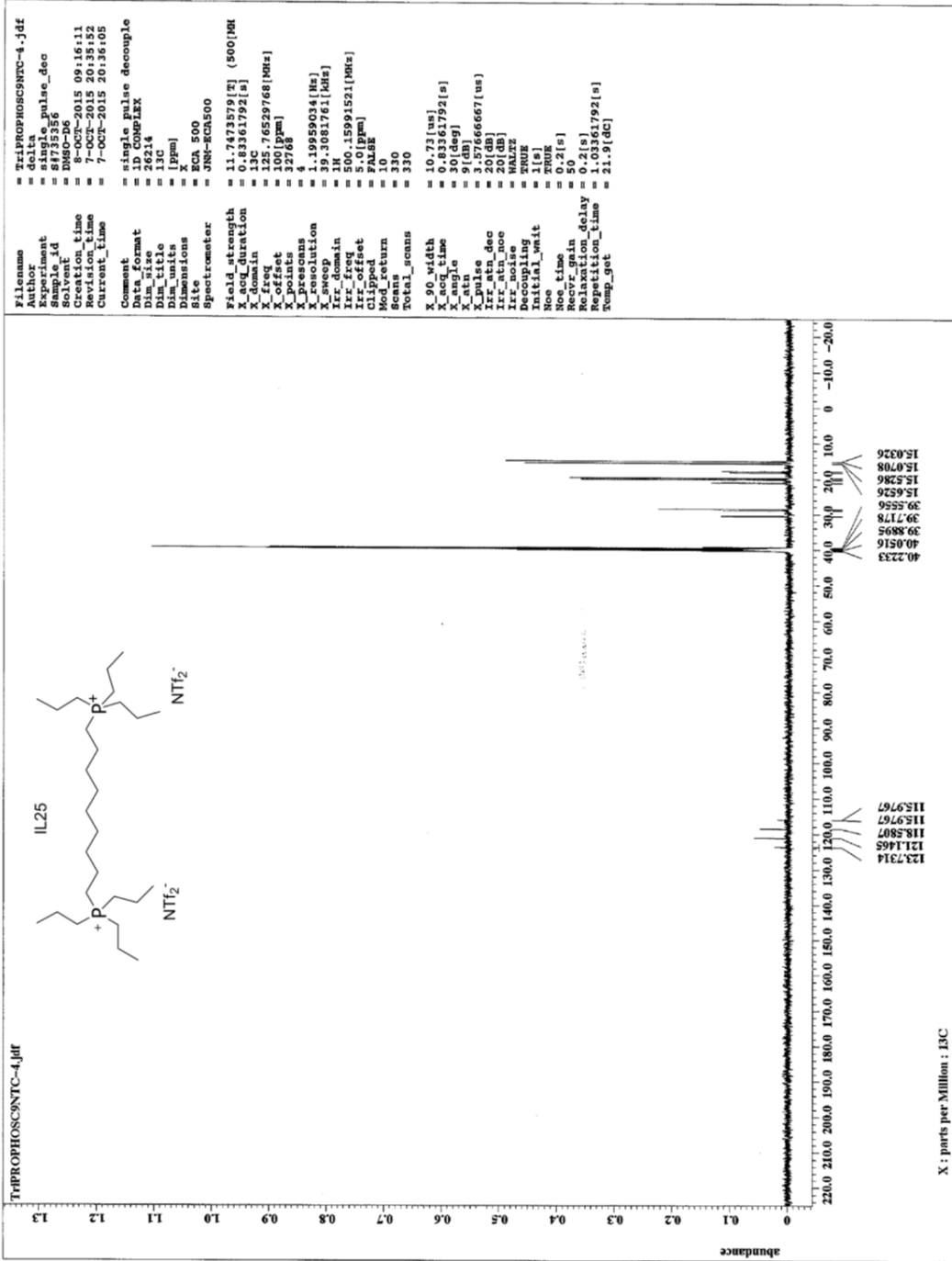




Appendix 17

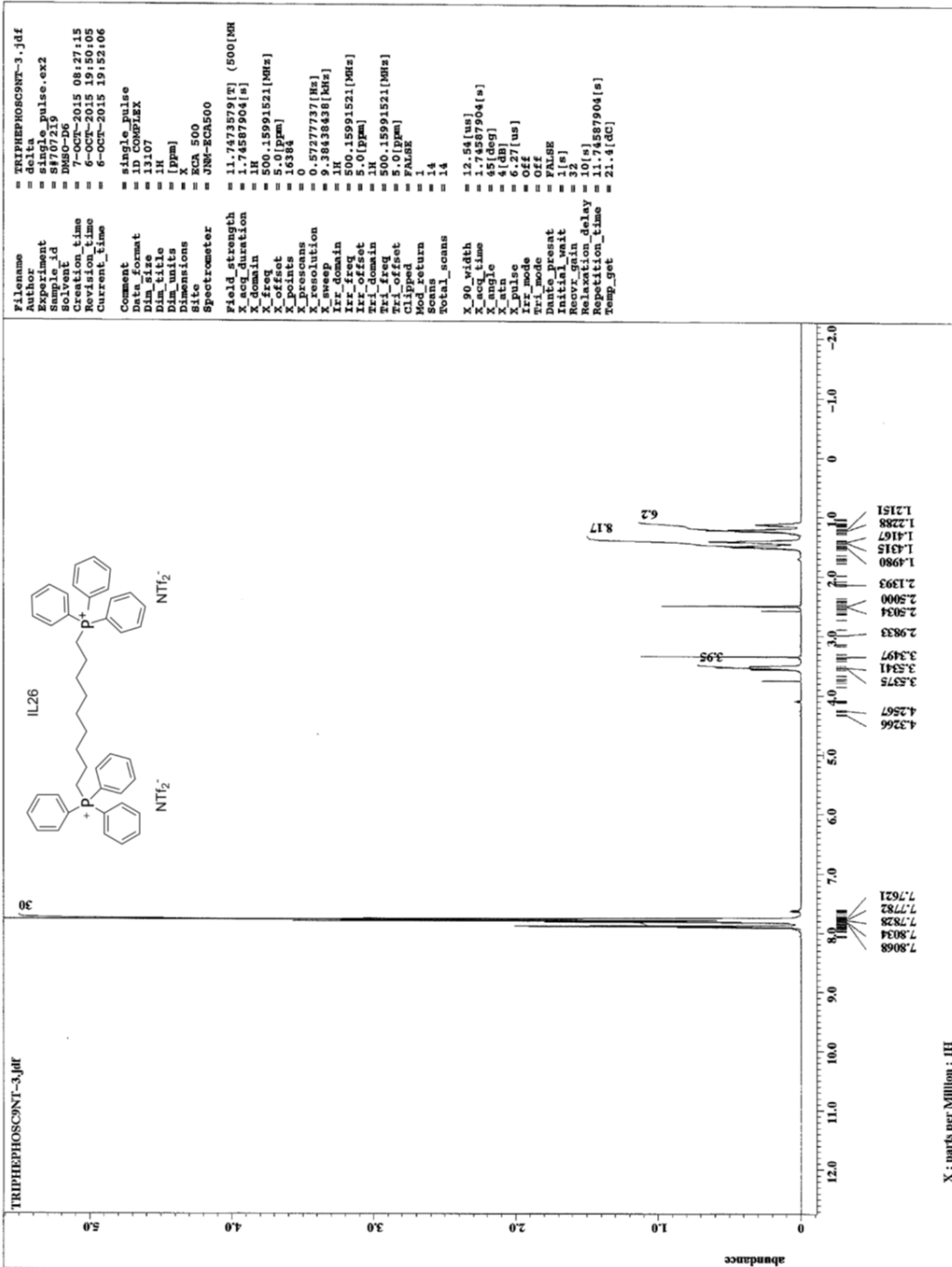
^1H NMR AND ^{13}C NMR OF $\text{C}_9(\text{pr}_3\text{p})_2\text{-NTf}_2$

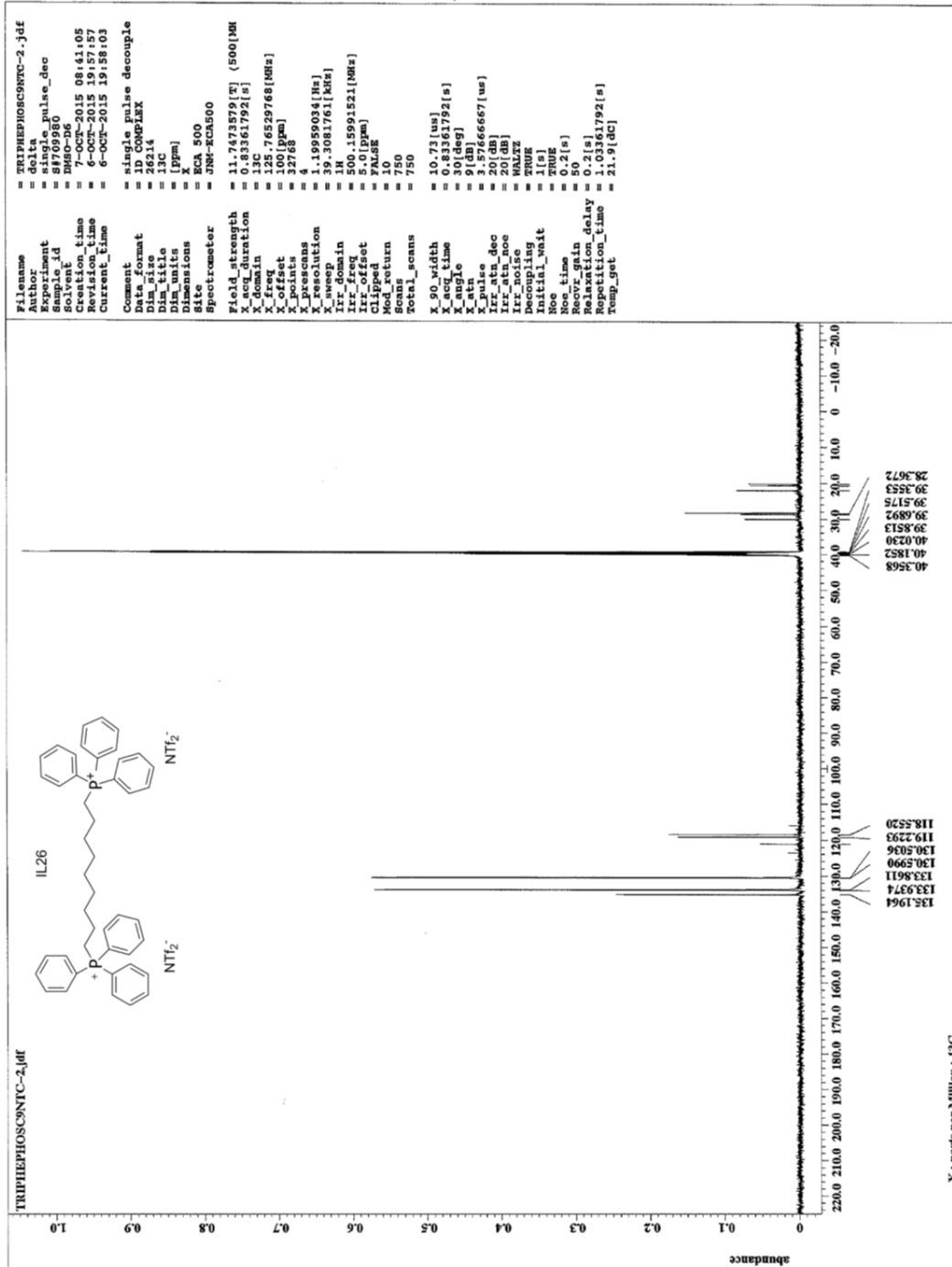




Appendix 18

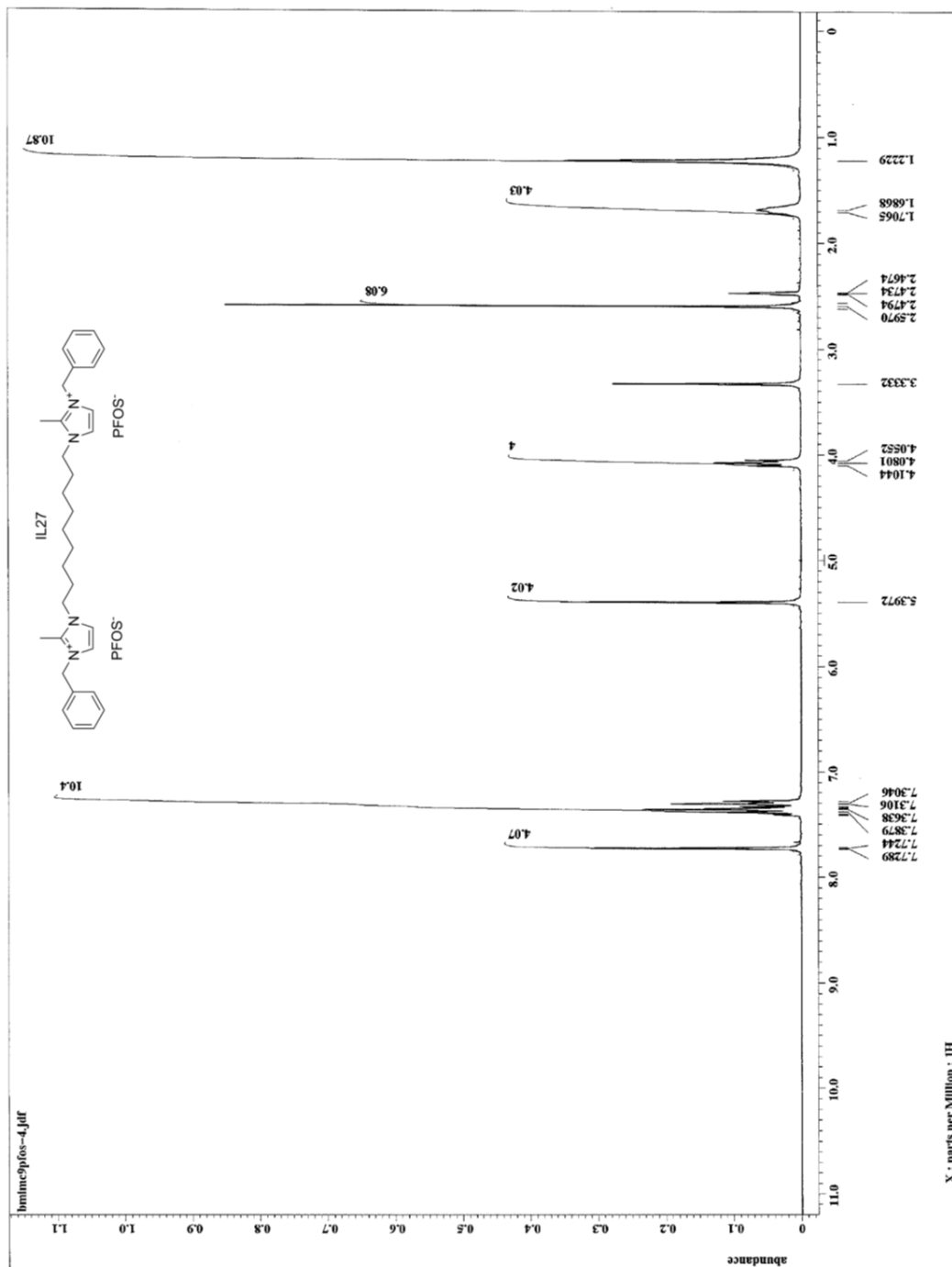
^1H NMR AND ^{13}C NMR OF $\text{C}_9(\text{ph}_3\text{p})_2\text{-NTf}_2$

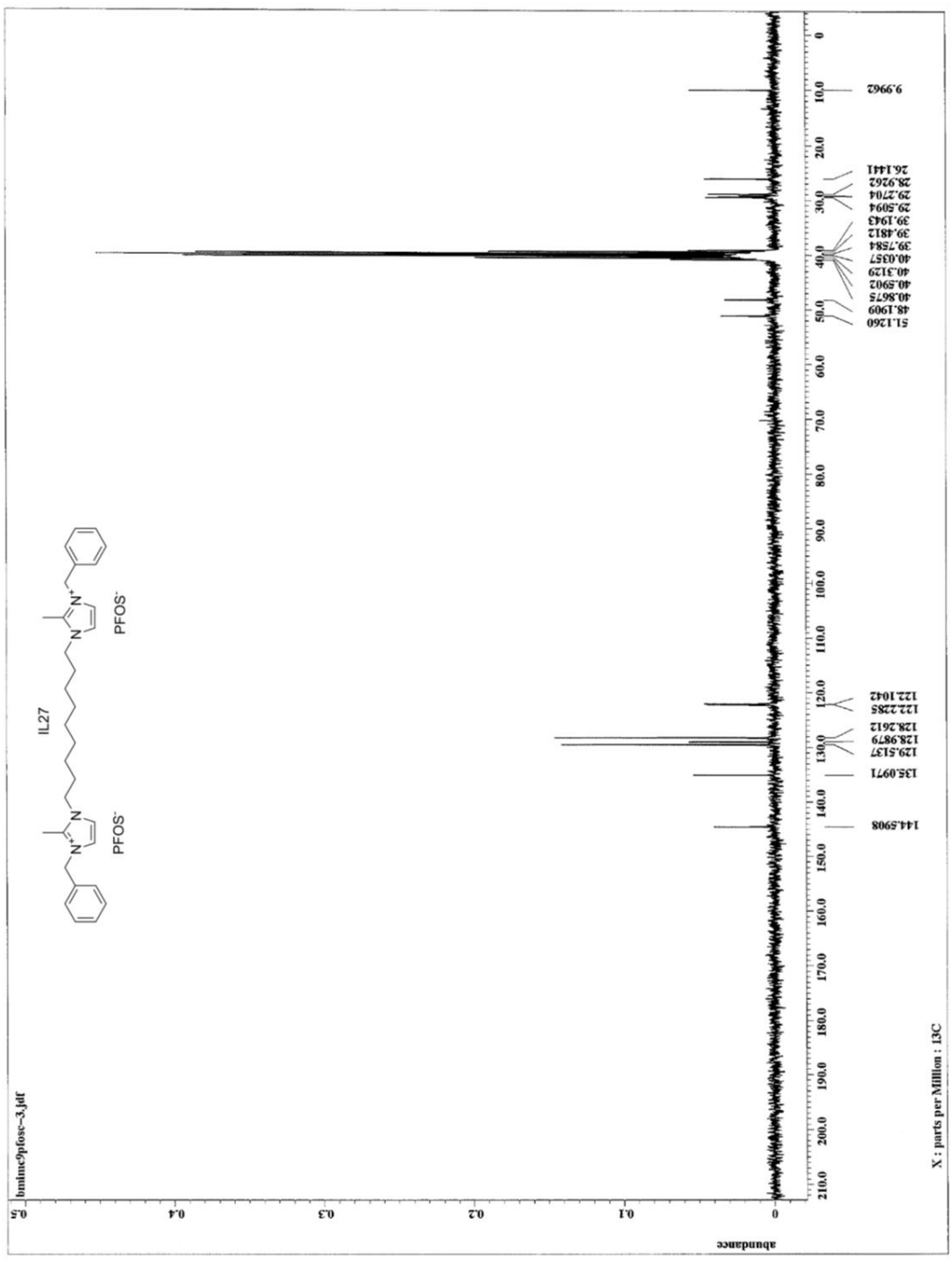




Appendix 19

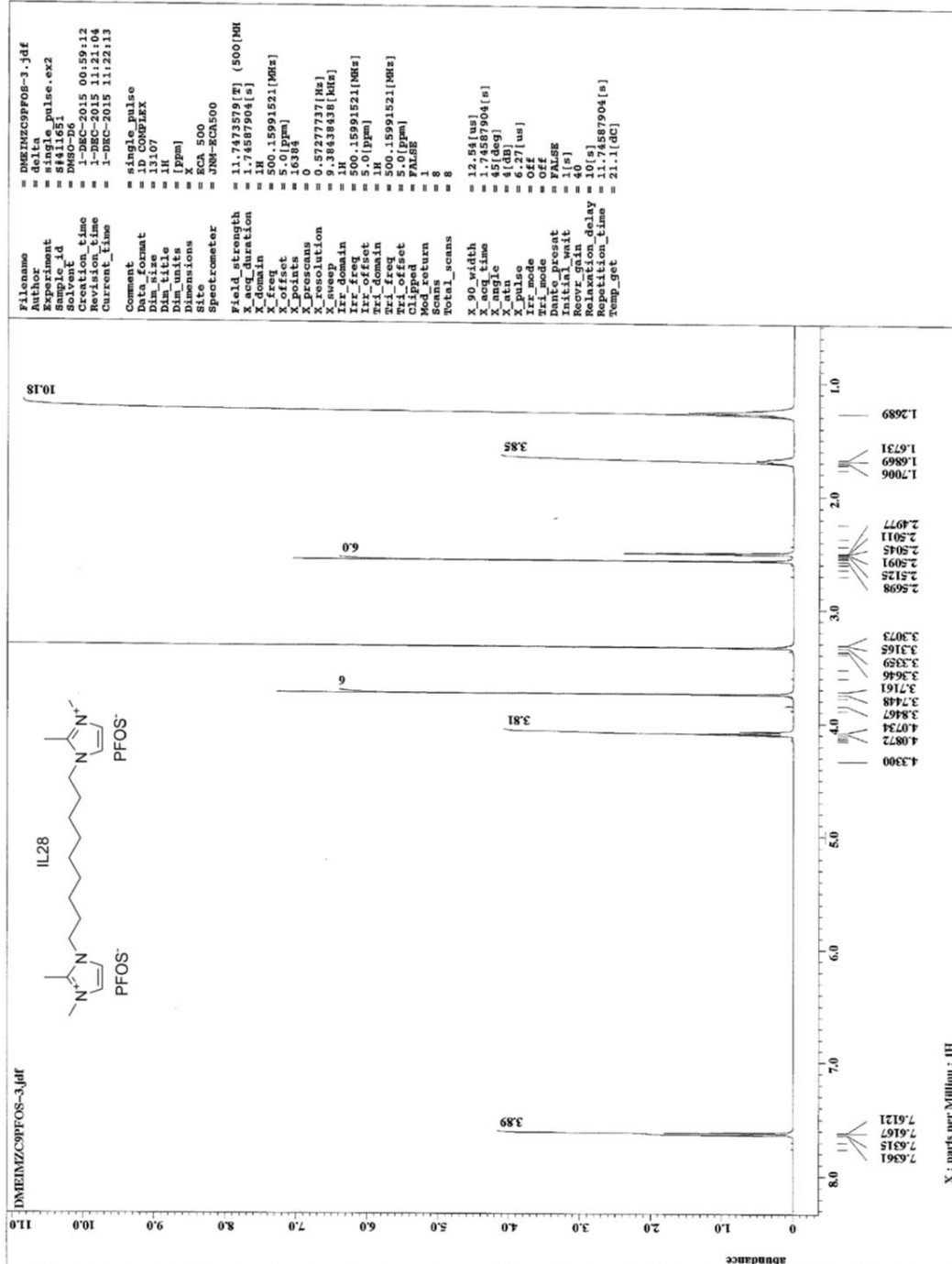
^1H NMR AND ^{13}C NMR OF $\text{C}_9(\text{bmim})_2\text{-PFOS}$

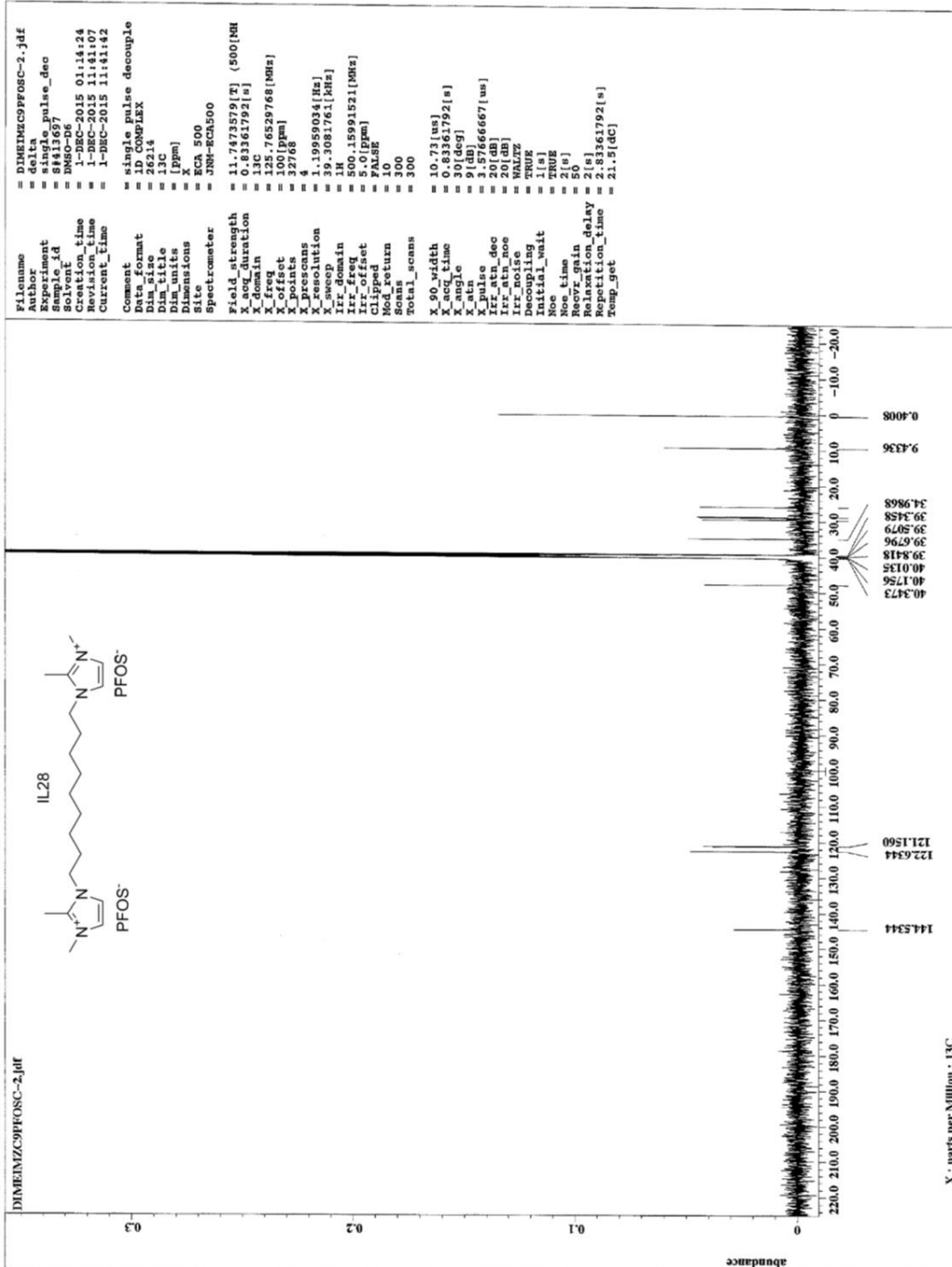




Appendix 20

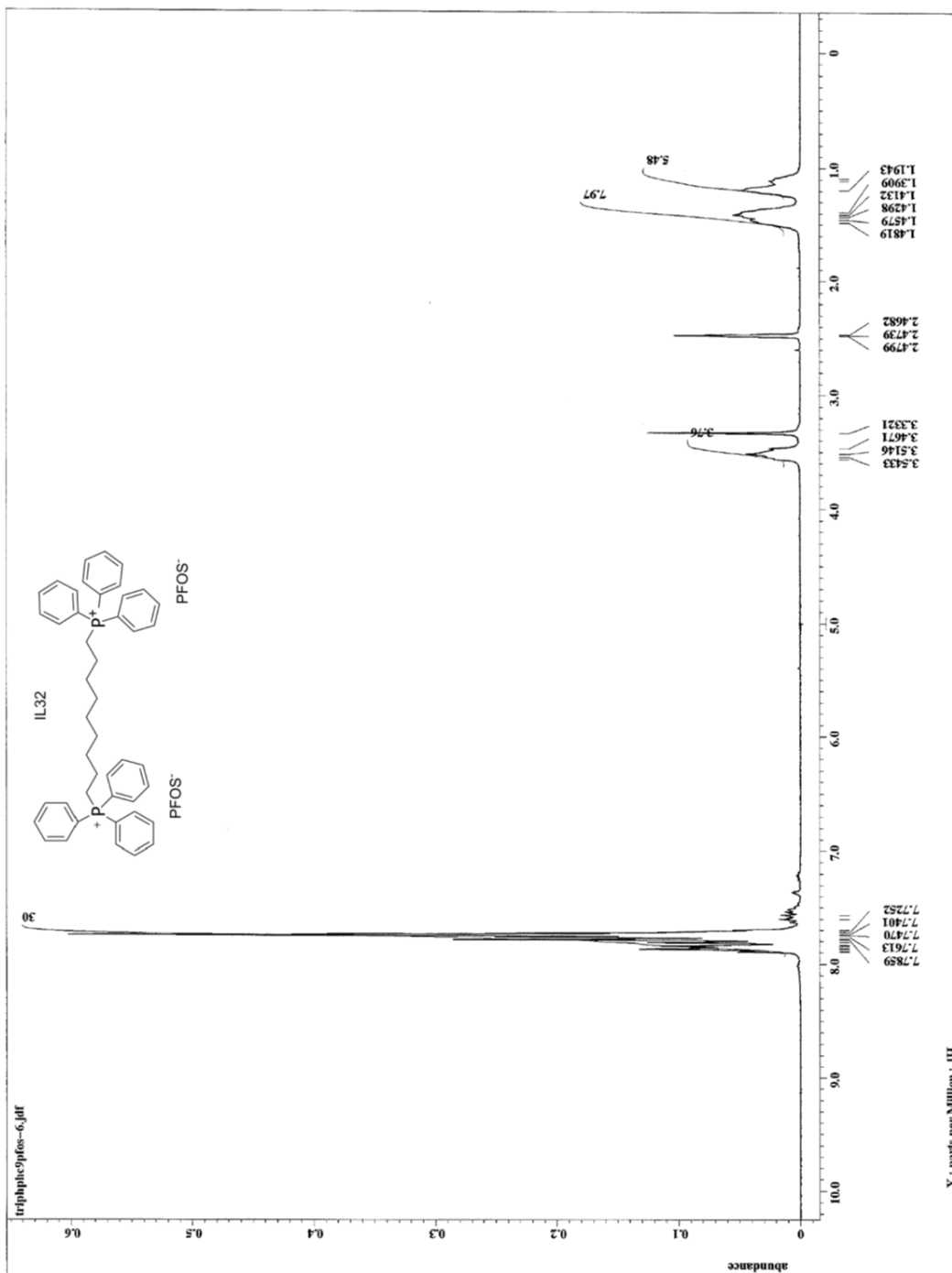
^1H NMR AND ^{13}C NMR OF $\text{C}_9(\text{mzim})_2\text{-PFOS}$

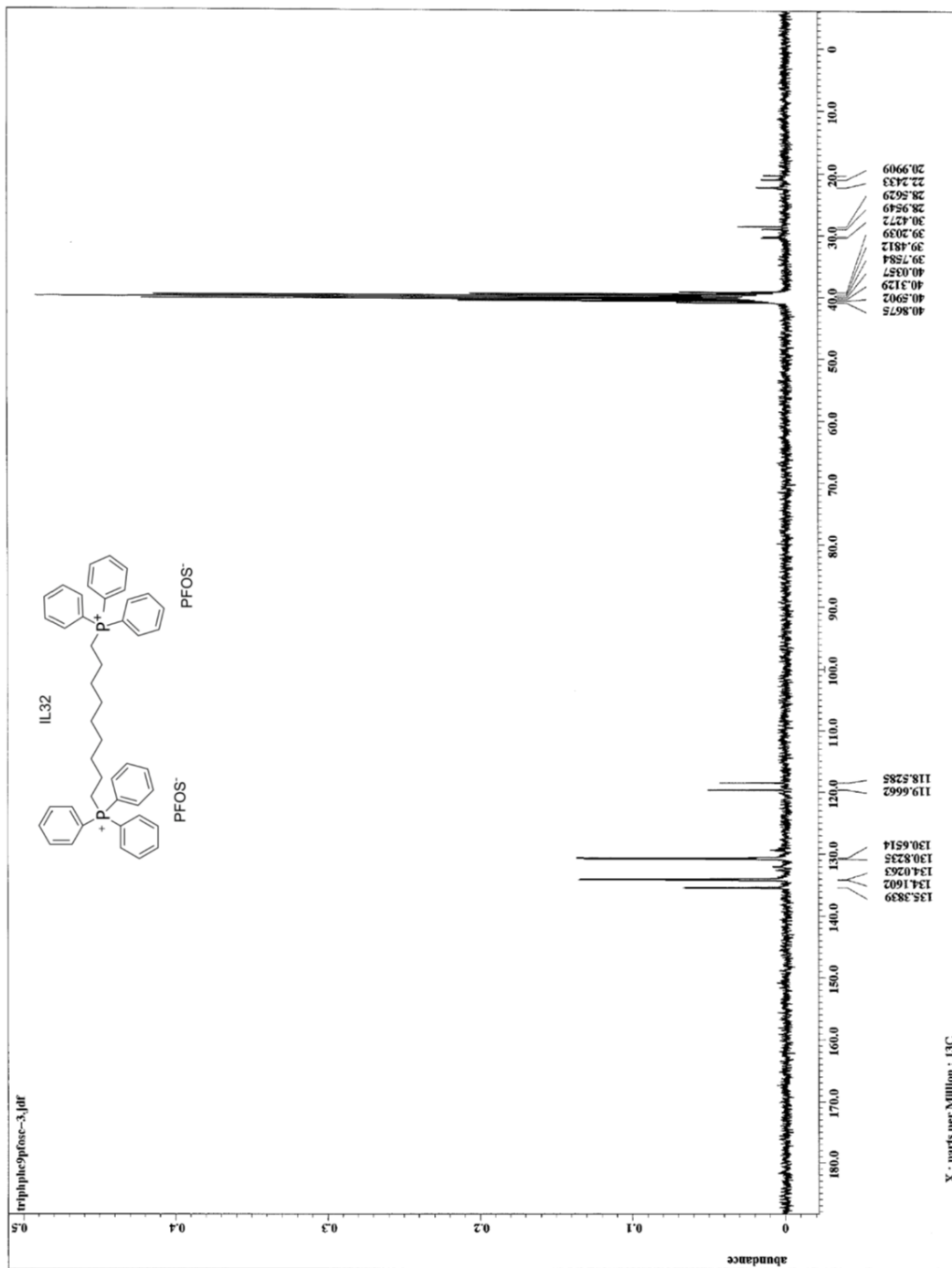




Appendix 21

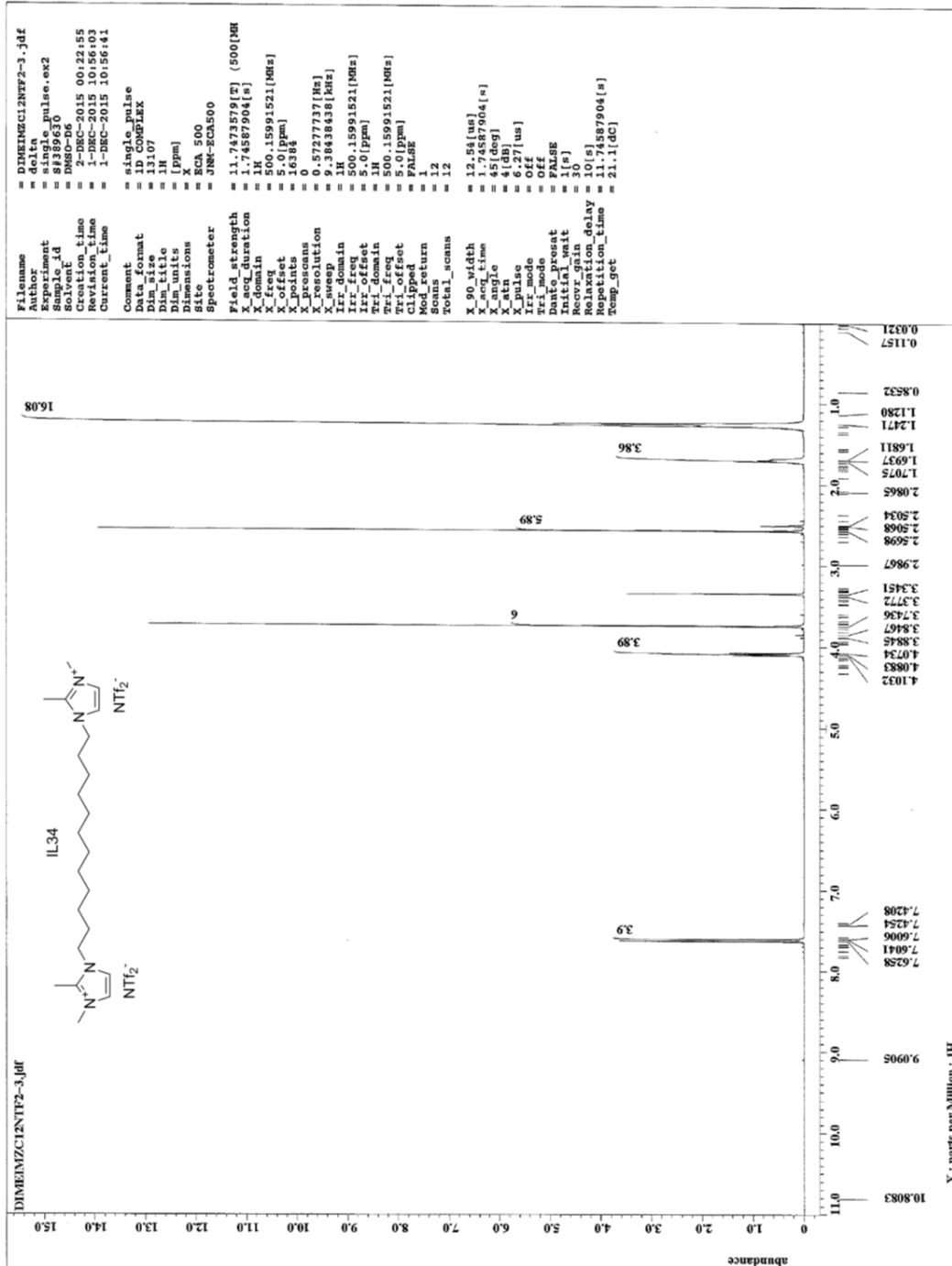
^1H NMR AND ^{13}C NMR OF $\text{C}_9(\text{ph}_3\text{p})_2\text{-PFOS}$

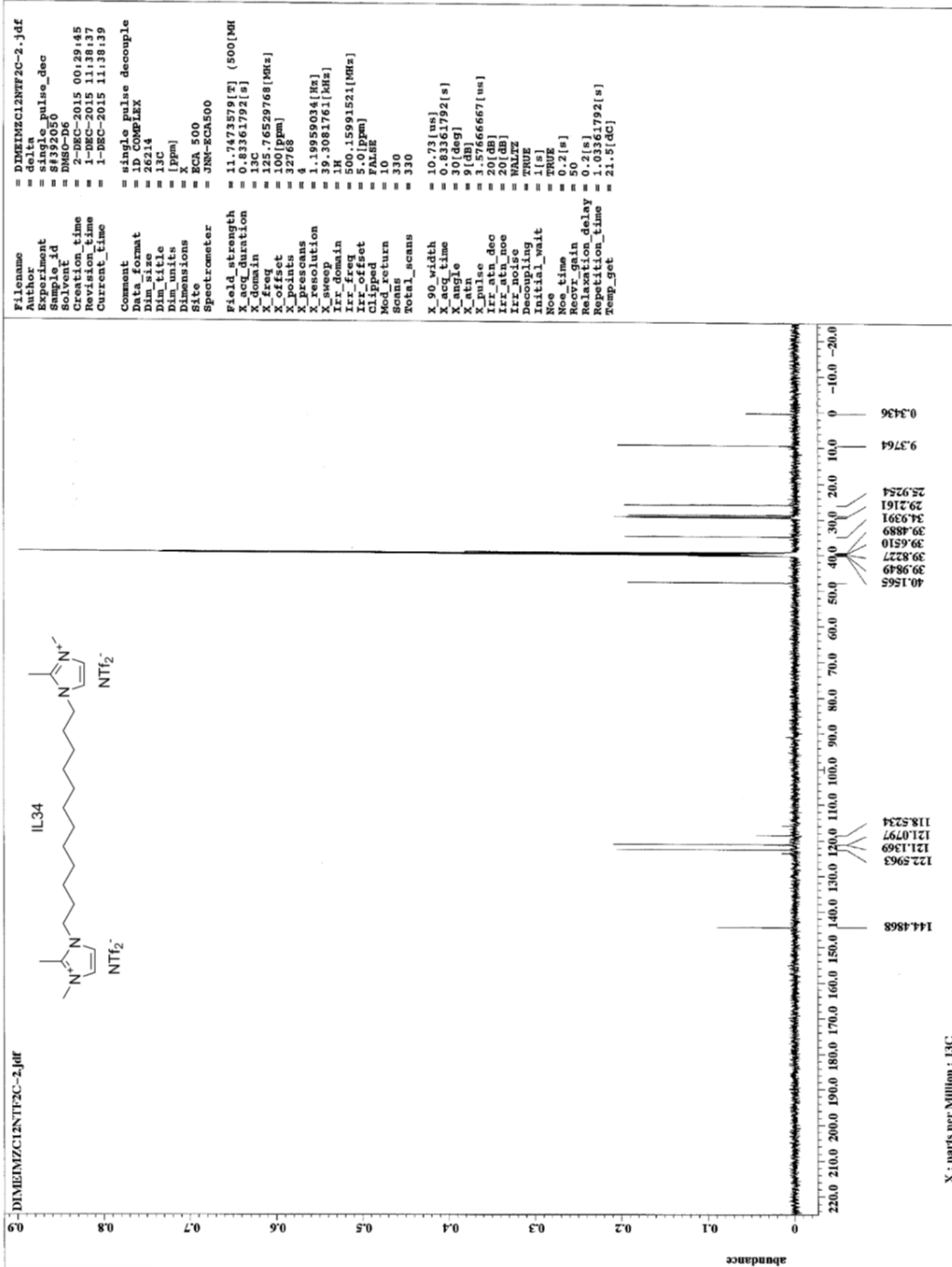




Appendix 22

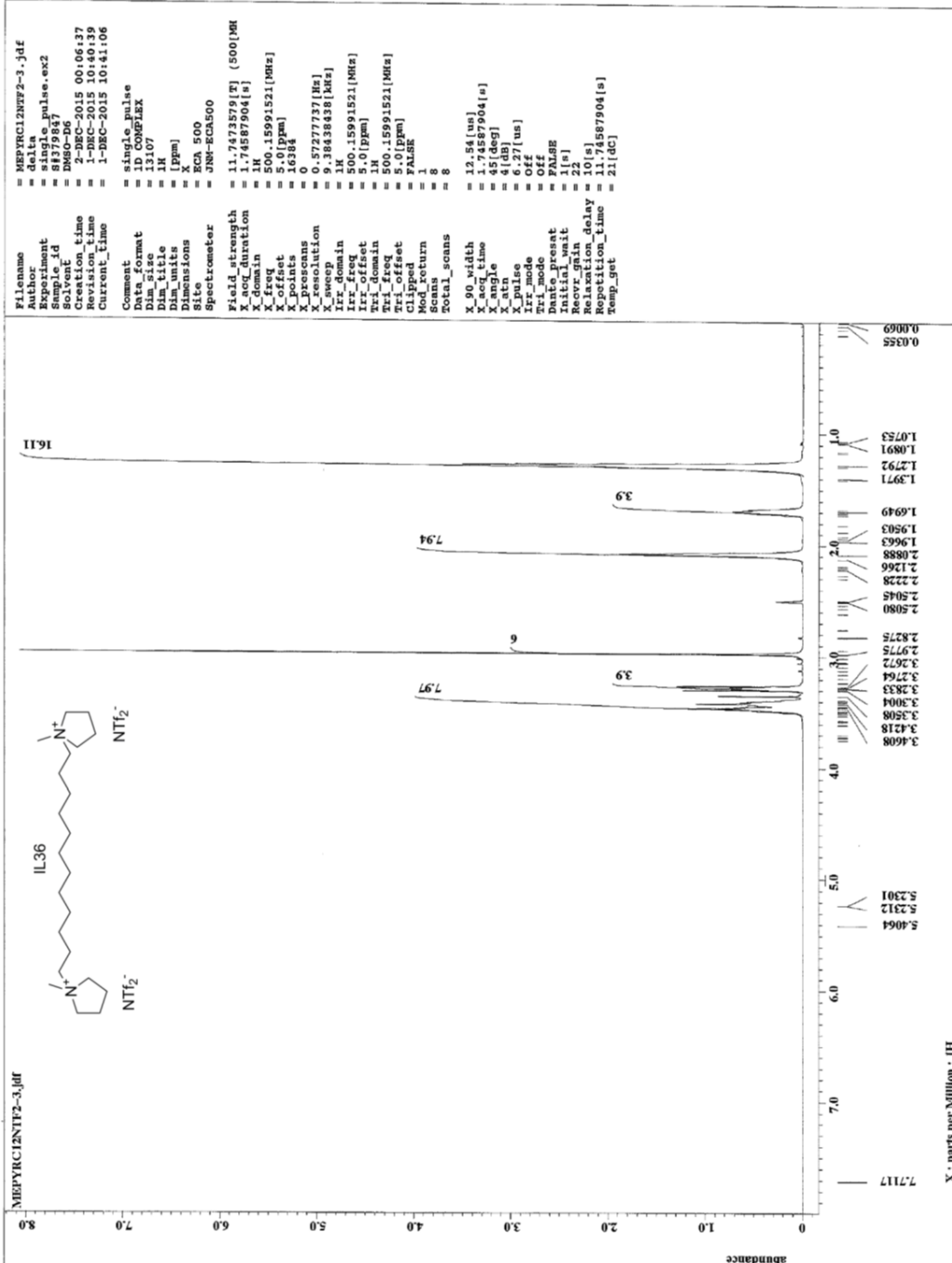
^1H NMR AND ^{13}C NMR OF $\text{C}_{12}(\text{mzim})_2\text{-NTf}_2$

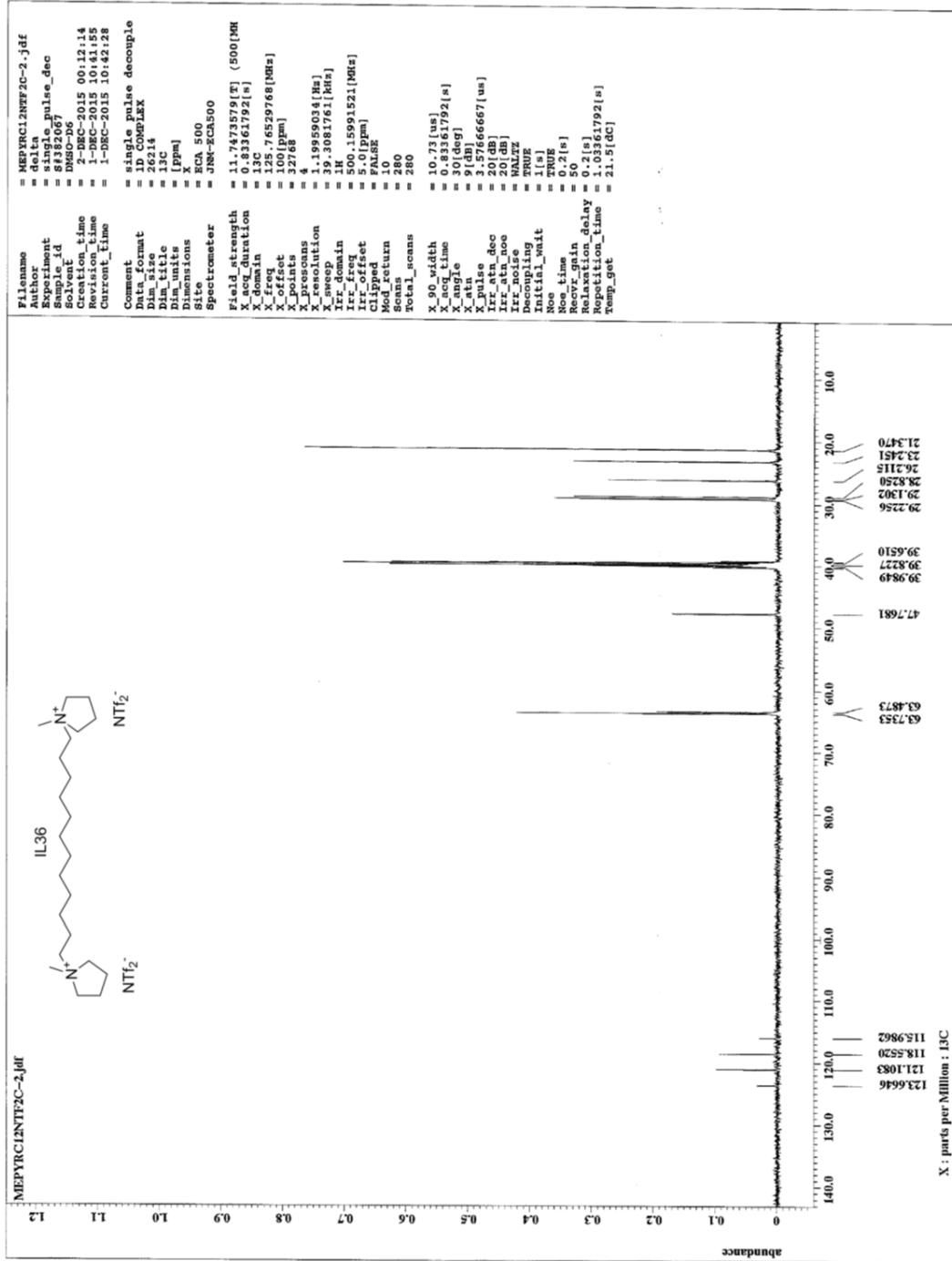




Appendix 23

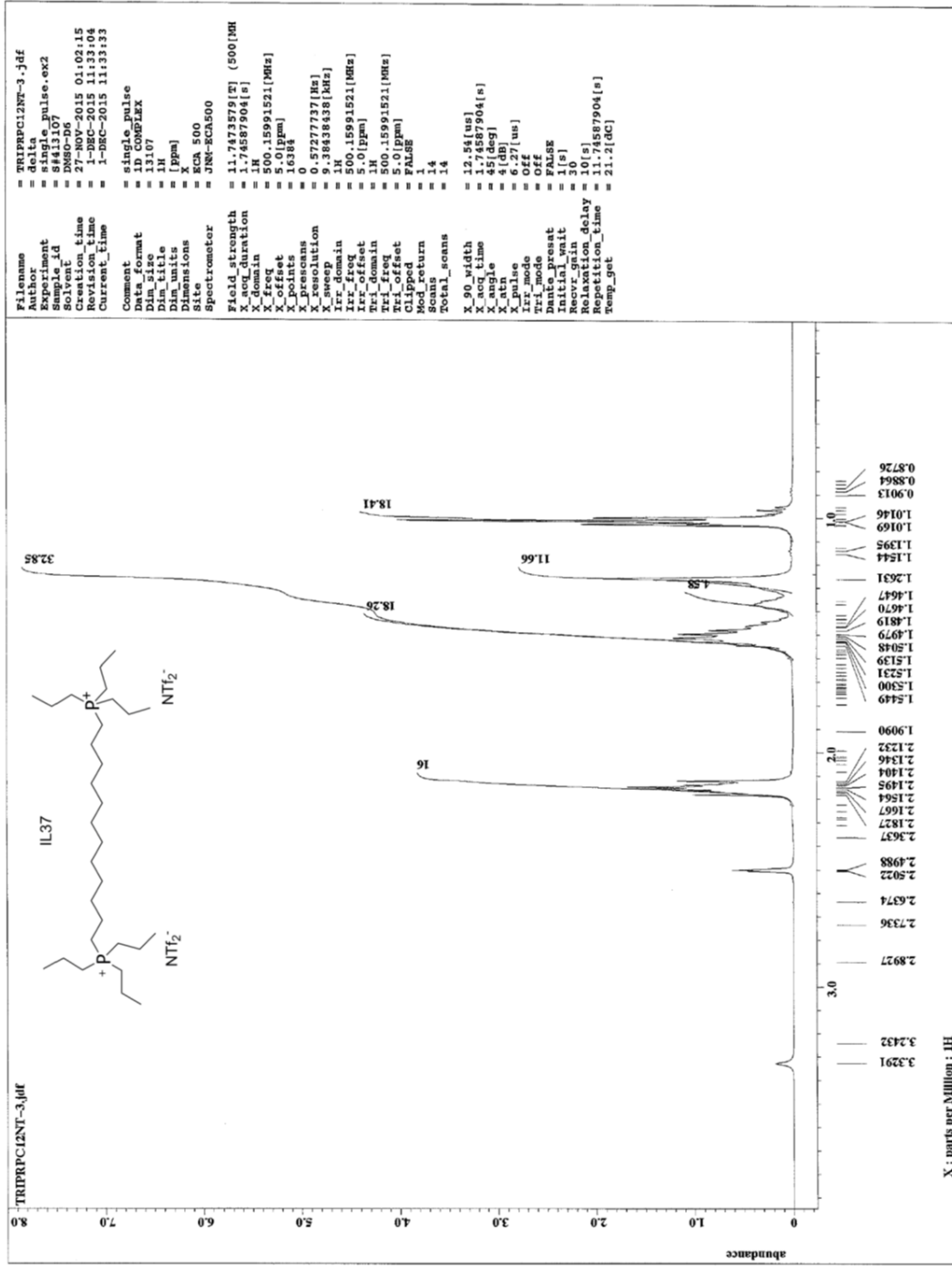
^1H NMR AND ^{13}C NMR OF $\text{C}_{12}(\text{mpy})_2\text{-NTf}_2$

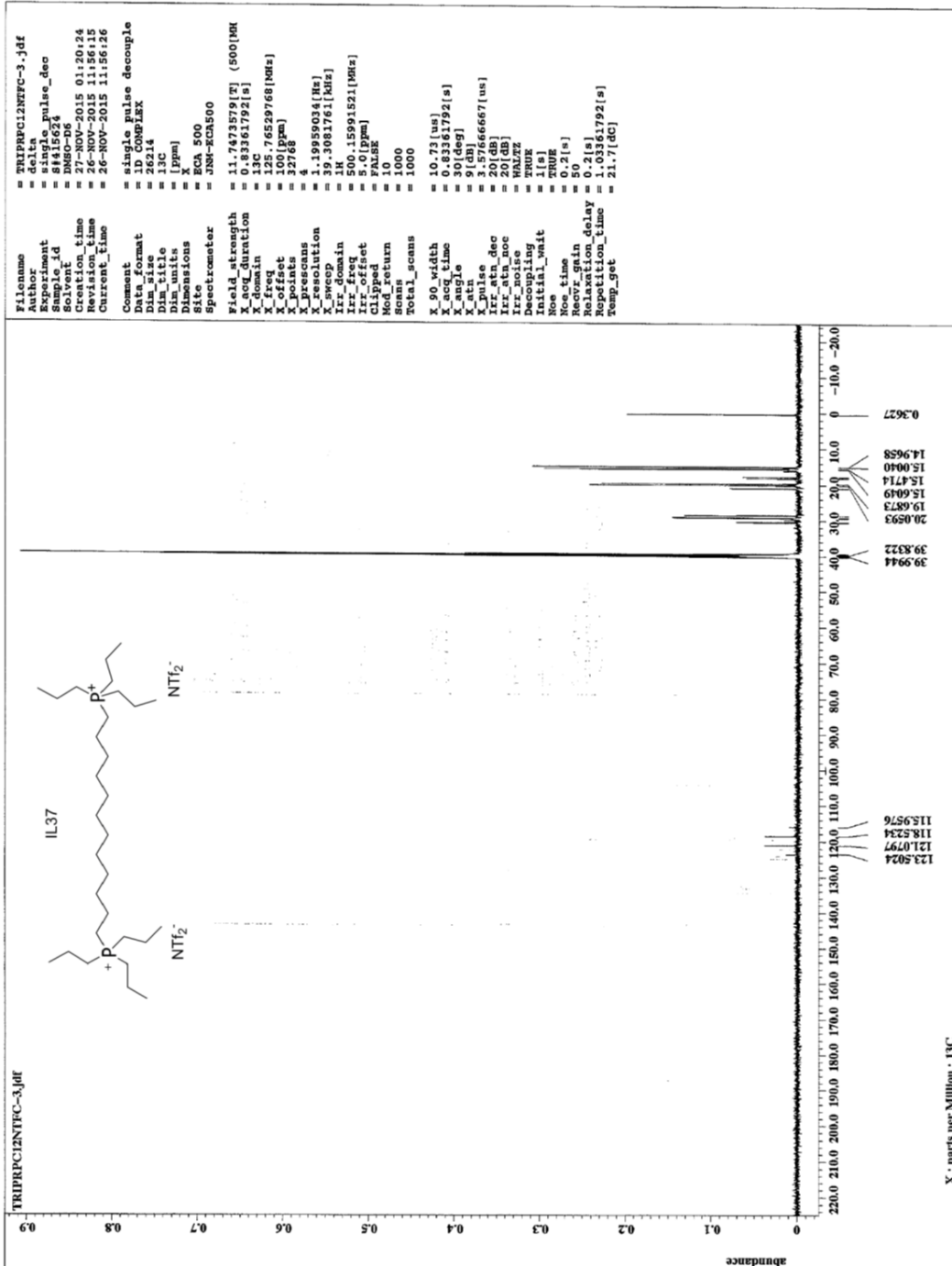




Appendix 24

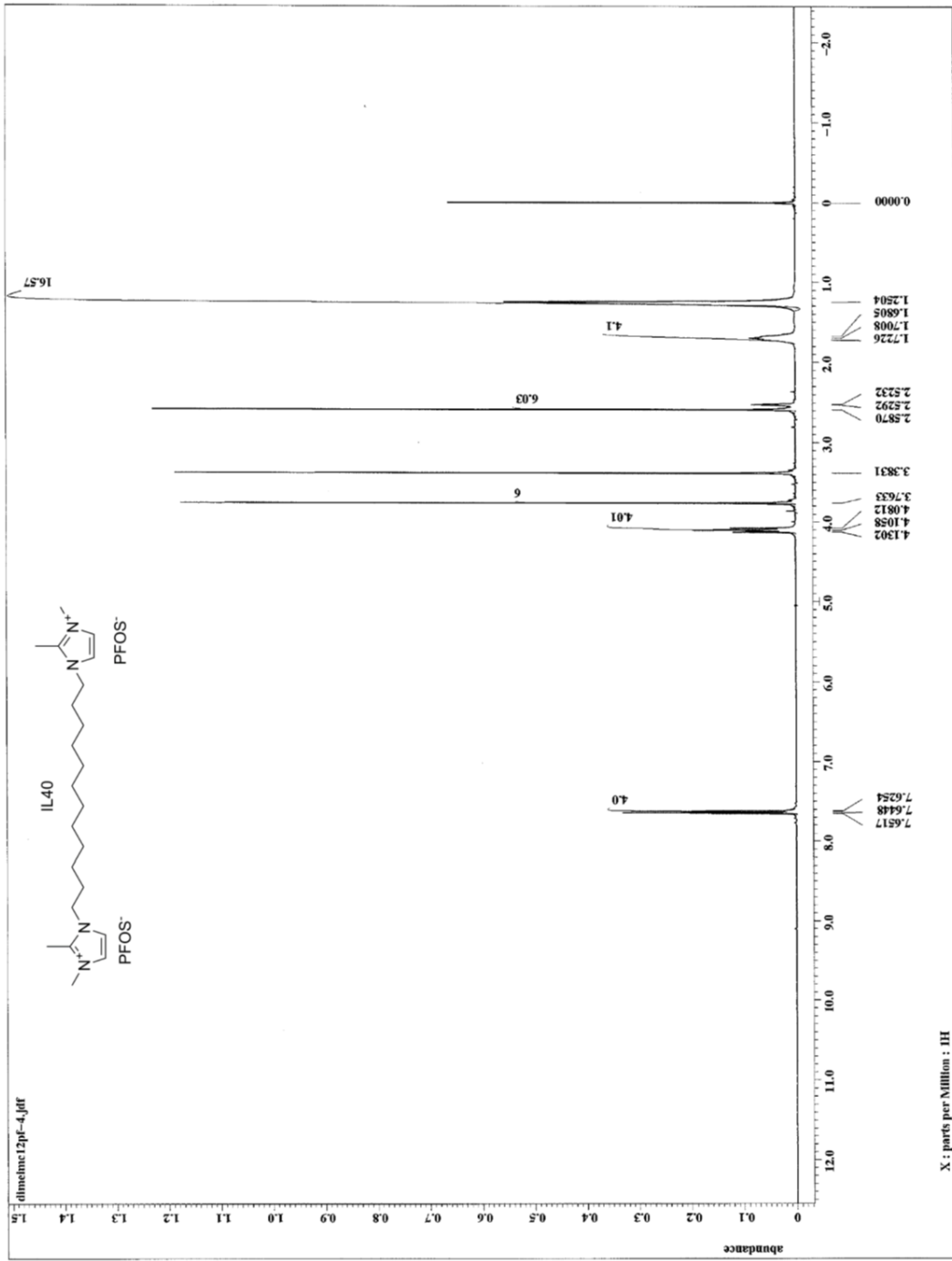
^1H NMR AND ^{13}C NMR OF $\text{C}_{12}(\text{pr}_3\text{p})_2\text{-NTf}_2$

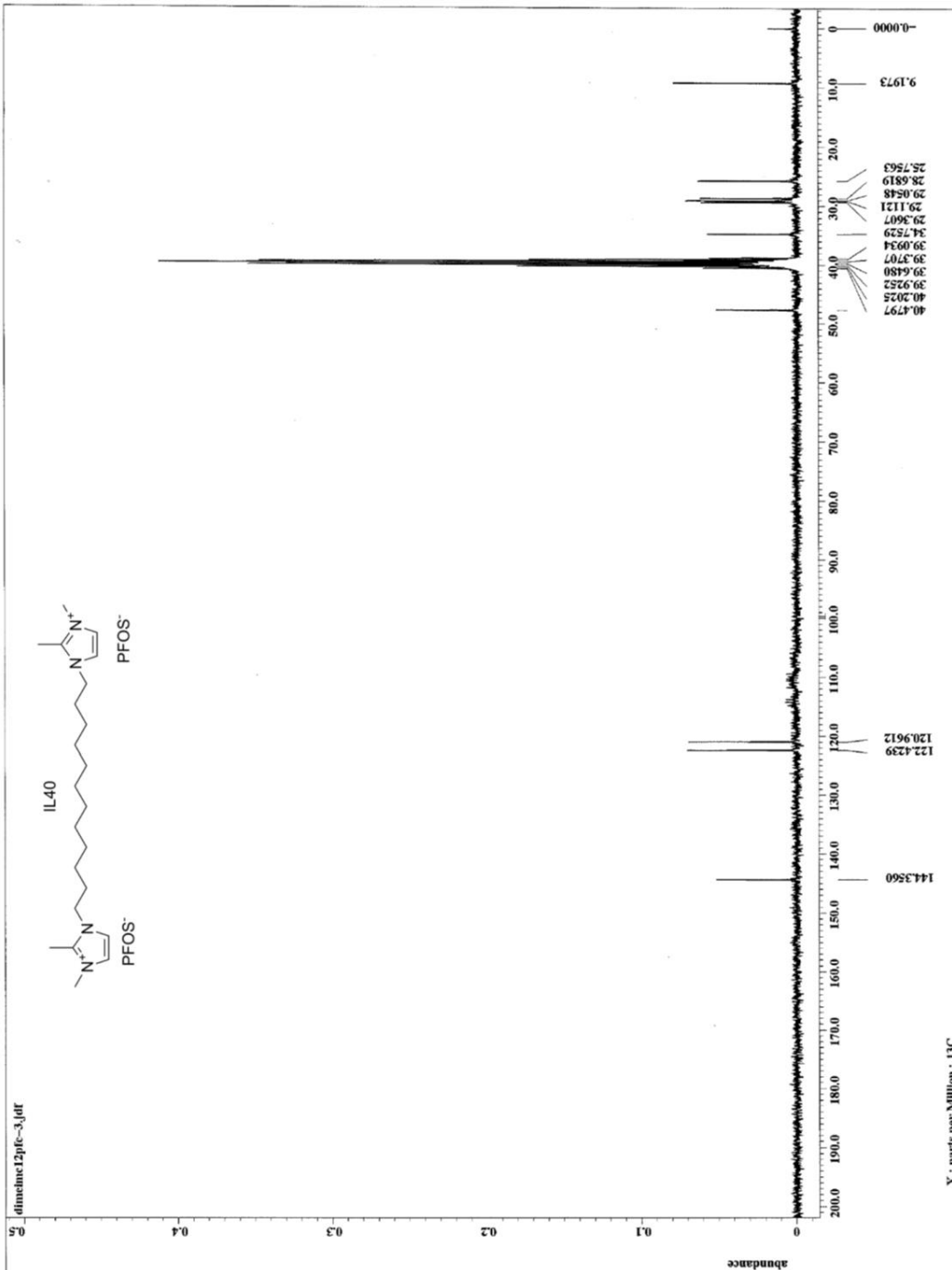




Appendix 25

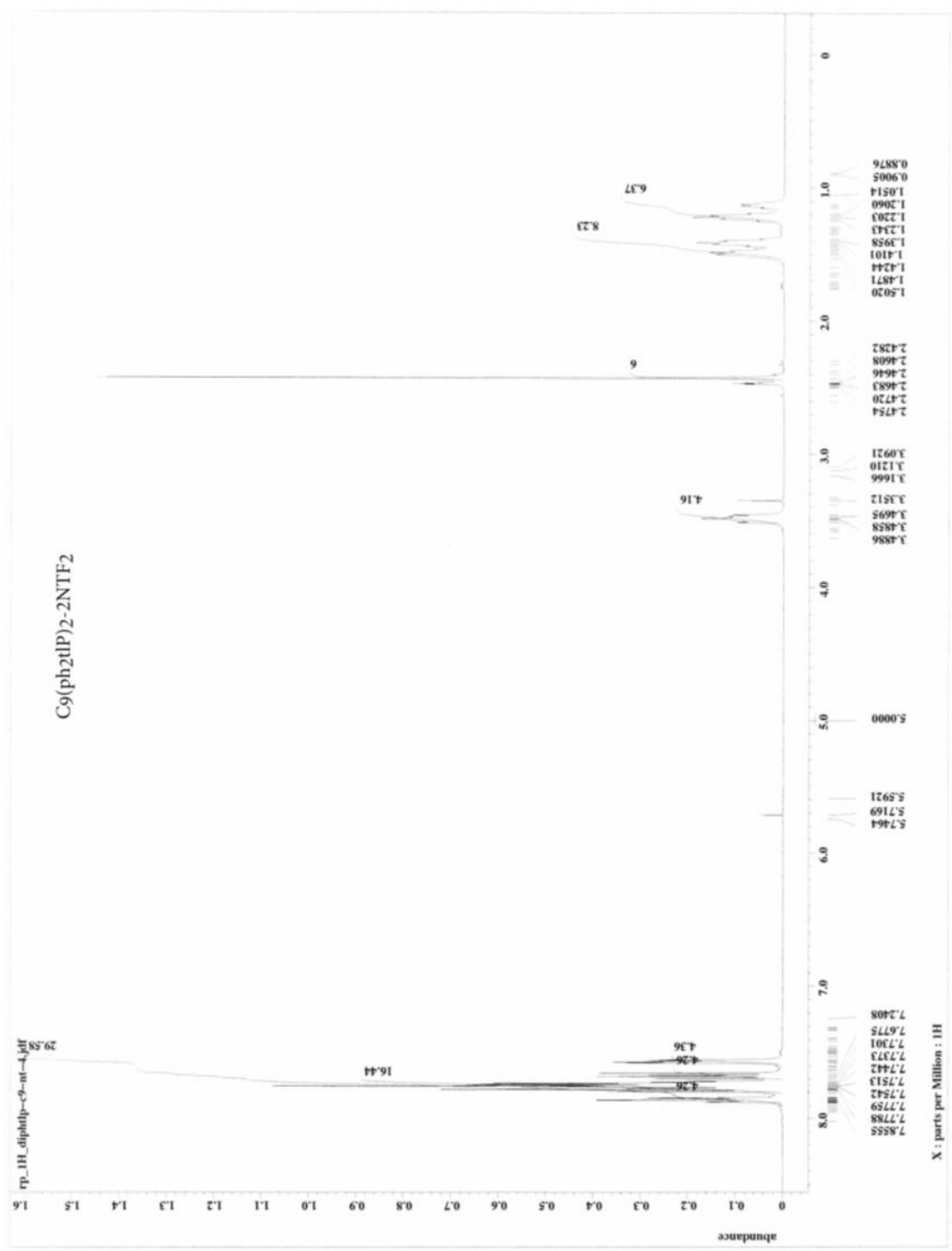
^1H NMR AND ^{13}C NMR OF $\text{C}_{12}(\text{mzim})_2\text{-PFOS}$

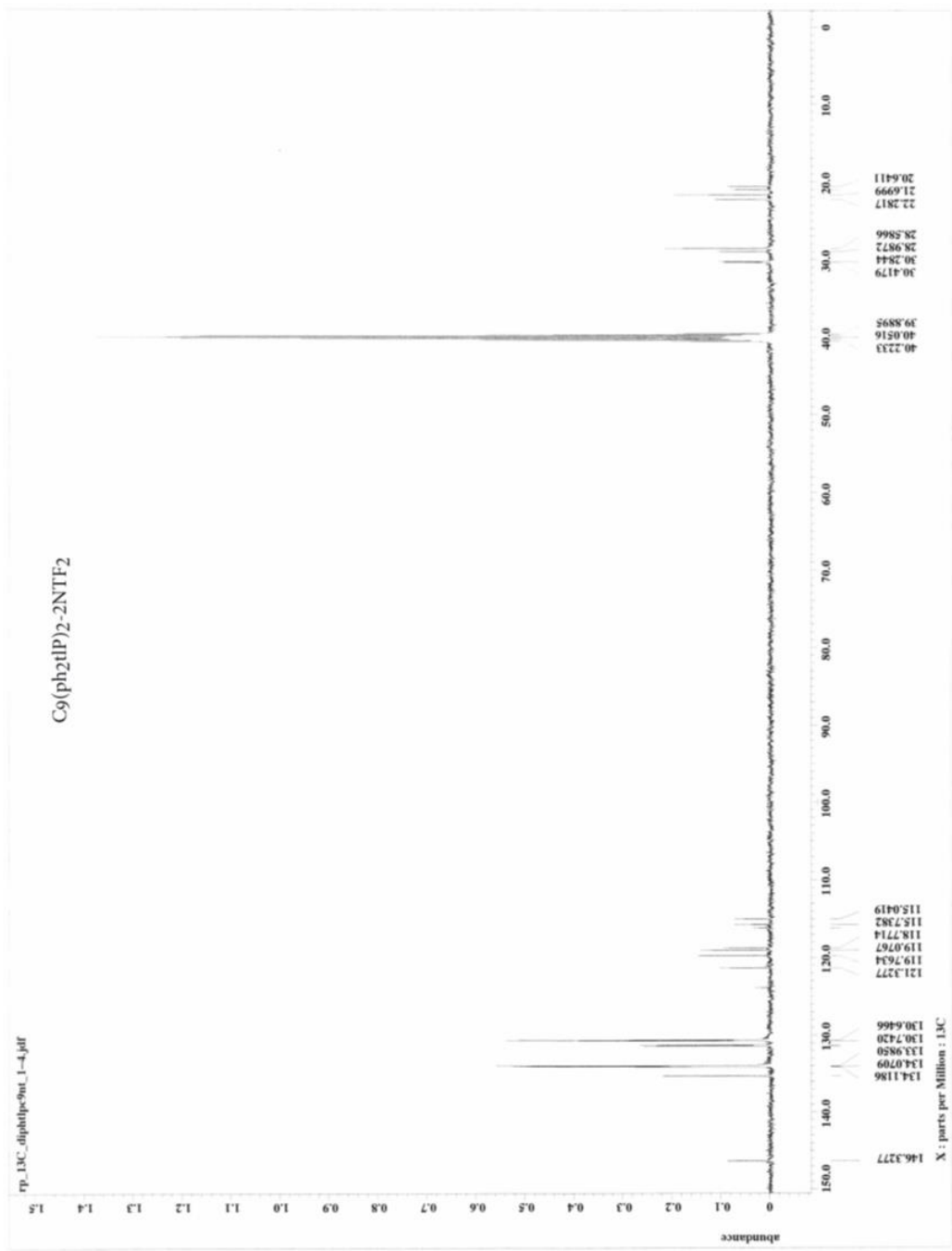




Appendix 26

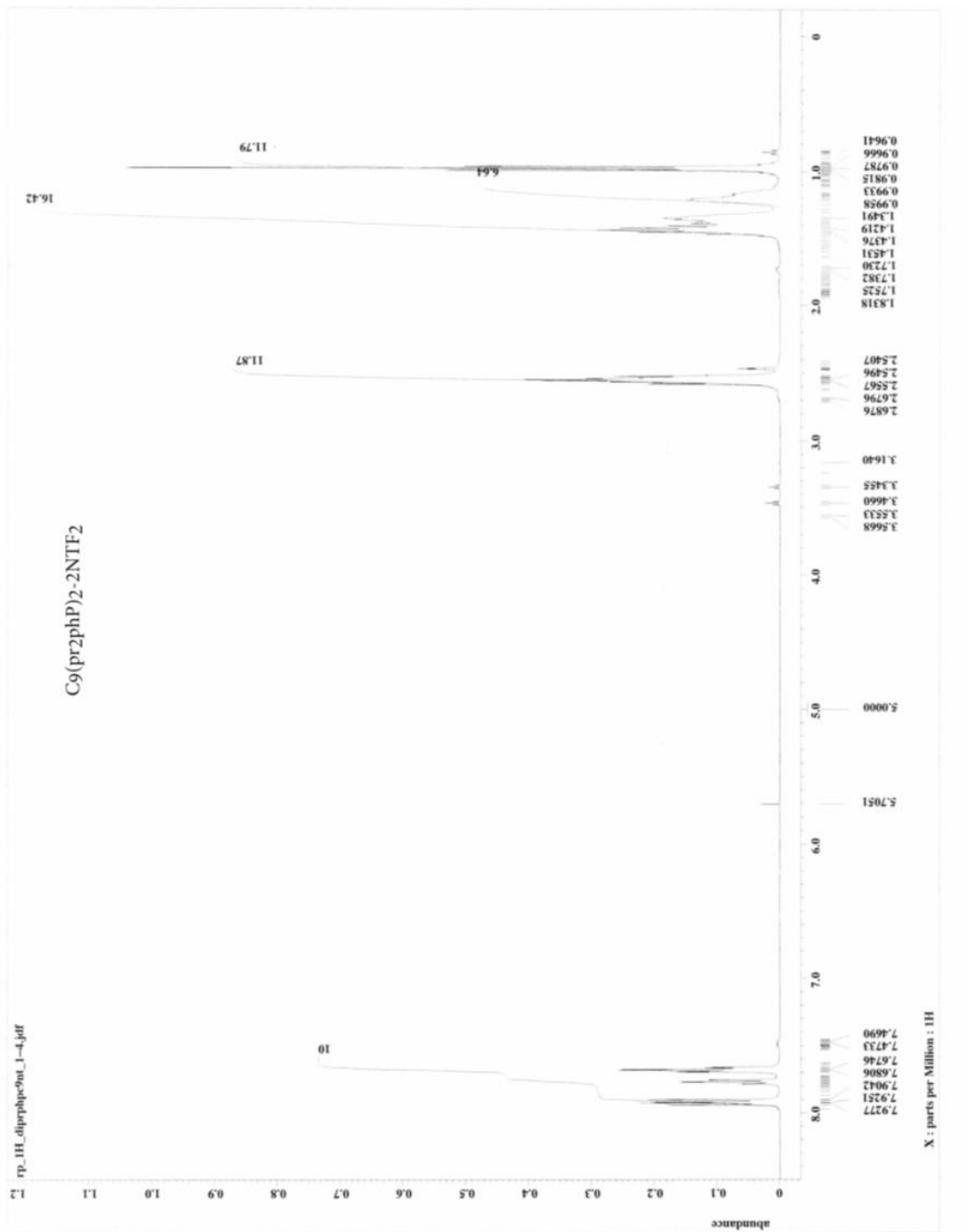
^1H NMR AND ^{13}C NMR OF $\text{C}_9(\text{ph}_2\text{tIP})_2\text{-2NTf}_2$

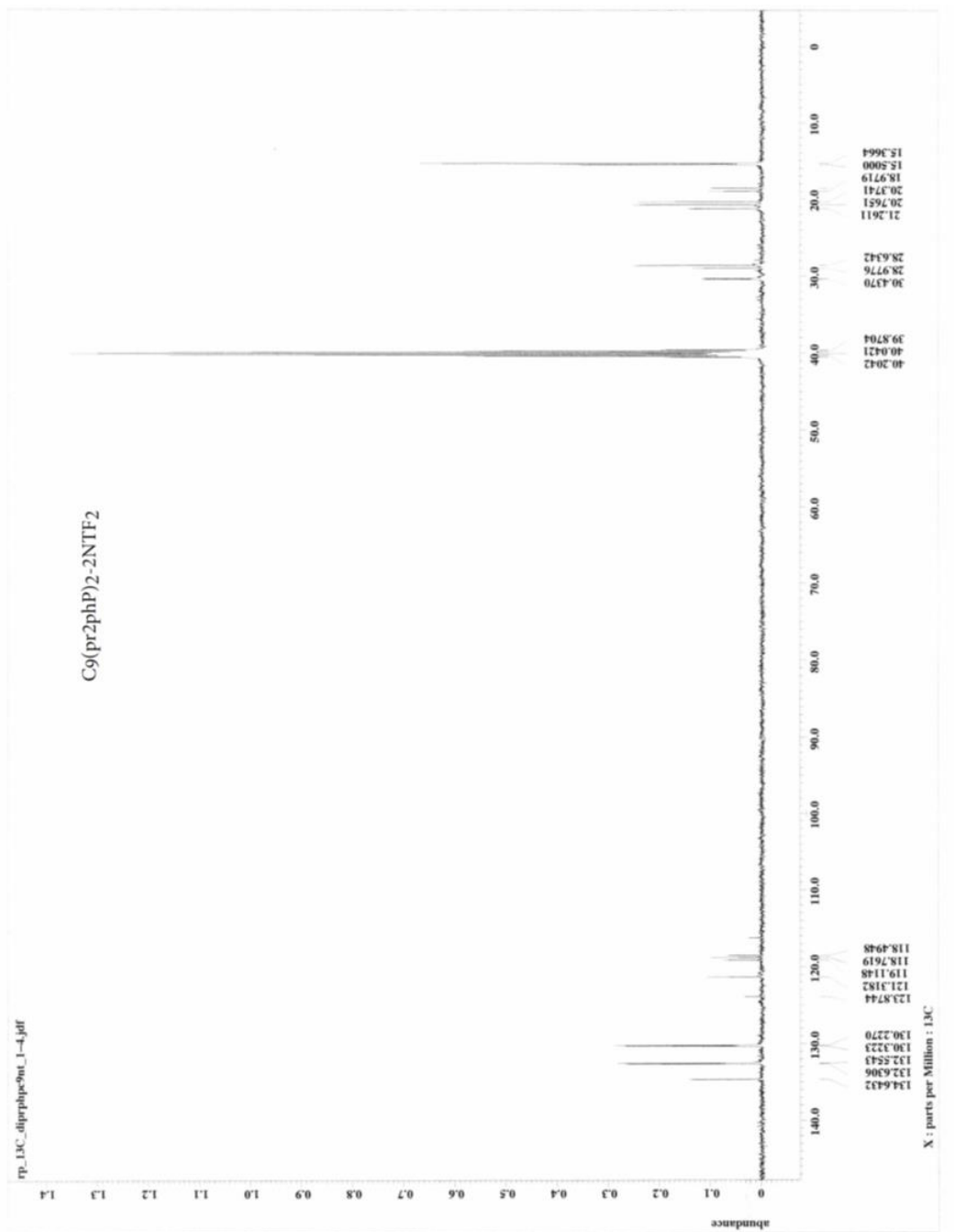




Appendix 27

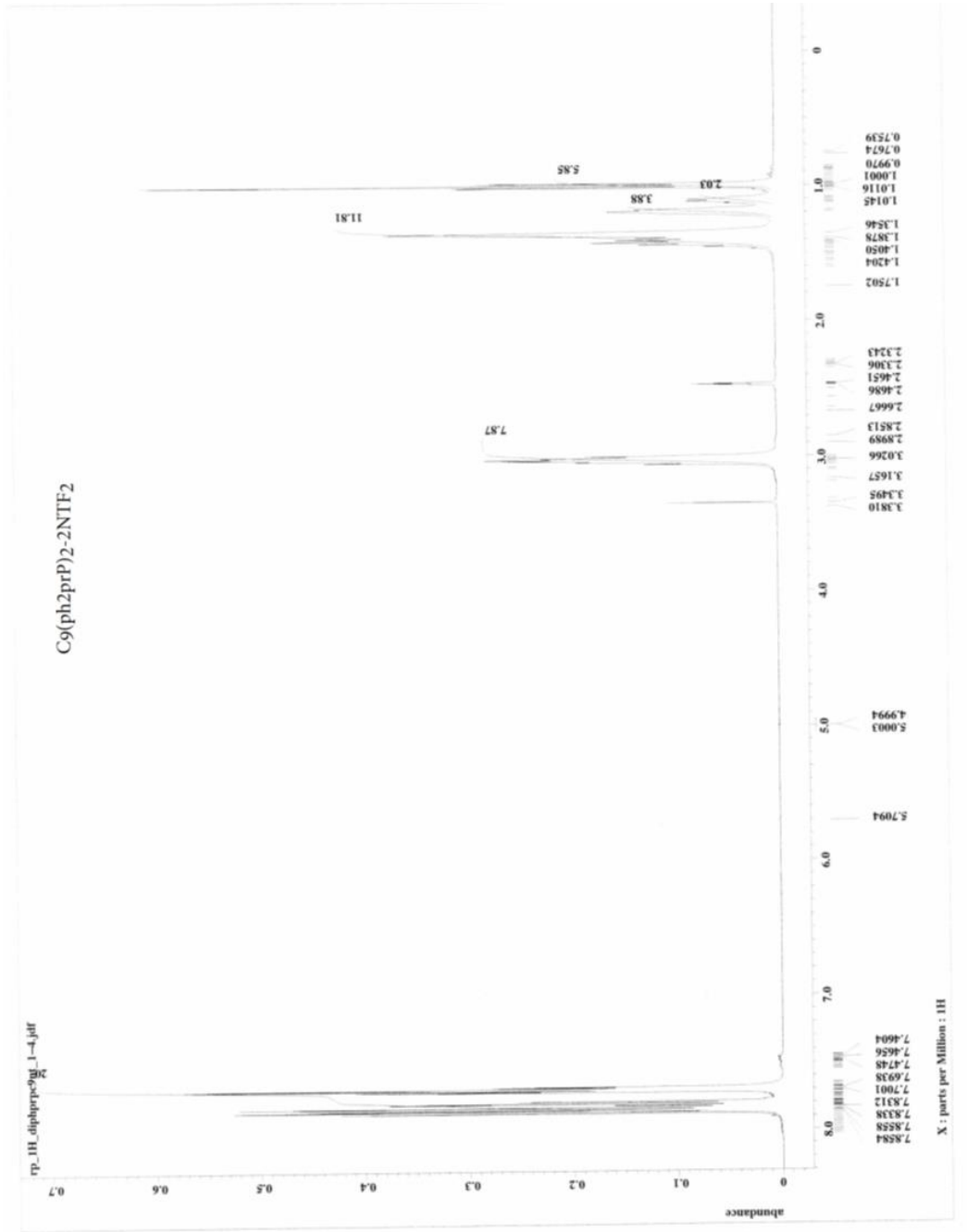
^1H NMR AND ^{13}C NMR OF $\text{C}_9(\text{pr}_2\text{phP})_2\text{-2NTf}_2$

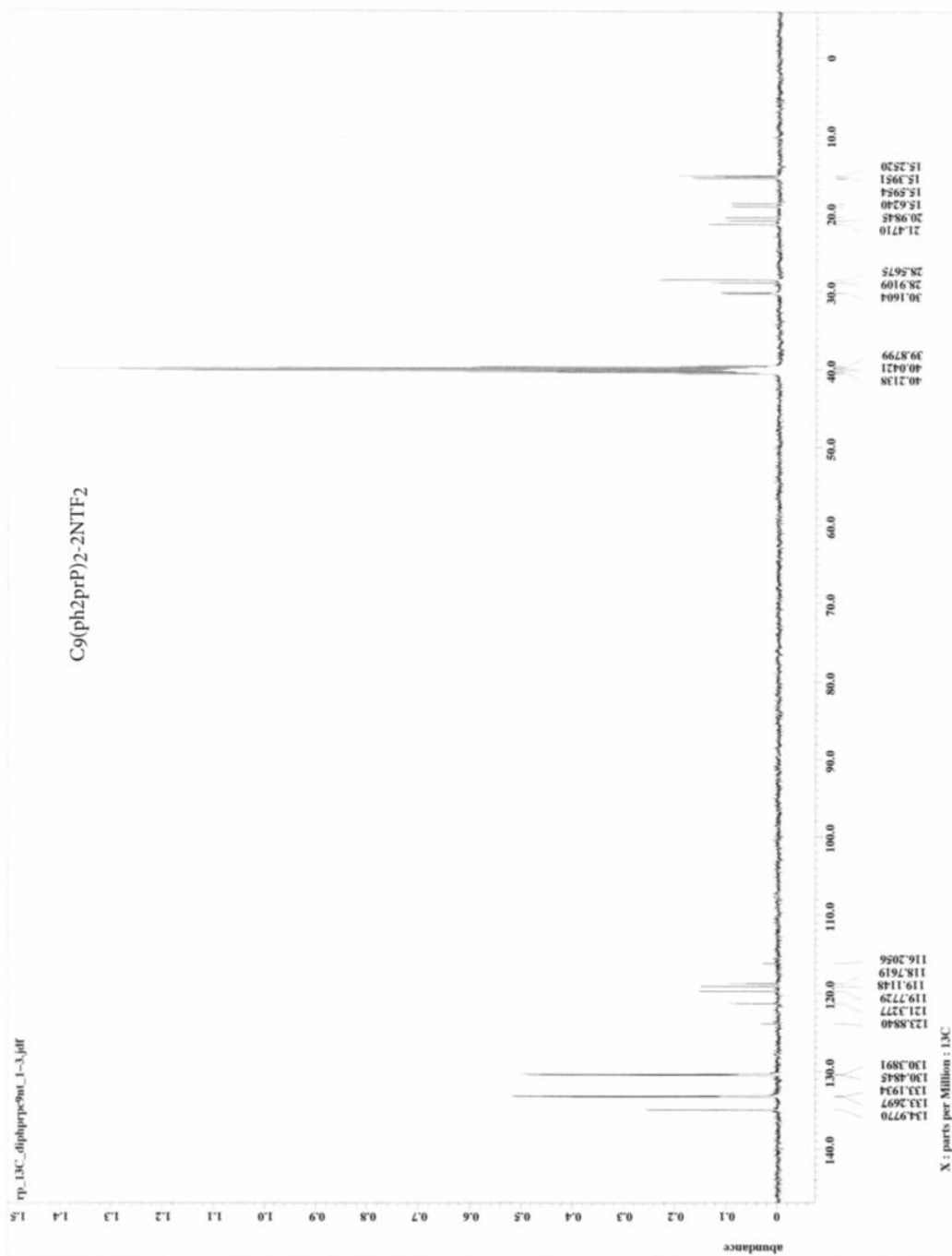




Appendix 28

^1H NMR AND ^{13}C NMR OF $\text{C}_9(\text{ph}_2\text{prP})_2\text{-2NTf}_2$





Appendix 29

PUBLICATION INFORMATION OF THE DISSERTATION

Chapter 2: Rahul. A. Patil, Mohsen Talebi, Chengdong Xu, Sumit S. Bhawal, Daniel W. Armstrong, Synthesis of Thermally Stable Geminal Dicationic Ionic Liquids and Related Ionic Compounds: An Examination of Physicochemical Properties by Structural Modification. *Chemistry of Materials*, 2016, 28, 4315-4323

Chapter 3: Rahul. A. Patil, Mohsen Talebi, Leonard M. Sidisky, Daniel W. Armstrong, Examination of Selectivities of Thermally Stable Geminal Dicationic Ionic Liquids by Structural Modification. *Chromatographia*, 2017, 80, 1563-1574

Chapter 4: Rahul. A. Patil, Mohsen Talebi, Alain Berthod, Daniel W. Armstrong. Dicationic Ionic Liquid Thermal Decomposition Pathways. *Analytical and Bioanalytical Chemistry*, 2018, 410, 4645-4655

Chapter 5: Rahul. A. Patil, Mohsen Talebi, Leonard M. Sidisky, Alain Berthod, Daniel W. Armstrong. GC Selectivity of New Phosphonium-based Dicationic Ionic Liquid Stationary Phases. *Journal of Separation Science*, accepted

Chapter 6: Sumit S. Bhawal, Rahul. A. Patil, Daniel W. Armstrong, Rapid Effective Deprotection of *tert*-butoxycarbonyl (Boc) Amino Acids and Peptides at high temperatures using a thermally stable ionic liquid. *RSC Advances*, 2015, 5, 95854-95856

Appendix 30
RIGHTS AND PERMISSIONS



RightsLink®

Home

Create Account

Help



ACS Publications
Most Trusted. Most Cited. Most Read.

Title: Synthesis of Thermally Stable Geminal Dicationic Ionic Liquids and Related Ionic Compounds: An Examination of Physicochemical Properties by Structural Modification

Author: Rahul A. Patil, Mohsen Talebi, Chengdong Xu, et al

Publication: Chemistry of Materials

Publisher: American Chemical Society

Date: Jun 1, 2016

Copyright © 2016, American Chemical Society

LOGIN

If you're a [copyright.com](#) user, you can login to RightsLink using your [copyright.com](#) credentials.

Already a [RightsLink](#) user or want to [learn more?](#)

PERMISSION/LICENSE IS GRANTED FOR YOUR ORDER AT NO CHARGE

This type of permission/license, instead of the standard Terms & Conditions, is sent to you because no fee is being charged for your order. Please note the following:

- Permission is granted for your request in both print and electronic formats, and translations.
- If figures and/or tables were requested, they may be adapted or used in part.
- Please print this page for your records and send a copy of it to your publisher/graduate school.
- Appropriate credit for the requested material should be given as follows: "Reprinted (adapted) with permission from (COMPLETE REFERENCE CITATION). Copyright (YEAR) American Chemical Society." Insert appropriate information in place of the capitalized words.
- One-time permission is granted only for the use specified in your request. No additional uses are granted (such as derivative works or other editions). For any other uses, please submit a new request.

BACK

CLOSE WINDOW

Copyright © 2018 [Copyright Clearance Center, Inc.](#) All Rights Reserved. [Privacy statement](#). [Terms and Conditions](#).
Comments? We would like to hear from you. E-mail us at customer@copyright.com

Chapter 2 reprinted with permission from Patil RA, Talebi M, Xu C, Bhawal SS, Armstrong DW (2016) Synthesis of Thermally Stable Geminal Dicationic Ionic Liquids and Related Ionic Compounds: An Examination of Physicochemical Properties by Structural Modification. Chem Mater 28 (12):4315-4323. Copyright 2016 American Chemical Society

**SPRINGER NATURE LICENSE
TERMS AND CONDITIONS**

Sep 09, 2018

This Agreement between University of Texas at Arlington -- Rahul Patil ("You") and Springer Nature ("Springer Nature") consists of your license details and the terms and conditions provided by Springer Nature and Copyright Clearance Center.

License Number	4424961478194
License date	Sep 09, 2018
Licensed Content Publisher	Springer Nature
Licensed Content Publication	Chromatographia
Licensed Content Title	Examination of Selectivities of Thermally Stable Geminal Dicationic Ionic Liquids by Structural Modification
Licensed Content Author	Rahul A. Patil, Mohsen Talebi, Leonard M. Sidisky et al
Licensed Content Date	Jan 1, 2017
Licensed Content Volume	80
Licensed Content Issue	10
Type of Use	Thesis/Dissertation
Requestor type	academic/university or research institute
Format	print and electronic
Portion	full article/chapter
Will you be translating?	no
Circulation/distribution	<501
Author of this Springer Nature content	yes
Title	Designing Thermally Stable Ionic Liquid Stationary Phases For Gas Chromatography And Examining Their Structure-Property Relationships
Instructor name	Daniel W. Armstrong
Institution name	University of Texas at Arlington
Expected presentation date	Oct 2018
Requestor Location	University of Texas at Arlington 700 Planetarium Place ARLINGTON, TX 76019 United States Attn: Rahul Patil
Billing Type	Invoice
Billing Address	University of Texas at Arlington 700 Planetarium Place ARLINGTON, TX 76019 United States Attn: Rahul Patil
Total	0.00 USD

**SPRINGER NATURE LICENSE
TERMS AND CONDITIONS**

Sep 09, 2018

This Agreement between University of Texas at Arlington -- Rahul Patil ("You") and Springer Nature ("Springer Nature") consists of your license details and the terms and conditions provided by Springer Nature and Copyright Clearance Center.

License Number	4424970217761
License date	Sep 09, 2018
Licensed Content Publisher	Springer Nature
Licensed Content Publication	Analytical and Bioanalytical Chemistry
Licensed Content Title	Dicationic ionic liquid thermal decomposition pathways
Licensed Content Author	Rahul A. Patil, Mohsen Talebi, Alain Berthod et al
Licensed Content Date	Jan 1, 2018
Licensed Content Volume	410
Licensed Content Issue	19
Type of Use	Thesis/Dissertation
Requestor type	academic/university or research institute
Format	print and electronic
Portion	full article/chapter
Will you be translating?	no
Circulation/distribution	<501
Author of this Springer Nature content	yes
Title	Designing Thermally Stable Ionic Liquid Stationary Phases For Gas Chromatography And Examining Their Structure-Property Relationships
Instructor name	Daniel W. Armstrong
Institution name	University of Texas at Arlington
Expected presentation date	Oct 2018
Requestor Location	University of Texas at Arlington 700 Planetarium Place ARLINGTON, TX 76019 United States Attn: Rahul Patil
Billing Type	Invoice
Billing Address	University of Texas at Arlington 700 Planetarium Place ARLINGTON, TX 76019 United States Attn: Rahul Patil
Total	0.00 USD

**SPRINGER NATURE LICENSE
TERMS AND CONDITIONS**

Sep 19, 2018

This Agreement between University of Texas at Arlington -- Rahul Patil ("You") and Springer Nature ("Springer Nature") consists of your license details and the terms and conditions provided by Springer Nature and Copyright Clearance Center.

License Number	4432670871127
License date	Sep 19, 2018
Licensed Content Publisher	Springer Nature
Licensed Content Publication	Analytical and Bioanalytical Chemistry
Licensed Content Title	PEG-linked geminal dicationic ionic liquids as selective, high-stability gas chromatographic stationary phases
Licensed Content Author	Ke Huang, Xinxin Han, Xiaotong Zhang et al
Licensed Content Date	Jan 1, 2007
Licensed Content Volume	389
Licensed Content Issue	7
Type of Use	Thesis/Dissertation
Requestor type	academic/university or research institute
Format	print and electronic
Portion	figures/tables/illustrations
Number of figures/tables/illustrations	1
Will you be translating?	no
Circulation/distribution	<501
Author of this Springer Nature content	no
Title	Designing Thermally Stable Ionic Liquid Stationary Phases For Gas Chromatography And Examining Their Structure-Property Relationships
Instructor name	Daniel W. Armstrong
Institution name	University of Texas at Arlington
Expected presentation date	Oct 2018
Portions	Figure 2
Requestor Location	University of Texas at Arlington 700 Planetarium Place ARLINGTON, TX 76019 United States Attn: Rahul Patil
Billing Type	Invoice
Billing Address	University of Texas at Arlington 700 Planetarium Place ARLINGTON, TX 76019 United States Attn: Rahul Patil
Total	0.00 USD



Note: Copyright.com supplies permissions but not the copyrighted content itself.

1
PAYMENT

2
REVIEW

3
CONFIRMATION

Step 3: Order Confirmation

Thank you for your order! A confirmation for your order will be sent to your account email address. If you have questions about your order, you can call us 24 hrs/day, M-F at +1.855.239.3415 Toll Free, or write to us at info@copyright.com. This is not an invoice.

Confirmation Number: 11749837
Order Date: 09/19/2018

If you paid by credit card, your order will be finalized and your card will be charged within 24 hours. If you choose to be invoiced, you can change or cancel your order until the invoice is generated.

Payment Information

Rahul Patil
University of Texas at Arlington
rahulapatil@mavs.uta.edu
+1 (817) 272-3834
Payment Method: n/a

Order Details

Chemical Society reviews

Order detail ID: 71561538
Order License Id: 4432661181952
ISSN: 1460-4744
Publication Type: e-Journal
Volume:
Issue:
Start page:
Publisher: ROYAL SOCIETY OF CHEMISTRY
Author/Editor: Royal Society of Chemistry (Great Britain)

Permission Status: **Granted**
Permission type: Republish or display content
Type of use: Thesis/Dissertation

Requestor type: Academic institution

Format: Print, Electronic

Portion: chart/graph/table/figure

Number of charts/graphs/tables/figures	1
The requesting person/organization	Rahul A Patil
Title or numeric reference of the portion(s)	Figure 2
Title of the article or chapter the portion is from	Ionic liquid thermal stabilities: decomposition mechanisms and analysis tools
Editor of portion(s)	N/A
Author of portion(s)	Cedric Maton, Nils De Vosa, Christian V. Stevens
Volume of serial or monograph	42
Page range of portion	5965
Publication date of portion	19 Apr 2013
Rights for	Main product
Duration of use	Life of current edition

Creation of copies for the disabled	no
With minor editing privileges	no
For distribution to	United States
In the following language(s)	Original language of publication
With incidental promotional use	no
Lifetime unit quantity of new product	Up to 499
Title	Designing Thermally Stable Ionic Liquid Stationary Phases For Gas Chromatography And Examining Their Structure-Property Relationships
Instructor name	Daniel W. Armstrong
Institution name	University of Texas at Arlington
Expected presentation date	Oct 2018

Note: This item will be invoiced or charged separately through CCC's **RightsLink** service. [More info](#)

\$ 0.00

Total order items: 1

This is not an invoice.

Order Total: 0.00 USD

**JOHN WILEY AND SONS LICENSE
TERMS AND CONDITIONS**

Oct 15, 2018

This Agreement between University of Texas at Arlington -- Rahul Patil ("You") and John Wiley and Sons ("John Wiley and Sons") consists of your license details and the terms and conditions provided by John Wiley and Sons and Copyright Clearance Center.

License Number	4450361108572
License date	Oct 15, 2018
Licensed Content Publisher	John Wiley and Sons
Licensed Content Publication	Journal of Separation Science
Licensed Content Title	GC selectivity of new phosphonium-based dicationic ionic liquid stationary phases
Licensed Content Author	Rahul A. Patil, Mohsen Talebi, Leonard M. Sidisky, et al
Licensed Content Date	Sep 27, 2018
Licensed Content Volume	0
Licensed Content Issue	ja
Licensed Content Pages	29
Type of use	Dissertation/Thesis
Requestor type	Author of this Wiley article
Format	Print and electronic
Portion	Full article
Will you be translating?	No
Title of your thesis / dissertation	Designing Thermally Stable Ionic Liquid Stationary Phases For Gas Chromatography And Examining Their Structure-Property Relationships
Expected completion date	Oct 2018
Expected size (number of pages)	1
Requestor Location	University of Texas at Arlington 700 Planetarium Place ARLINGTON, TX 76019 United States Attn: Rahul Patil
Publisher Tax ID	EU826007151
Total	0.00 USD

Chapter 6: Rapid, effective deprotection of tert-butoxycarbonyl (Boc) amino acids and peptides at high temperatures using a thermally stable ionic liquid. S. S. Bhawal, R. A. Patil and D. W. Armstrong, RSC Adv., 2015, 5, 95854 – Reproduced by permission of The Royal Society of Chemistry.

References

1. Weingärtner, H. *Angew. Chem. Int. Ed.* **2008**, *47* (4), 654-670.
2. Soukup-Hein, R. J.; Warnke, M. M.; Armstrong, D. W. *Annu. Rev. of Anal. Chem.* **2009**, *2*, 145-168.
3. Walden, P. *Bull. Acad. Imper. Sci.(St. Petersburg)* **1914**, 1800.
4. Wilkes, J. S. *Green Chem.* **2002**, *4* (2), 73-80.
5. Hurley, F. H.; Wler, T. P. *J. Electrochem. Soc.* **1951**, *98* (5), 207-212.
6. Welton, T. *Chem. Rev.* **1999**, *99* (8), 2071-2084.
7. Chauvin, Y.; Mußmann, L.; Olivier, H. *Angew. Chem.* **1995**, *107* (23-24), 2941-2943.
8. Chauvin, Y.; Mussmann, L.; Olivier, H. *Angew. Chem. Int. Ed. Engl.* **1996**, *34* (23-24), 2698-2700.
9. Bonhote, P.; Dias, A.-P.; Papageorgiou, N.; Kalyanasundaram, K.; Grätzel, M. *Inorg. Chem.* **1996**, *35* (5), 1168-1178.
10. Giernoth, R. *Angew. Chem. Int. Ed.* **2010**, *49* (16), 2834-2839.
11. Anderson, J. L.; Ding, R.; Ellern, A.; Armstrong, D. W. *J. Am. Chem. Soc.* **2005**, *127* (2), 593-604.
12. Payagala, T.; Huang, J.; Breitbach, Z. S.; Sharma, P. S.; Armstrong, D. W. *Chem. Mater.* **2007**, *19* (24), 5848-5850.
13. Breitbach, Z. S.; Armstrong, D. W. *Anal. Bioanal. Chem.* **2008**, *390* (6), 1605-1617.
14. Sharma, P. S.; Payagala, T.; Wanigasekara, E.; Wijeratne, A. B.; Huang, J.; Armstrong, D. W. *Chem. Mater.* **2008**, *20* (13), 4182-4184.
15. Wanigasekara, E.; Zhang, X.; Nanayakkara, Y.; Payagala, T.; Moon, H.; Armstrong, D. W. *ACS Appl. Mater. Interfaces* **2009**, *1* (10), 2126-2133.
16. Shirota, H.; Mandai, T.; Fukazawa, H.; Kato, T. *J. Chem.Eng. Data* **2011**, *56* (5), 2453-2459.
17. Huang, K.; Han, X.; Zhang, X.; Armstrong, D. W. *Anal. Bioanal. Chem.* **2007**, *389* (7-8), 2265-2275.
18. Zeng, Z.; Phillips, B. S.; Xiao, J.-C.; Shreeve, J. n. M. *Chem. Mater.* **2008**, *20* (8), 2719-2726.
19. Talebi, M.; Patil, R. A.; Armstrong, D. W. *J. Mol. Liq.* **2018**, *256*, 247-255.
20. Han, X.; Armstrong, D. W. *Org. Lett.* **2005**, *7* (19), 4205-4208.

21. Xiao, J.-C.; Shreeve, J. n. M. *J. Org. Chem.* **2005**, *70* (8), 3072-3078.
22. Anderson, J. L.; Armstrong, D. W. *Anal. Chem.* **2003**, *75* (18), 4851-4858.
23. Ho, T. D.; Yehl, P. M.; Chetwyn, N. P.; Wang, J.; Anderson, J. L.; Zhong, Q. *J. Chromatogr. A* **2014**, *1361*, 217-228.
24. Nacham, O.; Ho, T. D.; Anderson, J. L.; Webster, G. K. *J. Pharm. Biomed. Anal.* **2017**.
25. Wu, B.; Reddy, R.; Rogers, R. *Solar Engineering* **2001**, 445-452.
26. Jin, C.-M.; Ye, C.; Phillips, B. S.; Zabinski, J. S.; Liu, X.; Liu, W.; Jean'ne, M. S. *J. Mater. Chem.* **2006**, *16* (16), 1529-1535.
27. Qu, J.; Bansal, D. G.; Yu, B.; Howe, J. Y.; Luo, H.; Dai, S.; Li, H.; Blau, P. J.; Bunting, B. G.; Mordukhovich, G. *ACS Appl. Mater. Interfaces* **2012**, *4* (2), 997-1002.
28. Lin, X.; Kavian, R.; Lu, Y.; Hu, Q.; Shao-Horn, Y.; Grinstaff, M. W. *Chem. Sci.* **2015**, *6* (11), 6601-6606.
29. Fan, X.; Wang, L. *ACS Appl. Mater. Interfaces* **2014**, *6* (16), 14660-14671.
30. Liu, X.; Pu, J.; Wang, L.; Xue, Q. *J. Mater. Chem. A* **2013**, *1* (11), 3797-3809.
31. Maton, C.; De Vos, N.; Stevens, C. V. *Chem. Soc. Rev.* **2013**, *42* (13), 5963-5977.
32. Fredlake, C. P.; Crosthwaite, J. M.; Hert, D. G.; Aki, S. N.; Brennecke, J. F. *J. Chem. Eng. Data* **2004**, *49* (4), 954-964.
33. Heym, F.; Etzold, B. J.; Kern, C.; Jess, A. *Green Chem.* **2011**, *13* (6), 1453-1466.
34. Kosmulski, M.; Gustafsson, J.; Rosenholm, J. B. *Thermochim. Acta* **2004**, *412* (1-2), 47-53.
35. Bridges, N. J.; Visser, A. E.; Fox, E. B. *Energy & Fuels* **2011**, *25* (10), 4862-4864.
36. Kamavaram, V.; Reddy, R. G. *Int. J. Therm. Sci.* **2008**, *47* (6), 773-777.
37. Armstrong, D. W.; He, L.; Liu, Y.-S. *Anal. Chem.* **1999**, *71* (17), 3873-3876.
38. Anderson, J. L.; Armstrong, D. W. *Anal. Chem.* **2005**, *77* (19), 6453-6462.
39. Payagala, T.; Zhang, Y.; Wanigasekara, E.; Huang, K.; Breitbach, Z. S.; Sharma, P. S.; Sidisky, L. M.; Armstrong, D. W. *Anal. Chem.* **2008**, *81* (1), 160-173.
40. Anderson, J. L.; Ding, J.; Welton, T.; Armstrong, D. W. *J. Am. Chem. Soc.* **2002**, *124* (47), 14247-14254.
41. Sun, P.; Armstrong, D. W. *Anal. Chim. Acta* **2010**, *661* (1), 1-16.
42. Barber, D.; Phillips, C.; Tusa, G.; Verdin, A. *J. Chem. Soc.* **1959**, (JAN), 18-24.
43. Pacholec, F.; Butler, H. T.; Poole, C. F. *Anal. Chem.* **1982**, *54* (12), 1938-1941.
44. Pacholec, F.; Poole, C. *Chromatographia* **1983**, *17* (7), 370-374.

45. Pomaville, R. M.; Poole, S. K.; Davis, L. J.; Poole, C. F. *J. Chromatogr. A* **1988**, *438*, 1-14.
46. Sarda, S. R.; Jadhav, W. N.; Shete, A. S.; Dhopte, K. B.; Sadawarte, S. M.; Gadge, P. J.; Pawar, R. P. *Synth. Commun.* **2010**, *40* (14), 2178-2184.
47. Visser, A. E.; Swatloski, R. P.; Reichert, W. M.; Mayton, R.; Sheff, S.; Wierzbicki, A.; Davis, J. H.; Rogers, R. D. *Environ. Sci. Technol.* **2002**, *36* (11), 2523-2529.
48. Anderson, J. L.; Armstrong, D. W.; Wei, G.-T. *Anal. Chem.* **2006**, *78* (9), 2892-2902.
49. Anderson, J. L.; Pino, V.; Hagberg, E. C.; Sheares, V. V.; Armstrong, D. W. *Chem. Commun.* **2003**, (19), 2444-2445.
50. Boxall, D. L.; Osteryoung, R. A. *J. Electrochem. Soc.* **2004**, *151* (2), E41-E45.
51. Cadena, C.; Anthony, J. L.; Shah, J. K.; Morrow, T. I.; Brennecke, J. F.; Maginn, E. J. *J. Am. Chem. Soc.* **2004**, *126* (16), 5300-5308.
52. Carter, E. B.; Culver, S. L.; Fox, P. A.; Goode, R. D.; Ntai, I.; Tickell, M. D.; Traylor, R. K.; Hoffman, N. W.; Davis Jr, J. H. *Chem. Commun.* **2004**, (6), 630-631.
53. Earle, M. J.; Katdare, S. P.; Seddon, K. R. *Org. Lett.* **2004**, *6* (5), 707-710.
54. Fletcher, K. A.; Pandey, S. *Langmuir* **2004**, *20* (1), 33-36.
55. Gao, H.; Jiang, T.; Han, B.; Wang, Y.; Du, J.; Liu, Z.; Zhang, J. *Polymer* **2004**, *45* (9), 3017-3019.
56. Kaar, J. L.; Jesionowski, A. M.; Berberich, J. A.; Moulton, R.; Russell, A. J. *J. Am. Chem. Soc.* **2003**, *125* (14), 4125-4131.
57. Lee, J. K.; Kim, M.-J. *J. Org. Chem.* **2002**, *67* (19), 6845-6847.
58. Luo, H.; Dai, S.; Bonnesen, P. V.; Buchanan, A.; Holbrey, J. D.; Bridges, N. J.; Rogers, R. D. *Anal. Chem.* **2004**, *76* (11), 3078-3083.
59. Vijayaraghavan, R.; MacFarlane, D. *Chem. Commun.* **2004**, (6), 700-701.
60. Wasserscheid, P.; Hilgers, C.; Keim, W. *J. Mol. Catal. A: Chem.* **2004**, *214* (1), 83-90.
61. Wu, J.; Zhang, J.; Zhang, H.; He, J.; Ren, Q.; Guo, M. *Biomacromolecules* **2004**, *5* (2), 266-268.
62. Zhao, H.; Malhotra, S. V. *Biotechnol. Lett* **2002**, *24* (15), 1257-1259.
63. Zhou, Y.; Antonietti, M. *J. Am. Chem. Soc.* **2003**, *125* (49), 14960-14961.
64. Wang, R.; Jin, C.-M.; Twamley, B.; Shreeve, J. n. M. *Inorg. Chem.* **2006**, *45* (16), 6396-6403.
65. Bhawal, S. S.; Patil, R. A.; Armstrong, D. W. *RSC Adv.* **2015**, *5* (116), 95854-95856.

66. Ngo, H. L.; LeCompte, K.; Hargens, L.; McEwen, A. B. *Thermochim. Acta* **2000**, *357*, 97-102.
67. Wasserscheid, P.; Welton, T., *Ionic liquids in synthesis*. Wiley-VCH Verlag GmbH & Co. KGaA: Weinheim, Germany, 2008.
68. Dearden, J. *Sci. Total Environ.* **1991**, *109*, 59-68.
69. Izgorodina, E. I.; Forsyth, M.; MacFarlane, D. R. *Aust. J. Chem.* **2007**, *60* (1), 15-20.
70. Montanino, M.; Carewska, M.; Alessandrini, F.; Passerini, S.; Appetecchi, G. B. *Electrochim. Acta* **2011**, *57*, 153-159.
71. Rahman, M. M.; Liu, H. Y.; Prock, A.; Giering, W. P. *Organometallics* **1987**, *6* (3), 650-658.
72. Harvey, R. G., Environmental chemistry of PAHs. In *PAHs and related compounds*, Springer: 1998; pp 1-54.
73. Manzano, C.; Hoh, E.; Simonich, S. L. M. *Environ. Sci. Technol.* **2012**, *46* (14), 7677-7684.
74. Poster, D. L.; Schantz, M. M.; Sander, L. C.; Wise, S. A. *Anal. Bioanal. Chem.* **2006**, *386* (4), 859-881.
75. Ding, J.; Desikan, V.; Han, X.; Xiao, T. L.; Ding, R.; Jenks, W. S.; Armstrong, D. W. *Org. Lett.* **2005**, *7* (2), 335-337.
76. Cole, A. C.; Jensen, J. L.; Ntai, I.; Tran, K. L. T.; Weaver, K. J.; Forbes, D. C.; Davis, J. H. *J. Am. Chem. Soc.* **2002**, *124* (21), 5962-5963.
77. Dyson, P. J.; Ellis, D. J.; Welton, T.; Parker, D. G. *Chem. Commun.* **1999**, (1), 25-26.
78. Berthod, A.; He, L.; Armstrong, D. W. *Chromatographia* **2001**, *53* (1), 63-68.
79. Carda-Broch, S.; Berthod, A.; Armstrong, D. *Anal. Bioanal. Chem.* **2003**, *375* (2), 191-199.
80. Dai, S.; Ju, Y.; Barnes, C. *J. Chem. Soc., Dalton Trans.* **1999**, (8), 1201-1202.
81. Chun, S.; Dzyuba, S. V.; Bartsch, R. A. *Anal. Chem.* **2001**, *73* (15), 3737-3741.
82. Liu, R.; Liu, J.-f.; Yin, Y.-g.; Hu, X.-l.; Jiang, G.-b. *Anal. Bioanal. Chem.* **2009**, *393* (3), 871-883.
83. Armstrong, D. W.; Zhang, L.-K.; He, L.; Gross, M. L. *Anal. Chem.* **2001**, *73* (15), 3679-3686.
84. Carda-Broch, S.; Berthod, A.; Armstrong, D. W. *Rapid Commun. Mass Spectrom.* **2003**, *17* (6), 553-560.
85. Tholey, A.; Heinzle, E. *Anal. Bioanal. Chem.* **2006**, *386* (1), 24-37.

86. Chan, K.; Lanthier, P.; Liu, X.; Sandhu, J. K.; Stanimirovic, D.; Li, J. *Anal. Chim. Acta* **2009**, *639* (1), 57-61.
87. Crank, J. A.; Armstrong, D. W. *J. Am. Soc. Mass. Spectrom.* **2009**, *20* (10), 1790-1800.
88. Lagrost, C.; Carrie, D.; Vaultier, M.; Hapiot, P. *J. Phys. Chem. A* **2003**, *107* (5), 745-752.
89. Enders Dickinson, V.; Williams, M. E.; Hendrickson, S. M.; Masui, H.; Murray, R. W. *J. Am. Chem. Soc.* **1999**, *121* (4), 613-616.
90. Doyle, K. P.; Lang, C. M.; Kim, K.; Kohl, P. A. *J. Electrochem. Soc.* **2006**, *153* (7), A1353-A1357.
91. Nanayakkara, Y. S.; Moon, H.; Payagala, T.; Wijeratne, A. B.; Crank, J. A.; Sharma, P. S.; Armstrong, D. W. *Anal. Chem.* **2008**, *80* (20), 7690-7698.
92. Nanayakkara, Y. S.; Perera, S.; Bindiganavale, S.; Wanigasekara, E.; Moon, H.; Armstrong, D. W. *Anal. Chem.* **2010**, *82* (8), 3146-3154.
93. Ragonese, C.; Sciarrone, D.; Tranchida, P. Q.; Dugo, P.; Mondello, L. *J. Chromatogr. A* **2012**, *1255*, 130-144.
94. Krupčík, J.; Gorovenko, R.; Špánik, I.; Bočková, I.; Sandra, P.; Armstrong, D. W. *J. Chromatogr. A* **2013**, *1301*, 225-236.
95. Delmonte, P.; Fardin-Kia, A. R.; Rader, J. I. *Anal. Chem.* **2013**, *85* (3), 1517-1524.
96. Zeng, A. X.; Chin, S.-T.; Nolvachai, Y.; Kulsing, C.; Sidisky, L. M.; Marriott, P. J. *Anal. Chim. Acta* **2013**, *803*, 166-173.
97. Cagliero, C.; Bicchi, C.; Cordero, C.; Liberto, E.; Sgorbini, B.; Rubiolo, P. *J. Chromatogr. A* **2012**, *1268*, 130-138.
98. Delmonte, P.; Fardin-Kia, A. R.; Kramer, J. K.; Mossoba, M. M.; Sidisky, L.; Tyburczy, C.; Rader, J. I. *J. Chromatogr. A* **2012**, *1233*, 137-146.
99. Sanchez-Prado, L.; Lamas, J. P.; Garcia-Jares, C.; Llompарт, M. *Chromatographia* **2012**, *75* (17-18), 1039-1047.
100. Ragonese, C.; Sciarrone, D.; Tranchida, P. Q.; Dugo, P.; Dugo, G.; Mondello, L. *Anal. Chem.* **2011**, *83* (20), 7947-7954.
101. Ragonese, C.; Tranchida, P. Q.; Sciarrone, D.; Mondello, L. *J. Chromatogr. A* **2009**, *1216* (51), 8992-8997.
102. Frink, L. A.; Armstrong, D. W. *Anal. Chem.* **2016**, *88* (16), 8194-8201.
103. Frink, L. A.; Weatherly, C. A.; Armstrong, D. W. *J. Pharm. Biomed. Anal.* **2014**, *94*, 111-117.
104. Frink, L. A.; Armstrong, D. W. *J. Pharm. Sci.* **2016**, *105* (8), 2288-2292.

105. Frink, L. A.; Armstrong, D. W. *Food Chem.* **2016**, *205*, 23-27.
106. Talebi, M.; Frink, L. A.; Patil, R. A.; Armstrong, D. W. *Food Analytical Methods* **2017**.
107. Lambertus, G. R.; Crank, J. A.; McGuigan, M. E.; Kendler, S.; Armstrong, D. W.; Sacks, R. D. *J. Chromatogr. A* **2006**, *1135* (2), 230-240.
108. Sciarrone, D.; Tranchida, P. Q.; Ragonese, C.; Schipilliti, L.; Mondello, L. *J. Sep. Sci.* **2010**, *33* (4-5), 594-599.
109. Reid, V. R.; Crank, J. A.; Armstrong, D. W.; Synovec, R. E. *J. Sep. Sci.* **2008**, *31* (19), 3429-3436.
110. Patil, R. A.; Talebi, M.; Xu, C.; Bhawal, S. S.; Armstrong, D. W. *Chem. Mater.* **2016**, *28* (12), 4315-4323.
111. Dettmer, K. *Anal. Bioanal. Chem.* **2014**, *406* (20), 4931-4939.
112. Lin, C.-C.; Wasta, Z.; Mjøs, S. A. *J. Chromatogr. A* **2014**, *1350*, 83-91.
113. Grob, K.; Grob, G. *J. Chromatogr. A* **1978**, *156* (1), 1-20.
114. Grob, K.; Grob, G. *J. Chromatogr. A* **1981**, *219* (1), 13-20.
115. Han, X.; Armstrong, D. W. *Acc. Chem. Res.* **2007**, *40* (11), 1079-1086.
116. Ho, T. D.; Zhang, C.; Hantao, L. W.; Anderson, J. L. *Anal. Chem.* **2013**, *86* (1), 262-285.
117. Meng, Y.; Pino, V.; Anderson, J. L. *Anal. Chem.* **2009**, *81* (16), 7107-7112.
118. Li, T.; Joshi, M. D.; Ronning, D. R.; Anderson, J. L. *J. Chromatogr. A* **2013**, *1272*, 8-14.
119. Chang, Y. L.; Lee, Y. C.; Yang, W. B.; Chen, C. H. *J. Mass Spectrom.* **2011**, *46* (4), 367-375.
120. Bhattacharya, B.; Samanta, A. *J. Phys. Chem. B* **2008**, *112* (33), 10101-10106.
121. Qiu, H.; Liang, X.; Sun, M.; Jiang, S. *Anal. Bioanal. Chem.* **2011**, *399* (10), 3307-3322.
122. Shu Juan, L.; Feng, Z.; Xiao Hua, X.; Liang, Z.; Xia, L. *Chin. Chem. Lett.* **2004**, *15* (9), 1060-1062.
123. Xu, Y.; Wang, E. *J. Chromatogr. A* **2009**, *1216* (24), 4817-4823.
124. Mendes, A.; Branco, L. C.; Morais, C.; Simplicio, A. L. *Electrophoresis* **2012**, *33* (7), 1182-1190.
125. Minami, I.; Kamimura, H.; Mori, S. *Lubr. Sci.* **2007**, *24* (3), 135-147.
126. Qu, J.; Blau, P. J.; Dai, S.; Luo, H.; Meyer, H. M. *Tribol. Lett.* **2009**, *35* (3), 181-189.
127. Patil, R. A.; Talebi, M.; Sidisky, L. M.; Armstrong, D. W. *Chromatographia* **2017**.
128. Zhou, F.; Liang, Y.; Liu, W. *Chem. Soc. Rev.* **2009**, *38* (9), 2590-2599.
129. Clough, M. T.; Geyer, K.; Hunt, P. A.; Mertes, J.; Welton, T. *PCCP* **2013**, *15* (47), 20480-20495.

130. Lovelock, K. R.; Armstrong, J. P.; Licence, P.; Jones, R. G. *PCCP* **2014**, *16* (4), 1339-1353.
131. Nevshupa, R.; Conte, M.; Guerra, S.; Roman, E. *Lubricants* **2017**, *5* (3), 27.
132. Clough, M. T.; Crick, C. R.; Grasvik, J.; Hunt, P. A.; Niedermeyer, H.; Welton, T.; Whitaker, O. P. *Chem. Sci.* **2015**, *6* (2), 1101-1114.
133. Baranyai, K. J.; Deacon, G. B.; MacFarlane, D. R.; Pringle, J. M.; Scott, J. L. *Aust. J. Chem.* **2004**, *57* (2), 145-147.
134. Ohtani, H.; Ishimura, S.; Kumai, M. *Anal. Sci.* **2008**, *24* (10), 1335-1340.
135. Wooster, T. J.; Johanson, K. M.; Fraser, K. J.; MacFarlane, D. R.; Scott, J. L. *Green Chem.* **2006**, *8* (8), 691-696.
136. Talebi, M.; Patil, R. A.; Sidisky, L. M.; Berthod, A.; Armstrong, D. W. *Anal. Bioanal. Chem.* **2017**.
137. Sawada, M.; Takai, Y.; Chong, C.; Hanafusa, T.; Misumi, S.; Tsuno, Y. *Tetrahedron Lett.* **1985**, *26* (41), 5065-5068.
138. Silverstein, R. M.; Webster, F. X., *Spectrometric Identification of organic Compounds*. John Wiley and Sons: New York, 1998.
139. Ganguly, S.; Dana, K.; Mukhopadhyay, T. K.; Ghatak, S. *J. Therm. Anal. Calorim.* **2011**, *105* (1), 199-209.
140. Xie, W.; Xie, R.; Pan, W.-P.; Hunter, D.; Koene, B.; Tan, L.-S.; Vaia, R. *Chem. Mater.* **2002**, *14* (11), 4837-4845.
141. Cottrell, T. L., *The strengths of chemical bonds*. Academic Press: Butterworths, London, 1958.
142. Glastrup, J. *Polym. Degrad. Stab.* **1996**, *52* (3), 217-222.
143. Cao, Y.; Mu, T. *Ind. Eng. Chem. Res.* **2014**, *53* (20), 8651-8664.
144. Berthod, A.; Ruiz-Angel, M.; Carda-Broch, S. *J. Chromatogr. A* **2008**, *1184* (1-2), 6-18.
145. Poole, C. F.; Poole, S. K. *J. Sep. Sci.* **2011**, *34* (8), 888-900.
146. Yao, C.; Anderson, J. L. *J. Chromatogr. A* **2009**, *1216* (10), 1658-1712.
147. Xue, L.; Gurung, E.; Tamas, G.; Koh, Y. P.; Shadeck, M.; Simon, S. L.; Maroncelli, M.; Quitevis, E. L. *J. Chem. Eng. Data* **2016**, *61* (3), 1078-1091.
148. Chang, J.-C.; Ho, W.-Y.; Sun, I.-W.; Tung, Y.-L.; Tsui, M.-C.; Wu, T.-Y.; Liang, S.-S. *Tetrahedron* **2010**, *66* (32), 6150-6155.
149. D'Anna, F.; Gunaratne, H. N.; Lazzara, G.; Noto, R.; Rizzo, C.; Seddon, K. R. *Org. Biomol. Chem.* **2013**, *11* (35), 5836-5846.

150. Talebi, M.; Patil, R. A.; Sidisky, L. M.; Berthod, A.; Armstrong, D. W. *Anal. Chim. Acta* **2018**, <https://doi.org/10.1016/j.aca.2018.07.047>.
151. Fraser, K. J.; MacFarlane, D. R. *Aust. J. Chem.* **2009**, *62* (4), 309-321.
152. Bradaric, C. J.; Downard, A.; Kennedy, C.; Robertson, A. J.; Zhou, Y. *Green Chem.* **2003**, *5* (2), 143-152.
153. Rodríguez-Sánchez, S.; Galindo-Iranzo, P.; Soria, A. C.; Sanz, M. L.; Quintanilla-López, J. E.; Lebrón-Aguilar, R. *J. Chromatogr. A* **2014**, *1326*, 96-102.
154. Patil, R. A.; Talebi, M.; Sidisky, L. M.; Armstrong, D. W. *Chromatographia* **2017**, *80* (10), 1563-1574.
155. Zapadlo, M.; Krupčík, J.; Kovalczuk, T.; Májek, P.; Špánik, I.; Armstrong, D. W.; Sandra, P. *J. Chromatogr. A* **2011**, *1218* (5), 746-751.
156. Poole, C. F.; Lenca, N. *J. Chromatogr. A* **2014**, *1357*, 87-109.
157. Tukacs, J. M.; Király, D.; Strádi, A.; Novodarszki, G.; Eke, Z.; Dibó, G.; Kégl, T.; Mika, L. T. *Green Chem.* **2012**, *14* (7), 2057-2065.
158. Ros, M.; Escobar-Arnanz, J.; Sanz, M.; Ramos, L. *J. Chromatogr. A* **2018**, *1559*, 156-163.
159. Babich, M. A. **2010**, <https://www.cpsc.gov/s3fs-public/phthalover.pdf>, (last time accessed: June 16, 2018).
160. Nalin, F.; Sander, L. C.; Wilson, W. B.; Wise, S. A. *Anal. Bioanal. Chem.* **2018**, *410* (3), 1123-1137.
161. Kimbrough, R. D.; Jensen, A. A., *Halogenated biphenyls, terphenyls, naphthalenes, dibenzodioxins and related products*. Elsevier: Amsterdam, 1989; Vol. 4.
162. Bertazzi, P. A. *Sci. Total Environ.* **1991**, *106* (1-2), 5-20.
163. Wasserscheid, P.; Keim, W. *Angew. Chem. Int. Ed.* **2000**, *39* (21), 3772-3789.
164. Carmichael, A. J.; Earle, M. J.; Holbrey, J. D.; McCormac, P. B.; Seddon, K. R. *Org. Lett.* **1999**, *1* (7), 997-1000.
165. Snelders, D. J.; Dyson, P. J. *Org. Lett.* **2011**, *13* (15), 4048-4051.
166. Forsyth, S. A.; Gunaratne, H. N.; Hardacre, C.; McKeown, A.; Rooney, D. W. *Org. Process Res. Dev.* **2006**, *10* (1), 94-102.
167. Isambert, N.; Duque, M. d. M. S.; Plaquevent, J.-C.; Genisson, Y.; Rodriguez, J.; Constantieux, T. *Chem. Soc. Rev.* **2011**, *40* (3), 1347-1357.
168. Greene, T.; Wuts, P. J. *Wiley & Sons, New York* **1999**, 57-58.

169. Sartori, G.; Ballini, R.; Bigi, F.; Bosica, G.; Maggi, R.; Righi, P. *Chem. Rev.* **2004**, *104* (1), 199-250.
170. Kuttan, A.; Nowshudin, S.; Rao, M. *Tetrahedron Lett.* **2004**, *45* (12), 2663-2665.
171. Tom, N. J.; Simon, W. M.; Frost, H. N.; Ewing, M. *Tetrahedron Lett.* **2004**, *45* (5), 905-906.
172. Choy, J.; Jaime-Figueroa, S.; Jiang, L.; Wagner, P. *Synth. Commun.* **2008**, *38* (21), 3840-3853.
173. Kocienski, P. J., *Protecting Groups*. 3rd ed.; Georg Thieme: Stuttgart, New York, 2005.
174. Han, G.; Tamaki, M.; Hruby, V. J. *J. Pept. Res.* **2001**, *58* (4), 338-341.
175. Wang, J.; Liang, Y.-L.; Qu, J. *Chem. Commun.* **2009**, (34), 5144-5146.
176. Wang, G.; Li, C.; Li, J.; Jia, X. *Tetrahedron Lett.* **2009**, *50* (13), 1438-1440.
177. Handy, S. T.; Okello, M.; Dickenson, G. *Org. Lett.* **2003**, *5* (14), 2513-2515.
178. Majumdar, S.; De, J.; Chakraborty, A.; Roy, D.; Maiti, D. K. *RSC Adv.* **2015**, *5* (5), 3200-3205.
179. Dupont, J.; de Souza, R. F.; Suarez, P. A. *Chem. Rev.* **2002**, *102* (10), 3667-3692.
180. McNulty, J.; Dyck, J.; Larichev, V.; Capretta, A.; Robertson, A. *Lett. Org. Chem.* **2004**, *1* (2), 137-139.
181. Ludley, P.; Karodia, N. *Tetrahedron Lett.* **2001**, *42* (10), 2011-2014.

Biographical Information

Rahul A. Patil obtained his Master of Science degree in organic chemistry from Fergusson College affiliated to University of Pune at Pune, India in 2011. Subsequently, he worked at Lupin Limited (Research Park), Pune in analytical research and development department for two years. In 2014, he joined Dr. Daniel W. Armstrong's research group at University of Texas at Arlington for his Ph.D. studies. At UTA, Rahul did research on the development and applications of thermally stable ionic liquid gas chromatography stationary phases. During Ph.D., he was awarded two research poster awards; at the International Symposium for Capillary Chromatography (ISCC) in May 2017 and at the Chemistry Graduate Student Research Symposium (UTA) in April 2018.